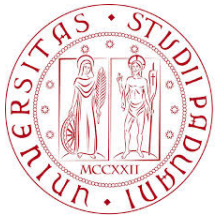

UNIVERSITÀ DEGLI STUDI DI PADOVA

Dipartimento di Fisica e Astronomia "Galileo Galilei"

Master Degree in Physics

Final Dissertation

Probing primordial non-Gaussianity via cosmological gravitational wave anisotropies

Thesis supervisor
Prof. Nicola Bartolo

Candidate
Martino Michelotti

Academic Year 2020/2021

Abstract

In modern Cosmology, primordial non-Gaussianity (PNG) is regarded as a fundamental and independent source of information about the physics of the early Universe. The ideal observable to measure the non-Gaussian nature of primordial perturbations, and its eventual scale dependence, is the cosmic microwave background (CMB) radiation. In this work another promising probe of primordial non-Gaussianity is considered, namely the cosmological gravitational wave background (CGWB) generated during inflation. An eventual detection of such a GW background in the near future may possibly provide with new and exciting information, inaccessible to CMB measurements. Signatures of primordial non-Gaussianity are in fact expected to be picked up via the GW propagation across large-scale scalar perturbations. Particular attention is given to the CGWB energy density anisotropies 3-point angular correlator, or bispectrum, as the lowest-order indicator of the presence of PNG. Explicit expressions can be derived in the case non-Gaussianity is parametrized in terms of the local ansatz for the primordial curvature perturbation. The inclusion of the scale dependence, or running, in the discussion is then achieved by means of a kernel approach for the non-linear parameter f_{NL} and of a subsequent matching with bispectrum templates recurring in the literature. A specific scenario of CGWB sourced at second order from enhanced small-scale scalar perturbations, arising with the formation of primordial black holes (PBHs), is also considered. In this context the presence of primordial non-Gaussianity would show up already at the emission, as an initial condition. The PBHs mass is taken to be such that they may as well comprise all of the dark matter (DM). If this was actually the case it would be remarkable, in presence of a sufficient running of non-Gaussianity, the possibility to obtain an arbitrarily anisotropic CGWB which is otherwise, in the non-running scenario, constrained to be highly isotropic due to cold dark matter isocurvature (CDI) bounds.

Alla mia cara nonna

Contents

Introduction

It is believed that at early times our Universe experiences a period of accelerated expansion, known as inflation [4], which in the most standard models is driven by the vacuum energy density of a scalar field, known as inflaton. Most importantly, other than solving a few shortcomings of the standard Big Bang model, the inflationary mechanism is able to provide an explanation for the production of primordial scalar perturbations [1], along with a primordial stochastic gravitational wave background [52, 53]. The former are at the origin of both the temperature and polarization anisotropies in the cosmic microwave background (CMB) radiation and the density inhomogeneities responsible for large-scale structure (LSS) formation at later times [41].

Primordial scalar perturbations are the result of inflaton quantum fluctuations during inflation, in such a way that they cannot be treated in a deterministic way. The right approach is to consider them as the different values assumed by a random field and thus to give a statistical description of the process. In practice this means to compute statistical correlators of quantities related to primordial perturbations, such as the CMB temperature angular anisotropies, which can then be compared to observations. The usual assumption, justified also by experimental data [10], is to take a zero-mean Gaussian as the probability density function from which primordial perturbations are drawn. If this is the case, all the information needed to describe such a distribution is represented by the variance and it is thus contained inside the 2-point correlation function. Its counterpart in Fourier space, then, is what is called the power spectrum.
Nevertheless, even if latest observations are compatible with the Gaussianity of primordial scalar perturbations, it is still interesting to consider the possibility of a deviation from this Gaussian behaviour, which is addressed to as non-Gaussianity [8]. In the specific case of primordial perturbations from inflation we refer to primordial non-Gaussianity (PNG). In such a context, higher-order statistical correlators have to be considered to fully describe a non-Gaussian random field. The lowest-order correlator to be an indicator of primordial non-Gaussianity is the the 3-point one, whose Fourier counterpart is the primordial bispectrum, in analogy to the definition of the power spectrum.
Primordial non-Gaussianity may then be regarded as an important and unique probe of the fundamental physics in the early Universe, since each inflationary model provides with a specific amount of PNG [12], in such a way that it can be exploited to confirm or rule out models depending on their predictions. It is also possible to consider an additional dependence of the non-Gaussian behaviour as a function of the scale of the perturbations. This generalization takes the name of running non-Gaussianity [12, 34] and a major part of this work is dedicated to deal with such a possibility.

In Cosmology, one of the main observables to retain information about primordial perturbations is the CMB. Primordial scalar perturbations can be expressed in the form of the gauge-invariant quantity ζ, known as primordial curvature perturbation [8]. The peculiarity of this quantity is that its evolution is frozen outside of the Hubble horizon, for the simplest models of inflation, in such a way that its value during inflation is transferred, practically unchanged, to later times after the horizon re-entry. In this way CMB temperature anisotropies can be directly referred to the inflationary period. In particular, CMB anisotropies inherit their statistics from the primordial curvature perturbation ζ, meaning that we can consider CMB statistical correlators, which are observable quantities, in order to study the presence of primordial non-Gaussianity and its nature [16].

Other than reviewing how the CMB may be regarded as a fundamental probe for PNG, we are interested in considering also another promising, possibly independent, source of information, namely the stochastic background of gravitational waves (GWs) of cosmological origin [52, 53]. Similarly to primordial scalar perturbations, quantum fluctuations during inflation are also expected to produce primordial tensor perturbations of the metric, which can be identified as a stochastic background of GWs. These are then expected to eventually pick up signatures of primordial non-Gaussianity during their propagation across large-scale scalar perturbations [49]. Since the scales probed by the cosmological GW background (CGWB) can be orders of magnitude different with respect to the CMB ones, there is the concrete possibility to recover unique constraints on primordial non-Gaussianity on such scales. This is one of the main focus of this Thesis, where the more original part actually consists in the generalization of the treatment to include the possibility of a scale-dependent non-Gaussianity.

The production of GWs early in the Universe is not exclusive to quantum fluctuations during inflation. Later in this work we will consider the stochastic background of GWs associated to the early formation of primordial black holes (PBHs) [81] and sourced by scalar perturbations at second order in perturbation theory [69, 70, 71, 20, 72, 73, 74, 75]. Any presence of non-Gaussianity in the primordial scalar perturbations is imprinted into this GW background directly at its emission [87]. In fact we will see how this may introduce anisotropies in the GW energy density and how this conclusion changes when accounting for the possibility of running non-Gaussianity. Moreover, a measurement of these anisotropies should also allow to constrain PNG, and its running, at scales much much smaller than the CMB ones.

The structure of this Thesis is organized as follows:
Chapter 1 introduces briefly to the main concepts in modern Cosmology, with a particular attention to the treatment of standard single-field models of inflation. The derivation of primordial scalar perturbations from quantum fluctuations is shown, along with the definition of the gauge-invariant curvature perturbation ζ. The necessity of a statistical description by means of the power spectrum is introduced.
Chapter 2 consists in a small, almost self-consistent, review of the cosmological perturbation theory (CPT) at linear order, which includes the main results of linearized Einstein equations. The topic of the gauge problem is then treated, and the expression for the curvature perturbation ζ is derived in an alternative way, as the result of a gauge-invariant construction.
In Chapter 3 the concept of primordial non-Gaussianity is introduced in the most generic context. The focus is in particular on the primordial bispectrum, as the main indicator of the presence of non-Gaussianity, which is described by a shape function and an amplitude parameter, whose eventual scale dependence corresponds to a running non-Gaussianity. The local shape is then considered, being it the simplest and most common way to parametrize non-Gaussianity and allowing also for a quite immediate generalization to the scale-dependent scenario, of which few possible cases are presented.
Chapter 4 is devoted to the treatment of the CMB temperature anisotropies as the result of primordial scalar perturbations. The standard derivation for the CMB angular power spectrum is presented. Analogously, the CMB angular bispectrum is computed in the presence of primordial non-Gaussianity and presented as a fundamental observable to probe deviation from Gaussian statistics in the early Universe. Specific expressions of the CMB bispectrum are also derived exploiting the local parametrization of non-Gaussianity.
In Chapter 5 the focus becomes the stochastic background of GWs of cosmological origin, the CGWB. Gravitational waves are presented as the solution to vacuum Einstein equations and the production of tensor metric perturbations arising from quantum fluctuations during inflation is treated. Via a Boltzmann-like approach, the CGWB is then described in strict analogy with the CMB, so that the effect of large-scale scalar perturbations on high-frequency GWs can be considered. This shows how primordial GWs from inflation may carry important information about PNG. Consequently, expression for the angular bispectrum, analogous to the ones for the CMB, are also derived.
In Chapter 6 a specific scenario of GW production in the early Universe is considered, associated to the formation of PBHs. This happens in presence of enhanced scalar perturbations at small

scales, which may then source at second order a background of GWs with sufficient amplitude to be detectable. The basic physics of GW production at second order from scalar perturbations and of PBH formation from enhanced density perturbations is briefly reviewed. The energy density of the CGWB is then introduced as a fundamental observable, and the effect that the presence of primordial non-Gaussianity has on it, in the considered scenario, is derived. The inclusion of running non-Gaussianity in the discussion is an original contribution to this work. Finally, isocurvature bounds on PBH abundance are considered in order for constraints on primordial local non-Gaussianity to be derived.
Formulae and relations useful for the discussions in the main text are reported in the Appendices, along with some of the more technical mathematical steps.

Chapter 1

Introduction to Cosmology

We start off the discussion with this introductory Chapter, in which we briefly recap the geometric and energetic aspects of our Universe. We focus in particular on the description of a FLRW background, homogeneous and isotropic as expected by the Cosmological Principle. A major portion of the Chapter is then devolved to introduce the inflationary hypothesis, along with the standard slow-roll model. A remarkable result, fundamental for the following treatment of primordial non-Gaussianity, is the production of primordial quantum scalar fluctuations during inflation, in the form of primordial curvature perturbations.

1.1 Background Cosmology

1.1.1 FLRW spacetime

If we look at our own Universe, on sufficiently large scale it appears almost exactly isotropic, where the deviations from this behaviour are of the order of 1 out of 10^5. Assuming that this property holds also when looking from any other point, meaning we do not occupy any special position (as stated by the Cosmological Principle), we can conclude that the Universe is also homogeneous. Furthermore, today we know that our Universe started hot and dense, cooled down while expanding during its thermal history, in the last 13.8 billions year, and ended up being what we observe today. Adopting Einstein's General Relativity as the theory governing gravity, all this features lead up to the Friedmann-Lemaitre-Robertson-Walker (FLRW) metric in spherical coordinates:

$$ds^2 = -dt^2 + a^2(t)\left(\frac{dr^2}{1-kr^2} + r^2\left(d\theta^2 + \sin^2\theta d\varphi^2\right)\right), \tag{1.1}$$

which describes the geometry of the background spacetime. Notice that we have assumed natural units, i.e. $c = 1$, and we will implicitly do the same throughout this work. The spatial curvature parameter k is a constant which can take three different values, in the case of a flat ($k = 0$), close ($k = +1$) or open ($k = -1$) spatial geometry. The scale factor $a(t)$, function of the cosmic time t, is a dimensionless quantity that accounts for the expansion of the Universe. We have introduced in (1.1) the comoving coordinate r, meaning that r remains fixed for a point following the Universe in his expansion. Physical distances, in Cartesian coordinates, are related to the comoving ones via the scale factor: $\vec{x}_{\rm phys} = a(t)\vec{x}_{\rm com}$.

Sometimes it is useful to introduce an alternative way of parametrizing the time coordinate. The conformal time is defined as:

$$\tau = \int_0^t \frac{dt'}{a(t')}, \tag{1.2}$$

so that $d\tau = \frac{dt}{a(t)}$. Substituting this expression inside (1.1), and setting $k = 0$, one finds the following result for the flat FLRW metric, written in Cartesian coordinate:

$$ds^2 = a^2(\tau)\big(-d\tau^2 + \delta_{ij}dx^i dx^j\big), \tag{1.3}$$

which corresponds to the Minkowski metric rescaled by an overall time dependent factor.

A photon traveling across the Universe experiences its expansion so that, when it reaches our detectors, its wavelength is stretched with respect to the one at emission. To quantify this we introduce the redshift z, defined as:

$$z \equiv \frac{\lambda_o - \lambda_e}{\lambda_e}, \tag{1.4}$$

where λ_o and λ_e are, respectively, the wavelength we observe today and the one emitted in the past. In the case of an expanding Universe we see that z is always bigger than unity and it basically quantifies how much a photon travelled before being picked up by some instrumentation on Earth. This suggests a relation between the redshift z and the scale factor a, which happens to be [1]:

$$1 + z(t) = \frac{a(t_0)}{a(t)}, \tag{1.5}$$

and it is then evident how z may be regarded as a time variable, something which is usually done in Cosmology.

1.1.2 Einstein's Equations and Energy Content

The evolution of the background metric (1.1) can be obtained starting from the following action:

$$S = \int d^4x\sqrt{-g}\Big(\frac{1}{16\pi G}R + \mathcal{L}_m(g_{\mu\nu}, \psi_m)\Big), \tag{1.6}$$

where g denotes the determinant of the metric and R the Ricci scalar (see Appendix A), as usual. The first term of (1.6) corresponds to the Einstein-Hilbert action, constructed from the metric and thus containing all the information about the geometry of the spacetime. The second term $\mathcal{L}_m(g_{\mu\nu}, \psi_m)$, instead, accounts for all the energetic content of the Universe, which acts as a source for the gravitational field $g_{\mu\nu}$. In this sense ψ_m is the field associated to any of the particles of the system.

Varying the action (1.6) with respect to the metric $g_{\mu\nu}$ one obtains the famous Einstein's equations:

$$G_{\mu\nu} \equiv R_{\mu\nu} - \frac{1}{2}g_{\mu\nu}R = 8\pi G T_{\mu\nu}, \tag{1.7}$$

where $R_{\mu\nu}$ and $G_{\mu\nu}$ are the Ricci and Einstein tensors, respectively. See Appendix A for more information on the geometric part of Einstein's equations.
We have defined the stress-energy tensor on the right side of (1.7) as:

$$T_{\mu\nu} = -\frac{2}{\sqrt{-g}}\frac{\delta(\sqrt{-g}\mathcal{L}_m)}{\delta g^{\mu\nu}}. \tag{1.8}$$

In Cosmology, when describing the background spacetime (1.1), usually one can assume the simple expression of the stress-energy tensor for a perfect fluid, isotropic and homogeneous [1]:

$$T_{\mu\nu} = u_\mu u_\nu(\rho + p) + p g_{\mu\nu}, \tag{1.9}$$

with u_μ the 4-velocity of the fluid. In its rest frame, where $u_\mu = (1, 0, 0, 0)$, it follows immediately $T^0_{\ 0} = -\rho$ and $T^i_{\ j} = p\delta^i_{\ j}$, where ρ is the background energy density and p is the background isotropic pressure. In evaluating them one has to account for all the possible contributions to the energy budget. Notice that the form (1.9) of the stress-energy tensor is compatible with the assumption made before of an homogeneous and isotropic background spacetime.
Writing explicitly the components of equation (1.7), in case of the metric (1.1), and using expression (1.9) for the stress-energy tensor, one derives the so called Friedmann equations:

$$H^2 \equiv \left(\frac{\dot{a}}{a}\right)^2 = \frac{8\pi G}{3}\rho - \frac{k}{a^2}, \tag{1.10}$$

from the (0-0)-component and:

$$\frac{\ddot{a}}{a} = -\frac{4\pi G}{3}(\rho + 3p), \tag{1.11}$$

from the (i-j)-component. In equation (1.10) we have also defined the Hubble parameter H, which identifies a characteristic time of expansion $\tau_H = H^{-1}$. Furthermore, from Bianchi identities $\nabla_\mu G^{\mu\nu} = 0$ for the metric (1.1), where ∇_μ is the covariant derivative, it follows the continuity equation:

$$\dot{\rho} + 3H(\rho + p) = 0. \tag{1.12}$$

We end up with a system of three equations, but it is possible to verify that only two out of these are independent. Therefore, we need one additional equation to solve the system for the three variables a, ρ and P, all as function of the cosmic time t. This is usually done by specifying the equation of state for a barotropic fluid:

$$p = w\rho, \tag{1.13}$$

where w is a constant, different for each one of the fluid components. Substituting (1.13) inside (1.12) one then obtains the evolution of the background energy density with respect to the scale factor:

$$\rho = \rho_0 \left(\frac{a}{a_0}\right)^{-3(1+w)}, \tag{1.14}$$

where we indicate with the subscript 0 the quantities evaluated today at $t = t_0$.
In the Standard Model of Cosmology ΛCDM the following cases are usually considered as components of the cosmic fluid:

- Matter: it includes both dark and ordinary matter, which have the peculiarity of having negligible pressure $|p| \ll \rho$. Setting $w = 0$ in (1.14) results in $\rho_m \propto a^{-3}$, an expected result since it accounts for the dilution due to the Universe expansion (vol $\propto a^3$).

- Radiation: it indicates not only photons but basically all the particles in a relativistic state, such as neutrinos or, at early times, particles with mass negligible with respect to the thermal energy. In this case $w = 1/3$, so that equation (1.14) gives $\rho_r \propto a^{-4}$, and it can be interpreted as the combined effect of dilution ($\propto a^{-3}$) and redshift ($\propto a^{-1}$).

- Cosmological Constant: this is the most simple and common way to describe dark energy, whose presence should be able to drive the late time accelerated expansion. Its name derives from the assumption that $\rho_\Lambda = \text{const}$, possible only if we set $p = -\rho$ inside equation (1.12). A negative pressure might seem strange, but we will see that it is required also during what is believed to be a fundemental phase of the primordial Universe, the inflation.

The evolution of these fluid components' energy densities is plotted in Figure 1.1.

Today the Universe is measured to be composed predominantly by cold dark matter and dark energy, which drives the late time accelerated expansion of the Universe and, within the ΛCDM model, is thought to be in the form of a cosmological constant Λ . They cover, respectively, around 25% and 70% of the energy budget today, with baryonic matter which constitutes the remaining 5%. The present contribution of radiation is negligible.
With the term baryonic matter we refer to all the particle content of the Standard Model of particle physics, whereas dark matter is still an unknown component of the Universe, with the property of interacting only gravitationally. So far its presence has only been stated indirectly by means of gravitational considerations on galaxies, which require the presence of additional yet not visible matter. Moreover, dark matter is necessary to allow the gravitational collapse of primordial perturbations into the large scale structures we observe today [1].

Starting from the present energy densities of the fluid components and evolving them back in time with equation (1.14) it is possible to recover different regimes:

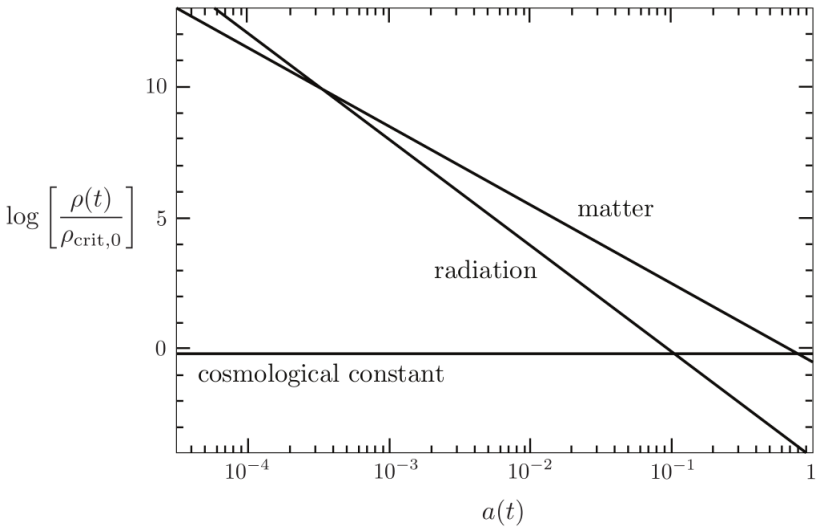

Figure 1.1: Energy densities evolution for radiation, matter and a cosmological constant. The critical energy density ρ_{crit} is defined in equation (1.15). It is immediate to deduce the different regimes and the epochs of equality between two fluid components. Taken from [2].

- Radiation domination until $z_{\text{eq}} \simeq 3000$,
- Matter domination from $z_{\text{eq}} \simeq 3000$ until $z_\Lambda \simeq 0.3$,
- Late time acceleration driven by dark energy from $z_\Lambda \simeq 0.3$ until today ($z_0 = 0$).

A specific regime is set by the dominating component of the fluid at a given moment and determines the dynamics of the Universe expansion. The transition between two different regimes happens when two components equally contribute to most of the total budget.

Before ending this preliminary section, it is worth spending few more words about the spatial curvature in the FLRW spacetime (1.1). From the first Friedmann equation (1.10), setting $k = 0$ and inverting, one obtains:

$$\rho_{\text{crit}}(t) = \frac{3H^2}{8\pi G}, \tag{1.15}$$

called the critical energy density, corresponding to the energy density one would measure in the case of a perfectly spatially flat Universe ($k = 0$). It is then useful to define the energy density parameter for the i-th fluid constituent:

$$\Omega_i(t) \equiv \frac{\rho_i(t)}{\rho_{\text{crit}}(t)}, \tag{1.16}$$

where the total energy density parameter $\Omega(t)$ is the sum of the energy density parameters of the single components. By definition, then, it would be $\Omega(t) = 1$ in case of a spatially flat FLRW spacetime with $k = 0$, with $\Omega(t) > 1$ and $\Omega(t) < 1$ for the close and open cases, respectively. From these considerations it follows that we can derive information about the geometry of the Universe by measuring its energy content. Furthermore, since k is a constant, we can determine its value today and the conclusion remains valid throughout all the history of the Universe.
From most recent observations we know the present density parameter of the main components of the cosmological fluid [3]:

$$\begin{aligned} \Omega_{c0}h^2 &= 0.120 \pm 0.001, \\ \Omega_{b0}h^2 &= 0.0224 \pm 0.0002, \\ \Omega_{\Lambda 0} &= 0.685 \pm 0.007, \end{aligned} \tag{1.17}$$

where h is defined such that the Hubble parameter today is $H_0 = 100h$ km s^{-1} Mpc^{-1}. The present energy contribution due to radiation is negligible. Since observationally [3] $H_0 = (67.36 \pm 0.54)$ km s^{-1} Mpc^{-1}, it can be verified that the components (1.17) almost add up to a total present energy budget $\Omega_0 \sim 1$, resulting with the experimental evidence that today we measure a density parameter compatible with a flat Universe. Because of this result, in the following discussion it is safe to set $k = 0$ inside the first Friedmann equation (1.10).
Starting from the experimental measurements (1.17) it is then possible to derive the values of the present energy densities as $\rho_{i0} = \Omega_{i0}\rho_{\text{crit},0}$. This allows to recover the results listed before for the epochs of equality by imposing $\rho_i(t_{\text{eq}}) = \rho_j(t_{\text{eq}})$ and using equation (1.14).

1.2 Inflation

The theory of inflation was first proposed by Guth in 1981 [4] as a way to solve the shortcomings of the Big Bang model. The idea behind it is that at very early time the Universe expands almost exponentially, driven by the vacuum energy density of a scalar field which takes the name of inflaton. Soon after the formulation of this theory, it was realized that inflation can provide also a mechanism to explain another fundamental aspect which a cosmological model necessarily have to deal with: the formation of large scale structures. We will see how the quantum fluctuations of the field driving inflation can be regarded as the seeds of the structures we observe today [1].

The first step is to understand what are the conditions needed in order to realize inflation. Starting from the second Friedmann equation (1.11) and imposing a positive acceleration $\ddot{a} > 0$, we find that the equation of state must satisfy:

$$w = \frac{p}{\rho} < -\frac{1}{3}. \tag{1.18}$$

This means that, in order to have inflation, it is necessary a mechanism which provides sufficiently negative pressure during that period. We have already seen an example of accelerated expansion provided by a cosmological constant. One would think an analogous assumption to be enough also in the inflationary case, but a fundamental requirement of the model is to be able to explain also how this accelerated phase ends and transitions to the standard Hot Big Bang. Before seeing how this is realized, we address briefly to the shortcomings that first led to the formulation of the inflationary hypothesis.

1.2.1 Shortcomings of the Hot Big Bang

We quickly review two of the historical inconsistencies, or shortcomings, of the standard Hot Big Bang model. They are usually called the horizon and the flatness problems, and we will see how a period of accelerated expansion in the early Universe, i.e. inflation, can solve both of them.

Number of e-foldings

Before presenting the details of the Hot Big Bang shortcomings, it has to be stressed that both the horizon and the flatness problem require not only a period of inflation, but actually a large enough amount of expansion. In both cases it is possible to explicitly compute the required amount, by asking these inconsistencies to be instead a natural consequence of the inflationary period. First of all, it is necessary to define a way in order to quantify the amount of inflation. This is done by defining the so called number of e-foldings:

$$N = \int_{t_i}^{t_f} H(t)dt = \ln\left(\frac{a_f}{a_i}\right), \tag{1.19}$$

which is essentially related to the ratio of the scale factors at the beginning (t_i) and at the end (t_f) of inflation. It is then possible to compute the minimum amount of e-foldings necessary in order

to solve the shortcomings of the Hot Big Bang. The requirement is that, both for the horizon and flatness problem, inflation must be able to start from generic initial conditions and evolve them such that they end up today in what we experimentally measure. Taking such an approach, the required number of e-foldings is found to be at least $N \sim 60 - 70$ [1], but usually inflationary models predict it to be much higher.

Horizon problem

In order to introduce the horizon problem it is necessary to understand how causality works in an expanding Universe. It is known that no signal can travel faster than light. It is the light signals what thus determine the causal connection between two points of the spacetime. It is useful, in particular, to compute what is the farthest distance from which we, or any other observer, can receive a signal. In this way one can find out what is the so called past causal cone of a given spacetime point. Assuming that a photon could have been emitted at the earliest at t=0, the particle horizon is defined as [1]:

$$R_H(t) = a(t) \int_0^t \frac{dt'}{a(t')}. \tag{1.20}$$

To evaluate this expression it is necessary to find the solution for $a(t)$ in an expanding Universe. Combining equations (1.10) and (1.14) one finds:

$$a(t) = a_* \left(\frac{t}{t_*} \right)^{\frac{2}{3(1+w)}}, \tag{1.21}$$

where t_* is an arbitrary reference time and $a_* = a(t_*)$. Substituting (1.21) inside (1.20) and performing the integration gives:

$$R_H(t) = \frac{3(1+w)t}{1+3w}, \tag{1.22}$$

and it follows that R_H is finite if and only if $w > -\frac{1}{3}$, i.e. $\ddot{a} < 0$. This suggests that the Standard Hot Big Bang model, which describes an always decelerating expansion, cannot explain the causal connection between points farther than the particle horizon distance. This contradicts the experimental evidence of an homogeneous CMB, as we will discuss in Chapter 4, since points separated by an angle of more than few degrees could not have been able to be in causal connection at the epoch of last scattering.
Actually the situation is even worse. The particle horizon is the distance from which an observer can receive a signal emitted any time after the Big Bang. But to have an homogeneous CMB a constant exchange of information between points is needed, so that they can share the same temperature. Such a causal connection is described by the Hubble radius:

$$R_c = \frac{1}{H(t)}, \tag{1.23}$$

and corresponds to the maximum distance between points that can exchange information over a Hubble time $\tau_H = H^{-1}$. What is interesting about Hubble radius is that the evolution of its comoving counterpart $r_c = (aH)^{-1}$ depends on the dynamics of the Universe. In fact:

$$\dot{r}_c = -\frac{\ddot{a}}{\dot{a}^2}. \tag{1.24}$$

It is then possible to define the comoving Hubble sphere, which contains all the points in causal contact, at a given instant, with the observer located at the centre. We see from equation (1.24) that, in the case of a decelerating Universe $\ddot{a} < 0$, such a sphere expands over time, such that the observer comes in causal contact with new, never seen before, points. It follows that we, as observers, are now in causal contact with points that could not have been able to communicate before the last scattering epoch, and thus we can explain the homogeneity of the CMB only by means of finely-tuned initial conditions. This is what is called the horizon problem.

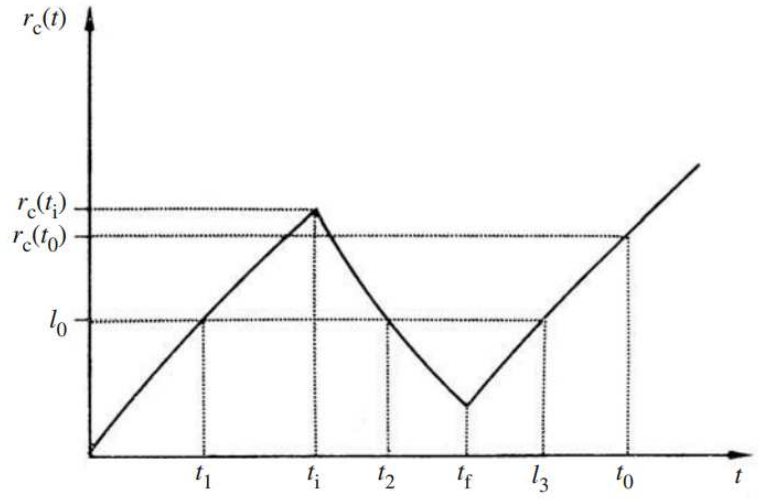

Figure 1.2: Evolution of the comoving Hubble radius r_c before $(0 < t < t_i)$, during $(t_i < t < t_f)$ and after $(t_f < t < t_0)$ inflation. Any fixed comoving distance l_0 remains instead constant throughout the evolution. The horizon problem is solved if $r_c(t_0) < r_c(t_i)$. Taken from [1].

Looking again at equation (1.24), it seems natural to try to solve this inconsistency by admitting an early time of accelerated expansion, during which the Hubble radius decreases and points in causal connection get pushed far apart. It is then sufficient to request the comoving Hubble radius today to be less than what it was before inflation:

$$r_c(t_0) < r_c(t_i), \tag{1.25}$$

and we obtain a past causal connection with all the points from which we can receive signals today. This situation is represented in Figure 1.2, in which it is plotted the evolution of the comoving Hubble radius r_c together with that of a comoving scale l_0.
Condition (1.25) can be made more explicit by combining the definition of comoving Hubble radius and equation (1.21) for the evolution of the scale factor. The latter assumes different values for different equation of states w, determined by the dominating fluid component during a certain period of expansion. Accounting, after the end of inflation, for a radiation dominated period followed by a matter dominated one, the condition (1.25) brings to the qualitative result:

$$N \gtrsim 60, \tag{1.26}$$

which is derived in details in [1].

Flatness problem

Another problem, similar to the horizon one, involves the measured spatial curvature of the spacetime. From our discussion in the previous section, we know that observationally the Universe is very close to be flat. This is due to the fact that today the density parameters of the various components add up almost exactly to a total $\Omega_0 \sim 1$, which corresponds to $k = 0$ inside the first Friedmann equation (1.10). The latter can be rewritten, exploiting (1.16), in the following way:

$$\Omega(t) - 1 = \frac{k}{(aH)^2} = kr_c^2, \tag{1.27}$$

where in the second equality we have applied the definition of the comoving Hubble radius. It is then possible to define the density parameter associated with the spatial curvature $\Omega_k(t) \equiv 1 - \Omega(t) = -kr_c^2$. From this definition, it follows that Ω_k vanishes in the spatially flat case and it is positive (negative) for a spatially open (close) spacetime. The latest measurements from the Planck

collaboration [3] constrain the value today to be $\Omega_{k0} = 0.001 \pm 0.002$. This value is compatible with a spatially flat Universe and it is way too small to be reasonable after the standard Hot Big Bang evolution. We can understand why by looking back to the first Friedmann equation (1.10) and analyzing the two terms on the right side: the first accounts for the energy contribution of the fluid components, whose energy density decreases at best as a^{-3} in the case of matter; the second term is, as already stressed, related to the spatial curvature and goes like a^{-2}. We can then conclude that, approaching early times, the curvature term, along with Ω_k, starts to become more and more negligible inside the Friedmann equation. The so called flatness problem lies in the fact that the measured value for Ω_{k0}, frequently expressed as $|\Omega_0 - 1| < 10^{-3}$, would require an initial condition, computed at Planck time t_P, of $|\Omega(t_P) - 1| \simeq |\Omega_0 - 1|10^{-60}$ [1], which is of course a finely-tuned assumption, in the same way as the initial homogeneity of the observable Universe was in the previous section.
The same conclusion can be deduced by taking the time derivative of the density parameter Ω_k:

$$\frac{d}{dt}\Omega_k = -k\frac{d}{dt}r_c^2 = 2kr_c\frac{\ddot{a}}{\dot{a}^2}. \tag{1.28}$$

This result tells us how the spatial curvature density parameter evolves when going back in time. It is straightforward to verify that, for a decelerating Universe $\ddot{a} < 0$, Ω_k approaches zero at early time, both in the case of positive or negative curvature. This leads to the same conclusion given before about the necessity for a fine-tuning at early times.

Once again the solution is to admit a period of inflation sufficiently long to satisfy, in analogy with (1.25), the inequality:

$$\frac{1 - \Omega_i^{-1}}{1 - \Omega_0^{-1}} \geq 1, \tag{1.29}$$

which corresponds to ask that the density parameter today Ω_0 must be closer to unity than the density parameter at the beginning of inflation Ω_i was. Furthermore, from the first Friedmann equation (1.10) it is possible to derive that the combination $(\Omega^{-1} - 1)\rho a^2 = \text{const}$ is actually conserved over time. Using this result inside (1.29), remembering (1.21) and splitting again the history of the Universe into the three periods of inflation ($w \simeq -1$), radiation domination ($w = \frac{1}{3}$) and matter domination ($w = 0$), it is possible [1] to recover the same amount of required inflation than the one computed by solving the horizon problem, which is approximately $N \gtrsim 60$. The evolution of the total energy density parameter, for both the cases of open and close Universe, is plotted in Figure 1.3.

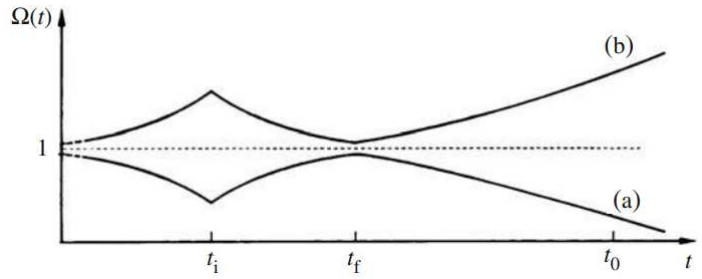

Figure 1.3: Evolution of the total density parameter before ($0 < t < t_i$), during ($t_i < t < t_f$) and after ($t_f < t < t_0$) inflation, for an open (a) and closed (b) Universe. The flatness problem is solved if $|\Omega(t_0) - 1| < |\Omega(t_i) - 1|$ Taken from [1].

1.2.2 Single scalar field inflation

We have seen that inflation should be capable of solving some of the shortcomings of the Big Bang model. It can actually achieve much more, namely it can explain the primordial origin of the

structures we observe today on cosmological scales. In order to see this we first need to understand how exactly it is possible to achieve such a period of early accelerated expansion.

The simplest way to obtain a period of inflation is to assume the presence, at very early time, of a scalar field, whose energy density drives the accelerated expansion. We call this scalar field the inflaton $\varphi(t, \vec{x})$. The starting point to study the single scalar field inflation is then the following action:

$$S = \int d^4x\sqrt{-g}\left(\frac{1}{16\pi G}R - \frac{1}{2}g^{\mu\nu}\nabla_\mu\varphi\nabla_\mu\varphi - V(\varphi)\right), \tag{1.30}$$

which basically corresponds to the action (1.6) where subdominant fields, other than the inflaton, have been neglected in $\mathcal{L}_m$. Apart from the Einstein-Hilbert sector, action (1.30) contains the most standard scalar field Lagrangian, with a canonical kinetic term and a self-interaction potential. In principle it is possible to construct different inflationary models by choosing various profiles for the potential, but later we will see that there are some underlying requirements which have to be fulfilled. An example is given in Figure 1.4.

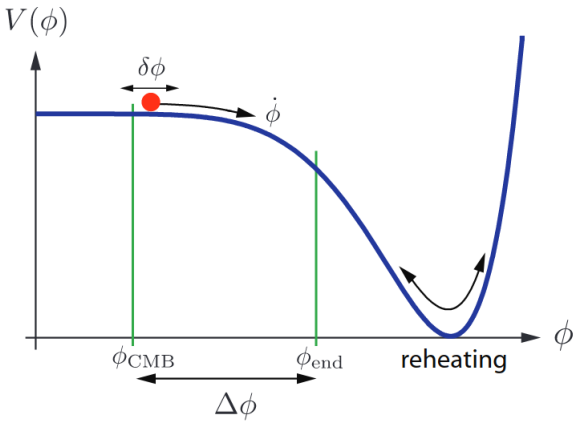

Figure 1.4: Example of slow-roll potential. During inflation the inflaton ϕ rolls down along the plateau of the potential. Taken from [6].

Varying the action (1.30) with respect to φ results in the Klein-Gordon equation for the inflaton:

$$\ddot{\varphi} + 3H\dot{\varphi} - \frac{\nabla^2\varphi}{a^2} = -\frac{\partial V}{\partial\varphi}. \tag{1.31}$$

Applying equation (1.8) for the inflaton part of the action (1.30) it is possible to compute the inflaton stress-energy tensor:

$$T_{\mu\nu} = \partial_\mu\varphi\partial_\nu\varphi - g_{\mu\nu}\left(\frac{1}{2}g^{\alpha\beta}\partial_\alpha\varphi\partial_\beta\varphi + V(\varphi)\right). \tag{1.32}$$

In order to proceed it is necessary to split the inflaton into its background value plus a small fluctuation around it [7]:

$$\varphi(t, \vec{x}) = \varphi_0(t) + \delta\varphi(t, \vec{x}), \tag{1.33}$$

with $\delta\varphi \ll \varphi_0$. The background value $\varphi_0(t)$ is allowed to be only a function of time due to the symmetries of the background FLRW spacetime. By definition $< \delta\varphi(t, \vec{x}) >= 0$, so that $< \varphi(t, \vec{x}) >= \varphi_0(t)$ is the inflaton vacuum expectation value. At first we will focus only on the background evolution, leaving the treatment of the fluctuations for later, when we will see how they can be regarded as the origin of the structures we observe today. A more detailed treatment of cosmological perturbations from a general point of view is given in Chapter 2.

Equation (1.32) evaluated for the background inflaton can be written in components:

$$\begin{aligned} T^0{}_0 &= -\rho_\varphi = -\left(\frac{1}{2}\dot{\varphi}^2 + V(\varphi)\right), \\ T^i{}_j &= p_\varphi \delta^i{}_j = \left(\frac{1}{2}\dot{\varphi}^2 - V(\varphi)\right)\delta^i{}_j, \end{aligned} \tag{1.34}$$

where from now on in this section we indicate the background inflaton just with φ. The first Friedmann equation (1.10) now reads:

$$H^2 = \frac{8\pi G}{3}\left(\frac{1}{2}\dot{\varphi}^2 + V(\varphi)\right), \tag{1.35}$$

where we have neglected the spatial curvature. This is possible because during inflation the curvature density parameter is pushed to zero, as can be deduced from equation (1.28).

We can finally verify how the inflaton stress-energy tensor can behave as the driving force of an inflationary period. Remembering the condition (1.18), and substituting (1.34), we get:

$$w_\varphi = \frac{p_\varphi}{\rho_\varphi} = \frac{\frac{1}{2}\dot{\varphi}^2 - V(\varphi)}{\frac{1}{2}\dot{\varphi}^2 + V(\varphi)} < -\frac{1}{3}, \tag{1.36}$$

which is the constraint that the equation of state of the inflaton must satisfy in order to achieve $\ddot{a} > 0$, i.e. accelerated expansion. In particular, making the assumption $V(\varphi) \gg \dot{\varphi}^2$, it follows $w_\varphi \simeq -1$, with the inflaton behaving almost like a cosmological constant. This is called slow-roll inflation, from the fact that the inflaton has little kinetic energy and slowly rolls down its potential. Again we stress that it can't be $w_\varphi = -1$ exactly because in such a case there would not be a way to end the period of accelerated expansion. In the slow-roll regime, considering the background value of the inflaton field, equations (1.31) and (1.35) can be approximated to:

$$\begin{aligned} 3H\dot{\varphi} &\simeq -V'(\varphi), \\ H^2 &\simeq \frac{8\pi G}{3}V(\varphi), \end{aligned} \tag{1.37}$$

where we have also assumed, reasonably, $\ddot{\varphi} \ll 3H\dot{\varphi}$ in the first equation. This condition ensures that the slow-roll requirement $\dot{\varphi}^2 \ll V(\varphi)$ is fulfilled for a long enough period.

We can now introduce some useful parameters, in order to better quantify the condition of slowly rolling we have just introduced. The first slow-roll parameter is defined in the following way:

$$\epsilon \equiv -\frac{\dot{H}}{H^2}. \tag{1.38}$$

Furthermore, we can write:

$$0 < \ddot{a} = \dot{a}H + a\dot{H} = aH^2(1-\epsilon), \tag{1.39}$$

from which it immediately follows the condition $\epsilon > 1$, necessary to obtain an accelerated expansion. However, inflation requires a more stringent constraint. Rearranging (1.38) in fact, with the help of the second of (1.37), results in $\epsilon \propto \frac{\dot{\varphi}^2}{V(\varphi)} \ll 1$. Exploiting also the first of (1.37) it is possible to obtain a constraint on the first order derivative of the potential:

$$\epsilon = \frac{1}{16\pi G}\left(\frac{V'}{V}\right)^2 \ll 1, \tag{1.40}$$

meaning that the inflaton potential has to be sufficiently flat. A second parameter may also be introduced, exploiting the assumption made on the inflaton acceleration $\ddot{\varphi} \ll 3H\dot{\varphi}$:

$$\eta \equiv -\frac{\ddot{\varphi}}{H\dot{\varphi}} \ll 1, \tag{1.41}$$

from which it follows a condition on the second derivative of the potential:

$$\eta_V \equiv \eta + \epsilon = \frac{1}{8\pi G}\frac{V''}{V}, \tag{1.42}$$

with $|\eta_V| \ll 1$. A whole hierarchy of slow-roll parameters may follow, of higher orders than the two just introduced, constraining higher order derivatives of the potential.

Therefore, the situation can be summed up as follows: during inflation the Universe undergoes an accelerating expansion, driven by the energy density (mostly potential) of a single scalar field, which slowly rolls along its potential. This goes on until the slow-roll conditions are satisfied (essentially until $\epsilon \sim 1$). At this point inflation ends and the inflaton energy density gets converted into all the particles needed to start the Hot Big Bang phase, via a process called reheating [7]. This situation is described in Figure 1.4, where a typical potential profile is represented. In particular, it can be observed that inflation occurs while the potential is sufficiently flat, so that the inflaton can slowly rolls on the plateau. Eventually, this flatness is spoilt and inflation ends: the inflaton starts oscillating around the true minimum of the potential and decays into other particles.

1.2.3 Primordial fluctuations from inflation

Now that we have seen the basic idea behind the background evolution in a single scalar field inflationary model, we can turn to a fundamental topic for the scope of this Thesis, which is the treatment of quantum fluctuations during inflation. In other words, we now consider the full $\varphi(t,\vec{x})$ as a quantum field, and see what is the evolution of the fluctuation $\delta\varphi(t,\vec{x})$ we have previously neglected. Because of this fluctuation, there will be local differences $\delta t(\vec{x})$ in the time when the inflation ends. This means that the local expansion history varies from one point to another and leads to the production of local inhomogeneities in the energy density $\delta\rho(\vec{x})$, which then evolve into the CMB temperature inhomogeneities $\delta T(\vec{x})$ we measure today. The aim of this section and the following one is to show how these perturbations generate from the primordial inflaton fluctuations $\delta\varphi(t,\vec{x})$.

We start by writing the perturbed part (linear in $\delta\varphi$) of the Klein-Gordon equation (1.31):

$$\ddot{\delta\varphi} + 3H\dot{\delta\varphi} - \frac{\nabla^2\delta\varphi}{a^2} = -V''(\varphi_0)\delta\varphi, \tag{1.43}$$

where we have used the following expansion around φ_0, up to first order, for the potential term:

$$V'(\varphi) = V'(\varphi_0) + V''(\varphi_0)\delta\varphi + O(\delta\varphi^2), \tag{1.44}$$

which in this way is explicitly written as a background term plus a first-order one. It is now convenient to perform the following rescaling:

$$\delta\varphi(t,\vec{x}) = \frac{\delta\tilde{\varphi}(t,\vec{x})}{a(t)}. \tag{1.45}$$

Using this, and passing to conformal time τ, equation (1.43) becomes:

$$\delta\tilde{\varphi}'' - \frac{a''}{a}\delta\tilde{\varphi} - \nabla^2\delta\tilde{\varphi} = -\frac{\partial^2 V}{\delta\varphi^2}(\varphi_0)\delta\tilde{\varphi}, \tag{1.46}$$

where the $'$ symbol denotes derivatives with respect to τ. In order to solve this equation it is useful to write it in Fourier space:

$$u''_{\vec{k}}(\tau) + \left[k^2 - \frac{a''}{a} + \frac{\partial^2 V}{\delta\varphi^2}(\varphi_0)\right]u_{\vec{k}}(\tau) = 0, \tag{1.47}$$

where $u_{\vec{k}}$ is defined as the Fourier transform of $\delta\tilde{\varphi}$:

$$\delta\tilde{\varphi}(\tau,\vec{x}) = \frac{1}{(2\pi)^3}\int d^3\vec{k}e^{i\vec{k}\vec{x}}u_{\vec{k}}(\tau). \tag{1.48}$$

We first consider the massless scalar field case, where $m_\varphi^2 = \frac{\partial^2 V}{\delta\varphi^2}(\varphi_0) = 0$. Equation (1.47), can be rewritten as:

$$u_{\vec{k}}'' + \omega_k^2 u_{\vec{k}} = 0, \tag{1.49}$$

so that each Fourier mode satisfies the harmonic oscillator equation of motion with frequency $\omega_k^2 = k^2 - \frac{a''}{a}$. Canonical quantization can thus be performed in analogy to the quantum harmonic oscillator [6]. We promote the perturbation $\delta\tilde{\varphi}(\tau, \vec{x})$ to a quantum operator $\delta\hat{\varphi}(\tau, \vec{x})$, such that the mode expansion can be written as:

$$\delta\hat{\varphi}(\tau, \vec{x}) = \frac{1}{(2\pi)^3}\int d^3\vec{k}\Big[u_k(\tau)\hat{a}_{\vec{k}}e^{i\vec{k}\vec{x}} + u_k^*(\tau)\hat{a}^\dagger_{-\vec{k}}e^{-i\vec{k}\vec{x}}\Big], \tag{1.50}$$

where $\hat{a}_{\vec{k}}$, $\hat{a}^\dagger_{\vec{k}}$ are, respectively, the annihilation and creation operators, i.e. $\hat{a}_{\vec{k}}|0\rangle = 0$ and $\langle 0|\hat{a}^\dagger_{\vec{k}} = 0$, where $|0\rangle$ is the vacuum state. The vector notation in u_k and u_k^* has been dropped since the frequency $\omega_k^2(\tau) = k^2 - \frac{a''}{a}$ depends only on the absolute value k and the same happens for the modes evolution [6]. Canonical quantization conditions read:

$$\begin{aligned}\big[\hat{a}_{\vec{k}}, \hat{a}_{\vec{k}'}\big] &= \big[\hat{a}^\dagger_{\vec{k}}, \hat{a}^\dagger_{\vec{k}'}\big] = 0,\\ \big[\hat{a}_{\vec{k}}, \hat{a}^\dagger_{\vec{k}'}\big] &= (2\pi)^3\delta^{(3)}(\vec{k} + \vec{k}'),\end{aligned} \tag{1.51}$$

and are ensured by the following normalization for the modes:

$$u_k'(\tau)u_k^*(\tau) - u_k(\tau)u_k^{*\prime}(\tau) = -i. \tag{1.52}$$

To fix the vacuum state $|0\rangle$, we exploit the information that at sufficiently early time ($\tau \to -\infty$) all modes of interest are still inside horizon $\left(k^2 \gg \frac{a''}{a}\right)$. Taking the sub-horizon limit in equation (1.49) results in $\omega_k = k$ and the solution at early times corresponds to a plane-wave in a flat spacetime:

$$\lim_{\tau\to-\infty} u_k(\tau) = \frac{1}{\sqrt{2k}}e^{-ik\tau}. \tag{1.53}$$

This initial condition for the mode functions defines what is called the Bunch-Davis vacuum.

We have already said that inflation needs some dynamics and the Universe cannot end up in a de-Sitter spacetime, since otherwise it would go on inflating forever. We thus want to solve equation (1.49) in a so called quasi de-Sitter spacetime, where, using the slow-roll parameter already introduced, $\epsilon = -\frac{\dot{H}}{H^2} \ll 1$. In this approximation it is possible to rewrite (1.49) in the form of a Bessel equation [8]:

$$u_k''(\tau) + \left[k^2 - \frac{\nu^2 - \frac{1}{4}}{\tau^2}\right]u_k(\tau) = 0, \tag{1.54}$$

where $\nu^2 = \frac{9}{4} + 3\epsilon$. Solutions of this equation can be found going into the sub-horizon or super-horizon limit. In the first case the result is basically proportional to the plane-wave in a flat spacetime (1.53) we have already discussed. Remembering the rescaling (1.45), it follows:

$$\delta\varphi_k = \frac{u_k}{a} = \frac{1}{a\sqrt{2k}}e^{-ik\tau}. \tag{1.55}$$

This tells us that, during inflation, modes inside the horizon oscillate while their amplitudes decreases as the inverse of the scale factor a. This behaviour goes on, for a given k, until the mode crosses the horizon when $k^2 \sim \frac{a''}{a}$. Without going too much into details, solving equation (1.54) in the super-horizon regime leads to the following result [8]:

$$|\delta\varphi_k| \simeq \frac{H}{\sqrt{2k^3}}\left(\frac{k}{aH}\right)^{\frac{3}{2}-\nu}, \tag{1.56}$$

with $\frac{3}{2} - \nu = -\epsilon$. This tiny scale dependence of order ϵ would be absent in the case of a pure de-Sitter spacetime. What the result (1.56) tells us is that, after crossing the horizon, an oscillating

k mode (with vanishing expectation value) freezes out with an almost constant amplitude, thus generating a classical perturbation of the field φ. A more in-depth treatment of equation (1.47) and its solutions, in the massless case, is performed in Chapter 5, dealing with primordial tensor perturbations.
In the more general case of a massive field the same result (1.56) holds, this time with $\frac{3}{2}-\nu = \eta_V - \epsilon$ [8], where $\eta_V = \frac{m_\varphi^2}{3H^2}$. The slow-roll condition $|\eta_V| \ll 1$ then requires φ to be very light (with respect to the Hubble parameter).

1.2.4 Primordial power spectrum

Now that we have found expression (1.56) for the primordial perturbations after the horizon-crossing, we are able to compute their power spectrum, which is the most important observable when dealing with a zero-mean random field such as $\delta\varphi$.

First, we introduce the concept of power spectrum in a more general way. Let $\delta(t,\vec{x})$ be the fluctuation around the background value of any field. The 2-point correlation function is then taken to be the following:

$$\xi(r) = \langle \delta(t,\vec{x}+\vec{r})\delta(t,\vec{x})\rangle, \tag{1.57}$$

where the angular brackets denote an ensamble average, ideally over different realizations of the Universe. Expression (1.57) basically represents the probability to have a configuration with the two fluctuations at a distance r one from another. The dependence on $r = |\vec{r}|$ is due to the homogeneity and isotropy of the background spacetime. Taking instead the 2-point correlation function of the Fourier transform, defined as in (1.48), we obtain:

$$\langle \delta(t,\vec{k})\delta(t,\vec{k}')\rangle = (2\pi)^3\delta^{(3)}(\vec{k}+\vec{k}')P(k), \tag{1.58}$$

where $P(k)$ is the power spectrum of the fluctuation δ. The dependence on $k = |\vec{k}|$ is due to isotropy, while homogeneity is encoded in the Dirac delta function. The power spectrum carries information about the mean power (quadratic in the fluctuation itself) of the fluctuation on a given scale. The just defined two quantities (1.57) and (1.58) are one the Fourier transform of the other, in fact:

$$\begin{aligned}\xi(r) = \langle \delta(t,\vec{x}+\vec{r})\delta(t,\vec{x})\rangle &= \frac{1}{(2\pi)^6}\int d^3\vec{k}\int d^3\vec{k}' e^{i\vec{k}(\vec{x}+\vec{r})}e^{i\vec{k}\vec{x}}\langle\delta(t,\vec{k})\delta(t,\vec{k}')\rangle \\ &= \frac{1}{(2\pi)^3}\int d^3\vec{k}e^{i\vec{k}\vec{r}}P(k).\end{aligned} \tag{1.59}$$

The variance of $\delta(t,\vec{x})$ can be regarded as the 2-point correlation function (1.57) computed for r=0:

$$\xi(0) = \langle\delta^2(t,\vec{x})\rangle = \frac{1}{(2\pi)^3}\int d^3\vec{k}P(k) = \int\frac{dk}{k}\mathcal{P}(k), \tag{1.60}$$

where the last equality defines the adimensional power spectrum:

$$\mathcal{P}(k) = \frac{k^3}{2\pi^2}P(k). \tag{1.61}$$

We can now compute the power spectrum of the primordial inflaton fluctuations. Taking the variance of expression (1.50) we get:

$$\begin{aligned}\langle|\delta\hat{\varphi}^2|\rangle &= \frac{1}{(2\pi)^6}\int d^3\vec{k}\int d^3\vec{k}'\langle 0|\big(u_k(\tau)\hat{a}_{\vec{k}}e^{i\vec{k}\vec{x}} + u_k^*(\tau)\hat{a}^\dagger_{-\vec{k}}e^{-i\vec{k}\vec{x}}\big) \\ &\times\big(u_{k'}(\tau)\hat{a}_{\vec{k}'}e^{i\vec{k}'\vec{x}} + u_{k'}^*(\tau)\hat{a}^\dagger_{-\vec{k}'}e^{-i\vec{k}'\vec{x}}\big)|0\rangle \\ &= \frac{1}{(2\pi)^6}\int d^3\vec{k}\int d^3\vec{k}' u_k u_{k'}^*\langle 0|\big[\hat{a}_{\vec{k}}\hat{a}^\dagger_{-\vec{k}'}\big]|0\rangle e^{-i(\vec{k}-\vec{k}')\vec{x}} \\ &= \frac{1}{(2\pi)^3}\int d^3\vec{k}|u_k|^2,\end{aligned} \tag{1.62}$$

where we have used the second of the (1.51) in the last passage. Remembering the rescaling (1.45), by comparing (1.62) with (1.60) we finally obtain the power spectrum of the inflaton perturbations:

$$P_{\delta\varphi}(k) = |\delta\varphi_k|^2 = \frac{H^2}{2k^3}\left(\frac{k}{aH}\right)^{3-2\nu}, \tag{1.63}$$

where in the second equality we have substituted the expression (1.56), since all modes of interest sooner or later leave the horizon during inflation. From (1.61), the adimensional power spectrum is then:

$$\mathcal{P}_{\delta\varphi}(k) = \left(\frac{H}{2\pi}\right)^2\left(\frac{k}{aH}\right)^{3-2\nu}. \tag{1.64}$$

In our previous treatment we have provided with the relation $3-2\nu = 2\eta_V - 2\epsilon$, when accounting for both the deviation from a pure de-Sitter spacetime and a light mass of the inflaton. Actually the situation is slightly more involved. Our simple model is based on the fact that, during inflation, the inflaton sources the vast majority of the energy content, such that we have also neglected any other possible contribution during that time. From Einstein equations it follows that the metric itself is sourced by the inflaton energy density, and in particular we conclude that it should be sensible to the inflaton fluctuations. To account for this, it is useful to introduce the so called comoving curvature perturbation [8]:

$$\mathcal{R} \equiv \hat{\psi} + H\frac{\delta\varphi}{\dot{\varphi}}, \tag{1.65}$$

where $\hat{\psi}$ is related to the spatial curvature perturbation of the metric, as we will see in the next Chapter. From the definition it is clear that $\mathcal{R}$ keeps trace of any perturbation in the inflaton field $\delta\varphi$, of which we have just computed the power spectrum (1.64). Actually, another quantity is usually considered when studying primordial scalar perturbations, whose relation with the inflaton perturbation is less manifest. It is called the curvature perturbation on uniform energy density hypersurfaces [8]:

$$\zeta \equiv -\hat{\psi} - H\frac{\delta\rho}{\dot{\rho}}, \tag{1.66}$$

where ρ designates generically the energy density of any component of the fluid which contributes to the total budget. The denomination of the two quantities (1.65) and (1.66) reflects the fact that both correspond to $\hat{\psi}$ in two different gauges: the comoving gauge and the spatially flat one, respectively. We will deepen more on this subject in the next Chapter, dealing with cosmological perturbation theory. In particular we will see that both $\mathcal{R}$ and ζ are gauge-invariant quantities by construction. Furthermore, we will show that their value remains constant on super-horizon scales, for the simplest models of inflation, making them great candidates to understand the evolution of primordial scalar perturbations of the inflaton field after they cross the horizon during inflation.
Figure 1.5 describes the constant behaviour of primordial perturbations outside the horizon. It is clear the advantage of using $\mathcal{R}$ instead of $\delta\varphi$: since $\dot{\mathcal{R}} \simeq 0$ on super-horizon scales, we can compute $\mathcal{R}$ at horizon-crossing, during inflation, and the same results holds also when the mode re-enters the horizon, well after inflation has ended. In practice, we can neglect the super-horizon evolution, since modes are nearly frozen during that time.
A more rigorous treatment of $\mathcal{R}$ and ζ is left for the next Chapter, but as of now we can at least derive the relation between these two quantities, since we are already in possession of all the instruments to do so. Assuming the slow-roll condition is satisfied during inflation, we know that the inflaton energy density can be identified with the potential, neglecting the kinetic one, i.e. $\rho_\varphi \simeq V(\varphi)$. From this we can write, on super-horizon scales:

$$\delta\rho_\varphi = V'(\varphi)\delta\varphi = -3H\dot{\varphi}\delta\varphi, \tag{1.67}$$

where in the last passage we have used the Klein-Gordon equation in the slow-roll regime (1.37). Substituting expressions (1.34) inside the continuity equation (1.12) we get:

$$\dot{\rho_\varphi} = -3H(\rho_\varphi + P_\varphi) = -3H\dot{\varphi}^2. \tag{1.68}$$

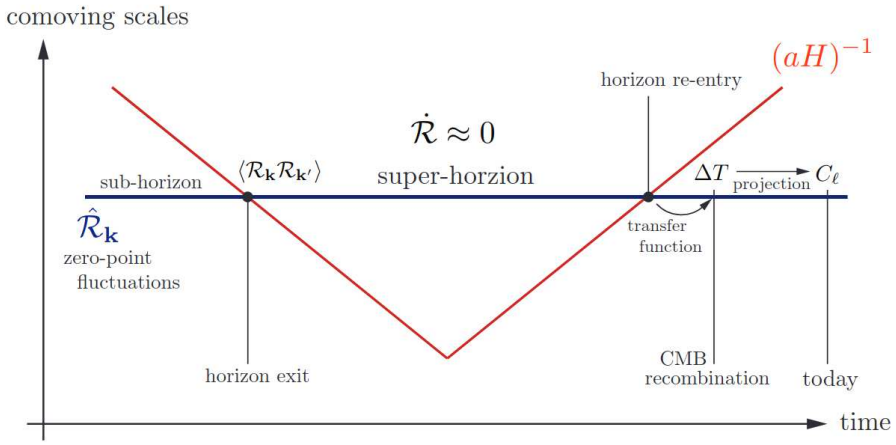

Figure 1.5: Time evolution of the primordial fluctuations during and after inflation. In particular, their value is frozen out of the horizon, ending up as the initial condition for the CMB temperature anisotropies. Taken from [6].

Putting together the previous results (1.67) and (1.68), and remembering the definitions of the gauge-invariant quantities (1.65) and (1.66), we finally obtain on super-horizon scales:

$$\zeta = -\hat{\psi} - H\frac{\delta\rho}{\dot{\rho}} = -\hat{\psi} - H\frac{-3H\dot{\varphi}\delta\varphi}{-3H\dot{\varphi}^2} = -\hat{\psi} - H\frac{\delta\varphi}{\dot{\varphi}} = -\mathcal{R}, \tag{1.69}$$

meaning that we can derive the power spectrum of the quantity ζ using the result already found for the inflaton perturbation (1.64). The convenience of using ζ resides in the fact that, as well as being gauge-invariant, it is also a conserved quantity outside the horizon, under the assumption of adiabaticity of the perturbations [8]. We will derive this result in the next Chapter.
All the arguments just provided lead to identify ζ as the right quantity to focus on in order to study the effects of primordial scalar perturbations on observables, such as the large scale structure (LSS) and the cosmic microwave background (CMB) radiation. Chapter 4 is devolved to the derivation of the CMB temperature anisotropies as a consequence of the primordial scalar perturbations re-entering the horizon.

Moving on, we can exploit the gauge invariance property to evaluate expression (1.66) for ζ in the spatially flat gauge, where $\hat{\psi} = 0$. Remembering the result (1.69), we conclude that:

$$\zeta\big|_{\hat{\psi}=0} = -H\frac{\delta\varphi}{\dot{\varphi}}, \tag{1.70}$$

such that expression (1.64) becomes:

$$\mathcal{P}_\zeta(k) = \left(\frac{H^2}{2\pi\dot{\varphi}}\right)^2 \left(\frac{k}{aH}\right)^{3-2\nu}, \tag{1.71}$$

which we refer to as the primordial power spectrum. This result can be rewritten using slow-roll equations (1.37) and the definition of ϵ (1.38). In fact, during slow-roll inflation, $\epsilon = -\frac{\dot{H}}{H^2} = \frac{4\pi G\dot{\varphi}^2}{H^2}$, and (1.71) becomes:

$$\mathcal{P}_\zeta(k) = \frac{H^2}{8\pi^2 M_P^2 \epsilon}\left(\frac{k}{aH}\right)^{3-2\nu}, \tag{1.72}$$

where we have introduced the reduced Planck mass $M_P = (8\pi G)^{-1/2}$. It is then possible to compute the so called scalar spectral index n_s, defined as:

$$n_s - 1 \equiv \frac{d\ln\mathcal{P}_\zeta}{d\ln k}, \tag{1.73}$$

which quantifies the scale dependence of the adimensional power spectrum of scalar primordial perturbations. To proceed with the computation, we evaluate equation (1.71) at horizon-crossing, exploiting the fact that ζ is constant on super-horizon scales:

$$\mathcal{P}_\zeta(k) = \left(\frac{H^2}{2\pi\dot{\varphi}}\right)^2_{k=aH}. \tag{1.74}$$

In this way at each scale corresponds a different instant in time, determined by solving the condition which identifies the horizon-crossing $k = aH$. Doing so the k dependence is made implicit inside time-dependent quantities in (1.74). From the horizon-crossing condition we have:

$$\ln k = \ln a + \ln H = N + \ln H, \tag{1.75}$$

where in the second equality we have applied the definition of e-foldings (1.19). From (1.75), neglecting the variation of H [9]:

$$d\ln k = H dt. \tag{1.76}$$

Combining equations (1.73), (1.74) and (1.76) it follows:

$$n_s - 1 = \frac{1}{\mathcal{P}_\zeta}\frac{d\mathcal{P}_\zeta}{Hdt} = \frac{\dot{\varphi}^2}{H^4}\frac{1}{H}2\frac{H^2}{\dot{\varphi}}\frac{2H\dot{H}\dot{\varphi} - \ddot{\varphi}H^2}{\dot{\varphi}^2} = 4\frac{\dot{H}}{H^2} - 2\frac{\ddot{\varphi}}{H\dot{\varphi}} = -4\epsilon + 2\eta = 2\eta_V - 6\epsilon, \tag{1.77}$$

where we have used expressions (1.38), (1.41), (1.42) for the slow-roll parameters. Equation (1.77) is the spectral index of the scalar perturbations, when one accounts both for the inflaton and the metric scalar perturbations.
From the latest result by Planck Collaboration [3], obtained considering CMB power spectra together with CMB lensing constraints, we know that experimentally $n_s = 0.9649 \pm 0.0042$. This is consistent with the prediction (1.77) of the single field slow-roll model of inflation. In particular, this value of the scalar spectral index tells us that primordial perturbations are nearly scale-invariant, with just a little red tilt (i.e. more power on smaller scales).

1.2.5 Primordial non-Gaussianity

Until now we have focused on the primordial scalar perturbations and their power spectrum, which is the equivalent of the 2-point correlation function in Fourier space. That would be enough for a complete statistical description only in the case perturbations were assumed to be Gaussian, which actually would be consistent with latest measurements by Planck collaboration [10].
Clear deviations from this Gaussian behaviour have yet to be observed, neither they have been excluded. Nevertheless, primordial non-Gaussianity (PNG) is expected to contain both exclusive and complementary information about the early Universe. For instance, a more precise measurements of the amount of PNG would be fundamental to help discriminating between different models of inflation [11].

Single field slow-roll models of inflation predict an amount of PNG of the order of the slow-roll parameters [12, 13]. Evidences of substantial deviations from Gaussianity would thus rule out this kind of models. Higher amounts of non-Gaussianity are predicted, typically, by models with non-canonical kinetic terms, multiple fields and/or higher order inflaton self-interactions [14].

The simplest way to probe PNG is to compute the 3-point correlation function of the primordial fluctuations. In fact, it vanishes in the Gaussian case and its value is directly proportional to the amount of non-Gaussianity predicted by a specific model. Statistical properties of the primordial perturbations would then be inherited by late time observables, affecting for example the expected CMB temperature anisotropies.
Simulated CMB maps are shown in Figure 1.6, for both temperature and polarization, in absence and presence of non-Gaussianities. At a first glance the effect of the non-Gaussianity is to move the power of the fluctuations to lower multipoles [15]. This is just an example but shows how PNG could have an influence on present observables, which in return would tell us fundamental information about the early Universe.

In this work we will treat at first CMB non-Gaussianities, which are vastly covered in the literature [16, 17], and then we will apply the same formalism to study non-Gaussianities in the cosmological gravitational wave background (CGWB). In particular we will focus on the primordial bispectrum and its imprint on the GW background, being it simple to treat yet containing much information on PNG already.

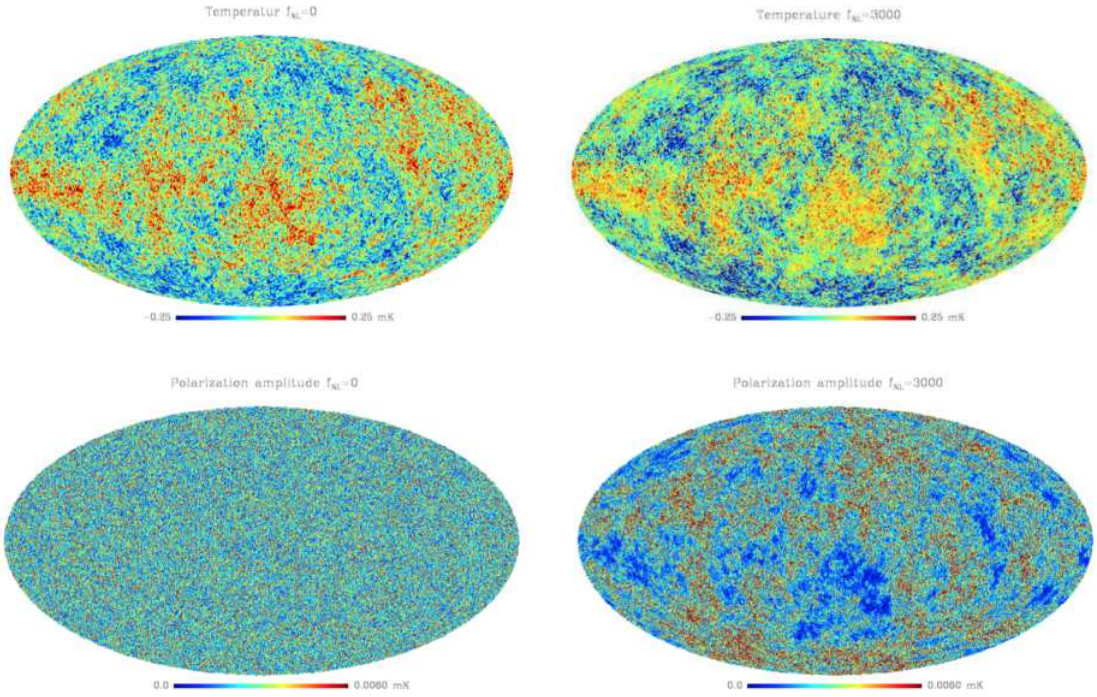

Figure 1.6: Simulated CMB maps for temperature (up) and polarization (down) anisotropies. In the left column Gaussian initial conditions are assumed, while the non-Gaussian case is represented in the right column. Taken from [15].

Chapter 2

Theory of Cosmological Perturbations

Dealing with the inflationary model in the previous Chapter, we have split the treatment of the inflaton evolution into its background and perturbations parts. This is a procedure which is frequently adopted in Cosmology, and in general it takes the name of Cosmological Perturbation Theory (CPT) [18, 19]. In this Chapter we focus on the linear perturbation theory, considering only first order fluctuations, and we introduce the so called gauge problem, seeing also what are the ways to solve it. Finally we formulate a more rigorous treatment of the curvature perturbation, already defined to study the evolution of scalar primordial fluctuations outside of the horizon.

2.1 Cosmological perturbations at first order

We have seen that the background metric (1.1) has a very simple expression. In reality the situation is quite different and the FLRW metric is not sufficient to describe aspects which deviate from the idea of an isotropic and homogeneous Universe, e.g. the formation of large scale structures. Nevertheless, we do not want to give up on the simplicity provided by such an idealized background spacetime. The idea behind CPT is thus to solve exactly a simpler version of a given problem, and then to include all the other complications as small perturbations around the background solution. In this way it is possible to treat, quite handily, also problems which would not have exact solutions. This is a general idea that can be applied to any tensor defined on the spacetime, so that each quantity can be split into a background value plus a fluctuation.
We have already followed this same procedure in equation (1.33), dealing with the inflaton and its fluctuations, where we have implicitly kept perturbative terms up to the first order. Now we can perform a more general and rigorous treatment, starting by defining the metric fluctuations.

2.1.1 The perturbed metric tensor

The full metric, describing the physical spacetime with all its features, can be expressed, in a similar fashion to equation (1.33), as:

$$g_{\mu\nu}(\tau, \vec{x}) = g^{(0)}_{\mu\nu}(\tau) + \delta g_{\mu\nu}(\tau, \vec{x}), \tag{2.1}$$

where $g^{(0)}_{\mu\nu}$ is the background FLRW metric (1.1) and $\delta g_{\mu\nu}$ represents the fluctuations around it. It is assumed $\delta g_{\mu\nu} \ll g^{(0)}_{\mu\nu}$, as requested by perturbation theory. A similar expression can be considered for any other tensor, keeping in mind that the background value must satisfy the same symmetry properties of the background spacetime, i.e. homogeneity and isotropy.
Usually, the metric fluctuation in equation (2.1) is further decomposed into scalar, vector and tensor components, according to their transformation behaviour under local rotations [20]. We can

thus expand the metric components, written in Cartesian coordinates, in the following way:

$$\begin{aligned} g_{00} &= -a^2(\tau)\left(1+2\sum_{r=1}^{+\infty}\frac{1}{r!}\phi^{(r)}\right), \\ g_{i0} &= g_{0i} = a^2(\tau)\sum_{r=1}^{+\infty}\frac{1}{r!}\hat{\omega}_i^{(r)}, \\ g_{ij} &= a^2(\tau)\left[\left(1-2\sum_{r=1}^{+\infty}\frac{1}{r!}\psi^{(r)}\right)\delta_{ij}+\sum_{r=1}^{+\infty}\frac{1}{r!}\hat{\chi}_{ij}^{(r)}\right], \end{aligned} \tag{2.2}$$

where $\hat{\chi}_{ij}(r)$ is a traceless tensor, i.e. $\hat{\chi}_i^{i(r)} = 0$. We have adopted the same notations used in [8]. All the newly introduced functions in (2.2), needed to parametrize the metric fluctuations, depend both on conformal time and space. Summations include all the different terms of the expansion, where r denotes the order of the perturbation.
A decomposition like (2.2) into scalar (S), vector (V) and tensor (T) component is often called an SVT decomposition [2]. In this way, a 3-vector can be split into the gradient of a scalar plus a divergenceless vector, so that:

$$\hat{\omega}_i^{(r)} = \partial_i\omega^{(r)} + \omega_i^{(r)}, \tag{2.3}$$

with $\partial^i\omega_i^{(r)} = 0$. In this context a divergenceless vector is also called transverse, since in Fourier space the condition becomes $k^i\omega_i^{(r)} = 0$, identifying the orthogonal direction with respect to the wavevector k^i. In a similar way a traceless tensor can be written as:

$$\hat{\chi}_{ij}^{(r)} = D_{ij}\chi^{(r)} + \partial_i\chi_j^{(r)} + \partial_j\chi_i^{(r)} + \chi_{ij}^{(r)}, \tag{2.4}$$

where, in analogy to the vector case, $\partial^i\chi_{ij}^{(r)} = 0$, thus designating $\chi_{ij}^{(r)}$ as transverse and traceless tensor degrees of freedom. Consistently with the fact that $\hat{\chi}_{ij}^{(r)}$ is a traceless tensor, we have introduced the traceless operator $D_{ij} \equiv \partial_i\partial_j - \frac{1}{3}\delta_{ij}\nabla^2$. As a result of the SVT decomposition, we check that the 10 degrees of freedom of the metric have been split up into 4 scalar, 4 divergenceless vector, and 2 divergenceless and traceless tensor degrees of freedom [18, 21]. Furthermore, the actual reason behind the SVT decomposition is that, at linear order, scalars, vectors and tensors evolve independently, meaning that it is possible to write evolution equations which do not mix different type of perturbations [8].

In writing decomposition (2.2) we have been generic and included perturbations up to any order. Neglecting all the terms of order higher than the first, the full perturbed line element has the following expression:

$$ds^2 = a^2(\tau)\Big[-(1+2\phi)d\tau^2 + 2\hat{\omega}_i d\tau dx^i + \big((1-2\psi)\delta_{ij} + \hat{\chi}_{ij}\big)dx^i dx^j\Big], \tag{2.5}$$

where from now on we omit the apex (1) since we will treat only the linear perturbation theory. Putting to zero all the perturbative terms in (2.5) the background FLRW metric is retrieved.
The next step is to use this linearly expanded metric inside Einstein equations (1.7) and to solve for the evolution of the different perturbations. In order to do so it is necessary to first compute the perturbed expressions for the affine connections and subsequently for the Ricci tensor and scalar. The results of these computations are reported in Appendix A.

2.1.2 The perturbed stress-energy tensor

The other necessary ingredient to write down Einstein equations is the stress-energy tensor, which accounts for the energy content of the Universe and thus acts as a source for the gravitational field. Dealing with the background evolution, in the previous Chapter we have written down expression (1.9) as the stress-energy tensor of a perfect fluid. This reflects, as we have already pointed out, the homogeneity and isotropy properties of the FLRW background spacetime. More in general, we

now want to account for fluctuations around the background value, so that the expression for the full perturbed stress-energy tensor becomes:

$$T_{\mu\nu} = T^{(0)}_{\mu\nu} + \delta T_{\mu\nu} = \rho u_\mu u_\nu + p h_{\mu\nu} + \Pi_{\mu\nu}, \tag{2.6}$$

where we have defined the projector $h_{\mu\nu} \equiv u_\mu u_\nu + g_{\mu\nu}$ orthogonal to the 4-velocity u^μ, i.e. $h_{\mu\nu}u^\mu = 0$. The perturbative term $\Pi_{\mu\nu}$ accounts for the presence of anisotropic stresses and thus has a vanishing background value. All the quantities in expression (2.6) can then be expanded up to any order, in the same way as we have done with the metric in (2.2):

- The 4-velocity can be expressed as:

$$u^\mu = \frac{1}{a}\left(\delta^\mu_{\ 0} + \sum_{r=1}^{\infty} v^{\mu(r)}(\tau, \vec{x})\right), \tag{2.7}$$

  where the first order perturbation is $v^\mu = (v^0, \hat{v}^i)$, with $\hat{v}^i$ the peculiar velocity of the fluid. Expanding the normalization condition $g_{\mu\nu}u^\mu u^\nu = -1$ at first order, it follows for the 0-component of the linear velocity perturbation:

$$v^0 = -\phi. \tag{2.8}$$

- For the energy density we write:

$$\rho(\tau, \vec{x}) = \rho^{(0)}(\tau) + \sum_{r=1}^{\infty} \delta\rho^{(r)}(\tau, \vec{x}), \tag{2.9}$$

  where the background value $\rho^{(0)}$ cannot depend on the spatial position, due to the symmetries of the underlying spacetime. The lowest order spatial dependence is then carried by the linear perturbation.

- Likewise, the isotropic pressure is:

$$p(\tau, \vec{x}) = p^{(0)}(\tau) + \sum_{r=1}^{\infty} \delta p^{(r)}(\tau, \vec{x}). \tag{2.10}$$

  Writing $p = p(\rho, S)$, with S being the entropy, its perturbation can also be split in the following way:

$$\delta p = \left(\frac{\partial p}{\partial \rho}\right)_S \delta\rho + \left(\frac{\partial p}{\partial S}\right)_\rho \delta S, \tag{2.11}$$

  where the second term accounts for non-adiabatic ($\delta S \neq 0$) contributions, while the first defines the adiabatic speed of sound $c_s^2 = \left(\frac{\partial p}{\partial \rho}\right)_S$, computed at constant entropy S.

The anisotropic stress $\Pi_{\mu\nu}$ has only non-vanishing spatial components $\hat{\Pi}_{ij}$, that can be further SVT decomposed:

$$\hat{\Pi}_{ij} = D_{ij}\Pi + \partial_i \Pi_j + \partial_j \Pi_i + \Pi_{ij}. \tag{2.12}$$

It is considered to be traceless, $\hat{\Pi}^i_{\ i}$, since its trace can be reabsorbed into the definition of the isotropic pressure p. In analogy to the spatial components of the metric, the tensor degrees of freedom Π_{ij} are defined as transverse $\partial^i \Pi_{ij} = 0$. We will consider only the linear part of perturbation (2.12), but in principle it includes terms up to any order.

Substituting the perturbative expansions back into equation (2.6), and keeping terms up to first order, it is possible to recover an explicit expression for the linear perturbation of the stress-energy tensor. This, combined with the geometric part from the previous section, allows to write down the perturbed linear order Einstein equations.

2.1.3 Perturbed Einstein equations

The evolution of metric perturbations in (2.5) is determined by the linearized Einstein equations. Expanding equation (1.7) up to first order and subtracting from it the background part we are left with just the linear components:

$$\delta G^{\mu}_{\ \nu} = 8\pi G \delta T^{\mu}_{\ \nu}, \tag{2.13}$$

where we have raised one index with respect to (1.7) since it makes the computations more feasible. We have already described the necessary ingredients to write down the components of this equation. General expressions for $\delta G^{\mu}_{\ \nu}$ are reported in Appendix A. For what concerns the stress-energy tensor, we have:

$$\delta T^{\mu}_{\ \nu} = \delta\left(g^{\mu\nu} T_{\mu\nu}\right) = \delta g^{\mu\nu} T_{\mu\nu} + g^{\mu\nu} \delta T_{\mu\nu}, \tag{2.14}$$

where we need to neglect terms of order higher than the first.
Remember now that, at linear order, Einstein equations only couple perturbations of the same nature, being them scalar, vector or tensor degrees of freedom. Because of this, it is possible to consider only a single type of perturbations at a time inside the linearized Einstein equations (2.13).
For the scope of this work we are mostly interested in the scalar metric perturbations and thus provide here with their evolution equations, which can be derived neglecting vector and tensor degrees of freedom.
The (0-0)-component of (2.13) gives:

$$\frac{1}{a^2}\left[3\mathcal{H}\left(\hat{\psi}' + \mathcal{H}\phi\right) - \nabla^2\left(\hat{\psi} + \mathcal{H}\sigma\right)\right] = -4\pi G \delta\rho, \tag{2.15}$$

where we have defined the curvature perturbation:

$$\hat{\psi} \equiv \psi + \frac{1}{6}\nabla^2\chi, \tag{2.16}$$

and the shear perturbation:

$$\sigma \equiv \frac{1}{2}\chi' - \omega. \tag{2.17}$$

From the (0-i)-component of linearized Einstein equations we get:

$$\frac{1}{a^2}\left(\hat{\psi}' + \mathcal{H}\phi\right) = -4\pi G(\rho_0 + p_0)(v + \omega), \tag{2.18}$$

where we have exploited the SVT decomposition of the vector components and neglected the divergenceless parts, since they do not affect the evolution of scalars. We have also introduced a simplified notation to designate the background zero-order values of the energy density ρ_0 and isotropic pressure p_0. Both equations (2.15) and (2.18) are not dynamical and can be regarded, respectively, as energy and momentum constraints. Actual evolution equations follow instead from the (i-j)-component of (2.13). Consistently with the previous treatment of the spatial metric perturbations, the trace and traceless parts provide with two independent equations. These are, respectively:

$$\frac{1}{a^2}\left[\hat{\psi}'' + 2\mathcal{H}\hat{\psi}' + \mathcal{H}\phi' + \left(2\mathcal{H}' + \mathcal{H}^2\right)\phi\right] = 4\pi G\left(\delta p + \frac{2}{3}\nabla^2\Pi\right), \tag{2.19}$$

and:

$$\frac{1}{a^2}\left(\sigma' + 2\mathcal{H}\sigma + \hat{\psi} - \phi\right) = 8\pi G\Pi, \tag{2.20}$$

where again we have SVT decomposed the tensor perturbations and considered only their scalar degrees of freedom. Equations (2.19) and (2.20) contains second-order time derivatives and thus describe the evolution of scalar perturbations.

In order to derive the physical implications of the equations we have just computed, it is first necessary to deal with an issue we have not considered up to now. Because of the symmetries of General Relativity and of the way perturbations are defined in Cosmology, in fact, our results, written in the way we have, actually contain redundant and nonphysical degrees of freedom we need to take care of. This will be the subject of the next section.

2.2 The gauge problem

It is time to address to a subtle but intrinsic ambiguity that arises when dealing with CPT. This is known as gauge problem, and refers to the fact that the perturbations for which we derived expressions in the previous sections are not uniquely defined [20].
Consider for example a generic tensor quantity T, which takes value on the full perturbed spacetime: its perturbation δT is then defined as the difference between the perturbed value T computed in a certain point of the physical spacetime and the zero-order value T_0 evaluated in the corresponding point of the background. This correspondence between points of the physical and of the background spacetime is realized by a map. The problem lies in the freedom of choosing such a map, so that different choices for the corresponding points are possible. This ultimately leads to different values for the perturbations, one for each possible choice of the map.
The change of map is achieved through a gauge transformation, in such a way that each map describes a different gauge choice. A gauge transformation, in practice, is realized by a change of coordinates in the physical spacetime. General Relativity is a theory invariant under generic diffeomorphisms, but the value of a perturbation δT does transform after a change of coordinates, and thus it depends on the gauge.
It is quite useful to think each coordinate system as a particular way of slicing the full spacetime into constant time τ hypersurfaces. In this way a gauge can be identified by the properties we want the spatial hypersurfaces to have. The freedom in choosing a particular slicing, i.e. gauge, can introduce non-physical contributions to the perturbations, which have to be identified and distinguished from the real physical values.

In order to illustrate better these ideas, let us show a simple concrete example [2]. Starting from the FLRW flat metric (1.1), we make the following change of spatial coordinates:

$$\tilde{x}^i = x^i + \xi^i(\tau, \vec{x}), \tag{2.21}$$

where ξ^i is assumed to be a small perturbation. The inverse change of coordinates is then, up to first order in ξ^i, $x^i = \tilde{x}^i - \xi^i(\tau, \tilde{\vec{x}})$. Space and time intervals transform with the Jacobian of the transformation law:

$$dx^\mu = \frac{\partial x^\mu}{\partial \tilde{x}^\nu} d\tilde{x}^\nu. \tag{2.22}$$

For the transformation (2.21) we are considering, the time component is left invariant while for the spatial ones we get:

$$dx^i = \frac{\partial x^i}{\partial \tilde{x}^\nu} d\tilde{x}^\nu = d\tilde{x}^i - \xi^{i\prime} d\tau - \partial_j \xi^i d\tilde{x}^j, \tag{2.23}$$

so that the FLRW metric in the new coordinates (2.21), at linear order in the perturbation ξ, has the following expression:

$$ds^2 = a^2\big[- d\tau^2 - 2\xi_i' d\tau d\tilde{x}^i + (\delta_{ij} + \partial_i \xi_j + \partial_j \xi_i) d\tilde{x}^i d\tilde{x}^j \big]. \tag{2.24}$$

Comparing this result with the generic expression (2.5), we see that we have apparently introduced metric perturbations, even if we know that FLRW spacetime is homogenous and isotropic. Indeed this is just an effect of the coordinate system in which we have decided to rewrite the metric, and the perturbations which have come up can be regarded as unphysical gauge artifacts.
In a similar but opposite way, by making a suitable change of coordinates it is also possible to instead remove real perturbations. A particular gauge choice can thus hide the true physical properties of our system, so that we need an unambiguous way to describe it uniquely.

2.2.1 Gauge transformations

Consider now the gauge transformation induced by a generic infinitesimal change of coordinates:

$$\tilde{x}^\mu = x^\mu - \xi^\mu(x), \tag{2.25}$$

where the presence of the minus sign is such that the results we find agree with the sign convention usually adopted in the literature. It is necessary to understand how a given quantity transforms as a consequence of (2.25). In order to do so we exploit the transformation properties of tensors. We know in fact that any given tensor T transforms with the Jacobian (and its inverse) of the change of coordinates, namely:

$$\tilde{T}^{\mu}_{\ \nu}(\tilde{x}) = \frac{\partial \tilde{x}^{\mu}}{\partial x^{\rho}} \frac{\partial x^{\sigma}}{\partial \tilde{x}^{\nu}} T^{\rho}_{\ \sigma}(x), \tag{2.26}$$

where the generalization to a different combination of indices is straightforward. We want to compute the consequences on T of a gauge transformation along the direction ξ. We thus combine equations (2.25) and (2.26) to obtain the relation between the new and old tensors, both evaluated at the same coordinate point:

$$\tilde{T}^{\mu}_{\ \nu} = (\delta^{\mu}_{\ \rho} - \partial_{\rho}\xi^{\mu})(\delta^{\sigma}_{\ \nu} + \partial_{\nu}\xi^{\sigma}) T^{\rho}_{\ \sigma}(x+\xi) = T^{\mu}_{\ \nu} - \partial_{\rho}\xi^{\mu} T^{\rho}_{\ \nu} + \partial_{\nu}\xi^{\rho} T^{\mu}_{\ \rho} + \xi^{\rho}\partial_{\rho} T^{\mu}_{\ \nu}, \tag{2.27}$$

where we have kept the linear order in ξ. A similar transformation law is valid for tensors of any order. All the first order terms in (2.27) can be grouped together into what is known as the Lie derivative of the tensor T along the direction ξ:

$$\mathcal{L}_{\xi} T^{\mu}_{\ \nu} = \partial_{\rho} T^{\mu}_{\ \nu} \xi^{\rho} - T^{\rho}_{\ \nu} \partial_{\rho} \xi^{\mu} + T^{\mu}_{\ \rho} \partial_{\nu} \xi^{\rho}, \tag{2.28}$$

where all the terms are evaluated at the same coordinate point. This reflects the independence on the coordinate system of the Lie derivative. Furthermore, the fact that all terms in (2.28) are already linear in the perturbations let us consider only the unperturbed part of a tensor T_0 inside the Lie derivative, when dealing with first order CPT.

It is now possible to derive what is the behaviour under a gauge transformation of all the metric and stress-energy tensor perturbations we have previously defined. In doing so it is useful to SVT decompose the infinitesimal displacement ξ^{μ} in the following way:

$$\begin{aligned} \xi^0 &= \alpha, \\ \xi^i &= \partial^i \beta + d^i, \end{aligned} \tag{2.29}$$

with $\partial_i d^i = 0$, so that the 4 degrees of freedom are split up between two scalars and one divergenceless vector.
Applying the transformation law (2.27) on the perturbations of the linearly perturbed metric (2.5), we can find how they behave under the infinitesimal change of coordinates (2.25):

$$\tilde{g}_{\mu\nu} = g_{\mu\nu} + \mathcal{L}_{\xi} g^{(0)}_{\mu\nu}. \tag{2.30}$$

As an example, we show the explicit computation for the perturbation ϕ of the $g_{00} = -a^2(1+2\phi)$ component:

$$-a^2(1+2\tilde{\phi}) = -a^2(1+2\phi) - 2aa'\alpha - 2a^2\alpha', \tag{2.31}$$

where we have applied equation (2.30) and used the decomposition (2.29) for the infinitesimal displacement ξ. Solving for $\tilde{\phi}$ we find the following gauge transformation law:

$$\tilde{\phi} = \phi + \mathcal{H}\alpha + \alpha', \tag{2.32}$$

with $\mathcal{H} \equiv \frac{a'}{a}$ defined in analogy with the Hubble parameter but using instead the conformal time τ. In a similar way it is possible to obtain an analogous expression for each of the perturbations in the metric (2.5). We just write down the results of the computations:

$$\begin{aligned} \tilde{\psi} &= \psi - \mathcal{H}\alpha - \frac{1}{3}\nabla^2\beta, \\ \tilde{\hat{\omega}}_i &= \hat{\omega}_i + \partial_i\alpha + \partial_i\beta' + d_i', \\ \tilde{\hat{\chi}}_{ij} &= \hat{\chi}_{ij} + 2D_{ij}\beta + \partial_i d_j + \partial_j d_i. \end{aligned} \tag{2.33}$$

Applying an SVT decomposition it is also possible to separate the scalar, vector and tensor degrees of freedom defined in (2.3) and (2.4):

$$\begin{aligned}\tilde{\omega} &= \omega - \alpha + \beta', \\ \tilde{\omega}_i &= \omega_i + d_i', \\ \tilde{\chi} &= \chi + 2\beta, \\ \tilde{\chi}_i &= \chi_i + d^i, \\ \tilde{\chi}_{ij} &= \chi_{ij},\end{aligned} \tag{2.34}$$

from which it is clear that (transverse and traceless) tensor components are gauge-invariant, at least at linear order in the perturbations.
Similarly, one can compute gauge transformations for the stress-energy tensor perturbations. The procedure is totally analogous to what we have done in the metric perturbations case. For the energy density it gives:

$$\tilde{\delta\rho} = \delta\rho + \rho_0'\alpha. \tag{2.35}$$

Considering instead the 4-velocity, and separating the temporal and spatial components, the gauge transformations are:

$$\begin{aligned}\tilde{v}^0 &= v^0 - \mathcal{H}\alpha - \alpha', \\ \tilde{\hat{v}}^i &= \hat{v}^i + \partial^i\beta + d^{i\prime}.\end{aligned} \tag{2.36}$$

The SVT decomposition allows to write $\hat{v}^i = \partial^i v + v^i$, so that it follows:

$$\begin{aligned}\tilde{v} &= v + \beta, \\ \tilde{v}^i &= v^i + d^{i\prime}.\end{aligned} \tag{2.37}$$

2.2.2 Gauge freedom and gauge choice

After having discussed the gauge problem, it is now clear how the freedom to choose one gauge or another can truly be a source of ambiguity, both during computations and in the interpretation of the final results. Therefore, a clever and powerful way out of this issue may actually be to come up with gauge-invariant quantities, exploiting the gauge transformations we have just computed and combining them in meaningful ways. We will do so in the next section.

An alternative would be to choose a given gauge and work out all the calculations in that gauge. From the discussion of the previous section we know that a gauge transformation is determined by the infinitesimal displacement ξ. The freedom in the choice of gauge corresponds to the freedom of choosing the components of ξ. In practice this can be used to arbitrarily fix the values of four degrees of freedom amongst the perturbation components. Doing so can be referred to as performing a gauge choice. Many different choices are possible and in principle there is no reason to prefer a gauge over another. Usually it is convenient to choose a gauge where equations of interest have a simpler form, solve the problem in that gauge and then exploit gauge transformations to generalize the result to any gauge. Even if this may simplify the actual computations, one should always be careful to the presence of possible gauge artifacts [5].

2.2.3 Gauge-invariant quantities

One way to deal with the gauge problem is to define specific quantities that have the useful property to be invariant under an arbitrary gauge transformation. One of the first attempt to implement this idea is due to Bardeen (1980), who introduced what now are called the Bardeen's potentials [21]:

$$\begin{aligned}\Phi &= \phi - \sigma' - \mathcal{H}\sigma, \\ \Psi &= \hat{\psi} + \mathcal{H}\sigma.\end{aligned} \tag{2.38}$$

It is straightforward to check that Φ and Ψ are indeed gauge-invariant quantities. They are called potentials since they appear inside a Poisson-like equation, derived from linearized Einstein equations for scalar perturbations, playing a role similar to the gravitational potential. This result is explicitly derived in the next section.

2.2.4 Linearized Einstein equations in the Poisson gauge

We can now exploit the gauge freedom to actually gain some physical insight from the components of linearized Einstein equations derived in section 2.1.3. These equations assume simpler expressions in the Poisson gauge, which is defined imposing the following conditions [8]:

$$\omega = 0, \quad \chi = 0, \quad \chi_i = 0. \tag{2.39}$$

In this way vector and tensor perturbations of the metric contain, respectively, only true (divergenceless) vector and true (divergenceless and traceless) tensor degrees of freedom. Notice that this corresponds to fix 4 degrees of freedom, as we have pointed out previously. It is then possible to focus on each type of perturbation at a time.

From conditions (2.39) it immediately follows that in the Poisson gauge the shear perturbation vanishes $\sigma = 0$, in such a way that also $\hat{\psi} = \psi$. Furthermore, the expressions of Bardeen's potentials (2.38) in this gauge reduce to:

$$\Phi = \phi, \quad \Psi = \psi. \tag{2.40}$$

Equation (2.20) thus simplifies and, in absence of anisotropic stresses $\Pi = 0$, which is actually the case for many ΛCDM models, we get:

$$\Phi - \Psi = 0. \tag{2.41}$$

This is a remarkable and simple result, which relates the two scalar potentials. Furthermore, it is written in terms of gauge-invariant quantity, so that it holds also for any other gauge choice, even if we explicitly derived it in the Poisson one.

Another interesting result can be obtained by combining equations (2.15) and (2.18), such that, in the Poisson gauge, it is possible to write:

$$-\nabla^2\Phi = -4\pi G a^2 \big[\delta\rho - 3\mathcal{H}(\rho_0 + p_0)(v + \omega)\big]. \tag{2.42}$$

Keeping the first order in perturbations, we can substitute the background continuity equation (1.12) and we obtain:

$$\nabla^2\Phi = 4\pi G a^2 \big[\delta\rho + \rho_0'(v + \omega)\big], \tag{2.43}$$

which is yet another gauge-invariant equation, since it can be verified that the combination on the right side $\delta\rho + \rho_0'(v+\omega)$ is indeed a gauge-invariant quantity. It corresponds to the energy density in the comoving gauge, defined by imposing the peculiar velocity of the fluid to vanish. Equation (2.43) thus resembles a Poisson-like equation where the Bardeen's potential plays the role of the Newtonian one, thus justifying the name given to the gauge-invariant quantity. Because of this result, the Poisson gauge also takes the name of Newtonian gauge when only scalar perturbations are considered.

2.3 Curvature perturbation

With the insight we have learnt on cosmological perturbations theory, we are now able, using the formalism adopted for the treatment of gauge-invariant quantities, to revisit and deepen the two different definitions of curvature perturbation, (1.65) and (1.66), first introduced in Chapter 1 dealing with primordial scalar perturbations.

2.3.1 Comoving curvature perturbation

For what concerns the comoving curvature perturbation, the starting point is to consider the intrinsic spatial curvature on constant time hypersurfaces [8]:

$${}^{(3)}R = \frac{4}{a^2}\nabla^2\hat{\psi}, \tag{2.44}$$

where we remember the definition (2.16). Notice that the quantity (2.44) is clearly not invariant under a gauge transformation, since $\hat{\psi}$ transforms in the following way:

$$\tilde{\hat{\psi}} = \hat{\psi} - \mathcal{H}\alpha, \tag{2.45}$$

where we have applied results (2.33) and (2.34). In particular, it is sensible only to a shift α of the time coordinate, responsible for a change of the slicing of spacetime.
Consider then the comoving gauge, where constant time hypersurfaces are orthogonal to the world-lines of comoving observers. Such observers do not measure any flux of energy, i.e. $T_{0i} = 0$, since they experience an isotropic expansion [18, 21]. During inflation this corresponds to measure a vanishing inflaton perturbation, $\delta\varphi_{\text{com}} = 0$. Applying the transformation law (2.27) to the full inflaton field (1.33), we find that:

$$\tilde{\delta\varphi} = \delta\varphi + \varphi_0'\alpha, \tag{2.46}$$

where $\delta\varphi$ has been regarded as the linear perturbations around the zero-order value φ_0. We have found that the inflaton perturbation transforms in a similar way to $\hat{\psi}$. This suggests that it should be possible to combine the two in such a way to obtain a gauge-invariant quantity.
Therefore, we can ask ourselves what is the required time displacement, $\xi^0 = \alpha$, necessary to pass from a generic gauge to the comoving one. The condition to impose is $\delta\varphi_{\text{com}} = \delta\varphi + \varphi_0'\alpha = 0$, from which:

$$\alpha = -\frac{\delta\varphi}{\varphi_0'}. \tag{2.47}$$

We can substitute this shift inside the transformation law (2.45) to recover the expression for $\hat{\psi}$ in the comoving gauge:

$$\hat{\psi}_{\text{com}} = \hat{\psi} + \mathcal{H}\frac{\delta\varphi}{\varphi_0'} = \hat{\psi} + H\frac{\delta\varphi}{\dot{\varphi}_0} \equiv \mathcal{R}, \tag{2.48}$$

which corresponds to the definition (1.65). It can be checked that $\mathcal{R}$ is, by construction, a gauge-invariant quantity and it goes by the name of comoving curvature perturbation. Indeed, in the comoving gauge $\delta\varphi_{\text{com}} = 0$, so that $\mathcal{R}_{\text{com}} = \hat{\psi}$.
We have already associated this quantity to the primordial scalar perturbations, and exploited the fact that, assuming a spatially flat gauge with $\hat{\psi} = 0$, $\mathcal{R}$ depends only on the inflaton perturbation and can thus be computed exploiting the results obtained for the scalar field slow-roll dynamics.
Another interesting property, fundamental to treat the evolution of primordial perturbations outside the horizon, is that on large scale the comoving curvature perturbation remains practically constant, under certain reasonable assumptions. In order to show this, we need to consider the other gauge-invariant quantity we have introduced during the treatment of primordial perturbations.

2.3.2 Curvature perturbation on uniform energy density hypersurfaces

Instead of the comoving one, we consider now a different way of performing the slicing, identifying constant time hypersurfaces charachterized by constant energy density, i.e. $\delta\rho = 0$. The time displacement to reach such a gauge would be, from equation (2.35):

$$\alpha = -\frac{\delta\rho}{\rho_0}. \tag{2.49}$$

Proceeding as in the previous case, the curvature perturbation $\hat{\psi}$ in the uniform energy density gauge is obtained via the following transformation:

$$\hat{\psi}\big|_{\delta\rho=0} = \hat{\psi} + \mathcal{H}\frac{\delta\rho}{\rho_0'} = \hat{\psi} + H\frac{\delta\rho}{\dot{\rho}_0} \equiv -\zeta, \tag{2.50}$$

which corresponds to (1.66) and is once again a gauge-invariant quantity, called curvature perturbation on uniform energy density hypersurfaces, since $\zeta\big|_{\delta\rho=0} = -\hat{\psi}$.

Super-horizon evolution

We have already shown that, during slow-roll inflation, the two gauge-invariant quantities are related by $\zeta = -\mathcal{R}$. We can now exploit the definition of ζ (2.50) to explicitly verify that perturbation modes are constant on super-horizon scales, after having exited the horizon during inflation.
To do this we need to perturb at first order the stress-energy tensor continuity equations $\nabla_\mu T^{\mu\nu} = 0$. On super-horizon scales it takes the following expression [19]:

$$\delta\rho' + 3\mathcal{H}(\delta\rho + \delta p) - 3\hat{\psi}'(\rho_0 + p_0) = 0. \tag{2.51}$$

It is possible to evaluate this equation in the uniform energy density gauge previously defined, so that $\delta\rho = 0$ and $\hat{\psi} = -\zeta$. In equation (2.11) we have split the pressure perturbation into adiabatic and non-adiabatic components. We know that $\delta p_{\text{adiabatic}} = c_s^2 \delta\rho$ and it follows that this component vanishes within our gauge choice, where equation (2.51) becomes:

$$\zeta' = -\frac{\mathcal{H}}{\rho_0 + p_0}\delta p_{\text{non-adiabatic}}. \tag{2.52}$$

If perturbations are adiabatic, which is the case for single field slow-roll inflation [8], then ζ remains constant on super-horizon scales. This result justifies the choice of using the curvature perturbation on uniform energy density hypersurfaces when dealing with primordial perturbations. As a consequence, the value of ζ at horizon-crossing during inflation, determined by the inflaton perturbations, is the one that enters inside the expressions for the late time observables, like the CMB temperature anisotropies. We thus have a concrete link between what happened during inflation and how the Universe evolves long after, during the standard hot Big Bang period. This result is represented in Figure 1.5.

Chapter 3

Primordial non-Gaussianity

In Chapter 1 we have briefly reviewed the standard slow-roll inflationary model, with particular focus on the production of primordial perturbations such a period of early acceleration is able to provide. In dealing with quantum random fluctuations we have then introduced the concept of power spectrum, needed describe their statistical properties. As we have already pointed out, the power spectrum would actually be sufficient to completely define a random field in the case it was drawn from a zero-mean Gaussian distribution, which for the primordial curvature ζ has the following expression:

$$P(\zeta) = \frac{1}{\sqrt{2\pi\sigma}} \exp\left(- \frac{\zeta^2}{2\sigma^2} \right), \tag{3.1}$$

where $\sigma^2 = \langle \zeta^2(t, \vec{x}) \rangle$ is the variance, defined as the 2-point correlation function when the two points coincide. In the standard slow-roll single field inflationary model the departure from Gaussianity can be computed to be of the order of the slow-roll parameters [13], a physically expected result since they quantify the deviation of the inflaton from being a free field, in which case the corresponding wave function in the ground state would be Gaussian [6]. Therefore, in order to generate a larger amount of primordial non-Gaussianity, it is required to violate any of the following conditions, which actually characterize the single field slow-roll inflation [22]:

- A single scalar field is responsible for driving inflation and for the production of primordial quantum fluctuations.
- The inflaton Lagrangian contains a canonical kinetic energy term, such that perturbations travel at the speed of light.
- As stated by the slow-roll assumption, the inflaton evolution has a much bigger timescale than the Hubble time H^{-1}.
- The initial condition for the inflaton is determined by the Bunch-Davis vacuum choice.

When all these conditions are satisfied simultaneously inflation predicts an undetectable amount of primordial non-Gaussianity. Detecting a consistent deviation from Gaussianity can thus be enough to rule out the most standard inflationary model. Furthermore, any other inflationary model, constructed by violating one or more of the conditions we have just listed, provides a different amount of predicted non-Gaussianity. In this sense primordial non-Gaussianity can be regarded as an independent probe of the physics in the early Universe.

In presence of non-Gaussianity, the power spectrum is not sufficient anymore to describe all of the statistics, and higher-order correlation functions can provide useful information about the nature of the perturbations.
The aim of this Chapter is then to introduce, in detail, to the possibility of a non-Gaussian behaviour of the primordial perturbations. We will focus in particular on the 3-point correlation function, as the leading non-Gaussian signature, and on its Fourier counterpart, the bispectrum.

3.1 The bispectrum

Computing higher order correlation functions is the standard method to measure non-Gaussianity. We know in fact that all the correlators beyond the power spectrum do not carry additional information about the statistics of a Gaussian random field. In that case the odd order correlators vanish while the even order ones can be written in function of the power spectrum, i.e. the connected part of higher order correlators vanish. It follows that measuring non-vanishing values of these correlators is a clear sign of the non-Gaussian nature of the random field.

The simplest indicator sensible to non-Gaussianity in the early Universe is then the 3-point correlation function of the primordial curvature perturbation ζ. Its Fourier transform takes the name of bispectrum B and is defined by the following expression:

$$\langle\zeta(\vec{k}_1)\zeta(\vec{k}_2)\zeta(\vec{k}_3)\rangle = (2\pi)^3\delta^{(3)}(\vec{k}_1+\vec{k}_2+\vec{k}_3)B_\zeta(k_1,k_2,k_3), \tag{3.2}$$

which may of course be generalized to any other kind of perturbation evaluated on a FLRW background. It is clear the analogy with the power spectrum (1.58), where this time the correlation is extended to three fluctuations instead of two. Once again, isotropy of the background ensures the bispectrum to depend only on the magnitude of wavevectors, while homogeneity is accounted for by the presence of the Dirac delta. This actually requires to have wavevectors which form a triangle in Fourier space, while the power spectrum only correlates two perturbations with the same wavenumber. It is thus necessary to account for the different possibilities in the shape of the triangle, on which should actually depends the value of the bispectrum. This is done usually by splitting the bispectrum into two different factors:

$$B_\zeta(k_1,k_2,k_3) = f_{NL}F(k_1,k_2,k_3), \tag{3.3}$$

where the shape dependence is contained inside the shape function F, which is instead kept separated from the overall amplitude f_{NL}. Given the relevance of these two functions just introduced, we now spend few words each to present their major features.

3.1.1 Shape function

The shape function F introduced in (3.3) carries information about how much power is associated to each possible triangle shape, while keeping fixed the overall scale. Different inflationary models predict different shape functions, corresponding to different configurations for which the signal peaks. Furthermore, it has been discovered that the violation of each of the conditions provided earlier is responsible for a primordial bispectrum with a specific triangular shape [22]. It is then possible to classify $F(k_1,k_2,k_3)$ based on which shape of the triangle corresponds to the maximum of the bispectrum. Different momenta configurations along with the relative shapes are represented in Figure 3.1.
Before looking more in depth at the different shapes and the respective expressions of the bispectrum, we fix some conventions useful for our discussion. First of all we can better quantify what we mean with the term overall scale, introduced before, by defining:

$$K = \frac{k_1+k_2+k_3}{3}, \tag{3.4}$$

such that it is the average of the three wavevectors correlated by the bispectrum. For sure it is then possible to construct different triangles by varying the angles and the individual sides length, but keeping fixed the quantity (3.4). If we now assume the shape function to be invariant on this overall scale K, it is straightforward to conclude that F should only have two degrees of freedom, corresponding to the ratios between the three wavevectors. As we will see shortly, any possible overall scale dependence would be accounted instead by the amplitude f_{NL}. We thus define the rescaled momenta:

$$x_i = \frac{k_i}{k_1}, \tag{3.5}$$

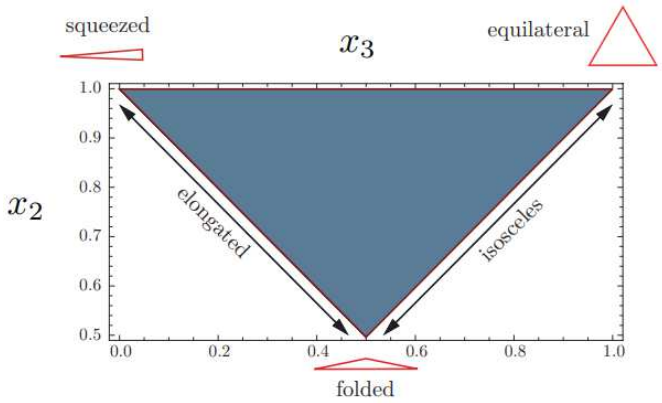

Figure 3.1: Parameter space of the rescaled momenta, where the three most common shapes of bispectrum predicted by inflationary models are highlighted. Taken from [6].

for $i = 2, 3$ and where we stick to the usual assumption of ordering the three momenta such that $x_3 \leq x_2 \leq 1$. Different combinations of rescaled momenta correspond to different shapes, with the ones shown in Figure 3.1 being the most common and studied in the literature [10]:

- **Local shape**. The signal is maximum for squeezed triangles with $x_3 \ll x_2 \sim 1$. Large amounts of this type of non-Gaussianity are usually predicted by multi-field models, like the curvaton model [8], which thus violate the first of the conditions listed above. The shape function can be written as [10]:

$$F_{\rm local}(k_1, k_2, k_3) = \frac{6}{5} A^2 \left[\frac{1}{k_1^{4-n_s} k_2^{4-n_s}} + \frac{1}{k_1^{4-n_s} k_3^{4-n_s}} + \frac{1}{k_2^{4-n_s} k_3^{4-n_s}} \right], \tag{3.6}$$

  where the normalization constant A is defined as the amplitude of the primordial power spectrum $P_\zeta(k) = Ak^{n_s-4}$. The name local comes from the fact that the non-linearity, responsible for non-Gaussianity, is parametrized in the following way, which was first considered in [23, 24, 25]:

$$\zeta(\vec{x}) = \zeta_g(\vec{x}) + \frac{3}{5} f_{NL} \left[\zeta_g(\vec{x})^2 - \langle \zeta_g(\vec{x}) \rangle^2 \right], \tag{3.7}$$

  so that the complete perturbation ζ is assumed to be, in real space, a local function of a Gaussian random field ζ_g. In particular, the deviation from non-Gaussianity is taken to be proportional to the amplitude parameter f_{NL}. The presence of the term $\langle \zeta_g(\vec{x}) \rangle^2$ ensures that ζ is a zero-mean field, i.e. $\langle \zeta(\vec{x}) \rangle = 0$. The local shape is particularly interesting since, in Fourier space, a considerable amount of non-Gaussianity arises from the correlation between long and short wavelenghts. This, plus the fact that a simple and explicit parametrization (3.7) there exists, makes the local shape a recurrent topic in the following discussions. Furthermore, a certain amount of non-Gaussianity with a local shape is expected also in the context of single field slow-roll inflation, with an amplitude proportional to the slow-roll parameters $f_{NL} = O(\epsilon, \eta)$ [12, 13, 26, 27].

- **Equilateral shape**. The bispectrum peaks for the equilateral configuration $x_3 \sim x_2 \sim 1$. This type of non-Gaussianity is produced by inflationary models containing non-canonical kinetic terms, i.e. higher derivative terms, in the inflaton Lagrangian. This happens, for example, in the Dirac-Born-Infeld model of inflation [12]. In these cases the correlation is between modes with comparable wavelengths, which cross the horizon nearly at the same time. The shape function of the equilateral type is [10]:

$$\begin{aligned} F_{\rm equil}(k_1, k_2, k_3) = \frac{18}{5} A^2 \Bigg\{ & - \frac{1}{k_1^{4-n_s} k_2^{4-n_s}} - \frac{1}{k_1^{4-n_s} k_3^{4-n_s}} - \frac{1}{k_2^{4-n_s} k_3^{4-n_s}} \\ & - \frac{2}{(k_1 k_2 k_3)^{2(4-n_s)/3}} + \left[\frac{1}{k_1^{(4-n_s)/3} k_2^{2(4-n_s)/3} k_3^{(4-n_s)}} + 5 \text{ perms} \right] \Bigg\}, \end{aligned} \tag{3.8}$$

where, in the second line, we have introduced a notation to account implicitly for all the possible permutations of a given term. This will be done extensively throughout the rest of this work.

- **Folded shape**. Violating the assumption of a Bunch-Davis vacuum as initial condition for the inflaton usually gives rise to a bispectrum peaking in the flattened configuration, with $x_3 \sim x_2 \sim \frac{1}{2}$.
- **Orthogonal shape**. It is then possible to consider another type of non-Gaussian bispectrum, which is defined to be orthogonal to the equilateral one and can thus be referred to as orthogonal shape. The signal has a maximum both for equilateral and folded triangle configurations [28]. In this case the shape function has the following expression [10]:

$$F_{\rm ortho}(k_1,k_2,k_3) = \frac{18}{5}A^2\Bigg\{ -\frac{3}{k_1^{4-n_s}k_2^{4-n_s}} - \frac{3}{k_1^{4-n_s}k_3^{4-n_s}} - \frac{3}{k_2^{4-n_s}k_3^{4-n_s}} - \frac{8}{(k_1k_2k_3)^{2(4-n_s)/3}} + \left[\frac{3}{k_1^{(4-n_s)/3}k_2^{2(4-n_s)/3}k_3^{(4-n_s)}} + 5 \text{ perms}\right]\Bigg\}. \tag{3.9}$$

In Figure 3.2 are plotted the shape functions for the local and the equilateral configurations. The normalization is such that $F(1,1,1) = 1$.

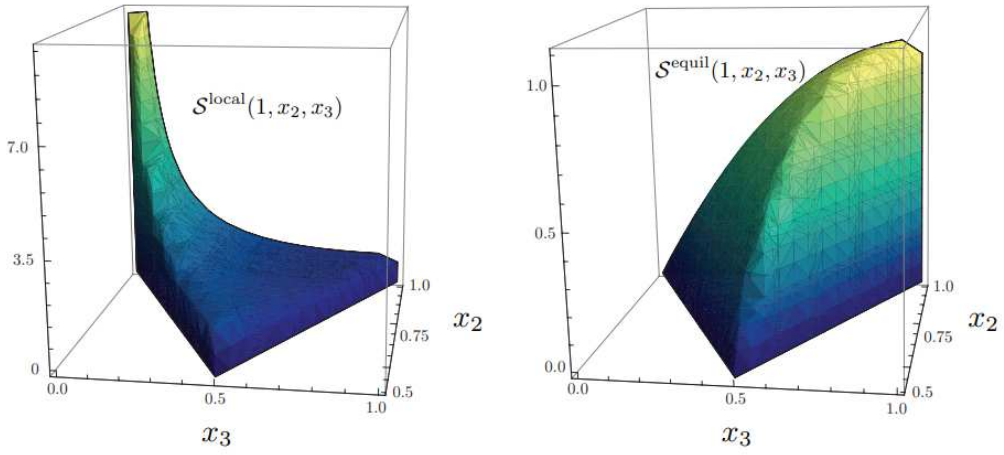

Figure 3.2: Plotted shape functions, indicated here as $\mathcal{S}$ instead of F, for the local (left panel) and equilateral (right panel) cases, as functions of rescaled momenta. Taken from [6].

3.1.2 Amplitude parameter

The amplitude, or non-linear, parameter f_{NL}, introduced in equation (3.3), accounts for the overall magnitude of the bispectrum. A more rigorous definition, which holds for arbitrary shapes, is obtained by fixing the following normalization [6]:

$$f_{NL} = \frac{5}{18}\frac{B_\zeta(k,k,k)}{P_\zeta^2(k)}, \tag{3.10}$$

where the bispectrum is computed in the equilateral configuration. The factor $\frac{5}{18}$ is chosen in such a way that the parameter f_{NL} in (3.7) corresponds with the one just defined (3.10). Using parametrization (3.7) it is also possible to recover that $B_\zeta \propto P_\zeta^2$, a result which actually holds also for other shapes. We will do so in the next section, performing the explicit calculation of the

bispectrum for the perturbation ζ parametrized as in (3.7).

Predictions on the amount of primordial non-Gaussianity from different inflationary models are usually expressed in terms of constraints on the value of f_{NL}, along with specifying the particular shape function predicted by the model. Referring to the definition (3.3) and to the three shape functions (3.6), (3.8) and (3.9), the latest observational constraints by the Planck Collaboration (2018) are [10]:

$$\begin{aligned} f_{NL}^{\text{local}} &= -0.9 \pm 5.1, \\ f_{NL}^{\text{equil}} &= -26 \pm 47, \\ f_{NL}^{\text{ortho}} &= -38 \pm 24. \end{aligned} \tag{3.11}$$

3.1.3 Running non-Gaussianity

We have not addressed yet to the possibility of a dependence of the amplitude parameter on the scale. We already know that the dependence on the triangular shapes, and thus on the ratio between the three momenta, is contained in the shape function. On the other hand, it is possible to account for a dependence of f_{NL} on the overall scale K (3.4). In analogy to the definition of the scalar spectral index n_s for the primordial power spectrum (1.73), it is natural to define the following parameter:

$$n_{f_{NL}} \equiv \frac{d\ln f_{NL}(k)}{d\ln k}, \tag{3.12}$$

which is known as running parameter, since it accounts for the possibility of having running non-Gaussianity, i.e. a scale-dependent f_{NL}. In this context the definition (3.10) can be rewritten in the following way [29]:

$$f_{NL}(k_1, k_2, k_3) = \frac{5}{6} \frac{B_\zeta(k_1, k_2, k_3)}{P_\zeta(k_1)P_\zeta(k_2) + 2 \text{ perms}}, \tag{3.13}$$

which is quite a more general definition for the amplitude parameter, since it is function of all the three momenta and so also of the shape of the triangle itself. In this case f_{NL} can be interpreted, directly from the definition (3.13), as the amplitude of the bispectrum with respect to the power spectrum squared.

Various explicit forms of running, in terms of the dependence on the wavenumbers, may be considered, as they arise from the different inflationary models. We know that multi-field models predict a local shape for the bispectrum (3.6), which is modified in case of a scale-dependent non-Gaussianity as [29]:

$$B_\zeta(k_1, k_2, k_3) \propto (k_1 k_2)^{n_s - 4} k_3^{n_{f_{NL}}} + 2 \text{ perms}, \tag{3.14}$$

if the curvature perturbation originates from only one of the scalar fields, while for a two-field model where both contribute to the primordial perturbations it is given by [29]:

$$B_\zeta(k_1, k_2, k_3) \propto (k_1 k_2)^{n_s - 4 + n_{f_{NL}}/2} + 2 \text{ perms}. \tag{3.15}$$

A mild running non-Gaussianity is also predicted by models which produce bispectra of the equilateral shape [10]. In this case the scale dependence can be expressed as [30]:

$$f_{NL}(k_1, k_2, k_3) = f_{NL}(k_p) \left(\frac{k_1 + k_2 + k_3}{3k_p} \right)^{n_{f_{NL}}}, \tag{3.16}$$

where k_p is a pivot scale and we recognize the explicit dependence on K defined in (3.4).
The 3 types of running just presented have been analyzed by the Planck collaboration (2018) and no evidence in favour of a scale-dependent primordial non-Gaussianity was found yet [10].

3.2 The local shape

Until now in this Chapter we have discussed the general features of primordial non-Gaussianity and provided with some of the most common results which can be found in the literature. It is interesting for the scope of this Thesis to deepen a bit more on the local parametrization (3.7):

$$\zeta(\vec{x}) = \zeta_g(\vec{x}) + \frac{3}{5} f_{NL}\big[\zeta_g^2(\vec{x}) - \langle\zeta_g^2(\vec{x})\rangle\big], \tag{3.17}$$

which we have rewritten here, being it the starting point of our discussion. This way of expressing the non-linearity of the primordial perturbation ζ allows to derive a simple result for the bispectrum (3.2). Furthermore, it is also straightforward to consider the case of running non-Gaussianity by introducing a dependence on the scale directly inside f_{NL} in (3.17).

In order to compute the primordial bispectrum (3.2) we need an expression for $\zeta(\vec{k})$ in Fourier space. Considering then the local ansatz (3.17), we find:

$$\zeta(\vec{k}) = \zeta_g(\vec{k}) + \frac{3}{5} f_{NL}\left[\int \frac{d^3\vec{p}}{(2\pi)^3}\zeta_g(\vec{p})\zeta_g(\vec{k}-\vec{p}) - (2\pi)^3\delta^{(3)}(\vec{k})\langle\zeta_g^2(\vec{x})\rangle\right] \equiv \zeta_g(\vec{k}) + \zeta_{ng}(\vec{k}), \tag{3.18}$$

where $\langle\zeta_g^2(\vec{x})\rangle^2$ is the variance in real space. For the time being the amplitude parameter is assumed to be scale-invariant. Substituting (3.18) inside the correlator (3.2) one obtains:

$$\begin{aligned}\langle\zeta(\vec{k}_1)\zeta(\vec{k}_2)\zeta(\vec{k}_3)\rangle &= \langle\big(\zeta_g(\vec{k}_1) + \zeta_{ng}(\vec{k}_1)\big)\big(\zeta_g(\vec{k}_2) + \zeta_{ng}(\vec{k}_2)\big)\big(\zeta_g(\vec{k}_3) + \zeta_{ng}(\vec{k}_3)\big)\rangle \\ &= \langle\zeta_g(\vec{k}_1)\zeta_g(\vec{k}_2)\zeta_g(\vec{k}_3)\rangle + \frac{3}{5} f_{NL}\Bigg[\Bigg(\int \frac{d^3\vec{p}}{(2\pi)^3}\langle\zeta_g(\vec{p})\zeta_g(\vec{k}_1-\vec{p}) \\ &\times \zeta_g(\vec{k}_2)\zeta_g(\vec{k}_3)\rangle - (2\pi)^3\delta^{(3)}(\vec{k}_1)\langle\zeta_g^2(\vec{x})\rangle\langle\zeta_g(\vec{k}_2)\zeta_g(\vec{k}_3)\rangle\Bigg) + 2 \text{ perms}\Bigg],\end{aligned} \tag{3.19}$$

where we have kept the linear order in the amplitude parameter f_{NL}. We see that, because of the parametrization (3.17), the result (3.19) is written in terms of correlators of the Gaussian random field ζ_g. Recalling the discussion, at the beginning of this Chapter, about the properties of such a perturbation, it follows for the 3-point correlation function:

$$\langle\zeta_g(\vec{k}_1)\zeta_g(\vec{k}_2)\zeta_g(\vec{k}_3)\rangle = 0, \tag{3.20}$$

and the same result holds for higher order odd correlators. The linear term in f_{NL} of (3.19) contains instead the 4-point correlation function, for which we know the connected part to vanish, and thus ends up being just a combination of 2-point correlators:

$$\langle\zeta_g(\vec{k}_1)\zeta_g(\vec{k}_2)\zeta_g(\vec{k}_3)\zeta_g(\vec{k}_4)\rangle = \langle\zeta_g(\vec{k}_1)\zeta_g(\vec{k}_2)\rangle\langle\zeta_g(\vec{k}_3)\zeta_g(\vec{k}_4)\rangle + 2 \text{ perms}, \tag{3.21}$$

such that it can be expressed in terms of the primordial power spectrum (1.58). Therefore, combining results (3.20) and (3.21) with equation (3.19), we obtain:

$$\begin{aligned}\langle\zeta(\vec{k}_1)\zeta(\vec{k}_2)\zeta(\vec{k}_3)\rangle =& \frac{3}{5} f_{NL}\Bigg[\Bigg(\int \frac{d^3\vec{p}}{(2\pi)^3}\Big((2\pi)^6\delta^{(3)}(\vec{k}_1)\delta^{(3)}(\vec{k}_2+\vec{k}_3)P_\zeta(p)P_\zeta(k_2) \\ &+ (2\pi)^6\delta^{(3)}(\vec{p}+\vec{k}_2)\delta^{(3)}(\vec{k}_1-\vec{p}+\vec{k}_3)P_\zeta(k_2)P_\zeta(k_3) \\ &+ (2\pi)^6\delta^{(3)}(\vec{p}+\vec{k}_3)\delta^{(3)}(\vec{k}_1-\vec{p}+\vec{k}_2)P_\zeta(k_3)P_\zeta(k_2)\Big) \\ &- (2\pi)^6\delta^{(3)}(\vec{k}_1)\delta^{(3)}(\vec{k}_2+\vec{k}_3)P_\zeta(k_2)\int \frac{d^3\vec{p}'}{(2\pi)^3}P_\zeta(p')\Bigg) + 2 \text{ perms}\Bigg],\end{aligned} \tag{3.22}$$

where the definition of (1.58) was used and the variance $\langle\zeta_g^2(\vec{x})\rangle^2$ was re-expressed as the Fourier counterpart of P_ζ (1.60). It follows that the first and the last line of (3.22) cancel out each other so that performing the integration over $\vec{p}$ on the remaining terms gives rise to two equal contributions. The final result can be written in the following way:

$$\langle\zeta(\vec{k}_1)\zeta(\vec{k}_2)\zeta(\vec{k}_3)\rangle = \frac{6}{5} f_{NL}(2\pi)^6\delta^{(3)}(\vec{k}_1+\vec{k}_2+\vec{k}_3)\big[P_\zeta(k_1)P_\zeta(k_2) + P_\zeta(k_2)P_\zeta(k_3) + P_\zeta(k_3)P_\zeta(k_1)\big], \tag{3.23}$$

in which we have explicitly written the contributions coming from all the possible permutations. Remembering definition (3.2), we obtain the expression of the primordial bispectrum arising from the local ansatz (3.17):

$$B_\zeta(k_1,k_2,k_3) = \frac{6}{5} f_{NL}\big[P_\zeta(k_1)P_\zeta(k_2) + 2 \text{ perms}\big]. \tag{3.24}$$

It is straightforward to check, setting $P_\zeta(k) = Ak^{n_s-4}$, that this result indeed corresponds to the local shape function (3.6), thus verifying a posteriori that the ansatz (3.17) gives rise to primordial non-Gaussianity of the local type. It is also worth to notice that in this case the power spectrum of the full, non-linear, perturbation ζ does not include linear term in f_{NL}, and thus remains unchanged from the Gaussian one, up to corrections of the second order in f_{NL}.
Another consistency check would be to substitute the bispectrum (3.24) inside the definition of the amplitude parameter (3.10) finding that, thanks to the chosen normalization, it corresponds to the f_{NL} introduced in (3.17), which a priori was not at all obvious.

3.2.1 The long-short split

One interesting property of the local parametrization (3.17) is that it couples Fourier modes with long and short wavelengths . Remember in fact that the local shape of non-Gaussianity peaks in the squeezed configuration, where the relation between wavenumbers can be expressed as $k_3 \ll k_1 \sim k_2$. This means that the bispectrum signal is maximum when it correlates one long wavelength perturbation with two short wavelength ones. We know that during inflation longer modes cross the horizon earlier. Therefore, in presence of primordial local non-Gaussianity, it is possible to imagine a situation in which $\zeta(\vec{k}_3)$ has already frozen out and acts as a background for the evolution of the other two shorter modes $\zeta(\vec{k}_1)$ and $\zeta(\vec{k}_2)$. We can refer to this phenomenon by saying that the short modes are modulated by the long one.

In order to study such a scenario, we express once again the non-linearity in the form of the local ansatz (3.17) and, moreover, we assume that the Gaussian perturbation $\zeta_g(\vec{x})$ can be split up as [31]:

$$\zeta_g(\vec{x}) = \zeta_s(\vec{x}) + \zeta_l(\vec{x}), \tag{3.25}$$

where ζ_s (ζ_l) is the part of ζ_g which receives contribution from short (long) wavelength modes. This can be better understood by going to Fourier space, where we have [32]:

$$\begin{aligned} \zeta_s(\vec{x}) &= \int \frac{d^3\vec{k}}{(2\pi)^3}\theta(k-k_H)\zeta_g(\vec{k})e^{i\vec{k}\vec{x}}, \\ \zeta_l(\vec{x}) &= \int \frac{d^3\vec{k}}{(2\pi)^3}\theta(k_H-k)\zeta_g(\vec{k})e^{i\vec{k}\vec{x}}. \end{aligned} \tag{3.26}$$

The step functions truncate the integration intervals at k_H, which is the arbitrary wavenumber we choose to separate long and short modes. Usually, it is natural to take $k_H \simeq aH$, corresponding to the comoving Hubble horizon (1.2). In this way only modes with sub-horizon wavelength contribute to the short part of the perturbation, and vice-versa for the long one. From expressions (3.26), we can write the Fourier counterpart of the split (3.25) in the following way:

$$\zeta_g(\vec{k}) = \zeta_s(\vec{k}) + \zeta_l(\vec{k}), \tag{3.27}$$

where we have defined:

$$\begin{aligned} \zeta_s(\vec{k}) &\equiv \theta(k-k_H)\zeta_g(\vec{k}), \\ \zeta_l(\vec{k}) &\equiv \theta(k_H-k)\zeta_g(\vec{k}). \end{aligned} \tag{3.28}$$

The split in Fourier space (3.27) is thus just a formal way to state that a single mode of perturbation can, trivially, either be short, if still inside the horizon, or long, if already out of it. Expressed in this way, the two components do not mix together and we can conclude that in a Gaussian scenario

they cannot influence each other, an expected result since we know that, in linear perturbation theory, different Fourier modes evolve independently. This is not the case anymore if one allows for the presence of primordial non-Gaussianity: in this case we have already said that a bispectrum of the local type gets the maximum contribution from the correlation between long and short wavelength perturbations. Thanks to this correlation, it becomes possible to think the sub-horizon evolution of the short mode as modulated by the long one, which is instead assumed to be super-horizon and thus frozen. To see this we substitute the split (3.25) inside the local ansatz (3.17), obtaining:

$$\zeta = \zeta_s + \zeta_l + \frac{3}{5} f_{NL}\big[\zeta_s^2 + 2\zeta_s\zeta_l - \langle\zeta_s\rangle^2\big], \tag{3.29}$$

where all the perturbations are computed at the same point $\vec{x}$ in real space. In writing expression (3.29) we have already exploited the fact that the evolution of the long wavelength component ζ_l is assumed to be frozen, so that $\zeta_l^2 \simeq \langle\zeta_l\rangle^2$ and the two terms cancel out. From (3.29) we can derive the expression for the full, non-linear, small scale perturbation ζ_S modulated by the fixed large scale one [31]:

$$\zeta_S = \zeta_s + \frac{3}{5} f_{NL}\big[\zeta_s^2 + 2\zeta_s\zeta_l - \langle\zeta_s\rangle^2\big]. \tag{3.30}$$

This result explicitly shows how, in presence of a local type of primordial non-Gaussianity (3.17), the evolution of a small-scale perturbation is affected by a larger scale one.

The long wavelength modulation has a direct consequence on the power spectrum of the modulated short perturbation (3.30). Similarly to equation (3.18), the expression for ζ_S in Fourier space can be written as:

$$\zeta_S(\vec{k}) = \zeta_s(\vec{k}) + \frac{3}{5} f_{NL}\Big[\big(\zeta_s \star \zeta_s\big)(\vec{k}) + 2\big(\zeta_s \star \zeta_l\big)(\vec{k}) - (2\pi)^3\delta^{(3)}(\vec{k})\langle\zeta_s^2(\vec{x})\rangle^2\Big], \tag{3.31}$$

where we have introduced a shorter notation for the convolution:

$$\big(\zeta \star \zeta\big)(\vec{k}) = \int \frac{d^3\vec{p}}{(2\pi)^3}\zeta(\vec{p})\zeta(\vec{k}-\vec{p}). \tag{3.32}$$

It is straightforward to compute the 2-point correlation function of expression (3.31), remembering that, under our assumptions, we can take ζ_l out of the averages. Keeping the linear order in f_{NL} we find the following non-vanishing contributions:

$$\begin{aligned}
\langle\zeta_S(\vec{k}_1)\zeta_S(\vec{k}_2)\rangle &= \langle\zeta_s(\vec{k}_1)\zeta_s(\vec{k}_2)\rangle + \frac{6}{5} f_{NL}\int \frac{d^3\vec{p}}{(2\pi)^3}\big[\zeta_l(\vec{k}_1-\vec{p})\langle\zeta_s(\vec{p})\zeta_s(\vec{k}_2)\rangle \\
&\quad + \zeta_l(\vec{k}_2-\vec{p})\langle\zeta_s(\vec{p})\zeta_s(\vec{k}_1)\rangle\big] \\
&= (2\pi)^3\delta^{(3)}(\vec{k}_1+\vec{k}_2)P_{\zeta_s}(k_1) + \frac{6}{5} f_{NL}\int \frac{d^3\vec{p}}{(2\pi)^3}\big[\zeta_l(\vec{k}_1-\vec{p}) \\
&\quad \times (2\pi)^3\delta^{(3)}(\vec{p}+\vec{k}_2)P_{\zeta_s}(k_2) + \zeta_l(\vec{k}_2-\vec{p})(2\pi)^3\delta^{(3)}(\vec{p}+\vec{k}_1)P_{\zeta_s}(k_1)\big] \\
&= (2\pi)^3\delta^{(3)}(\vec{k}_1+\vec{k}_2)P_{\zeta_s}(k_1) + \frac{6}{5} f_{NL}\zeta_l(\vec{k}_1+\vec{k}_2)\big[P_{\zeta_s}(k_1) + P_{\zeta_s}(k_2)\big].
\end{aligned} \tag{3.33}$$

Notice that the second term of expression (3.33) is proportional to $\zeta_l(\vec{k}_1+\vec{k}_2)$ which, remembering definition (3.28), implies the condition on the wavevectors $|\vec{k}_1+\vec{k}_2| < k_H$. This is a less stringent constraint than the one coming from the usual Dirac delta, $\vec{k}_1+\vec{k}_2 = 0$, and it introduces a correlation between two short modes with different wavenumbers. This new contribution in (3.33) is linear in the amplitude parameter.

3.2.2 Running non-Gaussianity

We can also exploit the local ansatz (3.17) to discuss the case of a scale-dependent amplitude parameter f_{NL}, namely the case of running non-Gaussianity. The first thing we need to understand clearly is how we can implement the scale dependence inside the parametrization. Were we

assuming a particular expression of the bispectrum, we could have just defined the running as in (3.13). Looking instead at the parametrization in Fourier space (3.18), it seems natural to simply generalize f_{NL} as a function of the wavenumber k, such that our new starting point becomes [33]:

$$\zeta(\vec{k}) = \zeta_g(\vec{k}) + \frac{3}{5} f_{NL}(k) \left[\int \frac{d^3\vec{p}}{(2\pi)^3} \zeta_g(\vec{p}) \zeta_g(\vec{k}-\vec{p}) - (2\pi)^3 \delta^{(3)}(\vec{k}) \langle \zeta_g^2(\vec{x}) \rangle \right]. \tag{3.34}$$

Notice that this ansatz is not local anymore, which is evident when we transform back to real space:

$$\zeta(\vec{x}) = \zeta_g(\vec{x}) + \frac{3}{5} \int \frac{d^3\vec{k}}{(2\pi)^3} e^{i\vec{k}\vec{x}} f_{NL}(k) (\zeta_g \star \zeta_g)(\vec{k}), \tag{3.35}$$

where the deviation from the local form is proportional to the amount of scale dependence of f_{NL}. Substituting parametrization (3.34) inside (3.2), and repeating the exactly same steps of the scale-independent case, we end up with the following expression for the bispectrum:

$$B_\zeta(k_1, k_2, k_3) = \frac{6}{5} \big[f_{NL}(k_1) P_\zeta(k_2) P_\zeta(k_3) + 2 \text{ perms} \big], \tag{3.36}$$

where the running of the amplitude parameter is manifest. The result (3.36) is quite general, since it allows to recover a local type primordial bispectrum in the presence of running non-Gaussianity. The only limitation is that it describes only the cases where f_{NL} can be written explicitly as a function of a single wavenumber. Nevertheless, substituting (3.36) inside (3.13) would return, in principle, an expression for $f_{NL}(k_1, k_2, k_3)$, with a dependence on all the three wavenumbers. This does not correspond to the scale-dependent f_{NL} introduced in (3.34). We conclude that the two definitions of the amplitude parameter are inconsistent and identify two distinct objects [33], while in the constant-f_{NL} case the two were equivalent. We will however stick with the notation of expression (3.36), since the interpretation of f_{NL} as the amplitude of bispectrum is still valid there. Hopefully this ambiguity should not be the source of any confusion.

In order to study a concrete case, we consider a simple, physically motivated, power-law dependence of $f_{NL}(k)$ [34]:

$$f_{NL}(k) = f_{NL}(k_p) \left(\frac{k}{k_p} \right)^{n_{f_{NL}}}, \tag{3.37}$$

which actually corresponds to equation (3.12) in the case of constant $n_{f_{NL}}$ and where k_p is an arbitrary reference scale. Remembering also the expression for the primordial power spectrum $P_\zeta(k) = A k^{n_s - 4}$, we obtain for the bispectrum (3.36):

$$B_\zeta(k_1, k_2, k_3) = \frac{6}{5} A^2 \frac{f_{NL}(k_p)}{k_p^{n_{f_{NL}}}} \big[k_1^{n_{f_{NL}}} (k_2 k_3)^{n_s - 4} + 2 \text{ perms} \big], \tag{3.38}$$

which corresponds to the result (3.14), obtained for multi-field inflationary models where only a single scalar field contributes to the primordial curvature perturbation [29]. The running non-Gaussianity parametrization (3.34) can thus describe such physical cases.

Large scale limit

Since the bispectrum (3.36) peaks on squeezed configurations, it is natural to make a further step and take the large scale limit $k_L \equiv k_3 \to 0$. As a result of this, terms in (3.36) proportional to $P_\zeta(k_L)$ (remember $n_s \sim 1$) would diverge so that, assuming also $f_{NL}(k)$ to be finite around $k = k_L$, we may write [31]:

$$B_\zeta(k_s, k_L) \simeq \frac{12}{5} f_{NL}(k_s) P_\zeta(k_s) P_\zeta(k_L), \tag{3.39}$$

where in the large scale limit $k_s \equiv k_1 \sim k_2$. The result is that in (3.39) appears only the dependence of f_{NL} on the small scale k_s. This is exactly what happens to expression (3.38) in the reasonable case where $n_{f_{NL}} > -3$:

$$B_\zeta(k_s, k_L) \simeq \frac{12}{5} A^2 \frac{f_{NL}(k_p)}{k_p^{n_{f_{NL}}}} k_s^{n_{f_{NL}} + n_s - 4} k_L^{n_s - 4}. \tag{3.40}$$

This suggests the possibility to consider an amplitude parameter $f_{NL}(k)$ with a dependence on only the shorter wavelengths. This is quite interesting since it allows to imagine a scenario with the presence of a very little and undetectable amount of non-Gaussianity on largest scales, which would be bumped on smaller ones by choosing a sufficiently positive value for the parameter $n_{f_{NL}}$.

3.2.3 Scale-dependent f_{NL} as a kernel

We can actually obtain an even more general expression for running non-Gaussianity, starting from the local parametrization (3.17). In order to do so we may consider a generic, non-local, kernel operator K which modifies the coupling in the quadratic term [36]:

$$\zeta(\vec{x}) = \zeta_g(\vec{x}) + \frac{3}{5}K[\zeta_g, \zeta_g](\vec{x}), \tag{3.41}$$

where we have included f_{NL} inside the definition of K, since we want to account for running non-Gaussianity. Actually we will assume that the deviation from the local parametrization (3.17) is entirely due to the scale dependence of f_{NL}. In this way we can exploit the kernel formalism [27, 35, 36, 37] to recover explicit expressions for the scale dependence of f_{NL}. This is achieved by performing a matching with expressions of running bispectra recurring in the literature [10, 29, 30], like the ones we have considered in section 3.1.3

In Fourier space equation (3.41) has the following expression:

$$\begin{aligned}\zeta(\vec{k}) &= \zeta_g(\vec{k}) + \frac{3}{5}\int \frac{d^3\vec{k}_1 d^3\vec{k}_2}{(2\pi)^3}\delta^{(3)}(\vec{k}-\vec{k}_1-\vec{k}_2)K(\vec{k}_1,\vec{k}_2)\zeta_g(\vec{k}_1)\zeta_g(\vec{k}_2) \\ &\equiv \zeta_g(\vec{k}) + \frac{3}{5}K_{\vec{k}}[\zeta_g,\zeta_g],\end{aligned} \tag{3.42}$$

where the second equality defines the expression of the kernel operator in Fourier space. As a reference, the Fourier transform of (3.17) can be rewritten in the following way:

$$\begin{aligned}\zeta(\vec{k}) &= \zeta_g(\vec{k}) + \frac{3}{5}f_{NL}(\zeta_g \star \zeta_g)(\vec{k}) \\ &= \frac{3}{5}f_{NL}\int \frac{d^3\vec{k}_1 d^3\vec{k}_2}{(2\pi)^3}\delta^{(3)}(\vec{k}-\vec{k}_1-\vec{k}_2)\zeta_g(\vec{k}_1)\zeta_g(\vec{k}_2).\end{aligned} \tag{3.43}$$

We can also exploit expression (3.42) to derive a more explicit form of the kernel operator in real space, introduced in equation (3.41):

$$K[\zeta_g,\zeta_g](\vec{x}) = \frac{3}{5}\int d^3\vec{y}d^3\vec{z}K(\vec{y},\vec{z})\zeta_g(\vec{x}-\vec{y})\zeta_g(\vec{x}-\vec{z}), \tag{3.44}$$

where the kernel function in real space is related to the Fourier counterpart as:

$$K(\vec{k}_1,\vec{k}_2) = \int d^3\vec{y}d^3\vec{z}e^{-i(\vec{k}_1\vec{y}+\vec{k}_2\vec{z})}K(\vec{y},\vec{z}). \tag{3.45}$$

Expression (3.42) is quite general, while we are interested in the case where the kernel accounts only for the scale dependence of f_{NL}. Comparing expressions (3.42) and (3.43) we can thus set $K(\vec{k}_1,\vec{k}_2) = f_{NL}(\vec{k}_1,\vec{k}_2)$, and we will continue to refer to it as the kernel. Furthermore, if we also assume statistical isotropy, f_{NL} can only be a function of the magnitude of the momenta and the angle between the two, meaning that we can rewrite its dependencies as $f_{NL}(k_1,k_2,k)$, where $k = |\vec{k}_1+\vec{k}_2|$ because of the Dirac delta in equation (3.42). We end up with the most general expression for running non-Gaussianity derived as a generalization of the local ansatz:

$$\zeta(\vec{k}) = \zeta_g(\vec{k}) + \frac{3}{5}\int \frac{d^3\vec{k}_1 d^3\vec{k}_2}{(2\pi)^3}\delta^{(3)}(\vec{k}-\vec{k}_1-\vec{k}_2)f_{NL}(k_1,k_2,k)\zeta_g(\vec{k}_1)\zeta_g(\vec{k}_2), \tag{3.46}$$

where $f_{NL}(k_1, k_2, k)$ is the kernel we want to explicitly determine.

Computing the 3-point correlation function of (3.46), it is possible to to recover the corresponding form of the primordial bispectrum (3.2) in terms of the primordial power spectrum:

$$\begin{aligned} B_\zeta(k_1, k_2, k_3) = \frac{6}{5}\big[&f^{12}_{NL}(k_1, k_2, k_3)P_\zeta(k_1)P_\zeta(k_2) + f^{23}_{NL}(k_2, k_3, k_1)P_\zeta(k_2)P_\zeta(k_3) \\ &+ f^{31}_{NL}(k_3, k_1, k_2)P_\zeta(k_3)P_\zeta(k_1)\big], \end{aligned} \tag{3.47}$$

where we have also accounted for the possibility that, in principle, f_{NL} may not be symmetric under exchange of its arguments and thus introduced the notation f^{ij}_{NL} to designate the term which is multiplied to the power spectra evaluated in k_i and k_j. Nonetheless, we want instead to preserve the symmetry under the exchange of these two momenta in a single term. Because of this, it is important to highlight the order in which the momenta appear inside the dependencies of $f^{ij}_{NL}(k_i, k_j, |\vec{k}_i + \vec{k}_j|)$, distinguishing in particular the third momenta from the other two, which are interchangeable.
The result (3.47) can now be compared with specific bispectra expressions, arising from running non-Gaussianity physical arguments. This allows to recover the solutions for the kernel $f^{ij}_{NL}(k_i, k_j, |\vec{k}_i + \vec{k}_j|)$ which generate such templates.

As a consistency check, we start by considering the template (3.14), for which we already know one explicit expression of the kernel. This form of bispectrum arises from the generalization of the local ansatz to a scale-dependent $f_{NL}(k)$ (3.34) parametrized as a power-law (3.37), which we have discussed in the previous section. Adopting the kernel formalism to deal with such a case, we already see that f_{NL} depends only on one out of the three possible momenta.
Remembering that the primordial power spectrum can be expressed as $P_\zeta(k) = Ak^{n_s-4}$, we impose the equality between (3.47) and (3.14).

$$f^{12}_{NL}(k_1, k_2, k_3)A^2(k_1k_2)^{n_s-4} + 2 \text{ perms} = A^2(k_1k_2)^{n_s-4}\mathcal{A}k_3^{n_{f_{NL}}} + 2 \text{ perms}, \tag{3.48}$$

where we have defined the dimensionful constant $\mathcal{A} \equiv \frac{f_{NL}(k_p)}{k_p^{n_{f_{NL}}}}$, independent on the chosen pivot scale k_p. If we focus on the symmetry properties of the two sides, we realize that the term explicited on the left can only be matched with terms on the right symmetric under the exchange of k_1 and k_2. There are two possible combinations, on the RHS, with such a symmetry property: the term $(k_1k_2)^{n_s-4}k_3^{n_{f_{NL}}}$ and the term $\big(k_1^{n_s-4}k_2^{n_{f_{NL}}} + k_2^{n_s-4}k_1^{n_{f_{NL}}}\big)k_3^{n_s-4}$. These will correspond to two different solutions for the kernel $f^{12}_{NL}(k_1, k_2, k_3)$. The first is trivial and leads to:

$$f^{12}_{NL}(k_1, k_2, k_3) = \mathcal{A}k_3^{n_{f_{NL}}}, \tag{3.49}$$

where the generalization for permutations of the arguments is straightforward. This is our expected parametrization of the running as a power-law (3.37). It is interesting to notice, in particular, that in this case the running is exclusively on $k_3 = |\vec{k}_1 + \vec{k}_2|$, which is the external momentum in (3.42). This is a conclusion which will become relevant in the discussion of the following Chapters, where we will use this simple expression of scale-dependent f_{NL} to perform explicit calculations.
If we consider instead the second possibility for the matching in (3.48), we recover a less trivial kernel solution:

$$f^{12}_{NL}(k_1, k_2, k_3) = \frac{\mathcal{A}}{2}\big(k_1^{4-n_s+n_{f_{NL}}} + k_2^{4-n_s+n_{f_{NL}}}\big)k_3^{n_s-4}, \tag{3.50}$$

This is indeed another expression for f_{NL} which, inserted in (3.47), allows to recover the bispectrum (3.14). More generically, this is true for a combination of the two solutions:

$$f^{12}_{NL}(k_1, k_2, k_3) = A\big[(1-u)k_3^{n_{f_{NL}}} + \frac{u}{2}\big(k_1^{4-n_s+n_{f_{NL}}} + k_2^{4-n_s+n_{f_{NL}}}\big)k_3^{n_s-4}\big], \tag{3.51}$$

where u is a free parameter [36]. In fact, inserting (3.51) in (3.47) we find:

$$B_\zeta(k_1, k_2, k_3) = \frac{6}{5}A^2\mathcal{A}\big[(k_1k_2)^{n_s-4}k_3^{n_{f_{NL}}} + 2 \text{ perms}\big], \tag{3.52}$$

which is consistent with (3.14). This confirms our hypothesis for the running as a power-law (3.37) and extends it with a more general expression for the kernel (3.51).

We now consider the form of primordial bispectrum (3.15), for which this time we have not yet a corresponding parametrization of the running. Again, we interpret the scale dependence of f_{NL} as a kernel which has to be inverted and explicited by performing a matching. We thus identify the combinations in (3.15) which are symmetric under the exchange of k_1 and k_2. Again there are two possibilities: $(k_1k_2)^{n_s-4+\frac{n_{f_{NL}}}{2}}$ and $\big(k_1^{n_s-4+\frac{n_{f_{NL}}}{2}}+k_2^{n_s-4+\frac{n_{f_{NL}}}{2}}\big)k_3^{n_s-4+\frac{n_{f_{NL}}}{2}}$. The first leads to the following kernel solution:

$$f^{12}_{NL}(k_1,k_2,k_3)=\mathcal{A}(k_1k_2)^{\frac{n_{f_{NL}}}{2}}, \tag{3.53}$$

which can be seen to depend only on the internal momenta k_1 and k_2, as opposed to dependence on the external momentum of the power-law (3.49) we have pointed out earlier.
Matching instead with the second possibility let us recover the following result:

$$f^{12}_{NL}(k_1,k_2,k_3)=\frac{\mathcal{A}}{2}\big(k_1^{4-n_s}k_2^{\frac{n_{f_{NL}}}{2}}+k_1^{\frac{n_{f_{NL}}}{2}}k_2^{4-n_s}\big)k_3^{n_s-4+\frac{n_{f_{NL}}}{2}}. \tag{3.54}$$

The general kernel solution is then:

$$f^{12}_{NL}(k_1,k_2,k_3)=\mathcal{A}\big[(1-u)(k_1k_2)^{\frac{n_{f_{NL}}}{2}}+\frac{u}{2}\big(k_1^{4-n_s}k_2^{\frac{n_{f_{NL}}}{2}}+k_1^{\frac{n_{f_{NL}}}{2}}k_2^{4-n_s}\big)k_3^{n_s-4+\frac{n_{f_{NL}}}{2}}\big], \tag{3.55}$$

which substituted in (3.42) leads to:

$$B_\zeta(k_1,k_2,k_3)=\frac{6}{5}\mathcal{A}\big[(k_1k_2)^{n_s-4+\frac{n_{f_{NL}}}{2}}+2\text{ perms}\big], \tag{3.56}$$

as expected.
It is also interesting to consider the large scale-limit in the template (3.15), since we have just recovered it from the generalization of the local shape to a scale-dependent f_{NL}. This is analogous to what we have done in expression (3.40) in the case of the bispectrum arising from the simple power-law parametrization of the running. We thus take the limit $k_L\equiv k_3\to 0$ inside (3.56), which, assuming $n_s\sim 1$ and $n_{f_{NL}}<6$, results in:

$$B_\zeta(k_s,k_L)\simeq\frac{12}{5}\mathcal{A}(k_sk_L)^{n_s-4+\frac{n_{f_{NL}}}{2}}, \tag{3.57}$$

where $k_s\equiv k_1\sim k_2$. We see that this actually corresponds to the scale-dependent non-linear parameter $f_{NL}(k_s,k_L)=\mathcal{A}(k_sk_L)^{\frac{n_{f_{NL}}}{2}}$, i.e. a running both on the small k_s and large k_L scale, as opposed to (3.40) which only has the running on the small scale.

In conclusion, starting from two different, physically meaningful, bispectrum templates, (3.14) and (3.15), we have found two different parametrization of the running, equations (3.51) and (3.55). Substituting these results in (3.46) we have then two different ways of generalizing the local ansatz (3.7) in the case of running non-Gaussianity.
This same procedure may be adopted also for other forms, not considered here, of primordial bispectra arising in the case of running non-Gaussianity, and should allow to recover, by matching with the general expression (3.47), the corresponding solution for the scale-dependent kernel $f^{ij}_{NL}(k_i,k_j,|\vec{k}_i+\vec{k}_j|)$ present in the generalization of the local ansatz (3.46).

Long-short split

It seems natural to also generalize the previously discussed long-short split for the case of scale-dependent non-Gaussianity. It is actually quite straightforward to do so by employing the kernel formalism we have just introduced.

We consider the real space expression (3.41) and we substitute the split (3.25), remembering also the explicit form of the kernel (3.44). In analogy with (3.30), we derive the expression of a small scale perturbation modulated by a large scale one:

$$\zeta_S(\vec{x}) = \zeta_s(\vec{x}) + \frac{3}{5}\int d^3\vec{y}d^3\vec{z}K(\vec{y},\vec{z})\big[\zeta_s(\vec{x}-\vec{y})\zeta_s(\vec{x}-\vec{z}) + 2\zeta_s(\vec{x}-\vec{y})\zeta_l(\vec{x}-\vec{z})\big], \tag{3.58}$$

where we have thus neglected terms including only long wavelength perturbations. In Fourier space it corresponds to:

$$\zeta_S(\vec{k}) = \zeta_s(\vec{k}) + \frac{3}{5}\int \frac{d^3\vec{k}_1 d^3\vec{k}_2}{(2\pi)^3}\delta^{(3)}(\vec{k}-\vec{k}_1-\vec{k}_2)f_{NL}(k_1,k_2,k)\big[\zeta_s(\vec{k}_1)\zeta_s(\vec{k}_2) + 2\zeta_s(\vec{k}_1)\zeta_l(\vec{k}_2)\big], \tag{3.59}$$

where we have explicitly expressed the kernel as the scale-dependent non-linear parameter f_{NL}. The long and short wavelength modes are defined as in (3.27). Since the external momentum $\vec{k}$ is the one relative to a short mode, we can express the modulated short mode, in analogy with (3.42), by means of the following kernel operator:

$$K^{(s)}_{\vec{k}}[\zeta_g,\zeta_g] \equiv \frac{3}{5}\int \frac{d^3\vec{k}_1 d^3\vec{k}_2}{(2\pi)^3}\delta^{(3)}(\vec{k}-\vec{k}_1-\vec{k}_2)f_{NL}(k_1,k_2,k)\big[\zeta_s(\vec{k}_1)\zeta_s(\vec{k}_2) + 2\zeta_s(\vec{k}_1)\zeta_l(\vec{k}_2)\big], \tag{3.60}$$

which does not vanish only for large external momentum $k > k_H$. This ensures that only the combinations of two short modes which couple to a large k are considered inside the integral. The modulated short mode is then expressed as:

$$\zeta_S(\vec{k}) = \zeta_s(\vec{k}) + K^{(s)}_{\vec{k}}[\zeta_g,\zeta_g]. \tag{3.61}$$

This result for the long-short split in the presence of running non-Gaussianity will prove to be useful in Chapter 6 when we will perform some explicit calculations.

Chapter 4

CMB anisotropies

The cosmic microwave background (CMB) radiation is regarded as one of the most important source of information in Cosmology [38, 39], theorized as a fundamental prediction of the standard Hot Big Bang model. The fortuitous measurement of the CMB in 1964, by Penzias and Wilson [40], was in fact considered as a striking evidence for the thermal evolution of the Universe, as opposed to the other possibility proposed at the time, the Steady State Universe [41], a scenario without any expansion.

The CMB is believed to be the direct consequence of an event called recombination, localized around 3×10^5 years after the Big Bang [1]. During its thermal history, the Universe expands while cooling down and its temperature at a given time greatly affects the behaviour of the particle content at that moment. In this discussion we are keeping a much qualitative approach, for more details about the thermal history see for example [7].
Recombination takes place when the Universe is cold enough to allow the formation, for the first time, of a bound state between a proton and an electron, what is known as an hydrogen atom. Qualitatively, this happens when the bound energy starts to prevail over the thermal energy, so that photons are unable to ionize the atoms. Before this time, the ionization is very efficient and protons and electrons exist in a free state. The important aspect to understand the origin of the CMB is that, before recombination, photons and free electrons interact through what is called the Compton scattering and its non-relativistic counterpart, the Thomson scattering. Because of this, photons are continuously scattered and are not able to free stream. Thus, before recombination, the Universe is opaque to electromagnetic radiation. All of this changes with the recombination: electrons end up in a bound state and the cross section for the scattering of photons reduces drastically. Photons start to free stream without being interrupted as much as before. In this context, the CMB radiation is produced when photons scatter the last time before recombination. It can be derived that this happened at a redshift $z_* \simeq 10^3$ [1], which corresponds to what is called the last scattering surface.

After recombination photons are able to freely stream, while their wavelength is being stretched due to the cosmic expansion, corresponding in a decrease of their energy. From equations (1.4) and (1.5), in fact, any physical wavelength evolves proportionally to the scale factor, just due to the expansion of the Universe, i.e. $\lambda_{\text{phys}} \propto a$. Consequently, the frequency, i.e. the energy, evolves like the inverse of the scale factor. Furthermore, before recombination the photon fluid is kept in thermodynamical equilibrium by the continuous scatterings on electrons. This suggests that CMB should have an almost perfect black-body spectrum, a fact which is confirmed by observations, like the measurements from the instrument FIRAS onboard of COBE satellite [42]. It is then possible to associate a temperature to the CMB spectrum, which evolves linearly with the frequency so that, approximately, it holds that $T \propto a^{-1}$ [41].

The latest measured value of the CMB temperature is $T_0 = 2.726 \pm 0.001K$ [43]. This temperature corresponds to wavelengths typical of microwaves, and thus gives the name to the CMB radiation. For many years T_0 had been measured to be the same in every possible direction of the

incoming photons, apart for an overall dipole due to our own motion [44], until COBE in 1992 mapped for the first time temperature anisotropies at a level of 10^{-5} [45]. As of today, the most precise measurements of CMB temperature anisotropies have been achieved by the Planck satellite [46], resulting in the map of Figure 4.1.

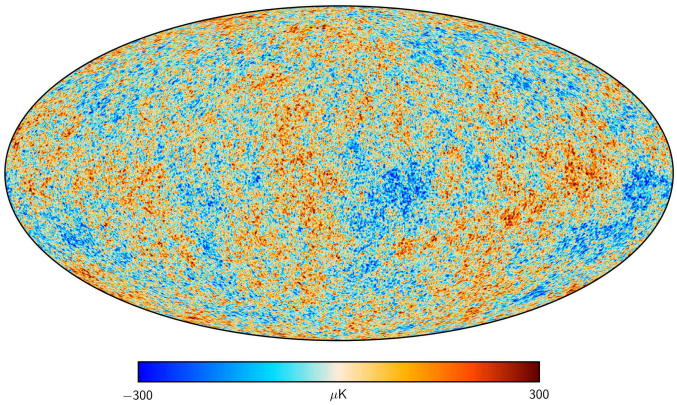

Figure 4.1: Map of CMB temperature, with anisotropies of the order of 10^{-5}. Taken from [47].

We have already seen how the theory of inflation was proposed in early eighties in order to explain, among other things, why at the time the CMB was measured to be homogeneous and isotropic [4]. Nevertheless, its most striking success is to be able to predict CMB anisotropies, interpreted as the consequence of quantum fluctuations during inflation. Those same anisotropies are then the seeds that lead, via gravitational instability, to the formation of the structures present today in our Universe [1]. In such a scenario, quantum fluctuations during inflation are responsible for deviations from a perfectly homogeneous and isotropic Universe. It is then important to understand how the initial conditions set by inflation do evolve throughout space and time. In particular, a fundamental step is to compute the predicted amount of anisotropies in the CMB temperature, produced by inflaton fluctuations which become classic once out of the horizon.

4.1 CMB angular power spectrum

If the CMB was perfectly homogeneous and isotropic, the value of the temperature would be sufficient to fully describes its properties, since it has a nearly perfect black-body spectrum. If this was the case, this observable would not be as interesting as it is today, since fundamental knowledge about the Universe and its evolution comes from studying the tiny fluctuations (at the level of 10^{-5}) around the background temperature, which require additional information in order to be described.
The starting point is then to assume the CMB temperature anisotropies as a direct consequence of primordial scalar quantum fluctuations, from which they inherit the random nature. As we have seen in the Chapter 1, when dealing with random fields the correct approach is to describe their statistical properties. In particular, in the case of the zero-mean field ζ, we have found the power spectrum to be the most simple and insightful statistical correlator, being it the Fourier counterpart of the 2-point correlation function. The aim of this section is thus to find an expression for the present power spectrum of CMB temperature anisotropies, seen as the result of the evolution of primordial fluctuations after they re-entered the horizon.

The statistical behaviour of the photon fluid, i.e. the CMB radiation, is described by its distribution function, which is the Bose-Einstein distribution in the case of a perfect black-body radiation, when the photons are in thermodynamical equilibrium. In this context, CMB temperature anisotropies can then be interpreted as a small departure of the photon distribution function

from the Bose-Einstein one [41]:

$$f(\vec{x},\vec{p},\tau) = \left[\exp\left(\frac{p}{T(\tau)\big(1+\Theta(\vec{x},\hat{p},\tau)\big)}\right) - 1\right]^{-1}, \tag{4.1}$$

which can be expanded, for small Θ, in the following way:

$$f(\vec{x},\vec{p},\tau) \simeq f^{(0)}(p,\tau) - p\frac{\partial f^{(0)}}{\partial p}(p,\tau)\Theta(\vec{x},\hat{p},\tau), \tag{4.2}$$

where $f^{(0)}$ is the background Bose-Einstein distribution function:

$$f^{(0)}(p,\tau) = \left[\exp\left(\frac{p}{T(\tau)}\right) - 1\right]^{-1}. \tag{4.3}$$

The function $\Theta(\vec{x},\hat{p},\tau)$ is thus defined as the first-order temperature perturbation $\frac{\Delta T}{T}$, such that the full CMB temperature field can be written in a way resembling the CPT approach of Chapter 2:

$$T(\vec{x},\hat{p},\tau) = T(\tau)\big[1+\Theta(\vec{x},\hat{p},\tau)\big]. \tag{4.4}$$

In agreement with the cosmological principle, the background temperature does depend only on the conformal time τ. In an analogous way, the zero-order Bose-Einstein distribution function (4.3) depends only on the time τ and on the magnitude of the momentum p, i.e. on the frequency of the photons. The perturbation Θ, instead, introduces two new dependencies:

- $\vec{x}$ is responsible for a spatial dependence, which breaks the homogeneity of the temperature field;
- $\hat{p}$ corresponds to the direction of the photons momentum, whose dependence breaks the isotropy of the system.

The expression (4.4) for the temperature field is as general as it can be, but we actually have to take into account that our observations can be performed only here ($\vec{x_0}$) and now (τ_0). Therefore we can appreciate, in our experiments, only the CMB temperature variation due to a change in the photons direction. This corresponds to a dependence on the polar coordinates θ and ϕ, which makes natural the projection of the first-order temperature perturbation Θ over the surface of a sphere. This is done mathematically by performing the following spherical harmonics expansion [41]:

$$\Theta(\vec{x},\hat{p},\tau) = \sum_{\ell=0}^{\infty}\sum_{m=-\ell}^{\ell} a_{\ell m}(\vec{x},\tau)Y_{\ell m}(\hat{p}), \tag{4.5}$$

where $a_{\ell m}$ are the coefficients of expansion and $Y_{\ell m}$ form an orthonormal basis on the sphere and are called spherical harmonics. The index ℓ is particularly meaningful since can be associated to the angular scale of the anisotropy described by $a_{\ell m}$, through the relation $\theta \sim \ell^{-1}$. More details on spherical harmonics and their properties can be found in Appendix B.2. Exploiting the normalization (B.8) it is then possible to invert equation (4.5) and obtain an expression for the $a_{\ell m}$ coefficients:

$$a_{\ell m}(\vec{x},\tau) = \int d\Omega Y^*_{\ell m}(\hat{p})\Theta(\vec{x},\hat{p},\tau). \tag{4.6}$$

In this way all the information about the temperature perturbation is now contained in the $a_{\ell m}$ coefficients, where the finite resolution of a given experiment determines the ℓ_{max} above which there is no more information.
It is then possible to focus on the statistical properties of the spherical harmonics coefficients $a_{\ell m}(\vec{x},\tau)$, instead of $\Theta(\vec{x},\hat{p},\tau)$. In particular the mean vanishes $\langle a_{\ell m}\rangle = 0$, while the variance C_ℓ is defined by the following 2-point correlator:

$$\langle a_{\ell m} a^*_{\ell' m'}\rangle = \delta_{\ell\ell'}\delta_{mm'}C_\ell, \tag{4.7}$$

and, in analogy with the definition of power spectrum (1.58), takes the name of angular power spectrum. It is interesting to notice, in comparison again with (1.58), that the independence on m of the coefficient C_ℓ stands for isotropy, while the Kronecker deltas ensure homogeneity.

In order to find an explicit expression for the 2-point correlation function (4.7), we actually need to write the coefficients $a_{\ell m}$ in a more manageable way than (4.6). In particular we want to understand how exactly we can compute the ensamble average $\langle \Theta\Theta^* \rangle$. Our goal is to derive an expression for the angular power spectrum today to compare it with observations. Therefore, from now on we fix the dependencies on $\vec{x_0}$ and τ_0 inside all the functions, as we have pointed out earlier. The value of the perturbation $\Theta(\vec{x_0}, \hat{p}, \tau_0)$ is then the result of two different processes: the production of quantum fluctuations during inflation and the following evolution until today. The first is a random process, while the second is deterministic. To account for both processes it is then useful to go into Fourier space and express Θ in the following way [41]:

$$\Theta(\vec{k}, \hat{p}, \tau_0) = \mathcal{T}(\vec{k}, \hat{p})\zeta(\vec{k}), \tag{4.8}$$

where ζ is the gauge-invariant primordial curvature perturbation (2.50), defined in previous Chapters, and $\mathcal{T}$ is the transfer function which accounts for the later evolution. It is remarkable the fact that Θ can be expressed as a linear function of ζ, meaning that the statistical behaviour of the primordial perturbations is recovered unaffected in the temperature anisotropies. In (4.8) we have passed to Fourier space in the usual way:

$$\Theta(\vec{x}, \hat{p}, \tau) = \int \frac{d^3\vec{k}}{(2\pi)^3} e^{i\vec{k}\vec{x}} \Theta(\vec{k}, \hat{p}, \tau). \tag{4.9}$$

We have already found out that the value of the primordial perturbation ζ is conserved while it is out of the horizon and thus it can be interpreted as an initial condition for Θ when the mode crosses the horizon during radiation domination. Therefore $\mathcal{T}$ accounts only for the evolution happening after inflation and inside the horizon, in such a way that it is not random and it can be uniquely determined in a deterministic way, regardless of the result of the primordial random processes. This is done by solving a set of Boltzmann-Einstein coupled equations, where the former describes the evolution of the phase space distribution functions of the cosmic fluid components, accounting for both their interactions and the expansion of the Universe [41]. In particular, in the CMB case, one has to consider two different regimes when the photon fluid behaves differently: at first it is tightly coupled to matter so that the two oscillate with the same frequency; then, at recombination ($z_* \simeq 1100$), the rate of these interactions starts to drop and photons are able to freely stream until today, as we have already reviewed earlier in this Chapter. Without going further into details (see [41]), the final result for Θ is usually given in terms of the coefficients Θ_ℓ of the following expansion:

$$\Theta(\vec{k}, \hat{p}, \tau) = \sum_{\ell=0}^{\infty} (-i)^\ell (2\ell + 1)\Theta_\ell(k, \tau) P_\ell(\hat{k} \cdot \hat{p}), \tag{4.10}$$

where P_ℓ are Legendre polynomials, defined in Appendix B.1. A similar expression holds for the transfer function $\mathcal{T}$, in such a way that relation (4.8) implies:

$$\Theta_\ell(\vec{k}, \tau_0) = \mathcal{T}_\ell(k)\zeta(\vec{k}). \tag{4.11}$$

Actually, in performing the expansion (4.10), we have implicitly assumed that the dependence $(\vec{k}, \hat{p})$ can be expressed as $(k, \hat{k} \cdot \hat{p})$. Exploiting now expansions (4.9) and (4.10), and remembering (4.11), expression (4.6), evaluated at $\vec{x} = \vec{x}_0$ and $\tau = \tau_0$, becomes:

$$\begin{aligned} a_{\ell m}(\vec{x}_0, \tau_0) &= \int d\Omega Y^*_{\ell m}(\hat{p}) \int \frac{d^3\vec{k}}{(2\pi)^3} e^{i\vec{k}\vec{x}_0} \sum_{\ell'=0}^{\infty} (-i)^{\ell'} (2\ell' + 1)\mathcal{T}_{\ell'}(k)\zeta(\vec{k}) P_{\ell'}(\hat{k} \cdot \hat{p}) \\ &= 4\pi(-i)^\ell \int \frac{d^3\vec{k}}{(2\pi)^3} e^{i\vec{k}\vec{x}_0} Y^*_{\ell m}(\hat{k}) \mathcal{T}_\ell(k)\zeta(\vec{k}), \end{aligned} \tag{4.12}$$

where, in the second step, we have expanded the Legendre polynomials over spherical harmonics (B.9) and applied the orthonormality condition (B.8). Computing now the 2-point correlator (4.7)

leads to:

$$\begin{aligned}\langle a_{\ell m} a^*_{\ell' m'}\rangle &= (4\pi)^2(-i)^\ell (i)^{\ell'} \int \frac{d^3\vec{k}}{(2\pi)^3}\int \frac{d^3\vec{k}'}{(2\pi)^3} e^{i\vec{k}\vec{x}_0} e^{-i\vec{k}'\vec{x}_0} \\ &\times Y^*_{\ell m}(\hat{k}) Y_{\ell' m'}(\hat{k}') \mathcal{T}_\ell(k) \mathcal{T}^*_{\ell'}(k') \langle \zeta(\vec{k})\zeta(\vec{k}')\rangle \\ &= (4\pi)^2 \int \frac{d^3\vec{k}}{(2\pi)^3} Y^*_{\ell m}(\hat{k}) Y_{\ell' m'}(\hat{k}) \mathcal{T}_\ell(k) \mathcal{T}^*_{\ell'}(k) P_\zeta(k) \\ &= \frac{2}{\pi}\delta_{\ell\ell'}\delta_{mm'} \int_0^\infty dk k^2 P_\zeta(k) |\mathcal{T}_\ell(k)|^2,\end{aligned} \tag{4.13}$$

where in the second line we have applied the definition of the primordial power spectrum (1.58) and integrated the resulting Dirac delta, while in the third we have used the spherical harmonics normalization condition (B.8). The ensamble average in (4.13) acts only on the random field ζ, since the transfer function $\mathcal{T}$ is fully determined, as we discussed previously. Equating (4.7) and (4.13), it immediately follows the expression for the angular power spectrum we have been looking for:

$$C_\ell = \frac{2}{\pi}\int_0^\infty dk k^2 P_\zeta(k) |\mathcal{T}_\ell(k)|^2. \tag{4.14}$$

This is a general result, which actually needs the expression of the transfer function $\mathcal{T}_\ell$, computed by solving the aforementioned Boltzmann-Einstein set of equations, in order to provide with an explicit prediction for C_ℓ comparable with observations. The derivation and solution of these equations is certainly beyond the scope of this Thesis and we will not treat them. Nevertheless, we present here the result of the computation, written as the value of the anisotropies today (at $\tau = \tau_0$) expressed as a function of the anisotropies at recombination (at $\tau = \tau_*$) [41]:

$$\begin{aligned}\Theta_\ell(k,\tau_0) &= \big[\Theta_0(k,\tau_*) + \phi(k,\tau_*)\big] j_\ell\big[k(\tau_0-\tau_*)\big] \\ &+ 3\Theta_1(k,\tau_*)\left(j_{\ell-1}\big[k(\tau_0-\tau_*)\big] - \frac{\ell(\ell+1) j_\ell\big[k(\tau_0-\tau_*)\big]}{k(\tau_0-\tau_*)}\right) \\ &+ \int_0^{\tau_0} d\tau e^{-\tau_D}\big[\phi'(k,\tau) + \psi'(k,\tau)\big] j_\ell\big[k(\tau_0-\tau)\big],\end{aligned} \tag{4.15}$$

where τ_D is the photons optical depth, not to be confused with the conformal time τ, and is defined such that $-\frac{1}{\tau_D'} = \lambda_{\text{MFP}}$ is the mean free path a photon travels in between two scatterings. In (4.15) we have introduced the spherical Bessel function $j_\ell(k\tau)$ of order ℓ, which quantifies the contribution of a plane-wave of wavenumber k to the anisotropy on an angular scale $\theta \sim \ell^{-1}$.
From equation (4.15) it is not immediately evident how to recover an explicit expression for the transfer function $\mathcal{T}_\ell$, since the linear dependence on ζ is not manifest as in (4.11). This is because the result is written as a function of quantities evaluated at recombination, which can themselves be computed solving the Boltzmann-Einstein equations in the tightly coupled regime, making thus explicit the dependence on ζ.
The final prediction for the CMB temperature anisotropies angular power spectrum is plotted in Figure 4.2 as the best fit curve in agreement with observational data [3].

Let us now briefly cover the three different terms which contribute to the present temperature anisotropies in equation (4.15).

- The first contribution is usually called the Sachs-Wolfe term. It includes the monopole of the distribution Θ_0, which corresponds to the intrinsic temperature anisotropy, and the gravitational potential ϕ, defined in Chapter 2, both evaluated at recombination. The presence of the latter accounts for a gravitational redshift effect, due to photons having to climb out of potential wells at the last scattering surface.

- The second term is the Doppler one, since it consists of the dipole moment Θ_1, again at recombination, mainly attributable to the relative velocity between the observer and the CMB rest frames.

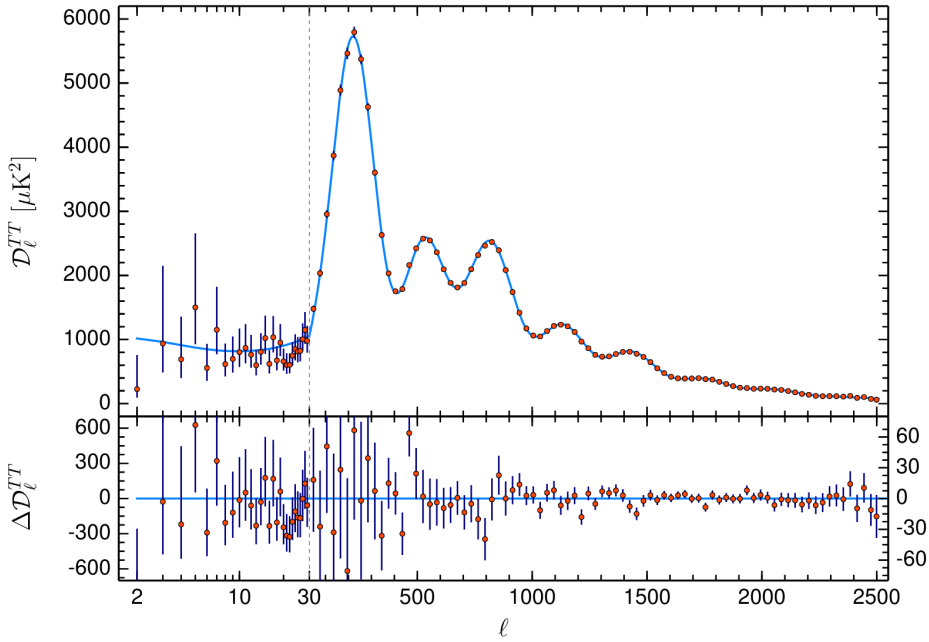

Figure 4.2: Planck 2018 [3] temperature power spectrum, $D_\ell^{TT} \equiv \ell(\ell+1)C_\ell^{TT}/2\pi$. The base-$\Lambda CDM$ theoretical spectrum best fit is plotted in light blue in the upper panel. Residuals with respect to this model are shown in the lower panel.

- The last is an integrated term, namely the Integrated Sachs-Wolfe (ISW) term. It depends on the time variation of the gravitational potentials throughout the history of the Universe, until the present $\tau = \tau_0$. This is the only term, out of the three, which accounts for later evolution after recombination.

In order to have a qualitative understanding we can focus on just the Sachs-Wolfe term, which allows us to explain the two main features of the CMB angular power spectrum profile: the plateau at low multipoles and the acoustic peaks at smaller scales.

4.1.1 Large angular scales

If we consider super-horizon perturbations at recombination we know that no causal physical process can affect them so that they are fully determined by the initial conditions set by the primordial fluctuations. It can be shown that in this scenario the Sachs-Wolfe term in (4.15) dominates and it can be expressed in terms of the primordial curvature perturbation [41]:

$$(\Theta_0 + \phi)(k, \tau_*) = -\frac{1}{5}\zeta(\vec{k}). \tag{4.16}$$

Furthermore, this term can be interpreted and motivated with simple physical arguments, since on largest scales the observed anisotropies are determined by the monopole at recombination Θ_0 plus the gravitational potential ϕ, which accounts for a gravitational redshift effect due to the fact that photons, at recombination, have to climb out of potential wells, losing energy in doing so. This phenomenon is known as the Sachs-Wolfe effect [48] and it dominates on largest scales.

It is then possible to compute the predicted angular power spectrum when accounting only for the Sachs-Wolfe term in (4.15). From (4.16) we can write:

$$\Theta_\ell^{SW}(k, \tau_0) \simeq -\frac{1}{5}\zeta(\vec{k}) j_\ell\big[k(\tau_0 - \tau_*)\big], \tag{4.17}$$

in such a way that it is possible, by comparison with equation (4.11), to find an explicit expression for the transfer function:

$$\mathcal{T}_\ell^{SW}(k) = -\frac{1}{5} j_\ell\big[k(\tau_0 - \tau_*)\big]. \tag{4.18}$$

We thus see that, dealing with large scale anisotropies, we are able to compute the result for the angular power spectrum today. Inserting (4.18) in (4.14) gives:

$$C_\ell^{SW} = \frac{2}{\pi}\frac{1}{25}\int_0^\infty dk k^2 \frac{2\pi^2}{k^3}\mathcal{P}_\zeta(k) j_\ell^2\big[k(\tau_0 - \tau_*)\big], \tag{4.19}$$

where we have used the expression of the adimensional power spectrum (1.61). Moreover, integrating the definition of the scalar spectral index (1.73), we can write $\mathcal{P}_\zeta = A_s\big(\frac{k}{k_p}\big)^{n_s-1}$, where A_s is a dimensionless amplitude and k_p a reference scale, so that (4.19) becomes:

$$C_\ell^{SW} = \frac{4\pi}{25} A_s k_p^{1-n_s}\int_0^\infty dk k^{n_s-2} j_\ell^2\big[k(\tau_0 - \tau_*)\big]. \tag{4.20}$$

In order to solve this integral it is useful to exploit relation (B.12) involving the spherical Bessel functions, making also use of the fact that $\tau_* \ll \tau_0$. The final result for the angular power spectrum in the Sachs-Wolfe regime is:

$$C_\ell^{SW} = \frac{4\pi}{25} A_s (k_p\tau_0)^{1-n_s} 2^{n_s-4}\pi \frac{\Gamma\Big(\ell + \frac{n_s}{2} - \frac{1}{2}\Big)\Gamma(3-n_s)}{\Gamma\Big(\ell + \frac{5}{2} - \frac{n_s}{2}\Big)\Gamma^2\Big(2 - \frac{n_s}{2}\Big)}, \tag{4.21}$$

where the Euler Gamma function Γ is defined in Appendix B.5. In the simple case of a scale-invariant power spectrum, i.e. $n_s = 1$, result (4.21) can be rearranged as:

$$\ell(\ell+1)C_\ell^{SW} = \frac{2\pi}{25} A_s, \tag{4.22}$$

which actually corresponds to a constant angular power spectrum per logarithmic interval. We have used properties (B.19) and (B.20) to compute explicitly the Gamma functions in (4.21). This scale-invariant behaviour is directly inherited from the primordial power spectrum and it is a confirm that on largest scales any kind of evolution is frozen. The result (4.22) may be recognized as the plateau in Figure 4.2 in correspondence to the lower multipoles, until $\ell \sim 30$, and it is the reason why usually in the literature the plotted quantity is $\ell(\ell+1)C_\ell$, instead of just C_ℓ.

4.1.2 Acoustic peaks

We have just seen that the treatment of super-horizon perturbations is quite simple, since they don't experience any evolution. But what if a given mode re-enters the horizon and does so before the epoch of recombination? When this happens the perturbation associated to the mode starts to be influenced once again by causal physics.

Before recombination the interactions between photons and matter are so efficient that the two species can be regarded as a single fluid, whose dynamics is essentially driven by two competing forces: the repulsion due to the photon pressure and the gravitational attraction experienced by baryons. The net result is an oscillating evolution of the fluid, with a frequency determined by the baryon density Ω_b. Therefore, the Sachs-Wolfe term, as a function of k, in (4.15) assumes different value depending on which stage of oscillation it is going through at recombination. The evolution until recombination of different modes is plotted in Figure 4.3. A mode, with wavenumber k, experiencing at τ_* a maximum compression or rarefaction corresponds to a peak in the angular power spectrum centered around $\ell \sim k\tau_0$, while the opposite happens for modes with vanishing amplitude at recombination, for which we expect a trough in the spectrum at the corresponding scale.

The description we have just given is a bit sketchy and certainly qualitative, but it at least physically motivates the presence of what are called the acoustic peaks, visible in the spectrum of Fig. 4.2 for $\ell \gtrsim 30$.

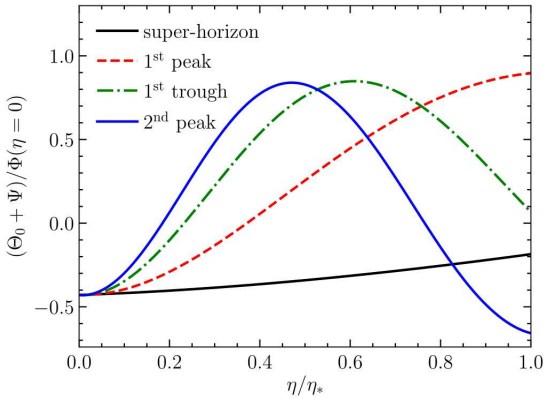

Figure 4.3: Time evolution of the Sachs-Wolfe term in the CMB temperature anisotropies. The evolution of modes with different wavenumber is shown. The amplitude at recombination is what determines the spectrum height at $\ell \sim k\tau_0$. In particular, it can be noticed that the super-horizon mode is shown to be not oscillating. In our notation $\Psi = \phi$ and $\Phi = -\psi$. Taken from [41].

4.2 CMB bispectrum

So far in this Chapter we have derived how the CMB temperature anisotropies are a product of the primordial perturbations evolution. In particular, the linear proportionality between Θ and ζ, expressed by relation (4.8), suggests that the CMB itself can be regarded as a source of information about the statistical properties of perturbations generated during inflation. We know, in fact, that the statistics of a given random field is described by the full set of n-point correlation functions. In the CMB case any n-point correlator of the present temperature anisotropy $\Theta(\vec{k}, \hat{p}, \tau_0)$ can be written schematically as:

$$\langle \Theta(\vec{k}_1)\Theta(\vec{k}_2)...\Theta(\vec{k}_n)\rangle = \left(\prod_{i=1}^{n} \mathcal{T}(\vec{k}_i)\right)\langle \zeta(\vec{k}_1)\zeta(\vec{k}_2)...\zeta(\vec{k}_n)\rangle. \tag{4.23}$$

It follows in particular that a non-vanishing higher order correlator of $\Theta(\vec{k}, \hat{p}, \tau_0)$ must be related to a non-vanishing correlator of the primordial perturbation $\zeta(\vec{k})$ of the same order. Furthermore, the proportionality factor is given deterministically by a product of transfer functions. In Chapter 3 we have introduced the primordial bispectrum as the main indicator of the presence of non-Gaussianity in some form. Setting $n = 3$ in relation (4.23) it is thus possible to probe primordial non-Gaussianity by means of the CMB bipectrum.

4.2.1 Angular bispectrum

In section 4.1 we have seen how it is natural, when dealing with CMB temperature anisotropies, to project the temperature field over the spherical sky by performing a spherical harmonics expansion. This has led us to compute the angular power spectrum (4.14), which is given by the 2-point correlation function of the expansion coefficients (4.7). In an analogous way it is possible to define the CMB temperature angular bispectrum, as the 3-point correlation function of the spherical harmonics expansion coefficients (4.6):

$$B^{m_1 m_2 m_3}_{\ell_1 \ell_2 \ell_3} = \langle a_{\ell_1 m_1} a_{\ell_2 m_2} a_{\ell_3 m_3}\rangle. \tag{4.24}$$

Assuming rotational invariance, we can average out the dependence on m without losing any physical information. We thus define the angle-averaged bispectrum as [16]:

$$B_{\ell_1 \ell_2 \ell_3} = \sum_{m_1 m_2 m_3} \begin{pmatrix} \ell_1 & \ell_2 & \ell_3 \\ m_1 & m_2 & m_3 \end{pmatrix} B^{m_1 m_2 m_3}_{\ell_1 \ell_2 \ell_3}, \tag{4.25}$$

where we have introduced the Wigner-3j symbol (Appendix B.4), which explicitly requires the angular bispectrum $B^{m_1m_2m_3}_{\ell_1\ell_2\ell_3}$ to satisfy the following triangle conditions and selection rules:

$$\begin{aligned} &m_1+m_2+m_3=0,\\ &\ell_1+\ell_2+\ell_3=\text{integer},\\ &|\ell_i-\ell_j|\leq\ell_k\leq\ell_i+\ell_j. \end{aligned} \tag{4.26}$$

As a result, it is possible to express $B^{m_1m_2m_3}_{\ell_1\ell_2\ell_3}$ in the following way [16]:

$$B^{m_1m_2m_3}_{\ell_1\ell_2\ell_3}=\mathcal{G}^{m_1m_2m_3}_{\ell_1\ell_2\ell_3}b_{\ell_1\ell_2\ell_3}, \tag{4.27}$$

where $b_{\ell_1\ell_2\ell_3}$ is called reduced bispectrum and carries all the physical information contained in $B^{m_1m_2m_3}_{\ell_1\ell_2\ell_3}$. The factor $\mathcal{G}^{m_1m_2m_3}_{\ell_1\ell_2\ell_3}$ is the Gaunt integral and satisfies all the geometrical conditions mentioned earlier. It is a real quantity defined by the integral:

$$\begin{aligned} \mathcal{G}^{m_1m_2m_3}_{\ell_1\ell_2\ell_3}&\equiv\int d\Omega Y_{\ell_1m_1}(\hat{n})Y_{\ell_2m_2}(\hat{n})Y_{\ell_3m_3}(\hat{n})\\ &=\sqrt{\frac{(2\ell_1+1)(2\ell_2+1)(2\ell_3+1)}{4\pi}}\begin{pmatrix}\ell_1&\ell_2&\ell_3\\0&0&0\end{pmatrix}\begin{pmatrix}\ell_1&\ell_2&\ell_3\\m_1&m_2&m_3\end{pmatrix}. \end{aligned} \tag{4.28}$$

It is clear the analogy of expression (4.27) with the definition of angular power spectrum (4.7): the Gaunt integral plays a similar role of the Kronecker deltas and ensures homogeneity, while isotropy is manifest from the m-independence of the reduced bispectrum.
Substituting (4.27) back inside (4.25) one obtains the relation between the angle-averaged and the reduced bispectrum:

$$B_{\ell_1\ell_2\ell_3}=\sqrt{\frac{(2\ell_1+1)(2\ell_2+1)(2\ell_3+1)}{4\pi}}\begin{pmatrix}\ell_1&\ell_2&\ell_3\\0&0&0\end{pmatrix}b_{\ell_1\ell_2\ell_3}, \tag{4.29}$$

where we have used the orthogonality relation (B.16). Since all the physical information is contained in the reduced bispectrum, or equivalently the angle-averaged one, we may regard it as the actual observable quantity, whereas the Gaunt integral ensures the geometrical properties (4.26) and allows to recover the full expression (4.24) of the angular bispectrum.

We can now compute explicitly the 3-point correlation function (4.24), by substituting the expression of the expansion coefficients written as a function of the primordial perturbation $\zeta(\vec{k})$ (4.12). We obtain the angular bispectrum in terms of the primordial one:

$$\begin{aligned} B^{m_1m_2m_3}_{\ell_1\ell_2\ell_3}&=(4\pi)^3(-i)^{\ell_1+\ell_2+\ell_3}\int\frac{d^3\vec{k}_1}{(2\pi)^3}\int\frac{d^3\vec{k}_2}{(2\pi)^3}\int\frac{d^3\vec{k}_3}{(2\pi)^3}e^{i(\vec{k}_1+\vec{k}_2+\vec{k}_3)\vec{x}_0}\\ &\times Y^*_{\ell_1m_1}(\hat{k}_1)Y^*_{\ell_2m_2}(\hat{k}_2)Y^*_{\ell_3m_3}(\hat{k}_3)\mathcal{T}_{\ell_1}(k_1)\mathcal{T}_{\ell_2}(k_2)\mathcal{T}_{\ell_3}(k_3)\langle\zeta(\vec{k}_1)\zeta(\vec{k}_2)\zeta(\vec{k}_3)\rangle\\ &=(4\pi)^3(-i)^{\ell_1+\ell_2+\ell_3}\int\frac{d^3\vec{k}_1}{(2\pi)^3}\int\frac{d^3\vec{k}_2}{(2\pi)^3}\int\frac{d^3\vec{k}_3}{(2\pi)^3}Y^*_{\ell_1m_1}(\hat{k}_1)Y^*_{\ell_2m_2}(\hat{k}_2)Y^*_{\ell_3m_3}(\hat{k}_3)\\ &\times\mathcal{T}_{\ell_1}(k_1)\mathcal{T}_{\ell_2}(k_2)\mathcal{T}_{\ell_3}(k_3)(2\pi)^3\delta^{(3)}(\vec{k}_1+\vec{k}_2+\vec{k}_3)B_\zeta(k_1,k_2,k_3), \end{aligned} \tag{4.30}$$

where we have exploited the definition of primordial bispectrum (3.2) in the second equality. In order to proceed we can expand the Dirac delta over spherical harmonics to get the following representation [49]:

$$\begin{aligned} \delta^{(3)}(\vec{k}_1+\vec{k}_2+\vec{k}_3)&=\int\frac{d^3\vec{r}}{(2\pi)^3}e^{i(\vec{k}_1+\vec{k}_2+\vec{k}_3)\vec{r}}\\ &=\int d^3\vec{r}\prod_{i=1}^{3}\left[2\sum_{\ell_im_i}i^{\ell_i}j_{\ell_i}(k_ir)Y^*_{\ell_im_i}(\hat{r})Y_{\ell_im_i}(\hat{k}_i)\right]. \end{aligned} \tag{4.31}$$

Therefore, going back to expression (4.30), we obtain:

$$\begin{aligned} B^{m_1m_2m_3}_{\ell_1\ell_2\ell_3} &= \int d^3\vec{r}\prod_{i=1}^{3}\left[\frac{2}{\pi}\sum_{L_iM_i}(-i)^{\ell_i}i^{L_i}Y^*_{L_iM_i}(\hat{r})\int_0^\infty dk_i k_i^2\mathcal{T}_{\ell_i}(k_i)j_{L_i}(k_ir)\right. \\ &\quad\left.\times\int d^2\hat{k}Y^*_{\ell_im_i}(\hat{k}_i)Y_{L_iM_i}(\hat{k}_i)\right]B_\zeta(k_1,k_2,k_3) \\ &= \mathcal{G}^{m_1m_2m_3}_{\ell_1\ell_2\ell_3}\int_0^\infty drr^2\prod_{i=1}^{3}\left[\frac{2}{\pi}\int_0^\infty dk_ik_i^2\mathcal{T}_{\ell_i}(k_i)j_{\ell_i}(k_ir)\right]B_\zeta(k_1,k_2,k_3), \end{aligned} \tag{4.32}$$

where in the second equality we have used the spherical harmonics normalization condition (B.8) and the definition of the Gaunt integral (4.28). Remembering equation (4.27), the reduced bispectrum is then:

$$b_{\ell_1\ell_2\ell_3} = \int_0^\infty drr^2\prod_{i=1}^{3}\left[\frac{2}{\pi}\int_0^\infty dk_ik_i^2\mathcal{T}_{\ell_i}(k_i)j_{\ell_i}(k_ir)\right]B_\zeta(k_1,k_2,k_3). \tag{4.33}$$

Equation (4.32), together with the analogous (4.33), is a general result which holds for any given expression of the primordial bispectrum. Measuring the observable CMB reduced bispectrum thus allows to recover information about the amplitude and the shape of the primordial non-Gaussianity.

4.2.2 CMB bispectrum from local primordial non-Gaussianity

Result (4.32) can be specified for the case of primordial bispectrum with a local shape. In Chapter 3 we computed the 3-point correlator of the primordial perturbation ζ parametrized by the local ansatz (3.7). Substituting the resulting bispectrum (3.24) inside equation (4.33), we obtain:

$$\begin{aligned} b_{\ell_1\ell_2\ell_3} &= \frac{6}{5}f_{NL}\int_0^\infty drr^2\left[\left(\frac{2}{\pi}\int_0^\infty dk_1k_1^2P_\zeta(k_1)\mathcal{T}_{\ell_1}(k_1)j_{\ell_1}(k_1r)\right)\right. \\ &\quad\left.\times\left(\frac{2}{\pi}\int_0^\infty dk_2k_2^2P_\zeta(k_2)\mathcal{T}_{\ell_2}(k_2)j_{\ell_2}(k_2r)\right)\left(\frac{2}{\pi}\int_0^\infty dk_3k_3^2\mathcal{T}_{\ell_3}(k_3)j_{\ell_3}(k_3r)\right)+2\text{ perm}\right]. \end{aligned} \tag{4.34}$$

It is then possible to define the following coefficients [30]:

$$\alpha_\ell(r) \equiv \frac{2}{\pi}\int_0^\infty dkk^2\mathcal{T}_\ell(k)j_\ell(kr), \tag{4.35}$$

$$\beta_\ell(r) \equiv \frac{2}{\pi}\int_0^\infty dkk^2P_\zeta(k)\mathcal{T}_\ell(k)j_\ell(kr), \tag{4.36}$$

in such a way that the reduced bispectrum (4.34) can be written as:

$$b_{\ell_1\ell_2\ell_3} = \frac{6}{5}f_{NL}\int_0^\infty drr^2\left[\alpha_{\ell_1}(r)\beta_{\ell_2}(r)\beta_{\ell_3}(r)+\alpha_{\ell_2}(r)\beta_{\ell_3}(r)\beta_{\ell_1}(r)+\alpha_{\ell_3}(r)\beta_{\ell_1}(r)\beta_{\ell_2}(r)\right]. \tag{4.37}$$

In general, this result can be directly implemented into a code to perform the numerical integration over r. In order to compute coefficients (4.35) and (4.36) explicit expressions for the primordial power spectrum and transfer function are needed. The latter is usually provided by Einstein-Boltzmann solvers, like CMBFAST [50] and CAMB [51], which solve the full system of equations accounting for the evolution of perturbations after they re-enter the horizon during the post-inflationary period.

Sachs-Wolfe regime

It is possible to analytically solve the integrals in equation (4.37) by assuming the explicit expression for the transfer function in the Sachs-Wolfe regime (4.18). Remember that it is valid for angular scales larger than the horizon at recombination, for which we have considered only the Sachs-Wolfe

term in the expression (4.15) of the temperature anisotropy today. We have already seen how this assumption simplifies the expression of the angular power spectrum, and a similar outcome follows for the reduced bispectrum. We then substitute the transfer function (4.18) inside the expressions for coefficients (4.35) and (4.36), obtaining:

$$\alpha_\ell^{SW}(r) = -\frac{2}{5\pi}\int_0^\infty dk k^2 j_\ell\big[k(\tau_0-\tau_*)\big] j_\ell(kr), \tag{4.38}$$

$$\beta_\ell^{SW}(r) = -\frac{2}{5\pi}\int_0^\infty dk k^2 P_\zeta(k) j_\ell\big[k(\tau_0-\tau_*)\big] j_\ell(kr). \tag{4.39}$$

Remembering the assumption $\tau_* \ll \tau_0$, we recognize in (4.38) the spherical Bessel function closure relation (B.11), so that it becomes:

$$\alpha_\ell^{SW}(r) = -\frac{1}{5}\frac{\delta(r-\tau_0)}{r^2}. \tag{4.40}$$

The resulting Dirac delta is used to perform the integration over r in equation (4.37) and we are left with:

$$\begin{aligned} b^{SW}_{\ell_1\ell_2\ell_3} = -\frac{6}{25} f_{NL}\Bigg[&\bigg(-\frac{2}{5\pi}\int_0^\infty dk_1 k_1^2 P_\zeta(k_1) j^2_{\ell_1}(k_1 r)\bigg) \\ &\times\bigg(-\frac{2}{5\pi}\int_0^\infty dk_2 k_2^2 P_\zeta(k_2) j^2_{\ell_2}(k_2 r)\bigg) + 2 \text{ perm}\Bigg], \end{aligned} \tag{4.41}$$

where the terms inside the parentheses are non other than the CMB angular power spectrum in the Sachs-Wolfe limit (4.19). It follows that the CMB temperature reduced bispectrum, in the Sachs-Wolfe regime, can be expressed in terms of the CMB temperature angular power spectrum in the following way:

$$b^{SW}_{\ell_1\ell_2\ell_3} = -6 f_{NL}\big[C^{SW}_{\ell_1} C^{SW}_{\ell_2} + C^{SW}_{\ell_2} C^{SW}_{\ell_3} + C^{SW}_{\ell_3} C^{SW}_{\ell_1}\big]. \tag{4.42}$$

As expected, this result holds only for large angular scales, when ℓ_1, ℓ_2 and ℓ_3 are all less than ~ 10 [16].

4.2.3 CMB bispectrum from running primordial non-Gaussianity

Exploiting the results of sections 3.2.2 and 3.2.3, we can now compute the CMB angular bispectrum in the case of a running non-Gaussianity parametrized as a generalization of the local model (3.7). We just need to consider the corresponding primordial bispectrum and substitute it inside expression (4.33) for the CMB reduced bispectrum. This leads to calculations almost identical to the one we have done in the previous section, such that the result can still be written as equation (4.37), with the only difference being the scale dependence of f_{NL} now has to be included in the definition of either α_ℓ and/or β_ℓ.
We are going to discuss the two simple parametrizations (3.49) and (3.53) for f_{NL} we have derived by generalizing the local ansatz as (3.46) and performing a matching with known primordial bispectrum templates.

In the first case, corresponding to the power-law parametrization of the running (3.37), we find the following reduced bispectrum:

$$b_{\ell_1\ell_2\ell_3} = \frac{6}{5} f_{NL}(k_p)\int_0^\infty dr r^2\big[\alpha_{\ell_1}(r)\beta_{\ell_2}(r)\beta_{\ell_3}(r) + \alpha_{\ell_2}(r)\beta_{\ell_3}(r)\beta_{\ell_1}(r) + \alpha_{\ell_3}(r)\beta_{\ell_1}(r)\beta_{\ell_2}(r)\big], \tag{4.43}$$

where the scale dependence of f_{NL} affects the expression of the α_ℓ coefficient in the following way:

$$\alpha_\ell(r) \equiv \frac{2}{\pi}\frac{1}{k_p^{n_{f_{NL}}}}\int_0^\infty dk k^{2+n_{f_{NL}}}\mathcal{T}_\ell(k) j_\ell(kr), \tag{4.44}$$

while $\beta_\ell(r)$ keeps instead the same expression of the constant-f_{NL} case (4.36). It seems natural to take the Sachs-Wolfe limit, for which (4.44) becomes:

$$\alpha_\ell^{SW}(r) = -\frac{2}{5\pi}\frac{1}{k_p^{n_{f_{NL}}}}\int_0^\infty dk k^{2+n_{f_{NL}}} j_\ell\big[k(\tau_0-\tau_*)\big] j_\ell(kr). \tag{4.45}$$

Unfortunately the scale dependence introduced by $f_{NL}(k)$ does not allow to recover an analytic solution of this integral, meaning that we cannot derive the analogous of expression (4.42) without making any further assumption.

The expression (3.15) for a scale-dependent f_{NL} leads to the same expression (4.43), where the coefficient $\alpha_\ell(r)$ is defined as in (4.35) and β_ℓ has to be modified in this way:

$$\beta_\ell(r) \equiv \frac{2}{\pi}\frac{1}{k_p^{n_{f_{NL}}/2}}\int_0^\infty dk k^{2+\frac{n_{f_{NL}}}{2}} P_\zeta(k)\mathcal{T}_\ell(k) j_\ell(kr). \tag{4.46}$$

Since $\alpha_\ell(r)$ is left untouched from the constant-f_{NL} case, this time it is possible to take the Sachs-Wolfe limit, for which the CMB reduced bispectrum becomes:

$$\begin{aligned} b^{SW}_{\ell_1\ell_2\ell_3} = -\frac{6}{25} f_{NL}(k_p)\Bigg[&\left(-\frac{2}{5\pi}\frac{1}{k_p^{n_{f_{NL}}/2}}\int_0^\infty dk_1 k_1^{2+\frac{n_{f_{NL}}}{2}} P_\zeta(k_1) j^2_{\ell_1}(k_1 r)\right) \\ &\times\left(-\frac{2}{5\pi}\frac{1}{k_p^{n_{f_{NL}}/2}}\int_0^\infty dk_2 k_2^{2+\frac{n_{f_{NL}}}{2}} P_\zeta(k_2) j^2_{\ell_2}(k_2 r)\right) + 2 \text{ perm}\Bigg]. \end{aligned} \tag{4.47}$$

Nevertheless, remember that the the CMB angular power spectrum is not affected, at first order, by non-Gaussian contributions, in such a way that its expression (4.19) in the Sachs-Wolfe regime holds even when considering a scenario with running non-Gaussianity. We thus conclude that the result (4.42), relating the CMB angular power spectrum and reduced bispectrum in the SW limit, is an exclusive feature of the local model of primordial non-Gaussianity (3.7) with constant f_{NL}.

Chapter 5

The Cosmological Gravitational Wave Background

In Chapter 4 we have seen how the CMB may be regarded as an observable to probe, among other things, the possible presence of non-Gaussianity of primordial scalar perturbations. The key point is that the CMB temperature anisotropies, on a given scale, are set by the corresponding mode of the gauge-invariant curvature perturbation ζ at the time when it crosses the horizon after inflation. Since all the subsequent evolution is deterministic, the statistical properties of the temperature anisotropies we measure today describe the statistical nature of the perturbation ζ during inflation and thus allow to test for the presence of primordial non-Gaussianity.

The main focus of the original part of this work is actually to consider another, independent, probe for primordial non-Gaussianity, which is represented by the so called cosmological gravitational wave background (CGWB) [52, 53]. First of all, we need to define what we refer to as a gravitational wave background and to understand why the CGWB can be considered a fundamental and unique observable to probe the early Universe.

5.1 Gravitational waves in a linearized theory of gravity

Gravitational waves (GWs) are a natural prediction of the theory of General Relativity and can be identified as the transverse and traceless tensor degrees of freedom of the perturbed metric, as we have already mentioned in Chapter 2 discussing Cosmological Perturbation Theory. In a linearized theory of gravity, we can define GWs to be a small perturbation around the Minkowski flat metric:

$$g_{\mu\nu} = \eta_{\mu\nu} + h_{\mu\nu}, \tag{5.1}$$

with $|h_{\mu\nu}| \ll 1$. Vacuum Einstein equations for the linearized metric (5.1) reads [54]:

$$\Box \bar{h}_{\mu\nu} = 0, \tag{5.2}$$

where we have assumed the de Donder gauge $\partial^\mu \bar{h}_{\mu\nu} = 0$ and introduced the trace-reversed metric perturbation:

$$\bar{h}_{\mu\nu} = h_{\mu\nu} - \frac{1}{2}\eta_{\mu\nu} h, \tag{5.3}$$

where $h \equiv h^\mu{}_\mu$ and for which $\bar{h} = -h$. It is now possible to show [54] that there are actually 4 redundant degrees of freedom not fixed by the gauge choice, represented by the infinitesimal coordinate transformation $x'^\mu = x^\mu + \xi^\mu$ with $\Box \xi^\mu = 0$. We can then choose ξ^μ in order to impose the conditions $h_{0i} = 0$ and $h = -\bar{h} = 0$, so that it is also $\bar{h}_{\mu\nu} = h_{\mu\nu}$. From the de Donder condition then it follows that the component h_{00} is constant in time and can be set to vanish, since we consider the GW itself to be just the time-dependent part. Such choices define the transverse and traceless (TT) gauge, where the remaining spatial components h_{ij} must satisfy the conditions $h^i{}_i = 0$ and $\partial^i h_{ij} = 0$. This explains why we have identified the transverse and traceless tensor

degrees of freedom χ_{ij} in (2.5) as gravitational waves in the first place.
In the TT-gauge, equation (5.2) maintains the same form $\Box h_{\mu\nu} = 0$ when going back to the $h_{\mu\nu}$ variable. It is a wave equation whose solution can in general be expressed as a superposition of Fourier modes:

$$h_{ij}(t, \vec{x}) = \int d^3\vec{k}\left[h_{ij}(\vec{k})e^{ik_\mu x^\mu} + h^*_{ij}(\vec{k})e^{-ik_\mu x^\mu}\right], \tag{5.4}$$

with $k^i h_{ij}(\vec{k}) = 0$ and $k^\mu k_\mu = 0$. We have neglected the $h_{0\mu}$ components since in the TT gauge they all vanish. Assuming a plane-wave traveling in the $\hat{z}$ direction, the solution (5.4) reduces to:

$$h_{ij}(z, t) = \begin{pmatrix} h_+ & h_\times & 0 \\ h_\times & -h_+ & 0 \\ 0 & 0 & 0 \end{pmatrix} e^{ik(z-t)}, \tag{5.5}$$

where the two transverse and traceless tensor degrees of freedom, h_+ and $h_\times$, correspond to the two possible polarization states of the gravitational waves, + and ×. This is a direct manifestation of the nature of the gravitational interaction whose mediator, the graviton, is a massless spin-two boson.
Here we have just provided with the main results of the linearized theory of gravity in flat space, leading to the gravitational wave solution (5.4). For more details see [54].

5.1.1 Gravitational waves in curved spacetime

Our discussion so far has been centered around the linearized metric (5.1), where a gravitational wave is interpreted as a small perturbation around the flat spacetime. Nevertheless, in Cosmology we are more interested in considering the scenario of gravitational waves traveling throughout the physical spacetime, which at the background level we know to be described by the FLRW metric (1.1). More in general, it is necessary to find a way to describe gravitational waves in a curved spacetime. In analogy to the linearized case (5.1) we can write:

$$g_{\mu\nu}(x) = \bar{g}_{\mu\nu}(x) + h_{\mu\nu}(x), \tag{5.6}$$

where this time the background metric is a function of the spacetime coordinate x. It follows that isolating the gravitational wave $h_{\mu\nu}$ may not happen to be a trivial task. In such a context, this is made possible by considering a separation of scales/frequencies [52]. The idea is quite simple: basically we can distinguish the gravitational wave from the background by means of the length-scale over which they vary. This is actually the case when the background $\bar{g}_{\mu\nu}$ varies over L_B, while GWs have a typical wavelength $\lambda \ll L_B$. An analogous distinction can be performed by means of the different variations over a period of time, where the typical frequency of the GWs is much larger than the frequency which characterizes the variations of the background $f \gg f_B$. In this way the GWs are seen as small perturbations on a smooth background or, equivalently, as rapidly varying perturbations on a slowly varying background.
In general, when the background is curved, it is not possible to write the metric perturbations in the TT gauge, where h_+ and $h_\times$ are the only degrees of freedom. From our discussion in Chapter 2 we know indeed that there are in total four additional physical degrees of freedom: two scalars and two transverse vectors. Nevertheless, it is possible to show [52] that h_+ and $h_\times$ are the two only physical radiative degrees of freedom, whereas the metric can contain also scalar and vector non-radiative ones.

5.2 Stochastic background of gravitational waves

We have seen how the transverse and traceless tensor metric perturbations h_{ij} can be associated to gravitational waves propagating on a sufficiently smooth background. We will refer to h_{ij} as the amplitude of GWs. Its physical degrees of freedom are the actual observables which detectors on Earth [55] are capable of measuring.

Since the first detection, GW150914 [56], all measured GW signals until now have been associated with localized astrophysical events. In this context, it is then possible to distinguish between transient GWs, due to binary inspirals or burst events, and continuous periodic ones, generating for example from pulsars [57].
In Cosmology we are instead mainly interested in a very different type of signal, namely a stochastic background of gravitational waves, coming from all direction and with the defining property of being describable only in a statistical way. In the case of a stochastic background, the amplitude h_{ij} is in fact regarded as a random variable, which as we already know can be described only by means of statistical correlators. We then refer to a stochastic background of cosmological origin as a cosmological gravitational wave background (CGWB). When searching for this background [58], to first approximation homogeneity and isotropy can be assumed, in a similar way as the CMB case. It is indeed a very similar concept to the CMB one, where the photons are substituted by gravitational waves, arising from some kind of cosmological process in the early Universe. Actually, a stochastic background of astrophysical nature is also expected to be produced by the superposition of a large number of independent sources [59] and it is thus necessary to be able to distinguish it from the CGWB. This can be achieved, for example, by separating different frequency dependencies, which are determined by the characteristic scales of the cosmological processes.

The detection of a stochastic background of GWs is not a simple task, since, unlike the other types of signal, its statistical nature would make it appear as noise in a single detector [57]. The signal is in fact a random field which can be expressed as:

$$s(t) = n(t) + h(t), \tag{5.7}$$

the sum of the GW amplitude $h(t)$ and of the noise $n(t)$. The magnitude of the stochastic background is expected to be very tiny and for sure much smaller than the noise $h(t) \ll n(t)$. Nevertheless, it is possible to isolate the GW signal by considering the 2-point correlator of the outputs of two different detectors:

$$\langle s_1(t)s_2(t)\rangle = \langle (n_1(t) + h_1(t))(n_2(t) + h_2(t))\rangle = \langle h_1(t)h_2(t)\rangle, \tag{5.8}$$

where the last passage is motivated by the fact that it is possible to assume the statistical independence between the noise measured by different detectors.

Up to now a direct signal of the stochastic gravitational wave background, either of astrophysical or cosmological origin, has yet to be detected. Several detection methods are expected to be able to achieve such a result in the near future, each probing a specific range of the frequency spectrum [57].
Ground-based detectors LIGO and Virgo [60] , already responsible for the detection of localized GW signals, can exploit the correlation between detectors mentioned earlier to probe the range from 20 Hz to 1000 Hz. Pulsar timing [61] (10^{-9} Hz - 10^{-8} Hz) and the space based gravitational wave detector LISA [62] (0.1 mHz - 100 Hz), launching in the 2030s, are other examples of methods to attempt the detection of a stochastic background of GWs.

5.2.1 CGWB as a probe of the early Universe

An early period of inflation is expected to be a fundamental source for the CGWB [52]. This can either be the direct result of the amplification of initial quantum fluctuations of the gravitational field, which is responsible for the so called irreducible contribution to the background, or a consequence of other mechanisms in action during such a period.
In both cases, the CGWB is retained as a unique probe of the fundamental physics at early times. In fact, the peculiarity of gravitational waves is that they interact only gravitationally, whereas the photons of the CMB, for example, mainly interact electromagnetically with baryons. Being the gravitational interaction very weak, it decouples at very early time during the thermal history of the Universe, in such a way that GWs are able to freely stream, without interacting with matter or radiation.

Qualitatively speaking, we can evaluate the strength of a given interaction in an expanding Universe by comparing its rate Γ with the Hubble rate H, which roughly corresponds to the frequency with which the Universe doubles its size. In the case of the gravitational interaction we have [52]:

$$\frac{\Gamma(T)}{H(T)} \sim \frac{G^2T^5}{T^2/M_P} \simeq \left(\frac{T}{M_P}\right)^3, \tag{5.9}$$

where the reduced Planck mass is defined as $M_P = (8\pi G)^{-1/2}$ and the Hubble parameter during the radiation era has been expressed as $H(T) \sim T^2/M_P$. The interaction rate has been computed assuming a weak interaction $\Gamma(T) = n\sigma v$, where the number density of particles is $n \sim T^3$ and their velocity is relativistic $v \sim 1$. The cross-section is the one typical of interactions mediated by massless gauge bosons (in this case the graviton) $\sigma \sim G^2T^2$.
An interaction is then said to be inefficient when $\Gamma < H$, which for the gravitational one happens for $T < M_P$, i.e. the gravitational waves decouple from the thermal plasma approximately one Planck time t_P after the Big Bang. This shows that GWs are free to propagate immediately after they are produced, carrying unique information about the processes which generated them. Primordial GWs from inflation can thus be assumed as a unique probe of very high energy scales, inaccessible to the other observables. As a comparison, we know that CMB radiation is produced shortly after the recombination epoch, when photons decouple from matter, and thus cannot carry any information about the state of the Universe prior to that time.

5.2.2 Energy density of the stochastic background

The natural quantity to describe the statistics of a stochastic background is the 2-point correlation function of the GW amplitude h_{ij}, which is what we will compute explicitly in the next section for primordial GWs generated by quantum fluctuations during inflation, ending up with an expression for the tensor power spectrum, analogous to the scalar one computed in Chapter 1.
Beside the amplitude power spectrum, another quantity of major interest for a stochastic background is the GW energy density ρ_{GW}. In the weak-field limit, GWs can be considered as small perturbations around a fixed background metric. It is thus possible to define how the presence of these perturbations affects the background. This is done by rewriting vacuum Einstein equations $G_{\mu\nu} = 0$ in the following way [53]:

$$\bar{G}_{\mu\nu} = 8\pi G t_{\mu\nu}, \tag{5.10}$$

where $\bar{G}_{\mu\nu}$ is computed using the background metric only and $t_{\mu\nu}$ is a stress-energy tensor accounting for the presence of GWs, expressed as:

$$t_{\mu\nu} = \frac{1}{32\pi G}\langle \partial_\mu h_{ij} \partial_\nu h^{ij} \rangle. \tag{5.11}$$

The angle brackets denote an average over the typical lengthscale on which the background metric varies, which corresponds to several GW wavelengths. The energy density is then proportional to the (0-0) component of this stress-energy tensor. For a FLRW background with conformal time τ, we explicitly find:

$$\rho_{GW} = \frac{1}{32\pi G a^2}\langle h'_{ij}(\tau,\vec{x}) h'^{ij}(\tau,\vec{x}) \rangle. \tag{5.12}$$

It is often useful to define also the GW energy density per per logarithmic frequency interval:

$$\Omega_{GW}(\tau,k) \equiv \frac{1}{\rho_c}\frac{d\rho_{GW}}{d\ln k}, \tag{5.13}$$

where ρ_c is the critical density introduced in equation (1.15). Here we have defined Ω_{GW} as homogeneous, which is the usual assumption in most of the studies on the CGWB. Nevertheless, later in this Chapter we are going to see how it may be interesting to introduce the possibility for a space dependence related to the anisotropies of the GW stochastic background.

5.3 Gravitational Waves from inflation

In this section we discuss how primordial tensor perturbations, corresponding to gravitational waves, are naturally generated during an early period of inflation. This is analogous to the production of primordial scalar perturbations from the inflaton quantum fluctuations we have discussed in Chapter 1.

We consider again the standard single field slow-roll model of inflation, characterized by the action (1.30):

$$S = \int d^4x\sqrt{-g}\left(\frac{1}{16\pi G}R - \frac{1}{2}g^{\mu\nu}\partial_\mu\varphi\partial_\nu\varphi - V(\varphi)\right). \tag{5.14}$$

In Chapter 1 we have derived from this action the equation of motion for the full inflaton $\varphi(t,\vec{x})$, including both the background and the small perturbations around it, namely the Klein-Gordon equation (1.31). We know from the discussion of the previous section that GWs are represented by the transverse and traceless tensor degrees of freedom of the metric perturbation. Furthermore, at linear order their evolution is decoupled from scalars and vectors, in such a way that we can express the perturbed FLRW metric (2.5) as:

$$ds^2 = -dt^2 + a^2(t)(\delta_{ij} + h_{ij})dx^i dx^j, \tag{5.15}$$

where only the gauge-invariant tensor degrees of freedom have been considered. Expanding the pure gravitational part of action (5.14) for the perturbed metric (5.15), we get:

$$S_g = \frac{1}{64\pi G}\int d^4x a^2(t)\left[\dot{h}_{ij}\dot{h}_{ij} - \frac{1}{a^2}(\vec{\nabla}h_{ij})^2\right], \tag{5.16}$$

where we have kept the second order of expansion in h_{ij}, since we want to derive the equations of motion at first order. These are obtained by varying action (5.16) with respect to h_{ij}, resulting in:

$$\ddot{h}_{ij} + 3H\dot{h}_{ij} - \frac{1}{a^2}\nabla^2 h_{ij} = 0, \tag{5.17}$$

which is just the equation for a free wave propagating in a FLRW spacetime, as we would have expected. It is then possible to decompose h_{ij} in Fourier space into the two polarization states $\lambda = (+,\times)$, in the following way:

$$h_{ij}(t,\vec{x}) = \sum_{\lambda=(+,\times)}\int \frac{d^3\vec{k}}{(2\pi)^3}h^{(\lambda)}(t,\vec{k})e^{(\lambda)}_{ij}(\hat{k})e^{i\vec{k}\vec{x}}, \tag{5.18}$$

where we have introduced the polarization tensors $e^{(\lambda)}_{ij}(\hat{k})$, which depend only on the unit vector $\hat{k}$ and are symmetric $e_{ij} = e_{ji}$, transverse $k^i e_{ij} = 0$ and traceless $e^i{}_i = 0$. They can be assumed to be real and to satisfy the condition $e_{ij}(-\vec{k}) = e_{ij}(\vec{k})$, in such a way that the reality of h_{ij} is ensured if $h^{(\lambda)*}(t,\vec{k}) = h^{(\lambda)}(t,-\vec{k})$. In order to solve equation (5.17) it is then useful to introduce the following variable:

$$v^{(\lambda)}_{\vec{k}}(\tau) = \frac{aM_P}{\sqrt{2}}h^{(\lambda)}(\tau,\vec{k}), \tag{5.19}$$

where we have also passed to the conformal time τ. Combining definitions (5.18) and (5.19), equation (5.17) can be rewritten, in Fourier space, in terms of the mode functions $v^{(\lambda)}_{\vec{k}}(\tau)$:

$$v^{(\lambda)\prime\prime}_{\vec{k}}(\tau) + \left(k^2 - \frac{a''}{a}\right)v^{(\lambda)}_{\vec{k}}(\tau) = 0. \tag{5.20}$$

By comparison with equation (1.47) for the inflaton fluctuations, we can see how each polarization of the tensor perturbation h_{ij} behaves, during inflation, like a massless scalar field in a FLRW spacetime, where the expansion of the Universe is accounted for by an effective mass squared term equal to $\frac{a''}{a}$ [53].

Before we perform the standard quantization of $v_{\vec{k}}^{(\lambda)}(\tau)$ and compute the power spectrum of primordial tensor perturbations, we can study the qualitative behaviour of equation (5.20). It is possible to identify two different regimes, which correspond either to a sub-horizon or super-horizon mode solution.
We know that a given perturbation mode of wavenumber k crosses the horizon during inflation when its wavelength is comparable to the Hubble radius, which we identify with the condition $k = aH$. Therefore, for a mode well inside the horizon it holds the relation $k \gg aH$, which can be rewritten in terms of the proper time τ as $k^2 \gg \frac{a''}{a}$. Analogously, the wavenumber of a mode out of the Horizon satisfies $k \ll aH$, or $k^2 \ll \frac{a''}{a}$.
We first consider the sub-horizon regime, where equation (5.20) reduces to:

$$v_{\vec{k}}'' + k^2 v_{\vec{k}} = 0. \tag{5.21}$$

As we have already seen in Chapter 1, this corresponds to the equation of a plane-wave in flat spacetime. Physically, modes with a large enough wavenumber experience the FLRW spacetime as flat, thus ignoring the expansion of the Universe. The general solution for a sub-horizon mode is then:

$$v_k(\tau) = A(k)e^{ik\tau} + B(k)e^{-ik\tau}, \tag{5.22}$$

where A and B are time-independent integration functions determined by initial conditions, of which we will talk about soon. This means, remembering the rescaling (5.19), that the amplitude of sub-horizon modes of h_{ij} decreases during inflation as the inverse of the scale-factor.
In the super-horizon regime the term $\frac{a''}{a}$ in (5.20) dominates over k^2, in such a way that we have to solve:

$$v_{\vec{k}}'' - \frac{a''}{a} v_{\vec{k}} = 0. \tag{5.23}$$

This time the solution does not oscillate and in general can be expressed as:

$$v_k(\tau) = A(k)a(\tau) + B(k)a^{-2}(\tau), \tag{5.24}$$

which corresponds to a constant and a decreasing solution for h_{ij}. We will be interested in particular in the former, since during inflation the scale-factor increases almost exponentially and the decreasing super-horizon solution becomes negligible very soon.

Knowing the qualitative behaviour of the solutions of equation (5.20) in the two main regimes, we now perform the standard quantization of the tensor field h_{ij}, which is analogous to what we have done in Chapter 1 for the inflaton perturbation $\delta\varphi$. We thus promote the mode function $v_{\vec{k}}$ to the corresponding quantum operator:

$$\hat{v}_{\vec{k}}^{(\lambda)} = v_k(\tau)\hat{a}_{\vec{k}}^{(\lambda)} + v_k^*(\tau)\hat{a}_{\vec{k}}^{(\lambda)\dagger}, \tag{5.25}$$

where $\hat{a}_{\vec{k}}^{(\lambda)}$, $\hat{a}_{\vec{k}}^{(\lambda)\dagger}$ are the annihilation and creation operators for the two polarization states. Each couple of operators satisfies the canonical quantization condition (1.51), introduced when dealing with the quantum inflaton perturbations. In analogy with (1.52), then, the modes are normalized in such a way that they satisfy:

$$v_k^* v_k' - v_k v_k^{*\prime} = -i. \tag{5.26}$$

The vacuum state $|0\rangle$ is defined by imposing that it is destroyed by the annihilation operator at past infinity, i.e. $\hat{a}_{\vec{k}}^{(\lambda)}|0\rangle = 0$ for $\tau \to -\infty$. This corresponds to the so called Bunch-Davis vacuum choice.
Until now we have just repeated the same steps of section 1.2.3, adapting the notation to the current case. This time we want to deal more in details with the solution of the quantized version of equation (5.20). We already know that it corresponds to the equation of motion of a quantum harmonic oscillator for each polarization state:

$$v_k'' + \omega_k^2 v_k = 0, \tag{5.27}$$

which oscillates with frequency:

$$\omega_k^2(\tau) \equiv k^2 - \frac{a''}{a}. \tag{5.28}$$

Equation (5.27) can then be rewritten in the form of a Bessel equation:

$$v_k'' + \left(k^2 - \frac{\nu^2 - \frac{1}{4}}{\tau^2}\right) v_k = 0, \tag{5.29}$$

with $\nu^2 = \frac{9}{4} + 3\epsilon$ and where we have used the fact that $\frac{a''}{a} \simeq \frac{2}{\tau^2}$ when neglecting contributions linear in the slow-roll parameter ϵ. The most general exact solution of this Bessel equation is [53]:

$$v_k(\tau) = \sqrt{-\tau}\Big[c_1 H_\nu^{(1)}(-k\tau) + c_2 H_\nu^{(2)}(-k\tau)\Big], \tag{5.30}$$

where $H_\nu^{(1)}$ and $H_\nu^{(2)}$ are Hankel functions of the first and second kind, respectively, and order ν. The integration constants c_1 and c_2 can be fixed by imposing the initial conditions mentioned earlier. The Bunch-Davis vacuum choice states that the solution at past infinity is a plane-wave. This is consistent with the fact that we expect sub-horizon modes to experience the spacetime as flat. Combining it with the normalization (5.26), and picking up the positive frequency mode, we find the following initial condition:

$$\lim_{\tau \to -\infty} v_k(\tau) = \frac{1}{\sqrt{2k}} e^{-ik\tau}. \tag{5.31}$$

This has now to be matched to the sub-horizon limit of solution (5.30). The condition $k^2 \gg \frac{a''}{a}$ can be rewritten as $-k\tau \gg 1$ by using the aforementioned approximation $\frac{a''}{a} \simeq \frac{2}{\tau^2}$ and remembering that the proper time τ is negative during inflation. We can then exploit the following asymptotic forms of the Hankel functions:

$$\begin{aligned} H_\nu^{(1)}(x \gg 1) &\sim \sqrt{\frac{2}{\pi x}} e^{i\left(x - \frac{\pi}{2}\nu - \frac{\pi}{4}\right)}, \\ H_\nu^{(2)}(x \gg 1) &\sim \sqrt{\frac{2}{\pi x}} e^{-i\left(x - \frac{\pi}{2}\nu - \frac{\pi}{4}\right)}. \end{aligned} \tag{5.32}$$

First of all we see that the Hankel function of the second kind has a negative frequency, so that we have to set $c_2 = 0$. Substituting the expression for $H_\nu^{(1)}(x \gg 1)$ inside (5.30) and matching it to the early time plane-wave (5.31) we get:

$$c_1 = \frac{\sqrt{\pi}}{2} e^{i\left(\nu + \frac{1}{2}\right)\frac{\pi}{2}}, \tag{5.33}$$

in such a way that the exact solution becomes:

$$v_k(\tau) = \frac{\sqrt{\pi}}{2} e^{i\left(\nu + \frac{1}{2}\right)\frac{\pi}{2}} \sqrt{-\tau} H_\nu^{(1)}(-k\tau). \tag{5.34}$$

In order to compute the primordial tensor power spectrum we need the super-horizon behaviour of this solution. In analogy to the scalar case, in fact, also the tensor modes are conserved while out of the horizon, before re-entering it during the post-inflationary evolution. This fact directly follows from the solution (5.24) in the super-horizon regime. The value assumed by the perturbation at horizon-crossing, during inflation, thus provides the initial condition for the evolution of the modes upon horizon re-entry. Furthermore, from the discussion in Chapter 2 we remember that, at linear order, transverse and traceless tensor perturbations h_{ij} are also automatically gauge-invariant, which was the main reason that has led us to introduce the comoving curvature perturbation ζ to be identified with primordial scalar perturbations.
On super-horizon scales we have $-k\tau \ll 1$, for which the Hankel function of the first kind has the following asymptotic behaviour:

$$H_\nu^{(1)}(x \ll 1) \sim \sqrt{\frac{2}{\pi}} e^{-i\frac{\pi}{2}} 2^{\nu - \frac{3}{2}} \frac{\Gamma(\nu)}{\Gamma\left(\frac{3}{2}\right)} x^{-\nu}, \tag{5.35}$$

which, substituted inside (5.34), leads to the mode solution:

$$v_k(\tau) = e^{i\left(\nu-\frac{1}{2}\right)\frac{\pi}{2}} 2^{\nu-\frac{3}{2}} \frac{\Gamma(\nu)}{\Gamma\left(\frac{3}{2}\right)} \frac{1}{\sqrt{2k}} (-k\tau)^{\frac{1}{2}-\nu}. \tag{5.36}$$

We can finally recover, remembering the rescaling (5.19), the super-horizon solution for the Fourier modes of the GW amplitude:

$$h_k^{(\lambda)}(\tau) = e^{i\left(\nu-\frac{1}{2}\right)\frac{\pi}{2}} 2^{\nu-\frac{3}{2}} \frac{\Gamma(\nu)}{\Gamma\left(\frac{3}{2}\right)} \frac{1}{a\sqrt{k}M_P} (-k\tau)^{\frac{1}{2}-\nu}, \tag{5.37}$$

which is the same for both polarization states.

5.3.1 Primordial GW power spectrum

In analogy to the primordial scalar perturbations treatment, the adimensional power spectrum of primordial gravitational waves has the following expression:

$$\mathcal{P}_h^{(\lambda)}(k) = \frac{k^3}{2\pi^2} |h_k^{(\lambda)}|^2. \tag{5.38}$$

The total tensor power spectrum is then defined as the 2-point correlator of the GW amplitude:

$$\langle h_{ij}(\vec{k}) h_{ij}^*(\vec{k}') \rangle = (2\pi)^3 \delta^{(3)}(\vec{k} - \vec{k}') \frac{2\pi^2}{k^3} \mathcal{P}_T(k), \tag{5.39}$$

where the T refers to tensor degrees of freedom. Remembering that we are working in the TT gauge, we can express the LHS as $2|h_k^+|^2 + 2|h_k^\times|^2$, in such a way that $\mathcal{P}_T(k) = 4\mathcal{P}_h(k)$. In order to compute it explicitly, we first simplify expression (5.37) for $h_k^{(\lambda)}$. The parameter ν is defined by the relation $\nu^2 = \frac{9}{4} + 3\epsilon$, which at first order in ϵ gives $\nu \simeq \frac{3}{2} + \epsilon$. In the slow-roll limit, where $\epsilon \to 0$, we can then write the following approximate solution:

$$|h_k^{(\lambda)}| = \frac{1}{a\sqrt{k}M_P} (-k\tau)^{\frac{1}{2}-\nu} = \frac{H}{M_P\sqrt{k^3}} \left(\frac{k}{aH}\right)^{-\epsilon}, \tag{5.40}$$

where in the second equality we have also used the fact that, neglecting corrections of order ϵ, $\tau \simeq -\frac{1}{aH}$ during slow-roll inflation. The total tensor power spectrum thus happens to have the following expression:

$$\mathcal{P}_T(k) = 4 \times \frac{k^3}{2\pi^2} |h_k^{(\lambda)}|^2 = \frac{8}{M_P^2} \left(\frac{H}{2\pi}\right)^2 \left(\frac{k}{aH}\right)^{-2\epsilon}. \tag{5.41}$$

We see that standard slow-roll inflation, characterized by the positive slow-roll parameter $\epsilon \ll 1$, predicts a slightly red-tilted power spectrum of primordial gravitational waves. This is made clear by defining the tensor spectral index:

$$n_T \equiv \frac{d\ln\mathcal{P}_T(k)}{d\ln k} \simeq -2\epsilon, \tag{5.42}$$

which is very small and negative.
Exploiting the fact that tensor modes are conserved on super-horizon scales, we can evaluate result (5.41) at horizon-crossing, where $k = aH$, so that it becomes:

$$\mathcal{P}_T(k) = \frac{8}{M_P^2} \left(\frac{H}{2\pi}\right)^2 \Bigg|_{k=aH}. \tag{5.43}$$

The power spectrum we have just computed is relative to the production of primordial gravitational waves as metric quantum fluctuations during inflation. This means that an eventual detection of such a stochastic background of GWs would be a direct confirmation of an early period of accelerated expansion. In this sense it is often referred to as the "smoking gun" of inflation.

Gravitational waves from inflation are also expected to leave some characteristic traces on the CMB radiation, in particular on its polarization field [63, 64] . Without going too much into details, we just mention that an eventual detection of a pattern of B-modes can be associated to the presence of a CGWB coming from inflation. Here the experimental challenge is to account correctly for other possible sources of polarized light, in order to isolate the net effect due only to primordial GWs.

Consistency relation

We conclude this section by addressing to a unique prediction of standard slow-roll inflationary models.

We compute the relative contribution of primordial GWs with respect to primordial curvature perturbations, by taking the ratio of the respective power spectra. This defines the tensor-to-scalar ratio:

$$r \equiv \frac{\mathcal{P}_T}{\mathcal{P}_\zeta} = \frac{\frac{2H^2}{\pi^2 M_P^2}}{\frac{H^2}{8\pi^2 M_P^2 \epsilon}} = 16\epsilon, \tag{5.44}$$

where in the second equality we have used the expressions of power spectra evaluated at horizon-crossing, (1.74) and (5.43).
Latest CMB measurements by Planck Collaboration (2018) [65] impose an experimental upper bound on the tensor-to-scalar ratio, evaluated at a pivot scale of 0.002 Mpc^{-1}, of $r_{0.002} < 0.056$ at 95% CL. This result is actually obtained by combining with B-mode polarization data of the BICEP2/Keck Array [66].

Recalling expression (5.42) for the tensor spectral index, it is now possible to write down the following relation between the parameters of the primordial power spectra:

$$r = -8 n_T, \tag{5.45}$$

which is independent on the explicit values of the slow-roll parameters. This result can be regarded as an actual consistency relation which only slow-roll models of inflation are able to provide. A proper measure of the tensor power spectrum, of both its amplitude and spectral index, is required in order to check the validity of the relation, whose violation would be the signature of a departure from the standard single field slow-roll inflationary models.

Parameter space

If we consider both the primordial power spectra, tensor and scalar, we need to fix a total of 4 parameters in order to uniquely determine their behaviour. To make this more clear, we parametrize them in the following way:

$$\begin{aligned} \mathcal{P}_\zeta &= \mathcal{P}_\zeta(k_p)\left(\frac{k}{k_p}\right)^{n_s - 1}, \\ \mathcal{P}_T &= \mathcal{P}_T(k_p)\left(\frac{k}{k_p}\right)^{n_T}, \end{aligned} \tag{5.46}$$

where k_p is an arbitrary pivot scale. We thus have 4 observables, consisting in the 2 amplitudes, measured at the pivot scale, and the 2 respective scalar indices.
If we assume the consistency relation (5.45) to be valid, we obtain a relation between the two amplitudes and the tensor spectral index, which reduces the number of degrees of freedom to 3. Furthermore, measurements of CMB temperature anisotropies constrain the scalar amplitude, usually indicated as A_s, at the pivot scale 0.05 Mpc^{-1} to the value $\ln(10^{10} A_s) = 3.044 \pm 0.014$ [3]. This leaves a viable parameter space with just 2 degrees of freedom, which are usually chosen to coincide with n_s and r. This is represented in Figure 5.1, where predictions on the parameters for several inflationary models are reported, along with confidence regions from latest observations [65].

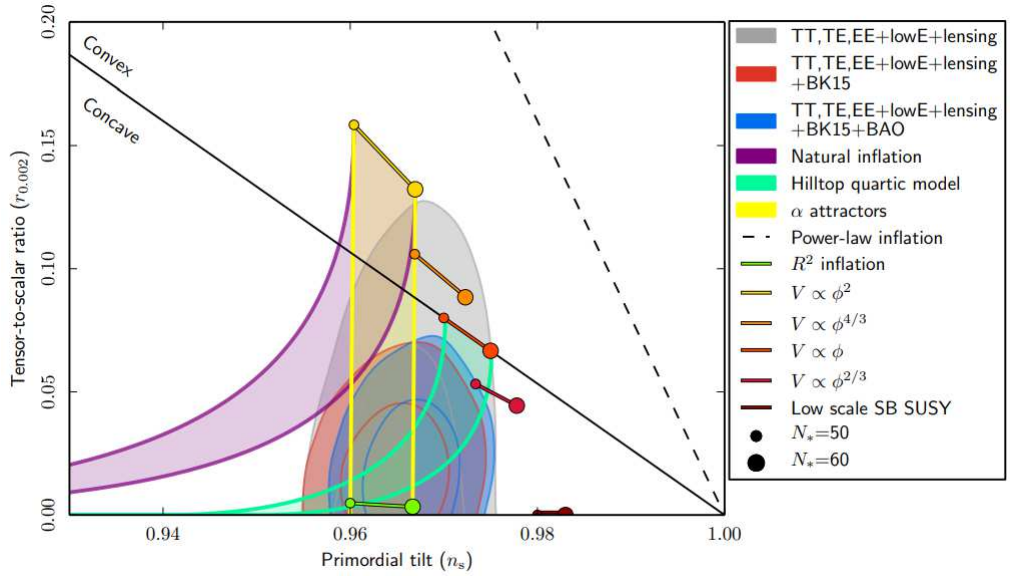

Figure 5.1: Confidence regions at 68% and 95% CL for n_s and r evaluated at the scale $k = 0.002$ Mpc^{-1}, along with theoretical predictions from several inflationary models. Taken from [65].

5.3.2 Primordial GWs from inflation as a source of information

A detection of CGWB generated during inflation would not only be a confirmation of the theory itself, but would also provide crucial information, otherwise inaccessible, about the physics of the early Universe. We present here two immediate conclusions one may draw from a direct measure of the tensor power spectrum, while assuming the standard slow-roll inflationary model.

Energy scale of inflation

The amplitude of the tensor power spectrum is strictly tied to the energy scale $E_{\rm inf} \simeq V^{\frac{1}{4}}$ at which the inflationary mechanism takes place, where $V(\varphi)$ is the inflaton potential in the slow-roll approximation. Notice in fact that expression (5.43) for $\mathcal{P}_T$ evaluated at horizon-crossing only depends on the Hubble parameter H. Moreover we know that, assuming the slow-roll approximation, during inflation the value of H is fully determined by the inflation potential $V(\varphi)$, via the first Friedmann equation in the slow-roll regime (1.37). Substituting the latter inside expression (5.43) we thus get a relation between the inflaton potential and the amplitude of primordial GWs power spectrum:

$$V = \frac{3}{2}\pi^2 M_P^4 \mathcal{P}_T. \tag{5.47}$$

This result can be rewritten in a more practical way, by exploiting the definition of the tensor-to-scalar ratio (5.44) and the estimate of the scalar amplitude on large scales obtained by the Planck Collaboration [65], which leads to:

$$V \simeq (10^{16}\ \text{GeV})^4 \frac{r}{0.01}, \tag{5.48}$$

from which it is clear that a measure of r would fix this energy scale.

Excursion of the inflaton field

In Chapter 1 we have introduced the concept of e-foldings (1.19) to quantify the duration of inflation, which is also related, as we will show shortly, to the excursion $\Delta\varphi$ experienced by the inflaton from the horizon-crossing of large-scale perturbations to the end of inflation. We now want

to show that the value of this $\Delta\varphi$ is directly related, once again, to the tensor-to-scalar ratio. By definition the excursion of the inflation field is:

$$\Delta\varphi = \int_{\varphi_{\rm CMB}}^{\varphi_{\rm end}} d\varphi, \tag{5.49}$$

where we have chosen to start the integration at the horizon-crossing of the CMB scale, i.e. the scale corresponding to the Hubble horizon at the epoch of last scattering. The relation with the number of e-foldings can be derived by combining definitions (1.19), (5.44) and the expression for the slow-roll parameter $\epsilon \simeq 4\pi G\varphi^2$, so that we can write:

$$r = \frac{8}{M_P^2}\left(\frac{d\varphi}{dN}\right)^2. \tag{5.50}$$

An expression for $\Delta\varphi$ is then derived by performing the following integration:

$$\Delta\varphi = M_P \int_{N(\varphi_{\rm CMB})}^{N(\varphi_{\rm end})} \left(\frac{r(N)}{8}\right)^{\frac{1}{2}} dN, \tag{5.51}$$

where we have made explicit the dependence of r on N. In the standard slow-roll inflationary models r can be taken to be constant [53], in such a way that:

$$\frac{\Delta\varphi}{M_P} \simeq \left(\frac{r}{8}\right)^{\frac{1}{2}} N(\varphi_{\rm CMB}). \tag{5.52}$$

Assuming the minimal amount of e-foldings necessary to solve both the horizon and the flatness problem, $N_{\rm min} \sim 60$ [1], a qualitative lower bound for the value of the inflaton excursion can be derived:

$$\frac{\Delta\varphi}{M_P} \gtrsim \left(\frac{r}{0.01}\right)^{\frac{1}{2}}. \tag{5.53}$$

5.3.3 Classical production of GWs during inflation

The CGWB generated from the quantum metric fluctuations during inflation is predicted to have the statistics described by the power spectrum (5.41). Actually, another way to produce GWs during inflation has to be taken into account, namely a classical mechanism. This takes place when the GW equation of motion in a FLRW spacetime (5.17) includes a source term, i.e. a non-vanishing term after the equality.
Possible sources of classically generated GWs can be associated with several different scenarios, such as particle production during inflation or the presence of additional scalar fields beyond the inflaton [53].

We are interested in particular in the classical production of GWs sourced by scalar perturbations, which is a second-order effect. Up to now we have neglected scalar and vector degrees of freedom of the metric fluctuations, since they do not influence the evolution of pure tensor degrees of freedom, but we know that this holds only at the linear level.
Already at the second order, equations of motions for the perturbations start to mix degrees of freedom of different nature. Among other things, this introduces the possibility of primordial GWs sourced, at second order, by a combination of first-order scalar perturbations. This is quite interesting because we know that, during inflation, scalar perturbations are always generated by quantum fluctuations of the inflaton, which then represent themselves a source for the classical production of primordial GWs at second order.
In principle we expect this contribution to the CGWB, being a second-order effect, to be negligible with respect to the one generated at first order from quantum metric fluctuations. Nevertheless, this may not be the case, for example, in a scenario where scalar perturbations are highly enhanced at very small scales, whereas the CMB constraints are satisfied at cosmological scales. In such a situation, second-order production of GWs from scalar perturbations would be greatly enhanced at small scales.

Large enough scalar perturbations may also lead to the formation of primordial black holes (PBHs). The description of the CGWB associated with PBH formation from enhanced scalar perturbation will be one of the the main focus of the next Chapter, where we will also provide with details about second-order primordial GWs sourced by scalar perturbations.

5.4 Characterization of the CGWB

Upon an actual detection of the CGWB in the foreseeable future, it arises the necessity to characterize the stochastic background in order to distinguish between different possible sources. The astrophysical and cosmological natures of the GW background, for instance, can be set apart by looking at the frequency dependence, since for each physical mechanism a different peaking scale is expected.
A natural alternative would be to focus instead on the GW background statistics, as we have already pointed out throughout this Chapter. In the previous section we have computed the tensor power spectrum as the 2-point correlation function of the amplitude h_{ij} of primordial GWs generated from quantum metric fluctuations during inflation. It is also possible to perform a statistical description analogous to the one presented in Chapter 4 for CMB temperature anisotropies. This is what we are actually going to do for the rest of this Chapter, which will eventually allow us to consider the effect of primordial non-Gaussianity on the CGWB. For this purpose we thus shift our focus, from now on, to the statistics of the GW energy density parameter Ω_{GW}, defined in (5.13), rather than the GW amplitude.

Our treatment of the CGWB anisotropies throughout this section follows quite closely the discussion presented in [49].

5.4.1 Boltzmann equation for gravitational waves

The statistical description of a GW stochastic background can be worked out within a Boltzmann equation approach [67], in complete analogy to the usual procedure developed for the treatment of CMB anisotropies [41].

Boltzmann equation regulates the evolution of a given distribution function of particles, accounting for all their possible interactions. The particles associated to gravitational waves are the gravitons, and we thus need to introduce the distribution function which describes their statistics.
In the weak-field limit it is possible to assume that massless gravitons travel along null geodesics of the background spacetime, like photons do. In fact, since gravitons themselves are a manifestation of the spacetime perturbations, such a description holds only as long as the typical wavelength of gravitational waves under study is much smaller than the lengthscale over which the background spacetime experiences sensible variations. This may resemble the geometric optics approach in the study of light propagation and it is usually referred to as the shortwave formalism [68].

We define the distribution function of gravitons $f(x, p, \lambda)$ as a function of the 4-position x^μ, the 4-momentum $p^\mu = \frac{dx^\mu}{d\lambda}$ and of the affine parameter λ, which parametrizes the null trajectories.
Boltzmann equation for f is then written schematically in the following way [67]:

$$\mathcal{L}[f(\lambda)] = \mathcal{C}[f(\lambda)] + \mathcal{I}[f(\lambda)], \tag{5.54}$$

where we have introduced $\mathcal{L}$, $\mathcal{C}$ and $\mathcal{I}$ as the Liouville, the collisional and the source operator, respectively. The first is simply the total derivative with respect to the affine parameter $\mathcal{L}[f(\lambda)] = \frac{df}{d\lambda}$ computed following the motion of the particles, which usually goes by the name of Lagrangian derivative. In absence of collisions and production of particles, Liouville's theorem then states that the distribution function is conserved along the trajectories, i.e. $\frac{df}{d\lambda} = 0$.
The collisional operator vanishes when dealing with GWs at linear order in the perturbations. Collisions between gravitons affect the distribution at higher orders and can thus be neglected, while interactions with other particle species become inefficient at very early times, as we have discussed in section 5.2.1. As a matter of fact, we neglect the collisional term in our treatment.

The source operator should account for all the possible emissions of GWs, being them astrophysical processes in the late Universe or cosmological ones, like the quantum fluctuations production during inflation we have discussed in the previous section. Since we are restricting ourselves to the description of a stochastic background of cosmological origin, i.e. a CGWB, we can treat the source term as an initial condition to be imposed at early times. This corresponds to the situation in which the CGWB is fully produced instantaneously and then left to evolve, without any other contribution from later emissions.
These considerations leave us with the free Boltzmann equation, in which we can replace the affine parameter with the conformal time τ:

$$\frac{df}{d\tau} \equiv \frac{\partial f}{\partial \tau} + \frac{\partial f}{\partial x^i}\frac{\partial x^i}{\partial \tau} + \frac{\partial f}{\partial p}\frac{\partial p}{\partial \tau} + \frac{\partial f}{\partial n^i}\frac{\partial n^i}{\partial \tau} = 0, \tag{5.55}$$

where the unit vector $\hat{n} = \hat{p}$ points in the GW direction of motion. The last term accounts for gravitational lensing effects and vanishes at linear order where gravitons are assumed to travel along straight lines, like CMB photons. The other, non-vanishing terms, describe the free-streaming and the redshifting of gravitons, where the latter includes effects analogous to the Sachs-Wolfe (SW) and the integrated Sachs-Wolfe (ISW) ones that we have discussed while dealing with CMB temperature anisotropies in Chapter 4.

We now need to express the free Boltzmann equation (5.55) in terms of the first-order metric perturbations around a FLWR background. In order to do so, we consider the metric written as in (2.5) and put ourselves in the Poisson gauge. Moreover, we can neglect transverse vector modes since they are not expected to be produced at linear order in standard inflationary models. We thus end up with the following expression for the linearly perturbed metric in the Poisson gauge:

$$ds^2 = a^2(\tau)\Big[-(1+2\phi)d\tau^2 + \big((1-2\psi)\delta_{ij} + \chi_{ij}\big)dx^i dx^j\Big], \tag{5.56}$$

where perturbations, both scalar and tensor, include only modes with wavelength much longer than the one of the GWs we are considering. In this way it is possible to separate the GW amplitude h_{ij} from the transverse and traceless tensor perturbations χ_{ij}, realizing concretely the idea behind the shortwave formalism introduced earlier. This allows us to consider the gravitons propagating along null geodesics of the perturbed background metric (5.56) and thus to derive the effects of the presence of scalar and tensor perturbations on the evolution of the graviton distribution function. Assuming the metric (5.56) and following the standard procedure developed for CMB anisotropies [77], we get the free Boltzmann equation (5.55) describing the evolution of gravitons in presence of scalar and tensor perturbations:

$$\frac{\partial f}{\partial \tau} + n^i\frac{\partial f}{\partial x^i} + \left[\frac{\partial \psi}{\partial \tau} - n^i\frac{\partial \phi}{\partial x^i} - \frac{1}{2}n^i n^j\frac{\partial \chi_{ij}}{\partial \tau}\right]q\frac{\partial f}{\partial q} = 0, \tag{5.57}$$

where we have also introduced the comoving momentum defined as $q \equiv pa$, in such a way that its value is not affected by the Universe expansion.
The solution of this equation can be expanded to first order as $f = f^{(0)} + f^{(1)}$, in the same way done in equation (4.2) for the CMB photon distribution function. From the zero-order part of equation (5.57), which simply reads $\frac{\partial f^{(0)}}{\partial \tau} = 0$, we conclude that the zero-order distribution function can be a function of the comoving momentum q only and it is thus homogeneous and isotropic. The other dependencies, on time, position and direction of motion, are accounted for by the first order correction. This is the case also for CMB photons, even if it is not immediately manifest. The zero-order photon distribution function is the Bose-Einstein one (4.3), which depends only on the ratio $\frac{p}{T}$. Moreover, at zero order the temperature varies only as a consequence of the Universe expansion and goes like $T \propto a^{-1}$, in such a way that also the photon distribution function depends only on the comoving momentum $\frac{p}{T} \propto pa = q$.
Keeping the analogy with the CMB treatment, we now express the first order contribution to the graviton distribution function in the following way:

$$f^{(1)}(\tau, \vec{x}, q, \hat{n}) \equiv -q\frac{\partial f^{(0)}}{\partial q}(q)\Gamma(\tau, \vec{x}, q, \hat{n}), \tag{5.58}$$

where we have defined the function Γ which accounts, as we will discuss in a moment, for the anisotropies in the CGWB energy density. By comparison with equation (4.2), we see that it is the analogous of the temperature anisotropy Θ in the CMB case.

5.4.2 Anisotropies in the CGWB energy density

Anisotropies in the graviton distribution function, parametrized by Γ, are related to anisotropies in the CGWB energy density. The latter, in fact, is obtained as the first moment of the distribution function:

$$\rho_{GW}(\tau,\vec{x}) = \frac{1}{a^4(\tau)}\int d^3\vec{q}qf(\tau,\vec{x},q,\hat{n}) \equiv \rho_c(\tau)\int d\ln q\Omega_{GW}(\tau,\vec{x},q), \tag{5.59}$$

where in the second equality we have applied the definition of energy density per per logarithmic frequency interval (5.13).
Equation (5.59) relates f and Ω_{GW} in the following way:

$$\Omega_{GW}(\tau,\vec{x},q) = \frac{1}{\rho_c}\left(\frac{q}{a}\right)^4\int d^2\hat{n}f(\tau,\vec{x},q,\hat{n}) \equiv \frac{1}{4\pi}\int d^2\hat{n}\omega_{GW}(\tau,\vec{x},q,\hat{n}), \tag{5.60}$$

where we have also introduced the contribution to Ω_{GW} per unit solid angle ω_{GW}. Remembering now the first-order expansion of the graviton distribution function, it is possible to define the homogeneous component of Ω_{GW} as:

$$\bar{\Omega}_{GW}(\tau,q) = \frac{1}{\rho_c}\left(\frac{q}{a}\right)^4\int d^2\hat{n}f^{(0)}(q) = \frac{4\pi}{\rho_c}\left(\frac{q}{a}\right)^4 f^{(0)}(q) \equiv \bar{\omega}_{GW}(\tau,q), \tag{5.61}$$

which is usually the main focus of studies on the CGWB. In this work we are interested instead in the generalization to a possible spatial dependence of Ω_{GW} and we will thus consider the full, anisotropic, GW energy density (5.60). We want to study in particular the anisotropies around the homogeneous background value $\bar{\Omega}_{GW}$. For this purpose we now introduce the GW density contrast, defined in this way:

$$\delta_{GW}(\tau,\vec{x},q,\hat{n}) \equiv \frac{\omega_{GW}(\tau,\vec{x},q,\hat{n}) - \bar{\omega}_{GW}(\tau,q)}{\bar{\omega}_{GW}(\tau,q)} = -\frac{q}{f^{(0)}}\frac{\partial f^{(0)}}{\partial q}\Gamma(\tau,\vec{x},q,\hat{n}), \tag{5.62}$$

where we have applied equations (5.60) and (5.61) in the second passage and the definition (5.58) in the third. In this way, we have written the GW density contrast in terms of the function Γ, introduced previously to parametrized the first order contribution to the graviton distribution function. Deriving the (5.61) we also get the following relation:

$$\frac{\partial\ln\bar{\Omega}_{GW}}{\partial\ln q} = 4 + \frac{\partial\ln f^{(0)}}{\partial\ln q}, \tag{5.63}$$

in such a way that equation (5.62) can be rewritten as:

$$\delta_{GW}(\tau,\vec{x},q,\hat{n}) = \left(4 - \frac{\partial\ln\bar{\Omega}_{GW}}{\partial\ln q}\right)\Gamma(\tau,\vec{x},q,\hat{n}). \tag{5.64}$$

From this result we conclude that the evolution of the anisotropies of the GW energy density Ω_{GW} is fully determined by the evolution of the function Γ, which we know to be described by the Boltzmann equation.

5.4.3 Evolution of the CGWB anisotropies

In order to study the evolution of the CGWB energy density anisotropies we need to write the first-order Boltzmann equation and solve it in terms of Γ. Neglecting the zero-order term in (5.57) and remembering the definition (5.58), we obtain the following expression for the Boltzmann equation:

$$\frac{\partial\Gamma}{\partial\tau} + n^i\frac{\partial\Gamma}{\partial x^i} = \frac{\partial\psi}{\partial\tau} - n^i\frac{\partial\phi}{\partial x^i} - \frac{1}{2}n^in^j\frac{\partial\chi_{ij}}{\partial\tau} \equiv S(\tau,\vec{x},\hat{n}), \tag{5.65}$$

where we have defined the source function S, which accounts for the effects of scalar and tensor first order perturbations on the primordial GW propagation. It is remarkable the independence of S on q, meaning that, at first order in perturbations, a dependence on the GW frequency can only originates from initial conditions rather than propagation effects [49].
Going in Fourier space with the usual convention (1.48), equation (5.65) becomes:

$$\Gamma' + ik\mu\Gamma = \psi' - ik\mu\phi - \frac{1}{2}n^i n^j \partial\chi'_{ij}, \tag{5.66}$$

where we have defined $\mu \equiv \hat{k}\cdot\hat{n}$. It is then possible to obtain the solution to this equation by performing a straightforward integration over τ, which gives [49]:

$$\begin{aligned}\Gamma(\tau,\vec{k},q,\hat{n}) = e^{-ik\mu(\tau-\tau_{\rm in})}\Big[\Gamma(\tau_{\rm in},\vec{k},q,\hat{n}) + \phi(\tau_{\rm in},\vec{k})\Big] \\ + \int_{\tau_{\rm in}}^{\tau} d\tau' e^{-ik\mu(\tau-\tau')}\left[\frac{\partial\Big(\psi(\tau',\vec{k}) + \phi(\tau',\vec{k})\Big)}{\partial\tau'} - \frac{1}{2}n^i n^j \frac{\partial\chi_{ij}(\tau',\vec{k})}{\partial\tau'}\right],\end{aligned} \tag{5.67}$$

where the lower extremum of integration $\tau_{\rm in}$ corresponds to the instant of emission of the CGWB we are considering. We may recognize 3 different contributions to this result:

- The first term, which is evaluated at $\tau_{\rm in}$, accounts for the presence of anisotropies in the initial conditions set by the mechanism generating the CGWB in the early Universe. Assuming that such a mechanism picks up initial conditions as the result of some random process, it is then possible to perform a statistical description of this term, analogous to the treatment of the primordial curvature perturbation ζ. Notice that the initial condition term carries an exclusive dependence on the frequency q, not present in the other terms, as we have previously anticipated.

- The terms including scalar metric perturbations ψ and ϕ can be identified, recalling result (4.15) for CMB temperature anisotropies, as the analogous of Sachs-Wolfe and integrated Sachs-Wolfe effects for the stochastic GW background. This suggests us that the CGWB may be exploited to probe large-scale primordial scalar perturbations, in addition to other already established observables, like the CMB. In particular, we can study the anisotropies in the stochastic background of primordial GWs in order to test the presence of primordial non-Gaussianity. This is exactly what we are going to do later in this Chapter.

- The last term accounts for the effect of (long-wavelength) transverse and traceless tensor modes on the GW propagation. In this work we will focus on the other two contributions, being the generalization to include also this term quite straightforward, even if mathematically a bit more involved.

The statistical description of the GW stochastic background now proceeds in analogy to the CMB treatment, with the final objective being the computation of angular correlators. The next step is thus to perform the usual spherical harmonics decomposition of the anisotropies to project them onto the spherical sky. We are going to do this separately for the initial condition and the scalar term (remember that we have decided to neglect the tensor contribution), so that it is convenient to split solution (5.67) into two parts:

$$\Gamma(\tau,\vec{k},q,\hat{n}) = \Gamma_I(\tau,\vec{k},q,\hat{n}) + \Gamma_S(\tau,\vec{k},\hat{n}), \tag{5.68}$$

where I and S identify the initial condition and scalar sourced term, respectively, defined as:

$$\Gamma_I(\tau,\vec{k},q,\hat{n}) \equiv e^{-ik\mu(\tau-\tau_{\rm in})}\Gamma(\tau_{\rm in},\vec{k},q,\hat{n}), \tag{5.69}$$

and

$$\Gamma_S(\tau,\vec{k},\hat{n}) \equiv e^{-ik\mu(\tau-\tau_{\rm in})}\phi(\tau_{\rm in},\vec{k}) + \int_{\tau_{\rm in}}^{\tau} d\tau' e^{-ik\mu(\tau-\tau')}\frac{\partial\Big(\psi(\tau',\vec{k}) + \phi(\tau',\vec{k})\Big)}{\partial\tau'}. \tag{5.70}$$

We address for a moment to the directional dependence in the initial condition term. In order to obtain statistically isotropic angular correlators we choose to limit the dependence on $\hat{n}$ in (5.69) to be just inside the μ term in the exponential, which corresponds to assuming an isotropic initial value of the random field $\Gamma(\tau_{\rm in}, \vec{k}, q, \hat{n}) = \Gamma(\tau_{\rm in}, \vec{k}, q)$.
In the following Chapter we will be interested to the CGWB anisotropies arising in a more specific context, where considering primordial GWs sourced at second order by scalar perturbations characterized by a certain amount of running non-Gaussianity. In such a context it may be reasonable to relax the hypothesis and consider the possibility of anisotropic correlators. Nevertheless, for now we stick to the simpler case of isotropic correlators, hence our previous assumption on the initial condition term.

Performing the expansion of the anisotropy Γ over spherical harmonics, in real space, allows us to obtain the following expansion coefficients:

$$\Gamma_{\ell m}(\tau_0, \vec{x}_0, q) = \int d^2\hat{n} Y^*_{\ell m}(\hat{n}) \Gamma(\tau_0, \vec{x}_0, q, \hat{n}), \tag{5.71}$$

which are the analogous of the $a_{\ell m}$ coefficients (4.6) in the CMB treatment. Notice how we have decided to evaluate both sides at the present time τ_0 and at our position $\vec{x}_0$, since we would ultimately want to make contact with quantities observationally accessible to us.
We now need to substitute (5.69) and (5.70), one at a time, inside the expression (5.71) for the coefficients $\Gamma_{\ell m}$, remembering also to transform back from Fourier space to the real one.

Initial condition term

We start with the initial condition term, for which we have:

$$\Gamma_{\ell m, I}(\tau_0, \vec{x}_0, q) = \int d^2\hat{n} Y^*_{\ell m}(\hat{n}) \int \frac{d^3\vec{k}}{(2\pi)^3} e^{i\vec{k}\vec{x}_0} e^{-ik\mu(\tau_0 - \tau_{\rm in})} \Gamma(\tau_{\rm in}, \vec{k}, q). \tag{5.72}$$

The integration over the GW direction $\hat{n}$ is performed by exploiting the following expansion of the exponential in a series of Legendre polynomials [49]:

$$e^{-i\vec{k}\vec{y}} = \sum_{\ell=0}^{\infty} (-i)^\ell (2\ell + 1) j_\ell(ky) P_\ell(\hat{k} \cdot \hat{y}). \tag{5.73}$$

Remembering also the spherical harmonics expansion of P_ℓ (B.9), and applying the orthonormality condition (B.8), we finally obtain:

$$\Gamma_{\ell m, I}(\tau_0, \vec{x}_0, q) = 4\pi(-i)^\ell \int \frac{d^3\vec{k}}{(2\pi)^3} e^{i\vec{k}\vec{x}_0} \Gamma(\tau_{\rm in}, \vec{k}, q) Y^*_{\ell m}(\hat{k}) j_\ell\big(k(\tau_0 - \tau_{\rm in})\big). \tag{5.74}$$

It has to be stressed that this result holds only for the isotropic case we have assumed, where $\Gamma(\tau_{\rm in}, \vec{k}, q)$ does not depend on the GW direction. This has allowed us to simply integrate over $\hat{n}$ by exploiting the spherical harmonics normalization condition (B.8). If this had not been the case we should have taken into account a non-trivial dependence on $\hat{n}$ while performing such an integration.

Scalar sourced term

We now perform the same steps for the scalar sourced term (5.70). In order to isolate the statistical behaviour inside this expression, we make use of the formalism of the transfer function, already introduced for the treatment of CMB anisotropies. We know that temperature anisotropies Θ on a given scale $\sim k^{-1}$ are set by the value of the curvature perturbation mode $\zeta_{\vec{k}}$ when it crosses the horizon after the end of inflation. This has allowed us to introduce the transfer function, defined in expression (4.8), in order to account for the subsequent deterministic evolution inside the horizon, while leaving the statistical behaviour of Θ to be inherited from ζ. A similar argument can be

given for the metric scalar perturbations ψ and ϕ. It is possible, in fact, to relate the value of these potentials, at late time after inflation, to the primordial curvature perturbation ζ [41]:

$$\begin{aligned}\psi(\tau,\vec{k}) &= \mathcal{T}_\psi(\tau,k)\zeta(\vec{k}),\\ \phi(\tau,\vec{k}) &= \mathcal{T}_\phi(\tau,k)\zeta(\vec{k}),\end{aligned} \tag{5.75}$$

in complete analogy with the CMB temperature anisotropies transfer function (4.8). Moreover, in absence of anisotropic stresses, we know from equation (2.20) that the two scalar potentials coincide $\psi = \phi$ in the Poisson gauge, so that their respective transfer functions are also the same, i.e. $\mathcal{T}_\psi = \mathcal{T}_\phi$.
With this premise in mind, we can now compute the spherical harmonics expansion coefficients for the scalar sourced terms:

$$\begin{aligned}\Gamma_{\ell m,S}(\tau_0,\vec{x}_0) &= \int d^2\hat{n} Y^*_{\ell m}(\hat{n}) \int \frac{d^3\vec{k}}{(2\pi)^3} e^{i\vec{k}\vec{x}_0}\Bigg[e^{-ik\mu(\tau_0-\tau_{\rm in})}\mathcal{T}_\phi(\tau_{\rm in},k)\\ &\quad + \int_{\tau_{\rm in}}^{\tau_0} d\tau' e^{-ik\mu(\tau_0-\tau')}\frac{\partial\Big(\mathcal{T}_\psi(\tau',k)+\mathcal{T}_\phi(\tau',k)\Big)}{\partial\tau'}\Bigg]\zeta(\vec{k})\\ &= 4\pi(-i)^\ell \int \frac{d^3\vec{k}}{(2\pi)^3} e^{i\vec{k}\vec{x}_0}\zeta(\vec{k})Y^*_{\ell m}(\hat{k})\Bigg[\mathcal{T}_\phi(\tau_{\rm in},k)j_\ell\big(k(\tau_0-\tau_{\rm in})\big)\\ &\quad + \int_{\tau_{\rm in}}^{\tau_0} d\tau' \frac{\partial\Big(\mathcal{T}_\psi(\tau',k)+\mathcal{T}_\phi(\tau',k)\Big)}{\partial\tau'} j_\ell\big(k(\tau_0-\tau')\big)\Bigg],\end{aligned} \tag{5.76}$$

where we have followed the same procedure detailed for the initial condition term. Notice how this result closely resembles the structure of the first (SW) and third (ISW) terms of the expression (4.15) for the CMB temperature anisotropies. We can further define:

$$\mathcal{T}^S_\ell(\tau_0,\tau_{\rm in},k) \equiv \mathcal{T}_\phi(\tau_{\rm in},k)j_\ell\big(k(\tau_0-\tau_{\rm in})\big) + \int_{\tau_{\rm in}}^{\tau_0} d\tau' \frac{\partial\Big(\mathcal{T}_\psi(\tau',k)+\mathcal{T}_\phi(\tau',k)\Big)}{\partial\tau'} j_\ell\big(k(\tau_0-\tau')\big), \tag{5.77}$$

in such a way that:

$$\Gamma_{\ell m,S}(\tau_0,\vec{x}_0) = 4\pi(-i)^\ell \int \frac{d^3\vec{k}}{(2\pi)^3} e^{i\vec{k}\vec{x}_0}\zeta(\vec{k})Y^*_{\ell m}(\hat{k})\mathcal{T}^S_\ell(\tau_0,\tau_{\rm in},k), \tag{5.78}$$

thus making complete the analogy with the $a_{\ell m}$ coefficients (4.12) expressed in terms of the primordial curvature perturbation ζ.

5.4.4 Angular correlators

We compute statistical correlators of our previous results, in order to extract physical information which may be eventually compared with observations. The two different contributions to the CGWB anisotropies we are considering, (5.74) and (5.78), are determined by the statistical behaviour of the random fields $\Gamma(\tau_{\rm in},\vec{k},q)$ and $\zeta(\vec{k})$, respectively. We have already described extensively the curvature perturbation ζ, by defining the primordial power spectrum:

$$\langle\zeta(\vec{k}_1)\zeta(\vec{k}_2)\rangle = (2\pi)^3\delta^{(3)}(\vec{k}_1+\vec{k}_2)P_\zeta(k_1), \tag{5.79}$$

and the primordial bispectrum:

$$\langle\zeta(\vec{k}_1)\zeta(\vec{k}_2)\zeta(\vec{k}_3)\rangle = (2\pi)^3\delta^{(3)}(\vec{k}_1+\vec{k}_2+\vec{k}_3)B_\zeta(k_1,k_2,k_3), \tag{5.80}$$

which for the latter we know to be non-vanishing only in the presence of primordial non-Gaussianity. The same treatment can also be applied to the anisotropy initial condition $\Gamma(\tau_{\rm in},\vec{k},q)$, which we assume to be the result of some primordial random process. We thus define the following 2-point:

$$\langle\Gamma(\tau_{\rm in},\vec{k}_1,q)\Gamma(\tau_{\rm in},\vec{k}_2,q)\rangle = (2\pi)^3\delta^{(3)}(\vec{k}_1+\vec{k}_2)P_I(q,k_1), \tag{5.81}$$

and 3-point correlation functions:

$$\langle \Gamma(\tau_{\rm in}, \vec{k}_1, q)\Gamma(\tau_{\rm in}, \vec{k}_2, q)\Gamma(\tau_{\rm in}, \vec{k}_3, q)\rangle = (2\pi)^3\delta^{(3)}(\vec{k}_1 + \vec{k}_2 + \vec{k}_3)B_I(q, k_1, k_2, k_3). \tag{5.82}$$

Notice in particular that the exclusive q-dependence of the initial condition term gets transferred to P_I and B_I.
We can now exploit the correlators just defined to compute the angular correlators of expression (5.71), starting with the angular power spectrum.

Angular power spectrum

We define the angular power spectrum in analogy to the CMB temperature one (4.7):

$$\langle \Gamma_{\ell_1 m_1}\Gamma^*_{\ell_2 m_2}\rangle = \delta_{\ell_1\ell_2}\delta_{m_1 m_2}\tilde{C}_{\ell_1}. \tag{5.83}$$

Exploiting the split (5.68), it is useful to also write expression (5.71) as:

$$\Gamma_{\ell m}(\tau_0, \vec{x}_0, q) = \Gamma_{\ell m, I}(\tau_0, \vec{x}_0, q) + \Gamma_{\ell m, S}(\tau_0, \vec{x}_0), \tag{5.84}$$

which substituted in (5.83) gives:

$$\tilde{C}_\ell = \tilde{C}_{\ell, I} + \tilde{C}_{\ell, S}, \tag{5.85}$$

where we have chosen to neglect the possibility of an eventual cross-correlation, in order to focus on the effects of the different physical mechanisms.
The 2-point correlators are then computed in the usual way, which we have already reported with all the details for the CMB case. Here we thus limit to provide with the results:

$$\tilde{C}_{\ell, I}(q) = 4\pi \int \frac{dk}{k}\left[j_\ell\big(k(\tau_0 - \tau_{\rm in})\big)\right]^2 \mathcal{P}_I(q, k), \tag{5.86}$$

$$\tilde{C}_{\ell, S} = 4\pi \int \frac{dk}{k}\big(\mathcal{T}^S_\ell(k, \tau_0, \tau_{\rm in})\big)^2 \mathcal{P}_\zeta(k). \tag{5.87}$$

It is interesting to consider the large-scale limit of this expressions. Remember in fact that, in the approximation of the shortwave formalism, we are considering only large-scale CGWB anisotropies produced by the propagation of high-frequency GWs across long-wavelength perturbation modes. We know that, for CMB temperature anisotropies, in the large-scale limit the SW term dominates over the ISW one and we expect now a similar outcome for the scalar sourced term (5.78). Actually, in this case we can give a slightly different explanation as to why we safely neglect the ISW contribution. For long-wavelength modes, which re-entered the horizon at later times during matter domination, we can safely neglect the evolution of the transfer functions and set them to be constant [41]:

$$\mathcal{T}_\psi = \mathcal{T}_\phi = \frac{3}{5}. \tag{5.88}$$

In this way, expression (5.77) reduces to:

$$\mathcal{T}^S_\ell(\tau_0, \tau_{\rm in}, k) = \frac{3}{5} j_\ell\big(k(\tau_0 - \tau_{\rm in})\big), \tag{5.89}$$

where in particular the contribution responsible for the ISW term vanishes since it is proportional to the time derivative of the transfer functions, which we are assuming constant.
We then exploit relation (B.12) to solve the integrals in (5.86) and (5.87), obtaining the following result for the CGWB anisotropies angular power spectrum in the large-scale limit:

$$\tilde{C}_\ell = \frac{2\pi}{\ell(\ell+1)}\left(\mathcal{P}_I(q) + \frac{9}{25}\mathcal{P}_\zeta\right), \tag{5.90}$$

where we have assumed a scale-invariant power spectrum for both the anisotropies initial condition and the curvature perturbation. The scalar sourced contribution of this result happens to be proportional to the CMB anisotropies spectrum in the Sachs-Wolfe regime (4.22), consistently with the fact that we have considered only the SW term in (5.77).

Angular bispectrum

In the previous Chapter we have computed the 3-point correlation function of CMB angular anisotropies and we have shown that it is strictly related to the non-Gaussianity of the primordial curvature perturbation ζ. A similar argument holds also for the CGWB anisotropies we are considering here, as it is evident from expression (5.78) for the contribution due to the GW propagation across scalar metric perturbations. The 3-point correlator of such a term can thus be regarded as a probe, alternative to the CMB, to test the presence of primordial non-Gaussianity. Before returning to this topic, which is one of the main focus of this Thesis, let us compute the angular bispectrum of the full anisotropy term (5.71), including also the contribution due to initial conditions.

The angular bispectrum of the CGWB anisotropies can be defined as:

$$\tilde{B}^{m_1 m_2 m_3}_{\ell_1 \ell_2 \ell_3} = \langle \Gamma_{\ell_1 m_1} \Gamma_{\ell_2 m_2} \Gamma_{\ell_3 m_3} \rangle, \tag{5.91}$$

in analogy with the angular bispectrum of CMB anisotropies (4.24). We can focus on the reduced bispectrum, defined in (4.27), without losing the physical information. In order to perform the explicit computation, we split the result in the usual way:

$$\tilde{b}_{\ell_1 \ell_2 \ell_3} = \tilde{b}_{\ell_1 \ell_2 \ell_3, I} + \tilde{b}_{\ell_1 \ell_2 \ell_3, S}, \tag{5.92}$$

where cross-correlations terms are neglected. The 3-point correlators of terms (5.74) and (5.78) are recovered in analogy with the CMB angular anisotropies one. We then refer to section 4.2.1 for the detailed calculations, which have just to be adapted for the current cases. The results of this procedure are the following reduced bispectra:

$$\tilde{b}_{\ell_1 \ell_2 \ell_3, I}(q) = \int_0^\infty dr r^2 \prod_{i=1}^{3} \left[\frac{2}{\pi} \int_0^\infty dk_i k_i^2 j_{\ell_i}\big(k(\tau_0 - \tau_{\rm in})\big) j_{\ell_i}(k_i r) \right] B_I(q, k_1, k_2, k_3), \tag{5.93}$$

$$\tilde{b}_{\ell_1 \ell_2 \ell_3, S} = \int_0^\infty dr r^2 \prod_{i=1}^{3} \left[\frac{2}{\pi} \int_0^\infty dk_i k_i^2 \mathcal{T}^S_{\ell_i}(k_i, \tau_0, \tau_{\rm in}) j_{\ell_i}(k_i r) \right] B_\zeta(k_1, k_2, k_3). \tag{5.94}$$

The reduced bispectrum of the scalar sourced contribution is in particular interesting since, as anticipated earlier, we can study the effect of primordial non-Gaussianity, and its possible running, on this term. Such a treatment is very similar to the one we have already detailed for the CMB bispectrum and it will be the focus of the remaining part of this Chapter.

5.5 Probing primordial non-Gaussianity via CGWB anisotropies

One interesting result we have found in our computations is that the statistics of the CGWB anisotropy term sourced by the scalar perturbations (5.78) is fully determined by the statistics of the primordial curvature perturbation ζ, which is exactly analogous to what happens for the CMB angular anisotropies (4.11). In Chapter 4 we have used this fact to study the effects of the non-Gaussianity of ζ, i.e. the primordial non-Gaussianity, on the expressions for CMB angular power spectrum and bispectrum. In return, observational measurements on the CMB statistics can then be used to constrain the amount of primordial non-Gaussianity. It is in this sense that the CMB can be considered as a probe to test primordial non-Gaussianity.
Therefore, it seems natural to conclude that the CGWB represents an additional and independent source of information for primordial non-Gaussianity. As we have said, this information is contained inside the contribution to anisotropies due to the scalar perturbations the GWs have to traverse along their path.

Given the previous considerations, in this section we want to compute the effects of primordial non-Gaussianity on the CGWB anisotropies angular correlators we have previously derived. In particular, the original aim of this Thesis was to derive the consequences of scale-dependent non-Gaussianity.
We anticipate that the results we are looking for closely resemble what we have already computed

in Chapter 4 in the CMB case. This should not come as a surprise, since our treatment of the CGWB has been done in complete analogy to the one developed for the CMB. Nevertheless we spend a few words on this topic, both beacuse the physical phenomenon under study is quite different, even if the mathematics is not, and because this was estabilished as one of the main focus of this Thesis. We leave for the next Chapter the treatment of a more original outcome of running non-Gaussianity on the CGWB anisotropies.

5.5.1 CGWB anisotropies and local non-Gaussianity

The starting point of the following discussion is result (5.94) for the reduced bispectrum of CGWB anisotropies sourced by primordial scalar perturbations. Being it proportional to the primordial bispectrum B_ζ, we see that the term vanishes for a Gaussian curvature perturbation ζ. We are thus interested in the less trivial scenario where primordial non-Gaussianity is indeed present.
We assume the usual non-linear coupling expressed by the local ansatz (3.7). We have already computed the primordial bispectrum (3.24) arising from such a parametrization, which we rewrite here in terms of the adimensional power spectrum (1.61):

$$B_\zeta(k_1,k_2,k_3) = \frac{6}{5} f_{NL} \left[\frac{2\pi^2}{k_1^3} \mathcal{P}_\zeta(k_1) \frac{2\pi^2}{k_2^3} \mathcal{P}_\zeta(k_2) + 2 \text{ perms} \right]. \tag{5.95}$$

Substituting this expression inside (5.94) allows to factorize the three integrals over k_i:

$$\begin{aligned} \tilde{b}_{\ell_1\ell_2\ell_3,S} = \frac{24}{5}\pi^4 f_{NL} \int_0^\infty dr r^2 \Bigg[& \left(\frac{2}{\pi} \int_0^\infty \frac{dk_1}{k_1} \mathcal{T}^S_{\ell_1}(k_1,\tau_0,\tau_{\text{in}}) j_{\ell_1}(k_1 r) \mathcal{P}_\zeta(k_1) \right) \\ & \times \left(\frac{2}{\pi} \int_0^\infty \frac{dk_2}{k_2} \mathcal{T}^S_{\ell_2}(k_2,\tau_0,\tau_{\text{in}}) j_{\ell_2}(k_2 r) \mathcal{P}_\zeta(k_2) \right) \\ & \times \left(\frac{2}{\pi} \int_0^\infty dk_3 k_3^2 \mathcal{T}^S_{\ell_3}(k_3,\tau_0,\tau_{\text{in}}) j_{\ell_3}(k_3 r) \right) + 2 \text{ perms} \Bigg]. \end{aligned} \tag{5.96}$$

Comparing this expression with (4.34), we see that results for the CGWB bispectrum may be simply obtained from the CMB ones by substituting the CMB transfer function $\mathcal{T}_\ell$ with the transfer function $\mathcal{T}^S_\ell$ for the scalar sourced contribution to the CGWB anisotropies.
If we assume expression (5.88) for the transfer functions, valid for modes re-entering the horizon during matter domination, the result (5.96) simplifies in a way similar to the CMB bispectrum in the Sachs-Wolfe regime (4.41). We can exploit in particular the closure relation of spherical Bessel functions (B.11) in order to solve the following integral:

$$\frac{3}{5}\frac{2}{\pi} \int_0^\infty dk k^2 j_\ell(k\tau_0) j_\ell(kr) = \frac{3}{5} \frac{\delta(r-\tau_0)}{r^2}, \tag{5.97}$$

where we have expressed $\mathcal{T}^S_\ell = j_\ell(k\tau_0)$, which comes from result (5.89) with the reasonable approximation $\tau_0 - \tau_{\text{in}} \simeq \tau_0$. Actually, we have been a little imprecise, since expression (5.88) is only valid for large-scale modes of the curvature perturbation. In practice this means that, in substituting this expression inside (5.96), we should cut off the k_i integrals at the maximum wavenumber for which the transfer function (5.88) holds. As a consequence, the exact relation (B.11) should be applied only for sufficiently low multipoles ℓ, in such a way that the contribution to the integral from the disregarded interval can be safely neglected. We see that, even if the reasons are a bit different, we end up in the same Sachs-Wolfe regime considered for the CMB and the following results will thus be valid only for low multipoles, i.e. large angular scales.
Substituting relation (5.97) in expression (5.96), it is possible to solve the integral over r and obtain:

$$\begin{aligned} \tilde{b}_{\ell_1\ell_2\ell_3,S} = 2 f_{NL} \Bigg[& \left(4\pi \frac{9}{25} \int_0^\infty \frac{dk_1}{k_1} j^2_{\ell_1}(k_1\tau_0) \mathcal{P}_\zeta(k_1) \right) \\ & \times \left(4\pi \frac{9}{25} \int_0^\infty \frac{dk_2}{k_2} j^2_{\ell_2}(k_2\tau_0) \mathcal{P}_\zeta(k_2) \right) + 2 \text{ perms} \Bigg]. \end{aligned} \tag{5.98}$$

We recognize in this result the expression for the scalar source contribution to the angular power spectrum (5.87), in such a way that we can write it in the following way:

$$\tilde{b}_{\ell_1\ell_2\ell_3,S} = 2f_{NL}(\tilde{C}_{\ell_1,S}\tilde{C}_{\ell_2,S} + \tilde{C}_{\ell_2,S}\tilde{C}_{\ell_3,S} + \tilde{C}_{\ell_3,S}\tilde{C}_{\ell_1,S}), \tag{5.99}$$

which is analogous to the CMB reduced bispectrum in the Sachs-Wolfe regime (4.42). Again, this result includes only the contribution coming from the SW term in (5.77) and it is valid only for anisotropies on large angular scales.

We remind that the expression for the angular power spectrum (5.87) holds in presence of non-Gaussianity when keeping the first order in f_{NL}. It is straightforward to verify that, assuming the local ansatz (3.7), the lowest non-Gaussian correction to the primordial power spectrum is indeed of second order in the non-linear parameter. In this way result (5.99) relates the CGWB anisotropies angular power spectrum and bispectrum in presence of non-Gaussianity, at first order in f_{NL}.

5.5.2 CGWB anisotropies and running non-Gaussianity

Results just derived may be generalized to the case of a scale-dependent non-Gaussianity. We have seen in Chapter 3 that it is possible to account for running non-Gaussianity by generalizing the simple non-linear coupling of the local ansatz (3.7), by substituting it with a less trivial kernel (3.41), quadratic in the curvature perturbation ζ. This actually corresponds to consider a scale dependence of the non-linear parameter f_{NL}, whose parametrization can be determined explicitly by performing a matching with a given template of running primordial bispectrum.
In order to account for a running of f_{NL}, it is useful to define the following r-dependent coefficients:

$$\tilde{\alpha}_\ell(r) \equiv \frac{2}{\pi}\int_0^\infty dk k^2 \mathcal{T}_\ell^S(k,\tau_0,\tau_{\rm in}) j_\ell(kr), \tag{5.100}$$

$$\tilde{\beta}_\ell(r) \equiv \frac{2}{\pi}\int_0^\infty dk k^2 P_\zeta(k) \mathcal{T}_\ell^S(k,\tau_0,\tau_{\rm in}) j_\ell(kr), \tag{5.101}$$

analogous to the CMB ones (4.35) and (4.36). The reduced bispectrum (5.96) can thus be expressed as:

$$\tilde{b}_{\ell_1\ell_2\ell_3} = \frac{6}{5} f_{NL}\int_0^\infty dr r^2 \left[\tilde{\alpha}_{\ell_1}(r)\tilde{\beta}_{\ell_2}(r)\tilde{\beta}_{\ell_3}(r) + \tilde{\alpha}_{\ell_2}(r)\tilde{\beta}_{\ell_3}(r)\tilde{\beta}_{\ell_1}(r) + \tilde{\alpha}_{\ell_3}(r)\tilde{\beta}_{\ell_1}(r)\tilde{\beta}_{\ell_2}(r)\right]. \tag{5.102}$$

In the presence of running, the scale-dependent $f_{NL}(k_1,k_2,k_3)$ would enter the definitions of coefficients (5.100) and (5.101), carrying an additional k-dependence, provided it is expressed in a factorizable form. This is actually the case for the power-law explicit parametrizations we have encountered so far.
The actual results are identical to the CMB ones we have already provided. For completeness we report them anyway.
In the case of a simple power-law non-Gaussianity (3.37), the coefficient $\tilde{\alpha}_\ell$ gets modified as:

$$\tilde{\alpha}_\ell(r) = \frac{2}{\pi}\frac{1}{k_p^{n_{f_{NL}}}}\int_0^\infty dk k^{2+n_{f_{NL}}} \mathcal{T}_\ell^S(k,\tau_0,\tau_{\rm in}) j_\ell(kr), \tag{5.103}$$

while for the kernel (3.53) it is the coefficient $\tilde{\beta}_\ell$ who gains a new dependence inside the integral:

$$\tilde{\beta}_\ell(r) = \frac{2}{\pi}\frac{1}{k_p^{n_{f_{NL}}}}\int_0^\infty dk k^{2+\frac{n_{f_{NL}}}{2}} P_\zeta(k) \mathcal{T}_\ell^S(k,\tau_0,\tau_{\rm in}) j_\ell(kr). \tag{5.104}$$

With these re-definitions, expression (5.102) for the reduced bispectrum holds also in the presence of running, where the constant f_{NL} in the front has to be replaced with $f_{NL}(k_p)$ evaluated at the pivot scale.
We have seen how taking the Sachs-Wolfe limit results in the constant transfer function (5.88). This simplifies the integrals inside coefficients $\tilde{\alpha}_\ell$ and $\tilde{\beta}_\ell$, but in general it is not possible to derive

an expression analogous to (5.99), directly relating the angular power spectrum and bispectrum, in the case of running non-Gaussianity. We have already pointed out this fact in section 4.2.3, dealing with the CMB running bispectrum.

Expression (5.102), and its generalization to include the presence of running non-Gaussianity, is the result for the reduced bispectrum of CGWB anisotropies, sourced by scalar perturbations, written in terms of the non-linear parameter f_{NL} and the primordial power spectrum P_ζ. Following an actual detection of the stochastic cosmological background of GWs, our results may indeed be exploited to constrain local non-Gaussianity, and its running, provided it is possible to isolate the scalar sourced contribution to the anisotropies. In principle, a similar procedure may be applied to probe different shapes of non-Gaussianity, other than the local one, and additional parametrizations of the running.

Chapter 6

CGWB anisotropies from enhanced scalar perturbations

In the previous Chapter we have performed a statistical analysis of the anisotropies in the cosmological gravitational wave background, computing the 2-point and 3-point correlators. In particular we have considered two distinct sources of anisotropies. The first can be identified with initial conditions set by the mechanism responsible for the production of the background itself at early times. The other contribution to the anisotropies is due instead to the propagation of high-frequency GWs across large-scale metric perturbations, an assumption which has allowed us to introduce the graviton distribution function and study its evolution by means of the Boltzmann equation. We have found in particular that the scalar sourced term inherit its statistics from the curvature perturbation. We have thus concluded that an experimental measurements of the reduced bispectrum (5.96) would allow to extract information and put constraints on primordial non-Gaussianity, and its running, in analogy to what is already done using CMB temperature anisotropies.

So far, in our discussion we have not made any specific assumption about the source of the CGWB, meaning that the results of the previous Chapter should hold whatever is the mechanism responsible for the production of GWs. We know that the latter is accounted for by the initial condition term (5.69), which we have considered to be an independent random field. Therefore, we have assumed the initial condition to the CGWB anisotropies to not carry any information about the statistics of primordial scalar perturbations and thus we have disregarded it while searching for signatures of primordial non-Gaussianity on the GW background.
In this Chapter we consider instead a more specific scenario, namely the stochastic background of GWs generated along with the formation of primordial black holes (PBHs). In such a context the GWs are produced classically at second order, sourced by primordial scalar perturbations [69, 70, 71, 20, 72, 73, 74, 75]. A particular attractive of this scenario is that it exclusively allows, as we will see, to probe the amount of non-Gaussianity at the small scales related to PBH formation. In this sense future detections of such a CGWB may provide with information about primordial non-Gaussianity which are otherwise inaccessible by CMB measurements.
We start the Chapter by reviewing the key points of the production of scalar sourced GWs at second order and introducing briefly to the physics of PBHs. Later on we will also compute how constraints on PBHs as dark matter may be relaxed with a specific parametrization of running non-Gaussianity. This was one of the main motivation behind this work, and can be considered to be the central original result.

6.1 Gravitational waves at second order from scalar perturbations

In the previous Chapter we have reviewed how primordial GWs are produced as quantum metric perturbations during standard slow-roll inflation. We have already pointed out that also other

mechanisms may be responsible for the production of a stochastic background.
The alternative in which we are interested here is the classical production of GWs sourced by scalar perturbations. This is a result which arises only at second order in perturbation theory and can provide an important contribution to the stochastic GW background if scalar perturbations are somehow enhanced at small scales, thus breaking the scale invariance property of large-scale perturbations. Nevertheless, a CGWB of this kind is always expected when scalar perturbations are produced, which we know to be the case during inflation. We now review how GWs can arise from scalar perturbations at second order. The first seminal papers dealing with second-order gravitational waves induced by scalar perturbations have been developed in [20, 76].

Going beyond linear order in CPT, the fact that metric perturbations of different nature do not couple remains valid only for perturbations of the same order. This means that, already at second order, we have that tensor perturbations, i.e. GWs, are inevitably sourced by first-order scalar perturbations. In order to better study this scenario, we introduce the following perturbed FLRW metric:

$$ds^2 = a^2(\tau)\Big[-(1+2\phi^{(1)})d\tau^2 + \big((1-2\psi^{(1)})\delta_{ij} + \frac{1}{2}h^{(2)}_{ij}\big)dx^i dx^j\Big], \tag{6.1}$$

where we have specified the order of the perturbations, which from now on will be made implicit. Notice that we are neglecting first-order tensors since the mechanism we are investigating is able to produce GWs only at second order or higher.
The equation of motion for h_{ij} is obtained by writing Einstein's equations for the perturbed metric (6.1). Expanding the transverce and traceless spatial part up to second order we obtain [20, 70, 72, 76] (see also, e.g. [73, 74]):

$$h''_{ij} + 2\mathcal{H}h'_{ij} - \nabla^2 h_{ij} = -4\mathcal{T}_{ij}^{\ lm}\mathcal{S}_{lm}, \tag{6.2}$$

where the source term $\mathcal{S}_{lm}$ is contributed by second-order combinations of first-order scalar perturbations and reads [20, 70, 72, 76] (see also, e.g. [27, 74]):

$$\begin{aligned}\mathcal{S}_{ij} &= 2\phi\partial_i\partial_j\phi - 2\psi\partial_i\partial_j\phi + 4\psi\partial_i\partial_j\psi + \partial_i\phi\partial_j\phi - \partial_i\phi\partial_j\psi - \partial_i\psi\partial_j\phi + 3\partial_i\psi\partial_j\psi \\ &- \frac{4}{3(1+w)\mathcal{H}^2}\partial_i(\psi'+\mathcal{H}\phi)\partial_j(\psi'+\mathcal{H}\phi) - \frac{2c_s^2}{3w\mathcal{H}^2}\big[3\mathcal{H}(\mathcal{H}\phi-\psi') + \nabla^2\psi\big]\partial_i\partial_j(\phi-\psi).\end{aligned} \tag{6.3}$$

The projector $\mathcal{T}_{ij}^{\ lm}$ extracts the transverse and traceless part of the tensor it acts on.
In Fourier space the GW amplitude can be decomposed in terms of the polarization tensors:

$$h_{ij}(\tau,\vec{x}) = \sum_{\lambda=(+,\times)}\int\frac{d^3\vec{k}}{(2\pi)^3}h^{(\lambda)}(\tau,\vec{k})e^{(\lambda)}_{ij}(\hat{k})e^{i\vec{k}\vec{x}}. \tag{6.4}$$

It is useful to express the polarization basis as:

$$\begin{aligned}e^{(+)}_{ij}(\hat{k}) &= \frac{1}{\sqrt{2}}\big[e_i(\hat{k})e_j(\hat{k}) - \bar{e}_i(\hat{k})\bar{e}_j(\hat{k})\big], \\ e^{(\times)}_{ij}(\hat{k}) &= \frac{1}{\sqrt{2}}\big[e_i(\hat{k})\bar{e}_j(\hat{k}) + \bar{e}_i(\hat{k})e_j(\hat{k})\big],\end{aligned} \tag{6.5}$$

where e_i and $\bar{e}_i$ form an orthonormal basis with $\hat{k}$, so that $e^{(\lambda)}_{ij}e^{(\lambda)ij} = 1$ and $e^{(\lambda)}_{ij}e^{(\lambda')ij} = 0$.
In terms of the polarization tensors, the TT projected source term is:

$$\mathcal{T}_{ij}^{\ lm}\mathcal{S}_{lm} = \sum_{\lambda=(+,\times)}\int\frac{d^3\vec{k}}{(2\pi)^3}e^{(\lambda)}_{ij}(\hat{k})e^{(\lambda)ij}(\hat{k})e^{i\vec{k}\vec{x}}\mathcal{S}_{lm}(\vec{k}). \tag{6.6}$$

It is then possible to write equation (6.2) in Fourier space for the mode function $h_{\vec{k}}$ with either polarization:

$$h''_{\vec{k}} + 2\mathcal{H}h'_{\vec{k}} + k^2 h_{\vec{k}} = \mathcal{S}(\tau,\vec{k}), \tag{6.7}$$

where the source term is defined as:

$$\mathcal{S}^{(\lambda)}(\tau,\vec{k}) \equiv -4e^{(\lambda)lm}(\vec{k})\mathcal{S}_{lm}(\vec{k}), \tag{6.8}$$

whose explicit expression is actually a convolution of two first-order scalar perturbations [20, 76, 74]. The mode solution of equation (6.7) can be expressed in the following way:

$$h_{\vec{k}}^{(\lambda)}(\tau) = \frac{4}{9}\frac{1}{k^3\tau}\int \frac{d^3\vec{p}}{(2\pi)^3} e^{(\lambda)}(\hat{k},\vec{p})\zeta(\vec{p})\zeta(\vec{k}-\vec{p})\left[\mathcal{I}_c(p,|\vec{k}-\vec{p}|)\cos(k\tau)+\mathcal{I}_s(p,|\vec{k}-\vec{p}|)\sin(k\tau)\right], \quad (6.9)$$

where the details of the calculation are reported in Appendix C, together with the definitions for the functions $\mathcal{I}_c$ and $\mathcal{I}_s$.

6.1.1 GW amplitude power spectrum

We now compute the 2-point correlation function of solution (6.9), corresponding to the power spectrum of GWs generated at second order from scalar perturbations:

$$\begin{aligned}\langle h_{\vec{k}_1}^{(\lambda)}(\tau) h_{\vec{k}_2}^{(\lambda')}(\tau)\rangle = &\left(\frac{4}{9}\right)^2 \frac{1}{k_1^3 k_2^3 \tau^2}\int \frac{d^3\vec{p}_1}{(2\pi)^3}\int \frac{d^3\vec{p}_2}{(2\pi)^3} e^{(\lambda)}(\hat{k}_1,\vec{p}_1)e^{(\lambda')}(\hat{k}_2,\vec{p}_2)\\ &\times\langle\zeta(\vec{p}_1)\zeta(\vec{k}_1-\vec{p}_1)\zeta(\vec{p}_2)\zeta(\vec{k}_2-\vec{p}_2)\rangle\\ &\times\left[\mathcal{I}_c(p_1,|\vec{k}_1-\vec{p}_1|)\cos(k_1\tau)+\mathcal{I}_s(p_1,|\vec{k}_1-\vec{p}_1|)\sin(k_1\tau)\right]\\ &\times\left[\mathcal{I}_c(p_2,|\vec{k}_2-\vec{p}_2|)\cos(k_2\tau)+\mathcal{I}_s(p_2,|\vec{k}_2-\vec{p}_2|)\sin(k_2\tau)\right],\end{aligned} \quad (6.10)$$

where the adimensional power spectrum of the curvature perturbation is defined in the usual way:

$$\langle\zeta(\vec{k}_1)\zeta(\vec{k}_2)\rangle = (2\pi)^3\delta^{(3)}(\vec{k}_1+\vec{k}_2)\frac{2\pi^2}{k_1^3}\mathcal{P}_\zeta(k_1). \quad (6.11)$$

In order to evaluate the 4-point correlator in (6.10) we assume, for the moment, that ζ possesses a Gaussian statistics, in such a way that we can write schematically:

$$\langle\zeta^4\rangle = \langle\zeta^2\rangle\langle\zeta^2\rangle + \langle\zeta^2\rangle\langle\zeta^2\rangle + \langle\zeta^2\rangle\langle\zeta^2\rangle, \quad (6.12)$$

meaning that the 4-point correlator can be expressed in terms of the 2-point one, i.e. its conneceted part vanishes. We will see in the next section how to generalize the treatment to the case of non-Gaussian statistics of ζ, which is actually the main focus of this Chapter.
Therefore, in terms of the primordial power spectrum, the 4-point correlation function of Gaussian ζ has two non-vanishing contributions for $\vec{k}_1, \vec{k}_2 \neq 0$:

$$\begin{aligned}\langle\zeta(\vec{p}_1)\zeta(\vec{k}_1-\vec{p}_1)\zeta(\vec{p}_2)\zeta(\vec{k}_2-\vec{p}_2)\rangle = &(2\pi)^6\delta^{(3)}(\vec{p}_1+\vec{p}_2)\delta^{(3)}(\vec{k}_1-\vec{p}_1+\vec{k}_2-\vec{p}_2)\\ &\times\frac{2\pi^2}{p_1^3}\mathcal{P}_\zeta(p_1)\frac{2\pi^2}{|\vec{k}_1-\vec{p}_1|^3}\mathcal{P}_\zeta(|\vec{k}_1-\vec{p}_1|)\\ &+(2\pi)^6\delta^{(3)}(\vec{p}_1+\vec{k}_2-\vec{p}_2)\delta^{(3)}(\vec{p}_2+\vec{k}_1-\vec{p}_1)\\ &\times\frac{2\pi^2}{p_1^3}\mathcal{P}_\zeta(p_1)\frac{2\pi^2}{p_2^3}\mathcal{P}_\zeta(p_2),\end{aligned} \quad (6.13)$$

and it is possible to show that the two terms contribute equally inside the integrals in (6.10). We choose to keep the first contribution and account for an overall factor 2. Exploiting the Dirac delta to integrate over $\vec{p}_2$ leads to:

$$\begin{aligned}\langle h_{\vec{k}_1}^{(\lambda)}(\tau) h_{\vec{k}_2}^{(\lambda')}(\tau)\rangle = &(2\pi)^3\delta^{(3)}(\vec{k}_1+\vec{k}_2)\left(\frac{4}{9}\right)^2\frac{2}{k_1^6\tau^2}\int\frac{d^3\vec{p}_1}{(2\pi)^3}e^{(\lambda)}(\hat{k}_1,\vec{p}_1)e^{(\lambda')}(-\hat{k}_1,-\vec{p}_1)\\ &\times\frac{2\pi^2}{p_1^3}\mathcal{P}_\zeta(p_1)\frac{2\pi^2}{|\vec{k}_1-\vec{p}_1|^3}\mathcal{P}_\zeta(|\vec{k}_1-\vec{p}_1|)\\ &\times\left[\mathcal{I}_c(p_1,|\vec{k}_1-\vec{p}_1|)\cos(k_1\tau)+\mathcal{I}_s(p_1,|\vec{k}_1-\vec{p}_1|)\sin(k_1\tau)\right]^2,\end{aligned} \quad (6.14)$$

where we have also exploited the second Dirac delta to set $\vec{k}_2 = -\vec{k}_1$. In order to solve the integral over $\vec{p}_1$ it is now useful to introduce the following variables [78]:

$$x = \frac{p_1}{k_1}, \qquad y = \frac{|\vec{k}_1 - \vec{p}_1|}{k_1}. \tag{6.15}$$

Moreover, we are allowed to assume, without losing generality, a coordinate system where $\vec{k}_1$ is oriented along the third axis, and to express the integral in (6.14) in spherical coordinates (p_1, θ, ϕ), where:

$$\cos\theta = \frac{1 + x^2 - y^2}{2x}. \tag{6.16}$$

We can first of all solve the integral over ϕ, with only the function $e^{(\lambda)}(\hat{k}_1, \vec{p}_1)$ carrying such a dependence. Its definition is given by (C.5) in Appendix C. It is possible to explicitly compute that [78]:

$$\int_0^{2\pi} d\phi e^{(\lambda)}(\hat{k}_1, \vec{p}_1) e^{(\lambda')}(-\hat{k}_1, -\vec{p}_1) = \frac{k_1^4 x^4}{2} \pi \left[1 - \frac{(1 + x^2 - y^2)^2}{4x^2}\right]^2 \delta^{\lambda\lambda'}. \tag{6.17}$$

Substituting this result in (6.14) and performing the change of variable (6.15) leads to:

$$\begin{aligned} \langle h^{(\lambda)}_{\vec{k}_1}(\tau) h^{(\lambda')}_{\vec{k}_2}(\tau)\rangle = (2\pi)^3 \delta^{(3)}(\vec{k}_1 + \vec{k}_2)\delta^{\lambda\lambda'} \frac{2\pi^2}{k_1^3} \times \frac{4}{81}\frac{1}{k_1^2\tau^2} \int\int_{\mathcal{S}} dxdy \frac{x^2}{y^2} \\ \times \left[1 - \frac{(1 + x^2 - y^2)^2}{4x^2}\right]^2 \mathcal{P}_\zeta(k_1 x)\mathcal{P}_\zeta(k_1 y) \\ \times \left[\mathcal{I}_c(x, y)\cos(k_1\tau) + \mathcal{I}_s(x, y)\sin(k_1\tau)\right]^2, \end{aligned} \tag{6.18}$$

where the integration domain is $\mathcal{S} = \{(x, y) | x > 0 \wedge |1 - x| \leq y < 1 + x\}$.
We recognize in this result the power spectrum of the GW amplitude, in the case of a second-order scalar source, defined in the usual way:

$$\langle h^{(\lambda)}_{\vec{k}_1}(\tau) h^{(\lambda')}_{\vec{k}_2}(\tau)\rangle = (2\pi)^3 \delta^{(3)}(\vec{k}_1 + \vec{k}_2)\delta^{\lambda\lambda'} \frac{2\pi^2}{k_1^3} \mathcal{P}_h(k_1), \tag{6.19}$$

with:

$$\begin{aligned} \mathcal{P}_h(\tau, k) = \frac{4}{81}\frac{1}{k^2\tau^2} \int\int_{\mathcal{S}} dxdy \frac{x^2}{y^2} \left[1 - \frac{(1 + x^2 - y^2)^2}{4x^2}\right]^2 \mathcal{P}_\zeta(kx)\mathcal{P}_\zeta(ky) \\ \times \left[\mathcal{I}_c(x, y)\cos(k\tau) + \mathcal{I}_s(x, y)\sin(k\tau)\right]^2. \end{aligned} \tag{6.20}$$

6.1.2 GW energy density

We are actually more interested in the energy density of the scalar sourced CGWB, rather than in the power spectrum of its amplitude. For the second-order tensor perturbation h_{ij} in (6.1), the energy density is defined in real space as [68, 79]:

$$\rho_{GW}(\tau, \vec{x}) = \frac{M_P^2}{16a^2} \langle h'_{ij}(\tau, \vec{x}) h'^{ij}(\tau, \vec{x})\rangle_T, \tag{6.21}$$

where the angle brackets denote a time average over an interval much greater than the GW period k^{-1} but much smaller than the Hubble time H^{-1}. The expected GW energy density is the 1-point correlator of (6.21), which we can compute starting from the mode solution (6.9) for $h_{\vec{k}}$ we have derived in the previous section. Remembering also the Fourier decomposition in terms of the

polarization tensors (6.4), we obtain the following expression:

$$\begin{aligned}\langle\rho_{GW}(\tau,\vec{x})\rangle &= \frac{M_P^2}{16a^2}\int\frac{d^3\vec{k}_1}{(2\pi)^3}\int\frac{d^3\vec{k}_2}{(2\pi)^3}e^{i(\vec{k}_1+\vec{k}_2)\vec{x}}\sum_{\lambda,\lambda'}\langle\langle h'^{(\lambda)}_{\vec{k}_1}(\tau)h'^{(\lambda')}_{\vec{k}_2}(\tau)\rangle_T e^{(\lambda)}_{ij}(\hat{k}_1)e^{(\lambda')ij}(\hat{k}_2)\\ &= \frac{M_P^2}{16a^2}\left(\frac{4}{9}\right)^2\frac{1}{\tau^2}\int\frac{d^3\vec{k}_1}{(2\pi)^3}\int\frac{d^3\vec{k}_2}{(2\pi)^3}\int\frac{d^3\vec{p}_1}{(2\pi)^3}\int\frac{d^3\vec{p}_2}{(2\pi)^3}\\ &\times e^{i(\vec{k}_1+\vec{k}_2)\vec{x}}\frac{1}{k_1^2k_2^2}\langle\zeta(\vec{p}_1)\zeta(\vec{k}_1-\vec{p}_1)\zeta(\vec{p}_2)\zeta(\vec{k}_2-\vec{p}_2)\rangle\\ &\times\langle\prod_{i=1}^{2}\left[\mathcal{I}_s(p_i,|\vec{k}_i-\vec{p}_i|)\cos(k_i\tau)-\mathcal{I}_c(p_i,|\vec{k}_i-\vec{p}_i|)\sin(k_i\tau)\right]\rangle_T\\ &\times\sum_{\lambda,\lambda'}e^{(\lambda)}_{ij}(\hat{k}_1)e^{(\lambda')ij}(\hat{k}_2)e^{(\lambda)}(\hat{k}_1,\vec{p}_1)e^{(\lambda')}(\hat{k}_2,\vec{p}_2).\end{aligned} \tag{6.22}$$

We have already computed the 4-point correlator of ζ in the Gaussian case (6.13), which lets us perform an immediate integration over $\vec{k}_2$ and $\vec{p}_2$:

$$\begin{aligned}\langle\rho_{GW}(\tau,\vec{x})\rangle &= \frac{M_P^2}{16a^2}\left(\frac{4}{9}\right)^2\frac{2}{\tau^2}\int\frac{d^3\vec{k}_1}{(2\pi)^3}\int\frac{d^3\vec{p}_1}{(2\pi)^3}\\ &\times\frac{1}{k_1^4}\frac{2\pi^2}{p_1^3}\mathcal{P}_\zeta(p_1)\frac{2\pi^2}{|\vec{k}_1-\vec{p}_1|^3}\mathcal{P}_\zeta(|\vec{k}_1-\vec{p}_1|)\\ &\times\langle\left[\mathcal{I}_s(p_1,|\vec{k}_1-\vec{p}_1|)\cos(k_1\tau)-\mathcal{I}_c(p_1,|\vec{k}_1-\vec{p}_1|)\sin(k_1\tau)\right]^2\rangle_T\\ &\times\sum_{\lambda,\lambda'}e^{(\lambda)}_{ij}(\hat{k}_1)e^{(\lambda')ij}(-\hat{k}_1)e^{(\lambda)}(\hat{k}_1,\vec{p}_1)e^{(\lambda')}(-\hat{k}_1,-\vec{p}_1).\end{aligned} \tag{6.23}$$

The time average of trigonometric functions over many periods k_1^{-1} has the following outcome:

$$\langle\cos^2(k_1\tau)\rangle_T=\langle\sin^2(k_1\tau)\rangle_T=\frac{1}{2},\qquad\langle\cos(k_1\tau)\sin(k_1\tau)\rangle_T=0. \tag{6.24}$$

Following the same logic of the previous Chapter, we now want to write the expression for the GW energy density per logarithmic frequency interval (5.13). We thus perform the trivial integration over the angular component of $\vec{k}_1$, in such a way that we are left with the integral over the frequency k_1, which can be factorized in the definition of Ω_{GW}. Again, to solve the integral over $\vec{p}_1$ we can assume the coordinate system with $\vec{k}_1$ along the third axis. Similar steps to the one performed before then lead to the following result:

$$\Omega_{GW}(\tau,k)=\frac{1}{972a^2H^2\tau^2}\int\int_{\mathcal{S}}dxdy\frac{x^2}{y^2}\left[1-\frac{(1+x^2-y^2)^2}{4x^2}\right]^2\mathcal{P}_\zeta(kx)\mathcal{P}_\zeta(ky)\mathcal{I}^2(x,y), \tag{6.25}$$

where we have defined $\mathcal{I}^2=\mathcal{I}_c^2+\mathcal{I}_s^2$. This is the expression for the energy density of a CGWB sourced at second order by scalar perturbations, for which we have not specified yet the form of the primordial power spectrum (for a similar computation, see also, e.g. [80]). Notice that the result we have found does not depend on the position $\vec{x}$.

In the previous Chapter we have seen how the propagation of primordial GWs across large-scale scalar perturbations can be a source of anisotropies in the GW energy density. We have also introduced a contribution to the anisotropies due to the initial conditions set by the mechanism responsible for the production of the CGWB. The description we have given there is quite general and holds for any kind of initial process. Without any further assumption, we have thus considered the effects of non-Gaussianity only on the scalar sourced part.

We are now considering the more specific scenario of primordial GWs sourced at second order by scalar perturbations. Therefore, it seems natural to conclude that any presence of primordial non-Gaussianity should affect the initial conditions of the CGWB and thus its anisotropies correlators. This is exactly what we are going to study, considering the concrete physical scenario of a background of gravitational waves produced at the formation of primordial black holes.

6.2 CGWB from Primordial Black Holes

Primordial black holes (PBHs) are expected to be created at small scales in the presence of sufficiently enhanced density perturbations (see, e.g., the review [81]). The production happens when the enhanced modes re-enter the horizon after inflation, and all the regions where the perturbation exceeds a certain threshold collapse into a black hole, which is what we identify as a PBH. These enhanced density perturbations are then related to scalar perturbations which inevitably generate gravitational waves at second order, as we have just discussed. The required density fluctuations in order to obtain a substantial amount of PBHs is so large that the respective scalar sourced CGWB may well exceed, at peak frequency, the first-order generated one, so that the GW amplitude could be large enough to become observable [82, 83, 84].

6.2.1 Primordial Black Holes

We pause for a moment the discussion around the GW background in order to introduce briefly to the physics of PBHs and, in particular, to the details about their formation in the early Universe.

PBH abundance

During radiation domination, a large enough overdensity can gravitationally collapse directly into a black hole. This is what we refer to as a primordial black hole. The actual formation happens when a perturbation exceeding a certain threshold re-enters the horizon, in which case gravity overcomes pressure and the region with the dimension of the perturbation collapses into a PBH with mass of the order of the horizon mass at that time. The threshold value is usually expressed in terms of the density perturbation and it is given by $\delta_c \sim 0.45$ [85]. We are instead more interested in dealing with the curvature perturbation ζ, for which the corresponding critical value is estimated to be around $\zeta_c \sim 1$. Density and curvature perturbation modes are actually related, during radiation domination, by the following expression [85]:

$$\delta(t,\vec{k}) = \frac{4}{9}\left(\frac{k}{aH}\right)^2 \zeta(\vec{k}), \tag{6.26}$$

with $(aH)^{-1}$ being the comoving Hubble radius at the time of PBH formation. It follows that, for long-wavelength modes, outside of the horizon ($k \ll aH$), density perturbations are suppressed with respect to the curvature ones. This explains why super-horizon modes have little effect on the formation of PBHs.

We can compute the mass fraction of the Universe which collapses into PBHs, defined as the fraction of the total energy density of the Universe contributed by the region collapsed into PBHs at the time of formation:

$$\beta \equiv \frac{\rho_{\rm PBH}(\tau_{\rm in})}{\rho_{\rm tot}(\tau_{\rm in})}. \tag{6.27}$$

This is obtained by integrating the probability density function of the curvature perturbation:

$$\beta = \int_{\zeta_c}^{\infty} d\zeta P(\zeta), \tag{6.28}$$

which corresponds to the probability that the random field ζ assumes a value equal to the PBH formation threshold ζ_c or greater. Assuming a Gaussian distribution function (3.1), this gives the following PBH fraction [85]:

$$\beta \simeq \sqrt{\frac{2\sigma^2}{\pi\zeta_c^2}} \exp\left(-\frac{\zeta_c^2}{2\sigma^2}\right). \tag{6.29}$$

The PBH mass fraction β can be directly related to the present density parameter of PBHs with a mass $M_{\rm PBH}$ [82]:

$$\Omega_{\rm PBH,0}(M_{\rm PBH}) \simeq 1 \times 10^{14} \beta(M_{\rm PBH}) \left(\frac{M_{\rm PBH}}{10^{20}\ {\rm g}}\right)^{-1/2}. \tag{6.30}$$

Consider now the bounds on the primordial power spectrum amplitude and spectral index coming from large-scales CMB measurements [65]. Latest observations constrain them to be $A_s \equiv \mathcal{P}_\zeta(k_{\rm CMB}) \simeq 2.2 \times 10^{-9}$ and $n_s - 1 \simeq -0.035$, where the pivot scale probed by CMB experiments is taken to be $k_{\rm CMB} = 0.05$ Mpc^{-1}. Assuming that the spectral index has no significant running, we can use these information to extrapolate the power spectrum amplitude at some arbitrary small scale $k_{\rm PBH} \gg k_{\rm CMB}$. Because of the red tilt, the estimated power spectrum at the PBHs scale would be for sure smaller than the one at CMB scales. This would correspond to a completely negligible fraction of PBHs. The reason for such a conclusion can be easily deduced from the fact that, in the case of a Gaussian ζ and taking for simplicity a scale-invariant spectrum, the width of the zero-mean distribution is $P_\zeta^{1/2} \sim 10^{-5}$, . It thus follows that PBHs form only in the extreme positive end of the distribution function, where $\zeta > \zeta_c$.
The assumption that the power spectrum behaviour does not change down to very small scales is however quite strong and we could instead imagine a scenario in which the curvature perturbation is highly enhanced at some given small scale, giving rise to a sufficiently high fraction of PBHs to be observationally interesting. This happens for a power spectrum of the order of $\mathcal{P}_\zeta(k_{\rm PBH}) \sim 10^{-2} - 10^{-1}$ [81], thus requiring a blue-tilted enough power spectrum, which is not so easy to realize in the standard slow-roll inflationary models and is ruled out at CMB scales by observations. The enhancement of the power spectrum at small scales can instead be achieved in alternative inflationary models, such as multi-field hybrid and curvaton models [81].

The PBH abundance is constrained by observations for a wide range of masses [81]. By now, PBHs with a mass up to 10^{15} g would have completely evaporated by emitting Hawking radiation. More massive ones are instead particularly interesting since they are considered to be a viable dark matter (DM) candidate. Depending on their masses, they can arrive to comprise a large fraction or even the totality of DM. This is true for PBHs with a mass in the range 10^{17} g $< M_{\rm PBH} < 10^{24}$ g [85] and with an abundance $\Omega_{\rm PBH,0} h^2 \simeq 0.1$.

PBH abundance in presence of non-Gaussianity

A factor that can have a strong influence on the PBH abundance is the presence of primordial non-Gaussianity, which in fact affects the shape of the tails of the curvature perturbation distribution function (see, e.g. [86]). We consider the usual local model of non-Gaussianity, parametrized as:

$$\zeta = \zeta_g + \frac{3}{5} f_{NL} (\zeta_g^2 - \sigma^2), \tag{6.31}$$

where we indicate the variance of the Gaussian distribution as $\sigma^2 \equiv \langle \zeta_g^2 \rangle$. To obtain the PBH abundance we need to compute the values of the Gaussian ζ_g corresponding to the value of the full ζ above the threshold ζ_c. Imposing $\zeta = \zeta_c$ we get the following solutions [85]:

$$\zeta_\pm = \frac{-5 \pm \sqrt{25 + 60 \zeta_c f_{NL} + 36 f_{NL}^2 \sigma^2}}{6 f_{NL}}. \tag{6.32}$$

The mass fraction is then computed as the integral of the Gaussian distribution, in analogy with (6.28), which for $f_{NL} \ll 1$ can be written as:

$$\beta = \int_{\zeta_+}^{\infty} d\zeta_g P(\zeta_g) \simeq \sqrt{\frac{2\sigma^2}{\pi \zeta_+^2}} \exp\left(- \frac{\zeta_+^2}{2\sigma^2} \right) \tag{6.33}$$

This practically results in a small variation of the critical value of the perturbation ζ needed for the formation of PBHs.

We are actually more interested in another consequence of primordial non-Gaussianity, which is the coupling between perturbation Fourier modes on large and small scales. We have derived in section 3.2.1, assuming the local non-Gaussianity parametrization (3.7) and performing the long-short split, how a short-wavelength perturbation can be modulated by a longer one. This

phenomenon directly affects the number of PBHs forming in different regions of the Universe. In particular, a peak in the long mode would correspond to an enhancement of the power of short-wavelength perturbations, effectively decreasing the threshold necessary to gravitationally collapse into a PBH. This is represented in Figure 6.1.

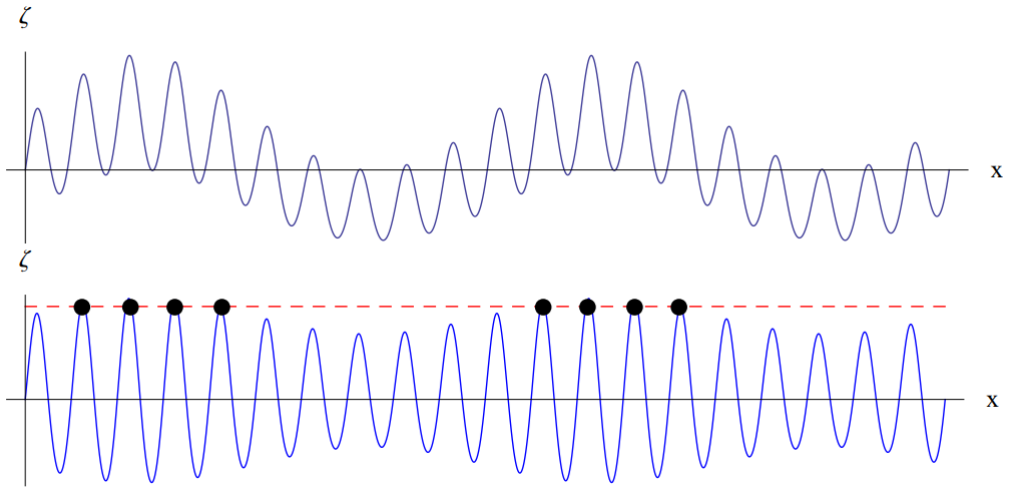

Figure 6.1: The top plot shows the curvature perturbation in the case it includes only one short and one long wavelength mode. The modulated short perturbation mode, described by equation (6.34), is shown in the bottom plot, along with a red line representing the PBH formation threshold. It is evident how the coupling with the long mode affects the spatial distribution of PBHs in different regions. Taken from [85].

Expression (3.30) for the modulated short mode can be rewritten as:

$$\zeta_S = \left(1 + \frac{6}{5} f_{NL} \zeta_l\right) \zeta_s + \frac{3}{5} f_{NL} \left(\zeta_s^2 - \sigma_s^2\right), \tag{6.34}$$

where $\sigma_s^2 \equiv \langle \zeta_s^2 \rangle$. Terms containing only the long mode cannot affect the PBH formation, which happens on the scales of the short mode, and thus have been neglected. It is possible to compute the new result for the PBH abundance, as a function of the long mode, by defining the following quantities [85]:

$$\begin{aligned} \tilde{\zeta}_g &\equiv \left(1 + \frac{6}{5} f_{NL} \zeta_l\right) \zeta_s, \\ \tilde{\sigma} &\equiv \left(1 + \frac{6}{5} f_{NL} \zeta_l\right) \sigma_s, \\ \tilde{f}_{NL} &\equiv \left(1 + \frac{6}{5} f_{NL} \zeta_l\right)^{-2} f_{NL}, \end{aligned} \tag{6.35}$$

in terms of which equation (6.34) assumes the structure of the local parametrization (6.31):

$$\zeta_S = \tilde{\zeta}_g + \frac{3}{5} \tilde{f}_{NL} \left(\tilde{\zeta}_g^2 - \tilde{\sigma}^2\right). \tag{6.36}$$

It is thus possible to recover the PBH abundance in the presence of the mode coupling by simply exploiting results (6.32) and (6.33), rewritten in terms of the quantities (6.35).
In order to quantify the effect of the long mode modulation on the PBH abundance, we define the following ratio:

$$\delta_\beta \equiv \frac{\beta - \bar{\beta}}{\bar{\beta}}, \tag{6.37}$$

where the background value $\bar{\beta}$ is computed as equation (6.33), while β accounts for the modulation and it is thus a function of ζ_l. At first order in ζ_l the explicit expression is [85]:

$$\delta_\beta = \frac{25 + 30\zeta_c f_{NL} + 36 f_{NL}^2 \sigma_s^2 - 5\sqrt{25 + 60\zeta_c f_{NL} + 36 f_{NL}^2 \sigma^2}}{3 f_{NL} \sigma_s^2 \sqrt{25 + 60\zeta_c f_{NL} + 36 f_{NL}^2 \sigma^2}} \zeta_l. \tag{6.38}$$

This result describes the spatial variation of the PBH abundance due to the modulation of the long mode ζ_l. We will see in the following how, if PBHs consist of a large part of DM, this spatial modulation is related to the presence of isocurvature modes. The latter are strongly constrained by the latest CMB measurements and thus allow to put upper bounds on the value of the non-linear parameter f_{NL}. We then generalize the conclusions in the case of a scale-dependent f_{NL}.

6.2.2 GW energy density for a Dirac delta curvature power spectrum

We have seen that, in order to produce a significant amount of PBHs, it is necessary to have a substantial increase of the amplitude of scalar perturbations on small scales with respect to the one measured at CMB scales. These same enhanced scalar perturbations are then expected to source at second order a possibly observable amount of primordial GWs.
Several inflationary models are able to provide the enhancement of curvature perturbation at small scales. In this work we consider the simple scenario, represented in Figure 6.2, of a primordial power spectrum peaked at some given scale k_*^{-1}, leading to the production of a significant amount of PBHs with a specific mass, along with a large amplitude CGWB of a characteristic peak frequency. It is possible to derive a relation between the two quantities [81]:

$$f_{GW} \simeq 3 \times 10^{-9} \text{ Hz} \left(\frac{M_{\text{PBH}}}{M_\odot} \right)^{-\frac{1}{2}}. \tag{6.39}$$

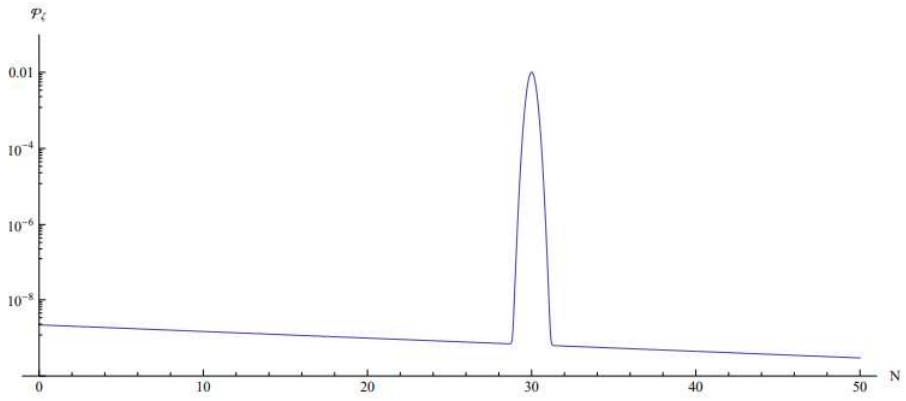

Figure 6.2: Example of primordial power spectrum with a peak at some given small scale, as a function of the number of e-folds N. Away from the peak the spectrum is small and with the spectral index $n_s = 0.96$, in such a way that at large scales it is compatible with latest CMB observations. Taken from [85].

We are interested into the possibility of PBHs consisting in the totality of dark matter, which is the case if we choose $M_{\text{PBH}} \sim 10^{-12} M_\odot$ (see, e.g. [87]). This corresponds to the GW frequency $f_{GW} \simeq 3 \times 10^{-3}$ Hz, which coincidentally falls in the range where LISA has the best sensitivity $\Omega_{GW} h^2 \sim 10^{-11}$ [82, 84]. This gives hope that a CGWB with such an origin may be observed in the next decades. Finally, from the GW frequency we derive the scale at which we assume the scalar perturbations to be enhanced, which is $k_* \simeq 2 \times 10^{12}$ Mpc^{-1} [83].
The scenario we are considering is thus characterized by a power spectrum with a sharp peak on the small scale responsible for the PBH formation, as visible in Figure 6.2. We may approximate it as a Dirac delta power spectrum:

$$\mathcal{P}_\zeta(k) = A_s k_* \delta(k - k_*). \tag{6.40}$$

Substituting this choice of the power spectrum inside expression (6.25), obtained for the GW energy density of a scalar sourced CGWB, we get:

$$\Omega_{GW}(\tau,k)=\frac{A_s^2}{15552a^2H^2\tau^2}\frac{k^2}{k_*^2}\left[\frac{4k_*^2}{k^2}-1\right]^2\theta(2k_*-k)\mathcal{I}^2\left(\frac{k_*}{k},\frac{k_*}{k}\right), \tag{6.41}$$

where, exploiting expressions (C.14):

$$\mathcal{I}^2\left(\frac{k_*}{k},\frac{k_*}{k}\right)=\frac{729}{16}\left(\frac{k}{k_*}\right)^{12}\left(3-\frac{2k_*^2}{k^2}\right)^4\left\{\left[4\left(2-\frac{3k^2}{k_*^2}\right)^{-1}-\log\left(\left|1-\frac{4k_*^2}{3k^2}\right|\right)\right]^2+\pi^2\theta\left(\frac{2k_*}{\sqrt{3}k}-1\right)\right\}. \tag{6.42}$$

Result (6.41) for the GW energy density is indeed independent on position in the case of Gaussian statistics for ζ we have assumed. The profile is shown in Figure 6.3. At the peak frequency $f_{GW}=\frac{k_*}{\sqrt{3}\pi}$, the typical amplitude is given by:

$$\Omega_{GW}h^2\simeq 6\times10^{-8}\left(\frac{A_s}{10^{-2}}\right)^2, \tag{6.43}$$

which, as expected, exceeds the first-order counterpart $\Omega_{GW}h^2\sim10^{-14}$ [82].

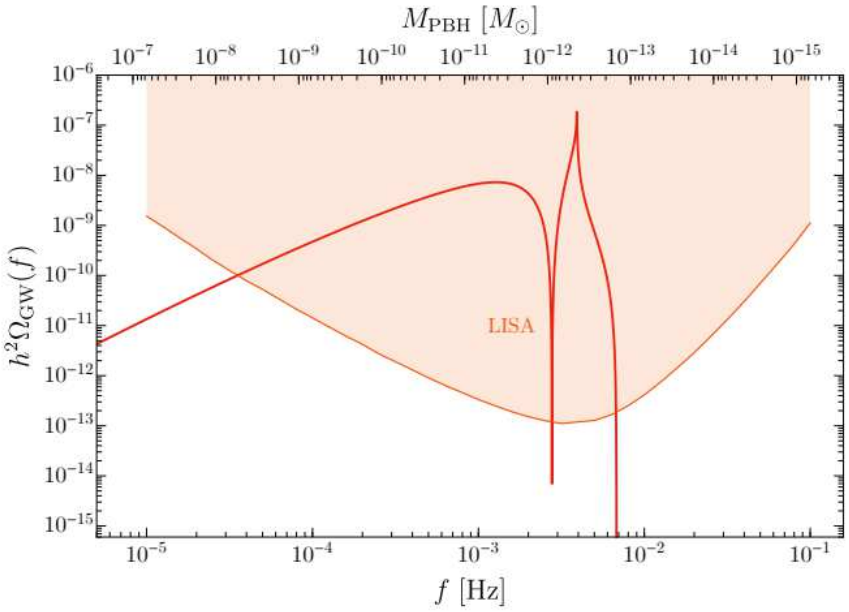

Figure 6.3: GW energy density per logarithmic frequency interval of the stochastic background sourced at second order by scalar perturbations with a Dirac delta spectrum peaked at the small scale k_*. The value $A_s=0.033$ has been chosen. Interesting features of this profile are the resonant peak at $k=\frac{2}{\sqrt{3}}k_*$ and the k^2 scaling at low frequencies. Moreover, the energy density vanishes for $k>2k_*$ due to the momentum conservation law. These features would be absent in the case of a more physical power spectrum, but the overall amplitude would be similar. The expected sensitivity curve of LISA is also plotted, showing that the stochastic background of GWs arising at the formation of $M_{\rm PBH}=10^{-12}M_\odot$ PBHs should be detectable. Taken from [84].

The fact that we recover an homogeneous result for the CGWB energy density is not that trivial. In principle, there is no actual reason to assume the GW production process to be perfectly homogeneous across the Universe. The level of anisotropies can then be evaluated as the 2-point correlation function of expression (6.21) for the energy density of scalar sourced GWs, i.e. $\langle\rho_{GW}(\vec{x})\rho_{GW}(\vec{y})\rangle$, which is only a function of the distance $|\vec{x}-\vec{y}|$ due to the statistical properties of the correlator.

It is indeed possible to show that the result is mainly contributed by the disconnected part of the correlator $\langle \rho_{GW} \rangle^2$, which we know from (6.41) to be in fact homogeneous. Qualitatively speaking, this conclusion can be understood by remembering that we are considering anisotropies on the scale $|\vec{x}-\vec{y}|$, which is much larger than the one associated to the CGWB production k_*^{-1}. Therefore, the enhanced Gaussian scalar perturbations on this small scale are not able to correlate over the large scales. Moreover, eventual inhomogeneities present at the production of the stochastic background would be averaged out, as a consequence of the central limit theorem, when measuring the GW energy density on angular scales several times larger than k_*^{-1} [87]. This shows that anisotropies in the CGWB energy density do not arise in a Gaussian scenario.
We will see in the next section that the presence of primordial local non-Gaussianity is necessary to induce a long-mode modulation of the small scale enhanced perturbation. In this way, the presence of the long modes both produces a spatial variation of the GW energy density and is responsible for the statistical correlation between regions separated by large angular distances. This is what gives rise to an anisotropic initial contribution of the CGWB energy density.
What we want to do now is thus to see how the homogeneous result (6.41) is altered in the presence of primordial local non-Gaussianity.

6.2.3 CGWB anisotropies in presence of non-Gaussianity

In the previous Chapter we have seen how anisotropies in the CGWB may arise from the GW propagation across scalar metric perturbations and how this imprints information about primordial non-Gaussianity on the stochastic background of GWs itself. We now focus instead on the anisotropies arising from the initial condition term Γ_I in the case of a scalar sourced CGWB. For such a case, we expect the presence of non-Gaussianity to directly affect the background of GWs already at their formation, in addition to the later propagation effects we have already considered. We now focus on the case with a constant non-linearity parameter f_{NL}, leaving the generalization to a scale-dependent non-Gaussianity for a later discussion.
Remember from (6.22) that the energy density of GW sourced at second order by scalar perturbations is a function of the 4-point correlator of the curvature perturbation ζ. This is basically due to ρ_{GW} being quadratic in h_{ij} which is quadratic itself in ζ. As always we consider primordial non-Gaussianity to be parametrized by the local ansatz (3.7). It is straightforward to realize that, neglecting corrections of second order or higher in f_{NL}, the non-Gaussianity of ζ does not affect the expression for the 4-point correlator (6.13) we have computed in the Gaussian case, being it an even-order correlator. What can actually produce anisotropies in the initial condition term of the CGWB is instead the coupling between long and short perturbation modes, which we already know to be responsible for spatial variations in the PBH abundance within different regions. Primordial local non-Gaussianity is then necessary in order to ensure such a coupling.

We consider the long-short split in real space (3.25), where ζ_s is the enhanced short wavelength perturbation responsible for the PBH formation, and the CGWB production, at the scale k_*^{-1}. Long modes are instead the ones relevant at cosmological scales, with a nearly scale-invariant spectrum, which do not affect the PBH production directly but only via the modulation on the short mode. This is accounted in the expression for the modulated short mode (3.30), for which we now compute the 4-point correlator and substitute it inside the GW energy density (6.22). The expression corresponding to (3.30) in Fourier space is given by (3.31) and we have already derived its 2-point correlator (3.33). In an analogous way, remembering to keep the long mode out of the ensamble average, since we assume it to be fixed, we get, up to the linear order in f_{NL}:

$$\begin{aligned}\langle \zeta_S(\vec{k}_1)\zeta_S(\vec{k}_2)\zeta_S(\vec{k}_3)\zeta_S(\vec{k}_4)\rangle = \langle \zeta_s(\vec{k}_1)\zeta_s(\vec{k}_2)\zeta_s(\vec{k}_3)\zeta_s(\vec{k}_4)\rangle + \frac{6}{5} f_{NL} \int \frac{d^3\vec{p}}{(2\pi)^3} \\ \times \left[\zeta_l(\vec{k}_1-\vec{p})\langle \zeta_s(\vec{p})\zeta_s(\vec{k}_2)\zeta_s(\vec{k}_3)\zeta_s(\vec{k}_4)\rangle + 3 \text{ perms}\right].\end{aligned} \tag{6.44}$$

Exploiting the Gaussianity of ζ_s, it is then possible to expand its 4-correlator in terms of the power spectrum P_{ζ_s}, in such a way that we can write:

$$\begin{aligned}\langle\zeta_S(\vec{p}_1)\zeta_S(\vec{k}_1-\vec{p}_1)\zeta_S(\vec{p}_2)\zeta_S(\vec{k}_2-\vec{p}_2)\rangle &= (2\pi)^6\delta^{(3)}(\vec{p}_1+\vec{p}_2)\delta^{(3)}(\vec{k}_1-\vec{p}_1+\vec{k}_2-\vec{p}_2)\\ &\times P_\zeta(p_1)P_\zeta(|\vec{k}_1-\vec{p}_1|)\\ &+ (2\pi)^6\delta^{(3)}(\vec{p}_1+\vec{k}_2-\vec{p}_2)\delta^{(3)}(\vec{p}_2+\vec{k}_1-\vec{p}_1)\\ &\times P_\zeta(p_1)P_\zeta(p_2)\\ &+ \frac{6}{5}f_{NL}\Big[\zeta_l(\vec{p}_1+\vec{p}_2)(2\pi)^3\delta^{(3)}(\vec{k}_1-\vec{p}_1+\vec{k}_2-\vec{p}_2)\\ &\times P_\zeta(|\vec{k}_1-\vec{p}_1|)\big[P_\zeta(p_1)+P_\zeta(p_2)\big]+3\text{ perms}\Big],\end{aligned} \tag{6.45}$$

where we have only considered the two possible non-vanishing contractions for $\vec{k}_1,\vec{k}_2\neq 0$. As already pointed out, in presence of local non-Gaussianity the long-mode modulation introduces the correlation of short modes with similar, not necessarily equal, wavenumber. In the terms linear in f_{NL}, in fact, the long mode ζ_l appears in place of one of the two Dirac delta, relaxing the condition on its argument. Considering for example the term explicitly reported in (6.45), the sum $\vec{p}_1+\vec{p}_2=\vec{k}_1+\vec{k}_2$ is no longer constrained to vanish, but it is only required to be the wavenumber of a long mode, i.e. $|\vec{k}_1+\vec{k}_2|<k_H$, where k_H is the wavenumber of the shortest long mode we are considering in making the split. This conclusion comes automatically from the step function included in the definition (3.28) of long and short modes.
We have already computed the contribution to the CGWB energy density coming from zero-order terms in (6.45), which gives the homogeneous result (6.25). We now focus on the term linear in f_{NL} explicitly written in (6.45). Substituting it inside the formula for the GW energy density (6.22) we get:

$$\begin{aligned}\langle\rho_{GW}(\tau,\vec{x})\rangle &= \frac{M_P^2}{81\tau^2a^2}\int\frac{d^3\vec{k}_1}{(2\pi)^3}\int\frac{d^3\vec{k}_2}{(2\pi)^3}\int\frac{d^3\vec{p}_1}{(2\pi)^3}\int\frac{d^3\vec{p}_2}{(2\pi)^3}e^{i(\vec{k}_1+\vec{k}_2)\vec{x}}\frac{1}{k_1^2k_2^2}\\ &\times\langle\prod_{i=1}^{2}\big[\mathcal{I}_s(p_i,|\vec{k}_i-\vec{p}_i|)\cos(k_i\tau)-\mathcal{I}_c(p_i,|\vec{k}_i-\vec{p}_i|)\sin(k_i\tau)\big]\rangle_T\\ &\times\sum_{\lambda,\lambda'}e_{ij}^{(\lambda)}(\hat{k}_1)e^{(\lambda')ij}(\hat{k}_2)e^{(\lambda)}(\hat{k}_1,\vec{p}_1)e^{(\lambda')}(\hat{k}_2,\vec{p}_2)\\ &\times\frac{6}{5}f_{NL}\zeta_l(\vec{p}_1+\vec{p}_2)(2\pi)^3\delta^{(3)}(\vec{k}_1-\vec{p}_1+\vec{k}_2-\vec{p}_2)\\ &\times P_\zeta(|\vec{k}_1-\vec{p}_1|)\big[P_\zeta(p_1)+P_\zeta(p_2)\big].\end{aligned} \tag{6.46}$$

We then integrate over $\vec{p}_2$, by making use of the Dirac delta, and we perform the change of variable $\vec{q}=\vec{k}_1+\vec{k}_2$, replacing the integration over $\vec{k}_2$ with the integration over $\vec{q}$. Doing so we obtain:

$$\begin{aligned}\langle\rho_{GW}(\tau,\vec{x})\rangle &= \frac{M_P^2}{81\tau^2a^2}\int\frac{d^3\vec{k}_1}{(2\pi)^3}\int\frac{d^3\vec{p}_1}{(2\pi)^3}\int\frac{d^3\vec{q}}{(2\pi)^3}e^{i\vec{q}\vec{x}}\frac{1}{k_1^2|\vec{q}-\vec{k}_1|^2}\\ &\times\langle\big[\mathcal{I}_s(p_1,|\vec{k}_1-\vec{p}_1|)\cos(k_1\tau)-\mathcal{I}_c(p_1,|\vec{k}_1-\vec{p}_1|)\sin(k_1\tau)\big]\\ &\times\big[\mathcal{I}_s(|\vec{q}-\vec{p}_1|,|\vec{k}_1-\vec{p}_1|)\cos(|\vec{q}-\vec{k}_1|\tau)\\ &-\mathcal{I}_c(|\vec{q}-\vec{p}_1|,|\vec{k}_1-\vec{p}_1|)\sin(|\vec{q}-\vec{k}_1|\tau)\big]\rangle_T\\ &\times\sum_{\lambda,\lambda'}e_{ij}^{(\lambda)}(\hat{k}_1)e^{(\lambda')ij}(\vec{q}-\vec{k}_1)e^{(\lambda)}(\hat{k}_1,\vec{p}_1)e^{(\lambda')}(\vec{q}-\vec{k}_1,\vec{q}-\vec{p}_1)\\ &\times\frac{6}{5}f_{NL}\zeta_l(\vec{q})P_\zeta(|\vec{k}_1-\vec{p}_1|)\big[P_\zeta(p_1)+P_\zeta(|\vec{q}-\vec{p}_1|)\big].\end{aligned} \tag{6.47}$$

By comparing this result with (6.23), we see that the long-short split has introduced new dependencies on the long mode wavevector $\vec{q}$. This actually results in a spatial dependence on $\vec{x}$ inside

(6.47), which has been previously canceled by the presence of the Dirac delta $\delta^{(3)}(\vec{p}_1 + \vec{p}_2)$. The physical interpretation of this fact is that the presence of the long modes, coupled to the short ones via local non-Gaussianity, is able to provide a correlation of the small-scale enhanced perturbations over large scales, which is exactly what is needed for anisotropies to arise in the GW energy density, as we have previously discussed. This idea is represented in Figure 6.4.

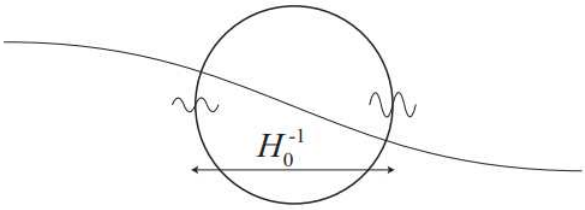

Figure 6.4: Representation of the spatial modulation of short-wavelength (sub-horizon) perturbation modes due to the presence of a long-wavelength (super-horizon) one, ensured by the coupling provided by local non-Gaussianity. In the context we are considering, this induces a large-scale correlation between patches of size k_*^{-1}, practically introducing anisotropies in the CGWB energy density. Taken from [89].

The next step is to realize that, at leading order of expansion in $\frac{q}{p_1} \ll 1$, it is possible to neglect the presence of $\vec{q}$ when it is combined with the wavevector $\vec{p}_1$ related to the short mode. A similar argument holds for $\frac{q}{k_1} \ll 1$, since we will ultimately identify k_1 with the GW frequency, which we know to be peaked around k_*. As a result, we are practically considering the leading order of expansion in $\frac{q}{k_*} \ll 1$. This allows us to perform the remaining integrals in (6.47) in the same way as we have already done in the Gaussian case. Furthermore, the contributions coming from the other 3 linear terms in (6.45) are obtained with either the substitutions $\vec{p}_1 \to \vec{k}_1 - \vec{p}_1$ or $\vec{p}_2 \to \vec{k}_2 - \vec{p}_2$ or both. It is possible to explicitly derive that, at least in the assumed approximation, this corresponds to an overall factor 4 we have to account in (6.47). Combining it with the previous result (6.23), we thus perform the remaining integrals in the usual way and obtain the following, position-dependent, expression:

$$\Omega_{GW}(\tau, \vec{x}, k) = \bar{\Omega}_{GW}(\tau, k)\left[1 + \frac{24}{5} f_{NL} \int \frac{d^3\vec{q}}{(2\pi)^3} e^{i\vec{q}\vec{x}} \zeta_l(\vec{q})\right], \tag{6.48}$$

which is the anisotropic energy density of a stochastic GW background sourced by the scalar perturbation ζ_S, enhanced at a given small scale and modulated, in presence of local non-Gaussianity, by longer perturbation modes on large scales. We have identified $\bar{\Omega}_{GW}(\tau, k)$ with the homogeneous result (6.41) derived in the Gaussian case. Following the more general treatment of the previous Chapter, we then compute the GW density contrast:

$$\delta_{GW}(\tau, \vec{x}, k) = \frac{24}{5} f_{NL} \int \frac{d^3\vec{q}}{(2\pi)^3} e^{i\vec{q}\vec{x}} \zeta_l(\vec{q}), \tag{6.49}$$

and, remembering equation (5.64), we obtain the initial condition term Γ_I contributing to the anisotropic energy density of the CGWB generated at PBH production we are considering:

$$\Gamma_I(\tau, \vec{x}, k) = \left(4 - \frac{\partial \ln \bar{\Omega}_{GW}}{\partial \ln k}\right)^{-1} \frac{24}{5} f_{NL} \int \frac{d^3\vec{q}}{(2\pi)^3} e^{i\vec{q}\vec{x}} \zeta_l(\vec{q}) = \frac{3}{5} \tilde{f}_{NL}(k) \int \frac{d^3\vec{q}}{(2\pi)^3} e^{i\vec{q}\vec{x}} \zeta_l(\vec{q}), \tag{6.50}$$

where the second equality defines the rescaled non-linear parameter:

$$\tilde{f}_{NL}(k) \equiv 8 f_{NL} \left(4 - \frac{\partial \ln \bar{\Omega}_{GW}}{\partial \ln k}\right)^{-1}. \tag{6.51}$$

It is clear that the initial contribution to the GW anisotropies Γ_I is sensible to the presence of primordial non-Gaussianity, being it proportional to the non-linear parameter f_{NL}. This is quite

different to what we have seen before for the scalar sourced anisotropies due to propagation, where instead the non-Gaussianity of ζ eventually shows up in the 3-point angular correlators, since its statistics is determined by the primordial bispectrum. We thus expect to be able to probe non-Gaussianity already via the lowest angular correlator, i.e. the angular power spectrum, of expression (6.50).

Angular power spectrum

The projection of the anisotropies onto the spherical sky is obtained in the usual way by expanding over spherical harmonics. Setting the observer at the origin, the position of the GW source is $\vec{x} = -\hat{n}(\tau_0 - \tau_{\rm in})$, where $\hat{n} \equiv \hat{k}$ points in the direction of propagation of the wave. We then substitute the expansion (5.73) for the exponential inside (6.50) and, applying spherical harmonics relations (B.8) and (B.9), we recover the following expression of the spherical harmonics expansion coefficients:

$$\Gamma_{\ell m,I}(k) = 4\pi(-i)^\ell \frac{3}{5}\tilde{f}_{NL}(k) \int \frac{d^3\vec{q}}{(2\pi)^3}\zeta_l(\vec{q})Y^*_{\ell m}(\hat{q})j_\ell\big(q(\tau_0 - \tau_{\rm in})\big). \tag{6.52}$$

Notice in particular, as anticipated in the previous Chapter, the dependence on the GW frequency k, exclusive of the initial condition contribution to the anisotropies, which we have indicated in (5.74) with q. Here $\vec{q}$ is instead the wavevector associated with the long modes of the scalar perturbation. This means that the integration in (6.52) is cut off at the higher extremum k_H, introduced as the largest wavenumber we associate to a long mode of the split.
Since the initial condition term already contains information about the non-Gaussianity of ζ we decide to focus on the 2-point correlator of (6.52), i.e. the angular power spectrum of the CGWB anisotropies. Before proceeding with the computation, we remember to allow also for later time anisotropies coming from the GW propagation across large-scale perturbations. This is accounted for in the scalar sourced term (5.78) computed in the previous Chapter. We also know that for perturbation modes re-entering the horizon during matter domination the transfer function is constant and the ISW-like term in (5.77) can be neglected. This is definitely the case for the long modes ζ_l we are considering.
Accounting for both the initial condition (6.52) and scalar sourced due to propagation (5.78) contributions we write the expansion coefficients of the CGWB energy density anisotropies as:

$$\Gamma_{\ell m,I+S}(k) = 4\pi(-i)^\ell \int \frac{d^3\vec{q}}{(2\pi)^3}\zeta_l(\vec{q})Y^*_{\ell m}(\hat{q})\mathcal{T}^{I+S}_\ell(\tau_0, \tau_{\rm in}, k, q), \tag{6.53}$$

where, remembering expression (5.89) for the scalar transfer function in the large-scale limit, we have defined:

$$\mathcal{T}^{I+S}_\ell(\tau_0, \tau_{\rm in}, k, q) = \frac{3}{5}\big[1 + \tilde{f}_{NL}(k)\big]j_\ell\big(q(\tau_0 - \tau_{\rm in})\big). \tag{6.54}$$

The result (6.53) is the quantity of which we actually want to compute the 2-point angular correlator.
We define the angular power spectrum of the CGWB anisotropies in the usual way:

$$\langle\Gamma_{\ell_1 m_1,I+S}(k)\Gamma^*_{\ell_2 m_2,I+S}(k)\rangle = \delta_{\ell_1\ell_2}\delta_{m_1 m_2}\tilde{C}_{\ell_1,I+S}(k), \tag{6.55}$$

where we keep highlighting the dependence on the GW frequency k. The 2-point correlation function has the following explicit expression:

$$\begin{aligned}\langle\Gamma_{\ell_1 m_1,I+S}(k)\Gamma^*_{\ell_2 m_2,I+S}(k)\rangle = (4\pi)^2(-i)^{\ell_1}(i)^{\ell_2}\int\frac{d^3\vec{q}_1}{(2\pi)^3}\int\frac{d^3\vec{q}_2}{(2\pi)^3}\langle\zeta_l(\vec{q}_1)\zeta^*_l(\vec{q}_2)\rangle \\ \times Y^*_{\ell_1 m_1}(\hat{q}_1)Y_{\ell_2 m_2}(\hat{q}_2)\left(\frac{3}{5}\right)^2\big[1+\tilde{f}_{NL}(k)\big]^2 \\ \times j_{\ell_1}\big(q_1(\tau_0-\tau_{\rm in})\big)j_{\ell_2}\big(q_2(\tau_0-\tau_{\rm in})\big),\end{aligned} \tag{6.56}$$

where the power spectrum of the long perturbation mode is:

$$\langle\zeta_l(\vec{q}_1)\zeta^*_l(\vec{q}_2)\rangle = (2\pi)^3\delta^{(3)}(\vec{q}_1 - \vec{q}_2)\frac{2\pi^2}{q_1^3}\mathcal{P}_{\zeta_l}(q_1). \tag{6.57}$$

The long mode ζ_l is the one whose statistics is constrained by the measurements on CMB large-scale anisotropies. We can thus safely approximate to a scale-invariant power spectrum for the long mode $\mathcal{P}_{\zeta_l}(q) = \mathcal{P}_{\zeta_l}$. Applying the spherical harmonics normalization (B.8) and the relation for spherical Bessel functions (B.12) with $n = 1$ we get the following result for the CGWB anisotropies angular power spectrum:

$$\tilde{C}_{\ell,I+S}(k) = \left[1 + \tilde{f}_{NL}(k)\right]^2 \frac{2\pi}{\ell(\ell+1)} \frac{9}{25} \mathcal{P}_{\zeta_l}. \tag{6.58}$$

It is interesting to compare this result with the expression for the GW angular power spectrum (5.90), obtained in the last Chapter where the initial condition term has been kept generic. We see that the two coincide by setting $\mathcal{P}_I(k) \equiv \frac{9}{25}\left(\tilde{f}_{NL}(k)\right)^2 \mathcal{P}_\zeta$ in (5.90) and accounting also for the contribution coming from the cross-correlation, which has been previously neglected.
Notice that that result (6.58) is only valid in the limit of low multipoles. This is due to the fact that the q-integrals in (6.56) are cut off at the wavenumber k_H, since ζ_l is a long-wavelength perturbation mode. Because of this, relation (B.12) cannot be applied exactly, but it is possible to show that it gives a sufficiently approximate result for the lowest multipoles, up to $\ell \sim k_H(\tau_0 - \tau_{\rm in})$. This is also consistent with the fact that we are considering only the constant SW-like term (5.88) of the scalar transfer function.

6.2.4 The effect of running non-Gaussianity on the CGWB anisotropies angular power spectrum

The result (6.58), for the anisotropies angular power spectrum of a stochastic GW background generated along with the formation of PBHs at the enhanced small scale k_*^{-1}, has been obtained under the assumption of a scale-independent non-Gaussianity. We stress again that the anisotropies in such a CGWB are induced by the modulation of longer perturbation modes on the enhanced short mode responsible for the PBHs production. This mode coupling is possible only in the presence of a (possibly squeezed) primordial non-Gaussianity, as we have shown explicitly by assuming the local parametrization (6.31).
Until now we have just recovered the same conclusions reported in [87]. We actually want to do a step further and try to account for the running of non-Gaussianity, in order to see what are the consequences on the results of the previous section. This was one of the main motivation behind this Thesis and arguably the most interesting original result of this work.

In section 5.5.2 we have derived the effect of running non-Gaussianity on the CGWB anisotropies angular bispectrum. What we have found is that the results resemble closely the ones for CMB temperature anisotropies. Specifically, this is the case when the anisotropy term due to the propagation of GWs across large-scale scalar perturbations is considered. Therefore, the natural conclusion is that a stochastic GW background with an unspecified cosmological origin may act as a probe for non-Gaussianity, either scale-dependent or not.
We are now considering instead a CGWB originated at PBHs formation, where the anisotropies in the energy density are set already by initial conditions. The latter are provided by the modulated short mode responsible for the PBHs production, with the modulation being proportional to the non-linear parameter f_{NL}. We have thus decided to just consider the angular power spectrum, being it the lowest statistical correlator which ideally allows to make contact with observations and recover information on primordial non-Gaussianity.

In order to generalize expression (6.58) in presence of running non-Gaussianity we now exploit the results obtained in section 3.2.3, concerning in particular the form of the long-short split (3.59), obtained from the local parametrization with a scale-dependent f_{NL}.
The starting point is yet again equation (6.22), corresponding to the expectation value of the GW energy density. This expression contains the 4-point correlator of the perturbation mode $\zeta(\vec{k})$ responsible for the production of the PBHs. We remember our previous assumption to be that the power spectrum has a sharp peak at a given small scale k_*^{-1}, which we approximate with a Dirac delta (6.40). Moreover, in presence of non-Gaussianity, we know that the short mode gets

modulated by longer modes on large observable scales, where the nearly scale-invariant spectrum is constrained by CMB measurements. In real space, this long-short coupling is linear in the non-linear parameter f_{NL} and therefore, the presence of a running in the non-Gaussianity would affect the modulation itself, leading to a different expression of the CGWB energy density (6.48).
We have already computed the expression in Fourier space (3.59) for the modulated short mode in presence of running non-Gaussianity. Remember that it accounts for the most generic form of scale dependence of the kernel $f_{NL}(k_1, k_2, k_3)$, where it is important the order in which the wavenumbers are written. We want in fact to keep the calculation as general as possible, at least until it becomes convenient to substitute a specific parametrization of the running in order to further simplify the results we obtain.

The 4-point correlator of (3.59) can be computed exploiting the Gaussianity of ζ_s and keeping the linear order in f_{NL}. Considering the combination of wavevectors needed inside (6.22), we find the following result:

$$\begin{aligned}\langle\zeta_S(\vec{p}_1)\zeta_S(\vec{k}_1-\vec{p}_1)\zeta_S(\vec{p}_2)\zeta_S(\vec{k}_2-\vec{p}_2)\rangle &= (2\pi)^6\big[\delta^{(3)}(\vec{p}_1+\vec{p}_2)\delta^{(3)}(\vec{k}_1-\vec{p}_1+\vec{k}_2-\vec{p}_2)\\ &\times P_\zeta(p_1)P_\zeta(|\vec{k}_1-\vec{p}_1|)\\ &+\delta^{(3)}(\vec{p}_1+\vec{k}_2-\vec{p}_2)\delta^{(3)}(\vec{k}_1-\vec{p}_1+\vec{p}_2)P_\zeta(p_1)P_\zeta(p_2)\big]\\ &+\frac{6}{5}(2\pi)^3\Big[\zeta_l(\vec{p}_1+\vec{p}_2)\delta^{(3)}(\vec{k}_1-\vec{p}_1+\vec{k}_2-\vec{p}_2)\\ &\times P_\zeta(|\vec{k}_1-\vec{p}_1|)\big[f_{NL}(p_1,|\vec{p}_1+\vec{p}_2|,p_2)P_\zeta(p_1)\\ &+f_{NL}(p_2,|\vec{p}_1+\vec{p}_2|,p_1)P_\zeta(p_2)\big]+3\text{ perms}\Big].\end{aligned} \tag{6.59}$$

Notice in particular that the non-linear parameter f_{NL} is a function of the same wavevectors whose combination appears as the argument of the long mode ζ_l. We then substitute inside (6.22) the explicitly written term linear in f_{NL} of the correlator (6.59) and repeat the same steps outlined for the constant-f_{NL} scenario, which lead to:

$$\begin{aligned}\langle\rho_{GW}(\tau,\vec{x})\rangle &= \frac{M_P^2}{81\tau^2a^2}\int\frac{d^3\vec{k}_1}{(2\pi)^3}\int\frac{d^3\vec{p}_1}{(2\pi)^3}\int\frac{d^3\vec{q}}{(2\pi)^3}e^{i\vec{q}\vec{x}}\frac{1}{k_1^2|\vec{q}-\vec{k}_1|^2}\\ &\times\langle\big[\mathcal{I}_s(p_1,|\vec{k}_1-\vec{p}_1|)\cos(k_1\tau)-\mathcal{I}_c(p_1,|\vec{k}_1-\vec{p}_1|)\sin(k_1\tau)\big]\\ &\times\big[\mathcal{I}_s(|\vec{q}-\vec{p}_1|,|\vec{k}_1-\vec{p}_1|)\cos(|\vec{q}-\vec{k}_1|\tau)\\ &-\mathcal{I}_c(|\vec{q}-\vec{p}_1|,|\vec{k}_1-\vec{p}_1|)\sin(|\vec{q}-\vec{k}_1|\tau)\big]\rangle_T\\ &\times\sum_{\lambda,\lambda'}e_{ij}^{(\lambda)}(\hat{k}_1)e^{(\lambda')ij}(\vec{q}-\vec{k}_1)e^{(\lambda)}(\hat{k}_1,\vec{p}_1)e^{(\lambda')}(\vec{q}-\vec{k}_1,\vec{q}-\vec{p}_1)\\ &\times\frac{6}{5}f_{NL}\zeta_l(\vec{q})P_\zeta(|\vec{k}_1-\vec{p}_1|)\big[f_{NL}(p_1,q,|\vec{q}-\vec{p}_1|)P_\zeta(p_1)\\ &+f_{NL}(|\vec{q}-\vec{p}_1|,q,p_1)P_\zeta(|\vec{q}-\vec{p}_1|)\big].\end{aligned} \tag{6.60}$$

At leading order in $\frac{q}{k_*}$, we now neglect the presence of the long-mode wavector $\vec{q}$ with respect to the short-mode wavevectors. This assumption is quite strong and it is mainly motivated by the fact that the computations would get much more involved already at first order in $\frac{q}{k_*}$. Actually, a treatment up to the linear order in $\frac{q}{k_*}$ has been one of the main focus of our work, even if in the end it has appeared to be incomplete. Therefore, we have decided to include these incomplete computations in Appendix D and to report here in the main text only the correct leading order result, which already provides with an interesting physical interpretation.
Accounting for all the contributions in (6.59), and proceeding in the usual way, we obtain:

$$\Omega_{GW}(\tau,\vec{x},k)=\bar{\Omega}_{GW}(\tau,k)\rangle\left[1+\frac{24}{5}\int\frac{d^3\vec{q}}{(2\pi)^3}e^{i\vec{q}\vec{x}}\zeta_l(\vec{q})f_{NL}(k_*,q,k_*)\right]. \tag{6.61}$$

As expected, the peculiarity of result (6.61), being a generalization of (6.48), is that it accounts for a generic scale dependence of the non-linear parameter. The latter depends on the wavenumber

k_*, characteristic of the enhanced short mode, and on the integrated wavenumber q of the longer modes responsible for the modulation of ζ_S.
We see in particular that the first and third wavenumber on which f_{NL} depends are identified with the enhanced scale k_*^{-1}. This is valid only in the approximation we have chosen to make, i.e. when keeping just the leading order term of the expansion in $\frac{q}{k_*}$. The third wavenumber, in particular, would not just be equal to k_* in the case we wanted to relax our assumptions. Specifically, it would also carry dependencies on q and on the direction $\hat{q}$, which may eventually lead to the introduction of off-diagonal terms in the angular power spectrum. This is evident from the discussion in Appendix D, where we derive a partial result for (6.61) at linear order in $\frac{q}{k_*}$. The precise treatment of such a case would additionally require a careful computation of the influence that the presence of $\vec{q}$ inside the time average and the polarization tensors in (6.60) would have. Nevertheless, as we will now discuss, some of the physical information is already present as a leading order effect.

By comparison between results (6.48) and (6.61), we can exploit the previous treatment to directly write down the spherical harmonics expansion coefficients of the CGWB anisotropies in presence of running non-Gaussianity:

$$\Gamma_{\ell m,I}(k) = 4\pi(-i)^\ell \frac{3}{5}\int \frac{d^3\vec{q}}{(2\pi)^3}\zeta_I(\vec{q})Y^*_{\ell m}(\hat{q})j_\ell\big(q(\tau_0-\tau_{\rm in})\big)\tilde{f}_{NL}(k,q), \tag{6.62}$$

where the scale-dependent, rescaled non-linear parameter is defined as:

$$\tilde{f}_{NL}(k,q) \equiv 8 f_{NL}(k_*,q,k_*)\left(4-\frac{\partial \ln\bar{\Omega}_{GW}}{\partial \ln k}\right)^{-1}. \tag{6.63}$$

Notice that this notation does not keep track of the specific dependencies inside $f_{NL}(k_*,q,k_*)$. Accounting also for CGWB anisotropies due to the GW propagation across large-scale cosmological perturbations, we then compute the 2-point angular correlator:

$$\begin{aligned}\langle \Gamma_{\ell_1 m_1,I+S}(k)\Gamma^*_{\ell_2 m_2,I+S}(k)\rangle = (4\pi)^2(-i)^{\ell_1}(i)^{\ell_2}\int\frac{d^3\vec{q}_1}{(2\pi)^3}\int\frac{d^3\vec{q}_2}{(2\pi)^3}\langle\zeta_I(\vec{q}_1)\zeta^*_I(\vec{q}_2)\rangle \\ \times Y^*_{\ell_1 m_1}(\hat{q}_1)Y_{\ell_2 m_2}(\hat{q}_2)\left(\frac{3}{5}\right)^2\big[1+\tilde{f}_{NL}(k,q_1)\big]\big[1+\tilde{f}_{NL}(k,q_2)\big] \\ \times j_{\ell_1}\big(q_1(\tau_0-\tau_{\rm in})\big)j_{\ell_2}\big(q_2(\tau_0-\tau_{\rm in})\big).\end{aligned} \tag{6.64}$$

In order to proceed with the computation, we now need to specify the parametrization of the running of f_{NL}. In particular, it is necessary to eventually account for any specific dependence on q in order to solve the respective integrals.

Power-law parametrization of the running

We first consider the simple case of a power-law running (3.37). As we know from (3.49), this means that f_{NL} depends only on the third wavenumber, which in this case corresponds to k_*, i.e. the wavenumber associated to the small scale at which scalar perturbations are enhanced and a sizeable amount of PBHs form. Explicitly, we consider:

$$\tilde{f}_{NL}(k,k_*) = 8\mathcal{A}k_*^{n_{f_{NL}}}\left(4-\frac{\partial\ln\bar{\Omega}_{GW}}{\partial\ln k}\right)^{-1}, \tag{6.65}$$

where the dependence on k_* has been highlighted in order to distinguish it from (6.51) in the constant-f_{NL} case. The dimensionful coefficient $\mathcal{A} \equiv \frac{f_{NL}(k_p)}{k_p^{n_{f_{NL}}}}$ is independent on the chosen pivot scale. Notice that parametrization (6.65) is independent on q. Therefore, substituting it inside (6.64), we can perform the integration in the usual way and we end up with the following result for the angular power spectrum of CGWB anisotropies:

$$\tilde{C}_{\ell,I+S}(k) = \big[1+\tilde{f}_{NL}(k,k_*)\big]^2\frac{2\pi}{\ell(\ell+1)}\frac{9}{25}\mathcal{P}_{\zeta_I}. \tag{6.66}$$

which is analogous to (6.58) in the non-running case, with the important detail that f_{NL} has to be evaluated at k_*. Actually, the simplicity of this result is a consequence of the level of precision we are keeping. Remember in fact that we have approximated, at leading order in $\frac{q}{k_*}$, thus setting $|\vec{q}-\vec{p}_1| \simeq p_1$ inside the f_{NL} dependence in (6.60). Relaxing this assumption would introduce new directional dependencies on $\hat{q}$ inside the integrals, which could possibly lead to additional, even off-diagonal, contributions to the angular power spectrum. For more details see Appendix D.
Nevertheless, the leading-order result (6.66) already gives useful insight about the effect of the running on the anisotropies of the CGWB. The power-law parametrization is in fact evaluated at the small scale k_*^{-1}, which differs many order of magnitude from the cosmological scales on which constraints on f_{NL} are usually derived. We thus see that even a small value of the running, i.e. a small positive value of the parameter $n_{f_{NL}}$, would greatly enhance the amount of expected CGWB anisotropies with respect to the scale-invariant result (6.58). This conclusion naturally leads to the discussion of the following section, where isocurvature constraints on the PBH abundance are taken into consideration.

Alternative parametrization

The outcome is less trivial if we choose the parametrization (3.53) of the running. In this case f_{NL} depends on the first two wavenumbers, in such a way that we have:

$$\tilde{f}_{NL}(k,k_*,q) = 8\mathcal{A}(k_*q)^{n_{f_{NL}}/2}\left(4-\frac{\partial \ln\bar{\Omega}_{GW}}{\partial \ln k}\right)^{-1}, \tag{6.67}$$

where this time we do have to account for this q-dependence in order to solve the integrals. Substituting (6.67) inside (6.64) we find the following expression for the angular power spectrum of CGWB anisotropies:

$$\begin{aligned}\tilde{C}_{\ell,I+S}(k) = 4\pi\frac{9}{25}\int_0^\infty \frac{dq}{q} j_{\ell_1}^2\big(q(\tau_0-\tau_{\rm in})\big) \\ \times\left[1+16\mathcal{A}\left(4-\frac{\partial \ln\bar{\Omega}_{GW}}{\partial \ln k}\right)^{-1}(k_*q)^{n_{f_{NL}}/2}\right. \\ \left.+64\mathcal{A}^2\left(4-\frac{\partial \ln\bar{\Omega}_{GW}}{\partial \ln k}\right)^{-2}(k_*q)^{n_{f_{NL}}}\right],\end{aligned} \tag{6.68}$$

where we have written explicitly the parametrization of the running, in order to account for the q-dependence. We now exploit relation (B.12), which we know to hold with a good approximation at low multipoles, in the three different cases $n=1$, $n=n_{f_{NL}}/2+1$ and $n=n_{f_{NL}}+1$. Assuming $n_{f_{NL}} \ll 1$ we can neglect its presence in the numerical coefficients, in such a way that we end up with the result:

$$\begin{aligned}\tilde{C}_{\ell,I+S}(k) &= \left[1+16\mathcal{A}\left(4-\frac{\partial \ln\bar{\Omega}_{GW}}{\partial \ln k}\right)^{-1}\left(\frac{k_*}{\tau_0-\tau_{\rm in}}\right)^{n_{f_{NL}}/2}\right. \\ &\quad\left.+64\mathcal{A}^2\left(4-\frac{\partial \ln\bar{\Omega}_{GW}}{\partial \ln k}\right)^{-2}\left(\frac{k_*}{\tau_0-\tau_{\rm in}}\right)^{n_{f_{NL}}}\right]\frac{2\pi}{\ell(\ell+1)}\frac{9}{25}\mathcal{P}_{\zeta_l} \\ &= \left[1+\tilde{f}_{NL}\big(k,k_*,(\tau_0-\tau_{\rm in})^{-1}\big)\right]^2\frac{2\pi}{\ell(\ell+1)}\frac{9}{25}\mathcal{P}_{\zeta_l},\end{aligned} \tag{6.69}$$

where in the second equality we have recognized the same structure of (6.67) and thus defined:

$$\tilde{f}_{NL}\big(k,k_*,(\tau_0-\tau_{\rm in})^{-1}\big) = 8\left(4-\frac{\partial \ln\bar{\Omega}_{GW}}{\partial \ln k}\right)^{-1} f_{NL}\big(k_*,(\tau_0-\tau_{\rm in})^{-1}\big), \tag{6.70}$$

with:

$$f_{NL}\big(k_*,(\tau_0-\tau_{\rm in})^{-1}\big) = \mathcal{A}\left(\frac{k_*}{\tau_0-\tau_{\rm in}}\right)^{n_{f_{NL}}/2}. \tag{6.71}$$

We see that this time the q-dependence inside (6.67), once integrated, induces a dependence in the result (6.69) on $(\tau_0 - \tau_{\rm in})^{-1}$, which is the wavenumber associated to the distance between the GW emission and the observer. This result does not come unexpected, since we know from the squeezed limit (3.57) that the parametrization of the running we are considering here has a dependence both on the large and small scale, with the latter being the one responsible for PBH formation k_*^{-1}. The large-scale wavenumber, instead, is originally identified with q, which we assume to be related with observable scales accessible by CMB measurements. The subsequent integration leads to a non-linear parameter f_{NL} evaluated at $(\tau_0 - \tau_{\rm in})^{-1}$, which can be seen as a dependence on the largest characteristic scale of the considered scenario.

6.3 Isocurvature constraints on CGWB anisotropies

We have seen that the coupling between long and short wavelength modes, induced by local-type non-Gaussianity, is responsible for fluctuations of the PBH abundance in different regions of the Universe. In the case PBHs contribute to a large fraction of the dark matter (DM), the fluctuations in DM distribution are then related to cold dark matter density isocurvature (CDI) perturbations, which are strictly constrained by CMB observations [65]. An isocurvature (or entropy) perturbation is such that the relative change $\frac{\delta X}{X}$ is different for each perturbed quantity, while the total energy density is kept constant [18, 19, 88]. It is the opposite of an adiabatic perturbation, which is instead equally shared by the different components, in such a way that the total entropy is kept constant.
Gravitational collapse is an irreversible process, which is thus expected to be related to some kind of entropy production. Moreover, at PBH formation, a fraction of the energy content of the Universe is transferred from radiation to matter, i.e. $\delta\rho_r \neq \delta\rho_m$ during the process, which is exactly the kind of behaviour associated to isocurvature perturbations. Spatial fluctuations in the PBH abundance due to the mode coupling can also be related to CDI perturbations and, in particular, it is possible to show [90] that this contribution is dominant with respect to the one due to the standard PBH formation in a Gaussian scenario. Therefore, CMB constraints on CDI perturbations may be exploited to derive bounds on the non-linear parameter f_{NL} of the local shape, which is the one responsible for the long-short modes coupling. Consequently, this also sets upper limits on the amount of CGWB anisotropies, since we have found the angular power spectrum of the latter to be proportional to f_{NL} [87].

Equation (6.38) expresses the spatial modulation of the PBH abundance as a function of the long wavelength perturbation ζ_l. If the latter is small, as it is in the scenario we are considering, it is then possible to introduce the so called scale-dependent bias b, in such a way that $\delta_\beta = b\zeta_l$ [90]. In our case we thus have explicitly:

$$b = \frac{25 + 30\zeta_c f_{NL} + 36 f_{NL}^2\sigma_s^2 - 5\sqrt{25 + 60\zeta_c f_{NL} + 36 f_{NL}^2\sigma_s^2}}{3 f_{NL}\sigma_s^2\sqrt{25 + 60\zeta_c f_{NL} + 36 f_{NL}^2\sigma_s^2}}, \tag{6.72}$$

where we recall ζ_c to be the critical value of ζ needed for the gravitational collapse into a PBH, and $\sigma_s \equiv \langle\zeta_s^2\rangle$ to be the variance of the short component of the perturbation. Expanding (6.72) at first order in f_{NL}, it simplifies as [85]:

$$b = \frac{6}{5}\left(1 + \frac{\zeta_c^2}{\sigma_s^2}\right) f_{NL}. \tag{6.73}$$

The scale-dependent bias then relates the power spectrum of isocurvature modes, arising as the spatial fluctuations in the PBH abundance δ_β in the case PBHs constitute all of DM, with the primordial curvature power spectrum in the following way:

$$\mathcal{P}_{\rm iso} = b^2\mathcal{P}_\zeta, \tag{6.74}$$

where $\mathcal{P}_\zeta$ is the nearly scale-invariant curvature power spectrum compatible with large-scale CMB measurements. The contribution of CDI perturbations to the total primordial power spectrum is

defined as the primordial isocurvature fraction [65]:

$$\beta_{\rm iso} = \frac{\mathcal{P}_{\rm iso}}{\mathcal{P}_\zeta + \mathcal{P}_{\rm iso}} = \frac{b^2}{1+b^2}, \tag{6.75}$$

where in the second equality we have substituted the result (6.74). Constraints on CDI perturbations are provided by the Planck collaboration latest TT,TE,EE+lowE+lensing results at 95% CL [65]:

$$\begin{aligned} &\beta_{\rm iso} < 0.00095 \quad \text{(fully correlated)}, \\ &\beta_{\rm iso} < 0.00107 \quad \text{(fully anti-correlated)}, \end{aligned} \tag{6.76}$$

where fully (anti-)correlated isocurvature perturbations correspond to positive (negative) values of the scale-dependent bias b. Combining these results with (6.75) we obtain the following constraints on b:

$$-0.0327 < b < 0.0308. \tag{6.77}$$

Exploiting now equation (6.73), we derive limits on the non-linear parameter f_{NL}:

$$-6.0 \times 10^{-4} < f_{NL} < 5.6 \times 10^{-4}, \tag{6.78}$$

where we have assumed the values $\zeta_c = 1$ and $\sigma_s = 0.15$ for the parameters, as reported in [85]. The conclusion is that, in the case PBHs make up for the totality of the dark matter, upper limits on isocurvature perturbations strongly constrain the amount of local-type primordial non-Gaussianity. As a consequence, also the stochastic background of GWs generated at the formation of these PBHs is constrained to be highly isotropic.
In order to evaluate the limits on the CGWB anisotropies angular power spectrum coming from CDI constraints, we express it in terms of the GW density contrast δ_{GW}, which should allow for a more intuitive physical description than the function Γ [87]. We thus introduce the following 2-point correlator:

$$\langle \delta_{GW,\ell_1 m_1} \delta^*_{GW,\ell_2 m_2} \rangle = \delta_{\ell_1 \ell_2} \delta_{m_1 m_2} \hat{C}_{\ell_1}(k), \tag{6.79}$$

and, remembering relation (5.64), we can rewrite the result (6.58) (in the case of constant f_{NL}) for the CGWB anisotropies angular power spectrum as:

$$\sqrt{\frac{\ell(\ell+1)}{2\pi}\hat{C}_\ell(k)} = \frac{3}{5}\mathcal{P}^{1/2}_{\zeta_\iota}\left|1+\tilde{f}_{NL}(k)\right|\left|4 - \frac{\partial \ln \bar{\Omega}_{GW}}{\partial \ln k}\right|. \tag{6.80}$$

Written in this way, the combination on the left side does not depend on the multipole ℓ, which is the same behaviour of the CMB temperature angular power spectrum at low multipoles, where it features the so called Sachs-Wolfe plateau. Substituting in (6.80) the constraints (6.78) on the non-linear parameter, and assuming the Planck normalization at CMB scales $\mathcal{P}_{\zeta_\iota} \simeq 2.2 \times 10^{-9}$ [65], we get the following estimate for the level of the CGWB anisotropies:

$$\sqrt{\frac{\ell(\ell+1)}{2\pi}\hat{C}_\ell(k_*)} \sim 3.0 \times 10^{-4}, \tag{6.81}$$

where we have evaluated the angular power spectrum at the peak frequency k_*. Remember that this result has been recovered within the assumption that PBHs consist of all of the dark matter. It is possible to generalize this conclusion for a scenario where PBHs constitute only a fraction of the DM, defined as the ratio $f_{\rm PBH} = \frac{\Omega_{\rm PBH,0}}{\Omega_{\rm DM,0}}$. In order to account for this possibility it is sufficient to notice that this directly affects the proportions between isocurvature and curvature perturbations, in such a way that the relation between the two power spectra becomes $\mathcal{P}_{\rm iso} = b^2 f^2_{\rm PBH} \mathcal{P}_\zeta$. Repeating the previous steps we end up with:

$$-\frac{6.0 \times 10^{-4}}{f_{\rm PBH}} < f_{NL} < \frac{5.6 \times 10^{-4}}{f_{\rm PBH}}. \tag{6.82}$$

We see that a sizeable amount of local non-Gaussianity, corresponding to a more anisotropic CGWB, would thus require that only a very tiny fraction of dark matter was in the form of PBHs.

This result is represented in Figure 6.5 which shows, following [87], a contour plot of the CGWB anisotropies angular power spectrum in the viable region for the parameters f_{NL} and $f_{\rm PBH}$. To produce such a plot, expression (6.72) has been used, rather than the (6.73) which holds only at first order in f_{NL}. Furthermore, the angular power spectrum is evaluated at $k = k_*$ where the corresponding background energy density $\bar{\Omega}_{GW}$ is close to the maximum, as visible in Figure 6.3.

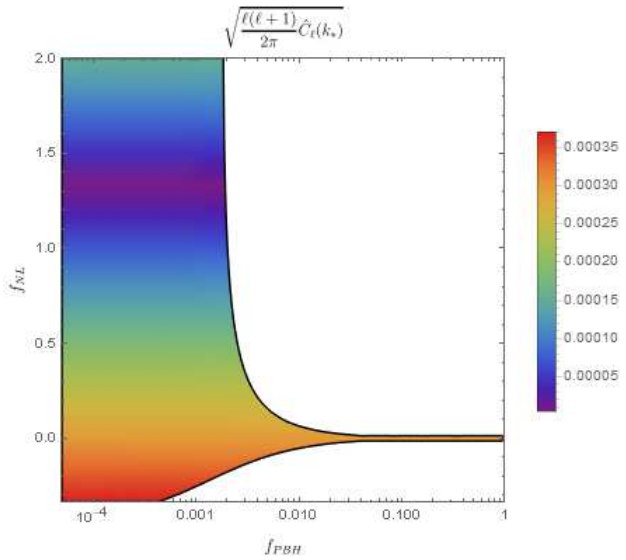

Figure 6.5: Contour plot of the angular power spectrum (6.80) of CGWB anisotropies evaluated at the frequency k_*, corresponding to the enhanced scale at which PBHs form. The actual plotted expression is the ℓ-independent combination $\sqrt{\ell(\ell+1)\hat{C}_\ell(k_*)/2\pi}$ in the allowed region for the parameters f_{NL} and $f_{\rm PBH}$, as derived from CDI constraints on CMB scales. The spectrum has its absolute minimum in correspondence of the dark spot, approximately for $f_{NL} \simeq 1.3$. We acknowledge [87] for the original idea to produce such a plot, along with the decision to take $f_{NL} = -1/3$ as the lower bound.

6.3.1 Isocurvature constraints and running non-Gaussianity

Up to now we have considered the case with constant f_{NL}, already covered in the literature [85, 87]. One interesting question we may ask ourselves is whether the presence of a running of f_{NL} can eventually evade the isocurvature bounds and allow for the possibility of an anisotropic CGWB, even arising from PBHs which constitute the totality of the dark matter.
We observe that equation (6.82) translates CDI constraints into limits on the non-linear parameter. In the case of constant f_{NL} these bounds on the non-linear parameter hold at all scales, even if they are derived within a very specific range. Constraints on CDI perturbations are in fact obtained in the range of scales probed by CMB anisotropies, i.e. 10^{-4} Mpc$^{-1} < k < 0.1$ Mpc^{-1} [31], which can be taken to be centered around the intermediate scale $k_{\rm CMB} \simeq 0.05$ Mpc^{-1} [65]. Then, the scale-invariance of f_{NL} requires the constraints on local non-Gaussianity to hold at any scale.

The conclusion is quite different in the case of a scale-dependent f_{NL}. CDI bounds only constrain non-Gaussianity on the CMB scales and a sufficient running can then enhance the value of f_{NL} on other scales. We know from the result (6.66) that, if the running is parametrized as a simple power-law (3.37), the angular power spectrum of the CGWB anisotropies we are considering depends on f_{NL} evaluated at the small scale k_*^{-1}, at which PBHs form. Given that the two scales k_*^{-1} and $k_{\rm CMB}^{-1}$ differ by many orders of magnitude, even a slightly positive running $n_{f_{NL}}$ would bring a constrained value $f_{NL}(k_{\rm CMB}) \ll 1$ to easily evade the isocurvature bounds at

$f_{NL}(k_*)$. Running local non-Gaussianity may thus allow to obtain an anisotropic CGWB even in the scenario where PBHs constitute all of the dark matter, which is instead not admitted in the case f_{NL} is constant.

Notice that, rigorously speaking, the case of scale-dependent f_{NL} should be dealt with by repeating, this time including the running, the steps which have led to expression (6.72) for the scale-dependent bias. We decide instead to proceed in a more approximate way, by assuming that the bounds (6.82), coming from CDI constraints, still hold at CMB scales for $f_{NL}(k_{\rm CMB})$. From these, we use the power-law parametrization (3.37) of the running to extrapolate upper limits on the local non-linear parameter at the enhanced PBH scale:

$$-\frac{6.0\times10^{-4}}{f_{\rm PBH}}\left(\frac{k_*}{k_{\rm CMB}}\right)^{n_{f_{NL}}}<f_{NL}(k_*)<\frac{5.6\times10^{-4}}{f_{\rm PBH}}\left(\frac{k_*}{k_{\rm CMB}}\right)^{n_{f_{NL}}}, \tag{6.83}$$

where we tassume $k_{\rm CMB}=0.05$ Mpc^{-1} and $k_*=2\times10^{12}$ Mpc^{-1}. Then, in order to have an enhancement of the CGWB anisotropies with respect to the non-running case, we need a positive value for $n_{f_{NL}}$, in such a way that f_{NL} increases at small scales. In the case of a power-law running, in analogy with (6.80), we evaluate the CGWB anisotropies as:

$$\sqrt{\frac{\ell(\ell+1)}{2\pi}\hat{C}_\ell(k)}=\frac{3}{5}\mathcal{P}_{\zeta_i}^{1/2}\left|1+\tilde{f}_{NL}(k,k_*)\right|\left|4-\frac{\partial\ln\bar{\Omega}_{GW}}{\partial\ln k}\right|, \tag{6.84}$$

where we have exploited equation (6.66). The running non-linear parameter $\tilde{f}_{NL}(k,k_*)$ is defined as in expression (6.65), for which we have yet to fix the value of $n_{f_{NL}}$. Given the huge discrepancy between the two scales in consideration, even a small positive running would be already sufficient to enhance the CGWB anisotropies at small scales, and we thus choose the quite conservative value $n_{f_{NL}}=0.1$ [34, 30]. For such a choice, the non-linear parameter is enhanced at small scales by a factor $f_{NL}(k_*)/f_{NL}(k_{\rm CMB})=(k_*/k_{\rm CMB})^{n_{f_{NL}}}\sim23$. This leads to the contour plot in Figure 6.6.

Notice first of all that the coloured viable parameter space is the same of Figure 6.5 for the non-running case. This is because we are considering $f_{NL}(k_{\rm CMB})$, evaluated at the CMB scale, which is the one directly constrained by CDI bounds. What actually changes is that the angular power spectrum is now a function of $f_{NL}(k_*)$, evaluated at the PBH scale, which, as we have said, is enhanced with respect to $f_{NL}(k_{\rm CMB})$ by the positive running. Overall, we can see that in the considered interval $[-1/3,2]$ for $f_{NL}(k_{\rm CMB})$, the power spectrum of the CGWB anisotropies is increased of roughly one order of magnitude for the case of power-law f_{NL} with $n_{f_{NL}}=0.1$. On the other hand, it is important to notice how the minimum of the spectrum (marked as the darkest part) shifts going from Figure 6.5 to Figure 6.6. The reason for this is that we need to evaluate the combination $\left|1+\tilde{f}_{NL}(k,k_*)\right|$ in equation (6.84) and not just $\tilde{f}_{NL}(k,k_*)$. As a result, in Figure 6.6 the minimum almost falls inside the interval where $f_{\rm PBH}$ is allowed to be of order unity. The consequences of this fact becomes clear if we set $f_{\rm PBH}=1$ and derive the maximum amount of anisotropies in the case of running f_{NL}. The result is practically the same as (6.81). This means that, if we focus on the scenario where PBHs constitute all of DM, a value of $n_{f_{NL}}=0.1$ is still not sufficient enough to appreciate differences with respect to the non-running case. In order for such a thing to happen a value of at least $n_{f_{NL}}\sim0.3$ is needed, for which the combination $\sqrt{\ell(\ell+1)\hat{C}_\ell(k_*)/2\pi}$ is allowed to range up to ~0.002, marking an order of magnitude increase with respect to previous cases. It is worth mentioning that in this case the CGWB anisotropies angular power spectrum starts to cover a wider range of values, while keeping also $f_{PBH}=1$, in such a way that also the value of $f_{NL}(k_{\rm CMB})$ for which $\hat{C}_\ell$ vanishes falls inside the CDI bounds (6.78).

Similar arguments to the one we have just provided may be repeated for the other parametrization of the running (3.53) considered in this work. Starting again from the CDI bounds (6.82) at the CMB scale $k_{\rm CMB}\simeq0.05$ Mpc^{-1}, we now want to extrapolate constraints on the value of the non-linear parameter which enters inside the expression for the angular power spectrum (6.69). This is expressed by equation (6.71), where we recall that f_{NL} is evaluated at the small PBH scale k_*^{-1}

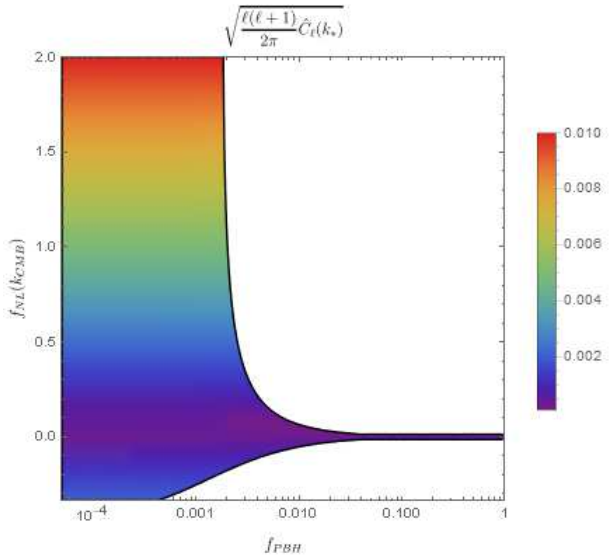

Figure 6.6: Contour plot of the angular power spectrum (6.84) of CGWB anisotropies evaluated at the frequency k_*, corresponding to the enhanced scale at which PBHs form, in the case of a power-law running non-Gaussianity (3.37). The actual plotted expression is the ℓ-independent combination $\sqrt{\ell(\ell+1)\hat{C}_\ell(k_*)/2\pi}$ in the allowed region for the parameters $f_{NL}(k_{\rm CMB})$, evaluated at $k_{\rm CMB}$, and $f_{\rm PBH}$, as derived from CDI constraints on CMB scales. The spectrum, which instead is proportional to $f_{NL}(k_*)$, has its absolute minimum in correspondence of the dark spot, approximately for $f_{NL}(k_{\rm CMB}) \simeq 0.06$, which is near the interval where $f_{\rm PBH}$ is allowed to range up to unity. Notice that the colour scale differs from the one in Figure 6.5.

and at the large observable scale $\tau_0 - \tau_{\rm in} \simeq \tau_0 \equiv k_{H,0}^{-1}$, which is of the order of magnitude of the present comoving Hubble horizon.
In such a scenario, from the CDI bounds (6.82) we then derive the following constraints:

$$-\frac{6.0\times10^{-4}}{f_{\rm PBH}}\left(\frac{k_*\cdot k_{H,0}}{k_{\rm CMB}^2}\right)^{n_{f_{NL}}/2} < f_{NL}(k_*,k_{H,0}) < \frac{5.6\times10^{-4}}{f_{\rm PBH}}\left(\frac{k_*\cdot k_{H,0}}{k_{\rm CMB}^2}\right)^{n_{f_{NL}}/2}, \tag{6.85}$$

where we have adopted the same notation of equation (6.71) by expressing explicitly the dependence of f_{NL} on the two wavenumbers k_* and $k_{H,0}$. We take the latter to be approximately $k_{H,0} \simeq 8.6\times10^{-5}$ Mpc^{-1} [16]. The result for the CGWB anisotropies in this case has the following expression:

$$\sqrt{\frac{\ell(\ell+1)}{2\pi}\hat{C}_\ell(k)} = \frac{3}{5}\mathcal{P}_{\zeta_l}^{1/2}\left|1+\tilde{f}_{NL}(k,k_*,k_{H,0})\right|\left|4-\frac{\partial\ln\bar{\Omega}_{GW}}{\partial\ln k}\right|, \tag{6.86}$$

where $\tilde{f}_{NL}(k,k_*,k_{H,0})$ is defined in equation (6.70). Setting again $n_{f_{NL}} = 0.1$ we find an enhancement at small scales of $f_{NL}(k_*,k_{H,0})/f_{NL}(k_{\rm CMB}) = \left(\frac{k_*\cdot k_{H,0}}{k_{\rm CMB}^2}\right)^{n_{f_{NL}}/2} \sim 3.5$. Consequently, we expect the departure of the amount of anisotropies from the constant-f_{NL} case to be less with respect to the one obtained with the power-law running. This is confirmed in Figure 6.7, which presents an overall level of CGWB anisotropies comprised between the two aforementioned cases. The minimum of the angular power spectrum is also found at an intermediate position. Predictably enough, if we focus on the scenario with $f_{PBH} = 1$, a value of $n_{f_{NL}} = 0.1$ is not sufficient to provide significant differences with respect to the non-running case. Since the parametrization considered here is less steep than the power-law one, we now need a value $n_{f_{NL}} \sim 0.7$ to start appreciating an enhanced level of anisotropies.

We see from our previous results that the capability of evading CDI bounds at PBH scales strongly depends on the chosen parametrization for the running. We can however conclude the discussion

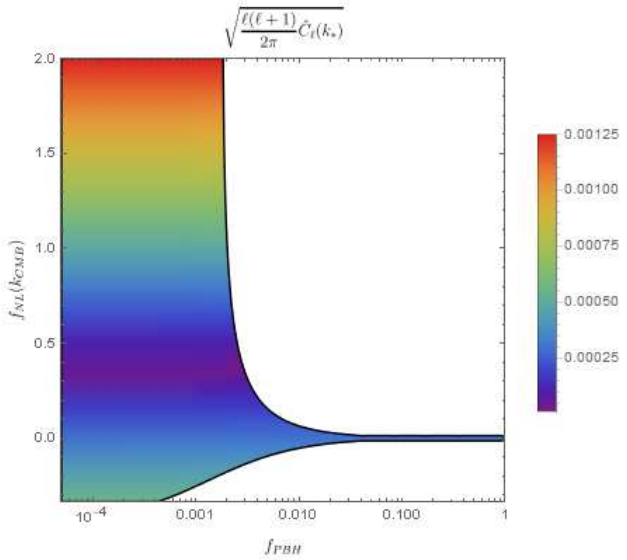

Figure 6.7: Contour plot of the angular power spectrum (6.86) of CGWB anisotropies evaluated at the frequency k_*, analogous to the one in Figure 6.6, for the alternative parametrization of the running (3.53). The spectrum has a minimum for $f_{NL}(k_{\rm CMB}) \simeq 0.4$.

by stating what is the model-independent condition necessary to deviate from the highly isotropic CGWB found for $f_{PBH} = 1$ in the non-running scenario [87]. This can be derived quite straightforwardly by noting that the level of anisotropies depends on the combination $|1 + \tilde{f}_{NL}|$, which in the constant-f_{NL} case approaches unity since CDI bounds (6.78) constrain $f_{NL} \ll 1$. Therefore, significant deviations from this situation only arise when the running is sufficient to enhance $|\tilde{f}_{NL}| \gtrsim 1$ at the PBH scale. This in fact happens for $n_{f_{NL}} \gtrsim 0.3$ and $n_{f_{NL}} \gtrsim 0.7$, respectively, for the two parametrizations we have considered.

Conclusions

Throughout this work we have centered our discussion on the topic of primordial non-Gaussianity, being it the deviation from the Gaussian statistics of the primordial perturbation ζ. After having reviewed the tools necessary to treat such a context, we have presented the CMB as the ideal observable to probe the presence of non-Gaussianity in the early Universe. Particular attention has been devoted to the local ansatz of non-Gaussianity, which has been assumed in order to recover explicit expressions for the CMB angular bispectrum, already present in the literature [16], and their generalizations to include a scale dependence of the non-linear parameter (see, e.g. [30]).
The discussion involving running non-Gaussianity, in particular, has been central in this work. What we have done, instead of considering the running arising from specific models of inflation [29], has been to start from the local parametrization and try to find the most general way to account for a scale dependence inside f_{NL}. This has resulted into a power-law parametrization as the simplest, but not the only, expression for a running within the local ansatz [33]. Nevertheless, the kernel approach to non-Gaussianity (see, e.g. [35, 36]) we have introduced should be general enough to allow for different, less trivial, parametrizations to be considered, leading to their respective expressions for the primordial bispectrum.

Primary focus of this Thesis has then been the cosmological gravitational wave background as a probe of primordial non-Gaussianity, which may possibly be a source of information on scales inaccessible to CMB and, consequently, provide with independent constraints on the amount of running non-Gaussianity. Exploiting the formalism developed for the treatment of CMB anisotropies [41] and non-Gaussianity [16], we have actually studied the stochastic GW background in a Boltzmann-like fashion [49, 67]. This has allowed to show that primordial non-Gaussianity may induce anisotropies in the GW energy density due to the propagation across large-scale scalar perturbations. Not surprisingly, given the formal analogy in the computations, the results written in terms of the CGWB anisotropies angular bispectrum strictly resemble the ones already available in the literature for the CMB [16]. The generalization to account also for running non-Gaussianity, which we have obtained by starting from the local model and admitting a scale-dependence of f_{NL} [33], can also be expressed with a notation similar to the one adopted for the treatment of such a context in the CMB case [30]. We conclude that the CGWB should represent an additional probe to test primordial non-Gaussianity, possibly even at scales inaccessible to the CMB. Therefore, an eventual detection of the CGWB in the near future, for example by means of space interferometers [62], is expected to shed more light, or at least provide with a new perspective, on the nature of primordial non-Gaussianity and its running.

Moving steps from the general treatment, we have come to consider the more specific context of a CGWB associated to PBH formation at small scales [87]. At second order in perturbation theory, GWs are sourced by scalar perturbations and, therefore, sufficiently enhanced modes, responsible for overdensities collapsing into PBHs, may produce a background of GWs with a characteristic frequency and possibly overcoming the CGWB arising from quantum fluctuations during inflation. The enhancement of scalar perturbations at small scales would actually require a deviation from the scale-invariant behaviour of the primordial power spectrum measured at large scales via CMB anisotropies [65]. Even though in the literature several inflationary models do exist capable of providing such a feature [81], in this work we have considered the idealized case of a Dirac delta curvature power spectrum, peaked at some given small scale.
We have shown explicitly that the presence of primordial local non-Gaussianity introduces inho-

mogeneities in the energy density of the GW background [87]. This is actually realized via a coupling between the short enhanced mode, responsible for the PBH production, and larger modes on observable scales, which otherwise would not affect the process. This also introduces spatial fluctuations of the PBH abundance within different regions [85, 90], which are then constrained by dark matter isocurvature bounds from CMB measurements [65]. As a result, it is possible to strictly limit the amount of local non-Gaussianity, in the case PBHs constitute a large amount or even the totality of dark matter [87].

As an original contribution to this Thesis, we have tried to consider the effect of the scale dependence of non-Gaussianity on the CGWB generated at PBH formation in the context just outlined. Exploiting the derived results on the parametrization of the running as a generalization of the local ansatz for non-Gaussianity, we have found that a sufficiently positive running should allow for the possibility of an arbitrarily anisotropic CGWB, even in the case of DM composed entirely by PBHs, contrary to what happens in the constant-f_{NL} scenario where the GW stochastic background is instead constrained to be highly isotropic [87]. We have to stress that this conclusion has been obtained by keeping only the leading order terms of expansion in $\frac{q}{k_*} \ll 1$, where q is the wavenumber of the long-wavelength component of the primordial perturbation ζ and k_*^{-1} the small scale at which PBHs form in the model we have considered. Nevertheless, we have still recovered the interesting result that CGWB anisotropies are determined by a non-linear parameter evaluated at the enhanced small scale k_*^{-1}, responsible for PBH formation. This is exactly what allows for large CGWB anisotropies in the presence of a positive enough running. Such a conclusion is exclusive of our treatment and cannot be realized within the constant-f_{NL} scenario [87]. A partial attempt to extend our computations up to linear order in $\frac{q}{k_*} \ll 1$ is discussed in Appendix D.
In this work we have not addressed to, and it is thus left open for further investigations, what an actual estimate could be on the minimum amount of CGWB anisotropies, and therefore of running non-Gaussianity, in order to be detectable at the interferometers [91]. Furthermore, constraints of different nature do exist on the curvature power spectrum at small scales [92] and it should be verified if these are compatible with the scenario we have considered. In general, we have addressed to the question whether the presence of running non-Gaussianity is capable of enhancing the anisotropies in the CGWB energy density, otherwise constrained by isocurvature bounds due to PBHs consisting of all the dark matter, but it still remains to be verified if the mechanism we have proposed is truly admitted by experimental bounds and within an established theoretical framework.

Appendix A

Perturbed Einstein tensor at first order

In this appendix we provide with the expressions for the components of the perturbed Einstein tensor δG^{μ}_{ν} at first order. We will only consider scalar perturbations of the metric (2.5), neglecting vector and tensor degrees of freedom, as we have done deriving Einstein equations components in Chapter 2.

The inverse of the perturbed metric (2.5) is found by imposing the condition $g_{\mu\nu}g^{\nu\rho} = \delta_{\mu}{}^{\rho}$, from which we get, at linear order:

$$g^{\mu\nu} = \begin{pmatrix} -1+2\phi & \partial^i\omega \\ \partial^i\omega & (1+2\psi)\delta^{ij} - D^{ij}\chi \end{pmatrix}. \tag{A.1}$$

In order to compute Einstein tensor we start from the affine connection coefficients, which in terms of the metric are expressed as:

$$\Gamma^{\mu}_{\nu\rho} = g^{\mu\sigma}\big(\partial_\nu g_{\rho\sigma} + \partial_\rho g_{\sigma\nu} - \partial_\sigma g_{\nu\rho}\big). \tag{A.2}$$

For the background FLRW metric, the non-vanishing unperturbed components are:

$$\Gamma^0_{00} = \frac{a'}{a}, \qquad \Gamma^i_{0j} = \frac{a'}{a}\delta^i{}_j, \qquad \Gamma^0_{ij} = \frac{a'}{a}\delta_{ij}. \tag{A.3}$$

The linear-order perturbation of expression (A.2) is:

$$\Gamma^{\mu}_{\nu\rho} = \eta^{\mu\sigma}\big(\partial_\nu \delta g_{\rho\sigma} + \partial_\rho \delta g_{\sigma\nu} - \partial_\sigma \delta g\nu\rho\big), \tag{A.4}$$

which has the following components:

$$\begin{aligned}
\delta\Gamma^0_{00} &= \phi', \\
\delta\Gamma^0_{0i} &= \partial_i\phi + \frac{a'}{a}\partial_i\omega, \\
\delta\Gamma^i_{00} &= \frac{a'}{a}\partial^i\omega + \partial^i\omega' + \partial^i\phi, \\
\delta\Gamma^0_{ij} &= -2\frac{a'}{a}\phi\delta_{ij} - \partial_i\partial_j\omega - 2\frac{a'}{a}\psi\delta_{ij} - \psi'\delta_{ij} - \frac{a'}{a}D_{ij}\chi + \frac{1}{2}D_{ij}\chi', \\
\delta\Gamma^i_{0j} &= -\psi'\delta^i{}_j + \frac{1}{2}D^i{}_j\chi', \\
\delta\Gamma^i_{jk} &= -\partial_j\psi\delta^i{}_k - \partial_k\psi\delta^i{}_j + \partial^i\psi\delta_{jk} - \frac{a'}{a}\partial^i\omega\delta_{jk} + \frac{1}{2}\partial_j D^i{}_k\chi + \frac{1}{2}\partial_k D^i{}_j\chi - \frac{1}{2}\partial^i D_{jk}\chi.
\end{aligned} \tag{A.5}$$

The Ricci tensor is defined as:

$$R_{\mu\nu} = \partial_\rho \Gamma^\rho_{\mu\nu} - \partial_\mu \Gamma^\rho_{\nu\rho} + \Gamma^\rho_{\sigma\rho}\Gamma^\sigma_{\mu\nu} - \Gamma^\rho_{\sigma\nu}\Gamma^\sigma_{\mu\rho}, \tag{A.6}$$

which has the following non-vanishing unperturbed components for a spatially flat FLRW background:

$$R_{00} = -3\frac{a''}{a} + 3\left(\frac{a'}{a}\right)^2, \qquad R_{ij} = \left[\frac{a''}{a} + 3\left(\frac{a'}{a}\right)^2\right]\delta_{ij}. \tag{A.7}$$

Perturbing expression (A.6) we get the following first-order perturbation:

$$\delta R_{\mu\nu} = \partial_\rho \delta\Gamma^\rho_{\mu\nu} - \partial_\mu \delta\Gamma^\rho_{\nu\rho} + \delta\Gamma^\rho_{\sigma\rho}\Gamma^\sigma_{\mu\nu} + \Gamma^\rho_{\sigma\rho}\delta\Gamma^\sigma_{\mu\nu} - \delta\Gamma^\rho_{\sigma\nu}\Gamma^\sigma_{\mu\rho} - \Gamma^\rho_{\sigma\nu}\delta\Gamma^\sigma_{\mu\rho}, \tag{A.8}$$

for which we compute the following components:

$$\begin{aligned}
\delta R_{00} &= \frac{a'}{a}\partial_i\partial^i\omega + \partial_i\partial^i\omega' + \partial_i\partial^i\phi + 3\psi'' + 3\frac{a'}{a}\psi' + 3\frac{a'}{a}\phi', \\
\delta R_{0i} &= \frac{a''}{a}\partial_i\omega + \left(\frac{a'}{a}\right)^2\partial_i\omega + 2\partial_i\psi' + 2\frac{a'}{a}\partial_i\phi + \frac{1}{2}\partial_k D^k{}_i\chi, \\
\delta R_{ij} &= \Bigg[-\frac{a'}{a}\phi' - 5\frac{a'}{a}\psi' - 2\frac{a''}{a}\phi - 2\left(\frac{a'}{a}\right)^2\phi - 2\frac{a''}{a}\psi - 2\frac{a''}{a}\phi \\
&\quad - 2\left(\frac{a'}{a}\right)^2\psi - \psi'' + \partial_k\partial^k\psi - \frac{a'}{a}\partial_k\partial^k\omega\Bigg]\delta_{ij} - \partial_i\partial_j\omega' + \frac{a'}{a}D_{ij}\chi' \\
&\quad + \frac{a''}{a}D_{ij}\chi + \left(\frac{a'}{a}\right)^2 D_{ij}\chi + \frac{1}{2}D_{ij}\chi'' + \partial_i\partial_j\psi - \partial_i\partial_j\phi - 2\frac{a'}{a}\partial_i\partial_j\omega \\
&\quad + \frac{1}{2}\partial_k\partial_i D^k_j\chi + \frac{1}{2}\partial_k\partial_j D^k_i\chi - \frac{1}{2}\partial_k\partial^k D_{ij}\chi.
\end{aligned} \tag{A.9}$$

The Ricci scalar is given by the following contraction:

$$R = g^{\mu\nu}R_{\mu\nu}, \tag{A.10}$$

which at zero order is:

$$R = \frac{6}{a^2}\frac{a''}{a}. \tag{A.11}$$

The first-order perturbation of (A.10) is:

$$\delta R = \delta g^{\mu\nu}R_{\mu\nu} + g^{\mu\nu}\delta R_{\mu\nu}, \tag{A.12}$$

such that it can be expressed as:

$$\begin{aligned}
\delta R = \frac{1}{a^2}\Bigg(&-6\frac{a'}{a}\partial_i\partial^i\omega - 2\partial_i\partial^i\omega' - 2\partial_i\partial^i\phi - 6\psi'' \\
&- 6\frac{a'}{a}\phi' - 18\frac{a'}{a}\psi' - 12\frac{a''}{a}\phi + 4\partial_i\partial^i\psi + \partial_k\partial^i D^k{}_i\chi\Bigg).
\end{aligned} \tag{A.13}$$

We can finally compute the Einstein tensor, given by the following combination:

$$G_{\mu\nu} = R_{\mu\nu} - \frac{1}{2}g_{\mu\nu}R, \tag{A.14}$$

We actually consider the components with mixed indices, since in this way the derivation of Einstein equations is simpler. On the unperturbed FLRW background the non-vanishing ones are:

$$G^0{}_0 = -\frac{3}{a^2}\left(\frac{a'}{a}\right)^2, \qquad G^i{}_j = -\frac{1}{a^2}\left[2\frac{a''}{a} - \left(\frac{a'}{a}\right)^2\right]\delta^i{}_j. \tag{A.15}$$

The linear-order perturbation of the Einstein tensor (A.14) has the following expression:

$$\delta G_{\mu\nu} = \delta R_{\mu\nu} - \frac{1}{2}\delta g_{\mu\nu} R - \frac{1}{2} g_{\mu\nu}\delta R, \tag{A.16}$$

whose components are:

$$\begin{aligned}
\delta G^0{}_0 &= \frac{1}{a^2}\left[6\left(\frac{a'}{a}\right)^2\phi 6\frac{a'}{a}\psi' + 2\frac{a'}{a}\nabla^2\omega - 2\nabla^2\psi - \frac{1}{2}\partial_k\partial^i D^k{}_i\chi\right],\\
\delta G^0{}_i &= \frac{1}{a^2}\left(-2\frac{a'}{a}\partial_i\phi - 2\partial_i\psi' - \frac{1}{2}\partial_k D^k_i\chi'\right),\\
\delta G^i_j &= \frac{1}{a^2}\left[\left(2\frac{a'}{a}\phi' + 4\frac{a''}{a}\phi - 2\left(\frac{a'}{a}\right)^2\phi + \nabla^2\phi + 4\frac{a'}{a}\psi' + 2\psi'' - \nabla^2\psi\right.\right.\\
&\quad \left. + 2\frac{a'}{a}\nabla^2\omega + \nabla^2\omega' + \frac{1}{2}\partial_k\partial^m D^k{}_m\chi\right)\delta^i{}_j - \partial^i\partial_j\phi + \partial^i\partial_j\psi - 2\frac{a'}{a}\partial^i\partial_j\omega\\
&\quad \left. - \partial^i\partial_j\omega' + \frac{a'}{a}D^i{}_j\chi' + \frac{1}{2}D^i{}_j\chi'' + \frac{1}{2}\partial_k\partial^i D^k{}_j\chi + \frac{1}{2}\partial_k\partial_j D^{ik}\chi - \frac{1}{2}\partial_k\partial^k D^i{}_j\chi\right].
\end{aligned} \tag{A.17}$$

Appendix B

Useful definitions and properties

In this appendix we list several definitions and properties useful throughout the computations in the main text.

B.1 Associated Legendre polynomials

The Legendre polynomials $P_\ell(x)$, of degree ℓ, are defined as the solutions of the following differential equation:

$$\frac{d}{dx}\left[(1-x^2)\frac{dP_\ell(x)}{dx}\right] + \ell(\ell+1)P_\ell(x) = 0. \tag{B.1}$$

The associated Legendre polynomials $P_\ell^m(x)$, of degree ℓ and order m, are then:

$$P_\ell^m(x) = (-1)^m(1-x^2)^{m/2}\frac{d^m}{dx^m}P_\ell(x), \tag{B.2}$$

in such a way that $P_\ell(x) \equiv P_\ell^0(x)$. They satisfy the following normalization condition:

$$\int_{-1}^{1} dx P_\ell^m(x)P_{\ell'}^m(x) = \frac{2(\ell+m)!}{(2\ell+1)(\ell-m)!}\delta_{\ell\ell'}. \tag{B.3}$$

The following recursive relations are also needed for the computations in Appendix D:

$$\sqrt{1-x^2}P_\ell^m(x) = -\frac{1}{2\ell+1}\left[P_{\ell+1}^{m+1}(x) - P_{\ell-1}^{m+1}(x)\right], \tag{B.4}$$

$$\sqrt{1-x^2}P_\ell^m(x) = \frac{1}{2\ell+1}\left[(\ell-m+1)(\ell-m+2)P_{\ell+1}^{m-1}(x) - (\ell+m-1)(\ell+m)P_{\ell-1}^{m-1}(x)\right], \tag{B.5}$$

$$xP_\ell^m(x) = \frac{1}{2\ell+1}\left[(\ell-m+1)P_{\ell+1}^m(x) + (\ell+m)P_{\ell-1}^m(x)\right]. \tag{B.6}$$

B.2 Spherical harmonics

Spherical harmonics can be defined in terms of the associate Legendre polynomials (B.2):

$$Y_{\ell m}(\theta,\phi) = \sqrt{\frac{2\ell+1}{4\pi}\frac{(\ell-m)!}{(\ell+m)!}}P_\ell^m(\cos\theta)\mathrm{e}^{im\phi}, \tag{B.7}$$

so that the following orthonormality condition is satisfied:

$$\int d\Omega Y_{\ell m}(\theta,\phi)Y^*_{\ell' m'}(\theta,\phi) = \delta_{\ell\ell'}\delta_{mm'}. \tag{B.8}$$

Spherical harmonics thus form an orthonormal basis over which functions depending on the angular variables θ and ϕ can be expanded. We use this property in the main text to project quantities

onto the full sky.
Legendre polynomials can be expanded over spherical harmonics, obtaining the following expression:

$$P_\ell(\hat{k}\cdot\hat{p}) = \frac{4\pi}{2\ell+1}\sum_{m=-\ell}^{\ell} Y^*_{\ell m}(\hat{k})Y_{\ell m}(\hat{p}). \tag{B.9}$$

B.3 Spherical Bessel functions

The spherical Bessel functions $j_\ell(x)$, of order ℓ, are one of the solutions of the Helmoltz equation:

$$x^2\frac{d^2 j_\ell(x)}{dx^2} + 2x\frac{dj_\ell(x)}{dx} + \big[x^2 - \ell(\ell+1)\big]j_\ell(x) = 0. \tag{B.10}$$

Qualitatively speaking, they are peaked near $\ell \sim x$, as can be seen in Figure B.1. This explains how a perturbation mode with wavenumber k is projected onto the anisotropy on a scale ℓ^{-1} in equation (4.15).

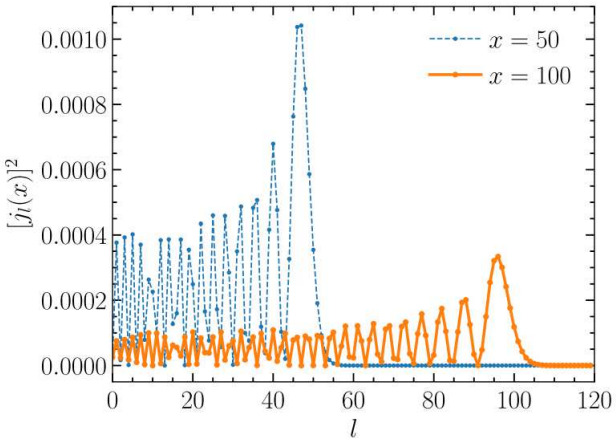

Figure B.1: Spherical Bessel functions squared as a function of ℓ, for $x = 50$ and $x = 100$. Notice how the peaks occur for ℓ slightly smaller than x. Taken from [41].

Spherical Bessel functions satisfy the following closure relation:

$$\int_0^\infty dx x^2 j_\ell(ax)j_\ell(bx) = \frac{\pi}{2a^2}\delta(a-b). \tag{B.11}$$

Another useful relation is the following:

$$\int_0^\infty dx x^{n-2} j_\ell^2(x) = 2^{n-4}\pi\frac{\Gamma\left(\ell+\frac{n}{2}-\frac{1}{2}\right)\Gamma(3-n)}{\Gamma\left(\ell+\frac{5}{2}-\frac{n}{2}\right)\Gamma^2\left(2-\frac{n}{2}\right)}, \tag{B.12}$$

where Γ is the Euler Gamma function described in Appendix B.5. Other relations needed in Appendix D are the following ones:

$$\begin{aligned}
&\int \frac{dx}{x} j_\ell^2(ax) = \frac{1}{2\ell(\ell+1)},\\
&\int dx j_\ell(ax)j_{\ell-1}(ax) = \frac{1}{2a\ell},\\
&\int dx j_\ell(ax)j_{\ell+1}(ax) = \frac{1}{2a(\ell+1)}.
\end{aligned} \tag{B.13}$$

B.4 Wigner 3-j symbols

The Wigner 3-j symbols are introduced in quantum mechanics to add angular momenta as an alternative to Clebsch-Gordan coefficients. They are written as:

$$\begin{pmatrix} \ell_1 & \ell_2 & \ell_3 \\ m_1 & m_2 & m_3 \end{pmatrix}, \tag{B.14}$$

and they vanish unless the following conditions are satisfied:

$$\begin{aligned} &m_1 + m_2 + m_3 = 0, \\ &\ell_1 + \ell_2 + \ell_3 = \text{integer (an even integer if } m_1 = m_2 = m_3 = 0), \\ &|\ell_i - \ell_j| \leq \ell_k \leq \ell_i + \ell_j. \end{aligned} \tag{B.15}$$

For our purposes, in the main text we just need the following orthogonality relation:

$$\sum_{m_1 m_2 m_3} \begin{pmatrix} \ell_1 & \ell_2 & \ell_3 \\ m_1 & m_2 & m_3 \end{pmatrix} \begin{pmatrix} \ell_1 & \ell_2 & \ell_3 \\ m_1 & m_2 & m_3 \end{pmatrix} = 1. \tag{B.16}$$

B.5 Euler Gamma function

The Euler Gamma function is a generalization to complex numbers of the factorial function, such that for any positive integer n:

$$\Gamma(n) = (n-1)! \tag{B.17}$$

For complex numbers with a positive real part it is defined by the following integral:

$$\Gamma(z) = \int_0^\infty x^{z-1} \mathrm{e}^{-z}. \tag{B.18}$$

A useful property is:

$$\Gamma(z+1) = z\Gamma(z), \tag{B.19}$$

while a fundamental value for a non-integer argument is:

$$\Gamma\left(\frac{1}{2}\right) = \sqrt{\pi}. \tag{B.20}$$

Appendix C

Details on GWs sourced by scalar perturbations at second order

In this appendix we share more details on the solution of equation (6.7) for the mode function $h_{\vec{k}}$. This can be obtained with the method of the Green's function, which gives the particular solution [74]:

$$h_{\vec{k}}^{(\lambda)}(\tau) = \frac{1}{a(\tau)} \int_{\tau_{\rm in}}^{\tau} d\tau' G_k(\tau,\tau') a(\tau') \mathcal{S}^{(\lambda)}(\tau', \vec{k}), \tag{C.1}$$

where G_k is the Green's function, solution of equation (6.7) with an impulse source:

$$G_k''(\tau,\tau') + \left(k^2 - \frac{a''}{a}\right) G_k(\tau,\tau') = \delta(\tau - \tau'). \tag{C.2}$$

In order to proceed, we remember that we are actually interested in second-order GWs produced when enhanced small-scale scalar perturbations re-enter the horizon, which happens early during radiation domination. In this case, the Green's function is found to be [74]:

$$G_k(\tau,\tau') = \frac{1}{k} \sin\big[k(\tau - \tau')\big] \theta(\tau - \tau'), \tag{C.3}$$

where θ is the Heaviside step function.
In the absence of anisotropic stresses, we know from Chapter 2 that first-order perturbed Einstein equations give $\phi = \psi$. The explicit expression of the source term in Fourier space (6.8) for $w = 1/3$ is then [78]:

$$\begin{aligned} \mathcal{S}^{(\lambda)}(\tau, \vec{k}) &= 4 \int \frac{d^3\vec{p}}{(2\pi)^3} e^{(\lambda)ij}(\hat{k}) p_i p_j \left[2\psi(\vec{p})\psi(\vec{k}-\vec{p}) + \left(\psi(\vec{p}) + \frac{1}{\mathcal{H}}\psi'(\vec{p})\right)\left(\psi(\vec{k}-\vec{p}) + \frac{1}{\mathcal{H}}\psi'(\vec{k}-\vec{p})\right)\right] \\ &\equiv \int \frac{d^3\vec{p}}{(2\pi)^3} e^{(\lambda)}(\hat{k}, \vec{p}) f(p, |\vec{k}-\vec{p}|, \tau) \zeta(\vec{p}) \zeta(\vec{k}-\vec{p}), \end{aligned} \tag{C.4}$$

where in the second line we have defined:

$$e^{(\lambda)}(\hat{k}, \vec{p}) \equiv e^{(\lambda)ij}(\hat{k}) p_i p_j, \tag{C.5}$$

and:

$$f(k_1, k_2, \tau) \equiv 4\left[2\mathcal{T}(\tau, k_1)\mathcal{T}(\tau, k_2) + \left(\mathcal{T}(\tau, k_1) + \frac{1}{\mathcal{H}}\mathcal{T}'(\tau, k_1)\right)\left(\mathcal{T}(\tau, k_2) + \frac{1}{\mathcal{H}}\mathcal{T}'(\tau, k_2)\right)\right]. \tag{C.6}$$

The function $\mathcal{T}(\tau, k)$ is the scalar transfer function defined in (5.75), relating scalar metric perturbations to the primordial curvature ζ. Since the source term only includes terms quadratic in the scalar perturbations, we just need to solve the linear evolution equation [82]:

$$\psi_{\vec{k}}''(\tau) + \frac{4}{\tau}\psi_{\vec{k}}'(\tau) + \frac{k^2}{3}\psi_{\vec{k}}(\tau) = 0 \tag{C.7}$$

which gives the following non-decaying solution for the transfer function:

$$\mathcal{T}(\tau,k)=\frac{6}{(k\tau)^2}\left[\frac{\sin(k\tau/\sqrt{3})}{k\tau/\sqrt{3}}-\cos(k\tau/\sqrt{3})\right], \tag{C.8}$$

and for super-horizon modes ($k\tau\ll 1$) reduces to $\mathcal{T}(\tau,k)=\frac{2}{3}$.
Substituting (C.3) and (C.4) back inside solution (C.1) we get:

$$\begin{aligned}h_{\vec{k}}^{(\lambda)}(\tau)&=\frac{1}{a(\tau)}\int_{\tau_{\rm in}}^{\tau}d\tau'\frac{1}{k}\sin\big[k(\tau-\tau')\big]a(\tau')\int\frac{d^3\vec{p}}{(2\pi)^3}e^{(\lambda)}(\hat{k},\vec{p})f(p,|\vec{k}-\vec{p}|,\tau')\zeta(\vec{p})\zeta(\vec{k}-\vec{p})\\&=\int\frac{d^3\vec{p}}{(2\pi)^3}\frac{1}{k^3\tau}e^{(\lambda)}(\hat{k},\vec{p})\zeta(\vec{p})\zeta(\vec{k}-\vec{p})\int_{k\tau_{\rm in}}^{k\tau}d(k\tau')k\tau'\big[\sin(k\tau)\cos(k\tau')-\cos(k\tau)\sin(k\tau')\big]f(p,|\vec{k}-\vec{p}|,\tau'),\end{aligned} \tag{C.9}$$

where we have exploited the fact that during radiation domination the scale factor goes like $a(\tau)\propto\tau$. It is possible to perform the integration over τ' and express the result in the following way:

$$h_{\vec{k}}^{(\lambda)}(\tau)=\frac{4}{9}\frac{1}{k^3\tau}\int\frac{d^3\vec{p}}{(2\pi)^3}e^{(\lambda)}(\hat{k},\vec{p})\zeta(\vec{p})\zeta(\vec{k}-\vec{p})\big[\mathcal{I}_c(p,|\vec{k}-\vec{p}|)\cos(k\tau)+\mathcal{I}_s(p,|\vec{k}-\vec{p}|)\sin(k\tau)\big], \tag{C.10}$$

where the functions $\mathcal{I}_c$ and $\mathcal{I}_s$ are defined as:

$$\begin{aligned}\mathcal{I}_c(p,|\vec{k}-\vec{p}|)&\equiv-\int_0^\infty d(k\tau')k\tau'\sin(k\tau')f(p,|\vec{k}-\vec{p}|,\tau'),\\\mathcal{I}_s(p,|\vec{k}-\vec{p}|)&\equiv\int_0^\infty d(k\tau')k\tau'\cos(k\tau')f(p,|\vec{k}-\vec{p}|,\tau').\end{aligned} \tag{C.11}$$

The factor 4/9 in front of (C.10) is present because $\mathcal{I}_c$ and $\mathcal{I}_s$ are written in terms of the transfer function normalized to the super-horizon scalar metric perturbation $\psi=\frac{2}{3}\zeta$ rather than the curvature perturbation ζ itself.
Integrals in (C.11) receive the main contribution in the interval between the horizon re-entry of the mode at $\tau\sim k^{-1}$ (which we have previously identified with the instant of production of the GW background) and a time a few order of magnitude larger than k^{-1}. Since $\tau_0\gg k^{-1}$, it is reasonable to extend the integration to future infinity. The choice of $\tau_{\rm in}=0$ is instead due to the fact that in principle one should account also for the source mode while it is super-horizon, even if damped [78]. In order to perform the analytical integration it is useful to introduce the following variables:

$$d=\frac{1}{\sqrt{3}}|x-y|,\qquad s=\frac{1}{\sqrt{3}}(x+y), \tag{C.12}$$

with:

$$x=\frac{p}{k},\qquad y=\frac{|\vec{k}-\vec{p}|}{k}. \tag{C.13}$$

The analytical integration gives then the following results [78]:

$$\begin{aligned}\mathcal{I}_c(d,s)&=-36\pi\frac{(s^2+d^2-2)^2}{(s^2-d^2)^3}\theta(s^2-1),\\\mathcal{I}_s(d,s)&=-36\frac{(s^2+d^2-2)}{(s^2-d^2)^2}\left[\frac{(s^2+d^2-2)}{(s^2-d^2)}\ln\left(\frac{1-d^2}{|s^2-1|}\right)+2\right].\end{aligned} \tag{C.14}$$

Appendix D

Linear corrections to the anisotropies of CGWB from PBHs

In this appendix we discuss about linear corrections in expression (6.60) for the GW energy density of the stochastic background arising at PBH formation, and consequently how they influence the result for the anisotropies angular power spectrum. Recall, in fact, that in the main text we have decided to stick with just the leading-order terms of expansion in $\frac{q}{k_*} \ll 1$, which has allowed to greatly simplify the actual computations. Because of such a drastic approximation, there is the risk that some interesting features do not show up in the final result, and arise instead only when accounting for higher-order contributions.
We thus want here to extend the computation in order to also account for terms linear in the expansion parameter $\frac{q}{k_*}$. The starting point is expression (6.60) for the energy density of the CGWB, which we rewrite here explicitly, accounting for all the contributions arising from the first order terms in (6.59):

$$
\begin{aligned}
\langle \rho_{GW}(\tau,\vec{x})\rangle = \frac{M_P^2}{81\tau^2 a^2}\int\frac{d^3\vec{k}_1}{(2\pi)^3}\int\frac{d^3\vec{k}_2}{(2\pi)^3}\int\frac{d^3\vec{p}_1}{(2\pi)^3}\int\frac{d^3\vec{p}_2}{(2\pi)^3}e^{i(\vec{k}_1+\vec{k}_2)\vec{x}}\frac{1}{k_1^2k_2^2}\\
\times\langle\prod_{i=1}^{2}\left[\mathcal{I}_s(p_i,|\vec{k}_i-\vec{p}_i|)\cos(k_i\tau)-\mathcal{I}_c(p_i,|\vec{k}_i-\vec{p}_i|)\sin(k_i\tau)\right]\rangle_T\\
\times\sum_{\lambda,\lambda'}e_{ij}^{(\lambda)}(\hat{k}_1)e^{(\lambda')ij}(\hat{k}_2)e^{(\lambda)}(\hat{k}_1,\vec{p}_1)e^{(\lambda')}(\hat{k}_2,\vec{p}_2)\\
\times\frac{6}{5}(2\pi)^3\Big[\zeta_l(\vec{p}_1+\vec{p}_2)\delta^{(3)}(\vec{k}_1-\vec{p}_1+\vec{k}_2-\vec{p}_2)P_\zeta(|\vec{k}_1-\vec{p}_1|)\\
\times\left[f_{NL}(p_1,|\vec{p}_1+\vec{p}_2|,p_2)P_\zeta(p_1)+f_{NL}(p_2,|\vec{p}_1+\vec{p}_2|,p_1)P_\zeta(p_2)\right]\\
+\zeta_l(\vec{p}_1+\vec{k}_2-\vec{p}_2)\delta^{(3)}(\vec{k}_1-\vec{p}_1+\vec{p}_2)P_\zeta(|\vec{k}_1-\vec{p}_1|)\\
\times\left[f_{NL}(p_1,|\vec{p}_1+\vec{k}_2-\vec{p}_2|,|\vec{k}_2-\vec{p}_2|)P_\zeta(p_1)\right.\\
\left.+f_{NL}(|\vec{k}_2-\vec{p}_2|,|\vec{p}_1+\vec{k}_2-\vec{p}_2|,p_1)P_\zeta(|\vec{k}_2-\vec{p}_2|)\right]\\
+\zeta_l(\vec{k}_1-\vec{p}_1+\vec{p}_2)\delta^{(3)}(\vec{p}_1+\vec{k}_2-\vec{p}_2)P_\zeta(p_1)\\
\times\left[f_{NL}(|\vec{k}_1-\vec{p}_1|,|\vec{k}_1-\vec{p}_1+\vec{p}_2|,p_2)P_\zeta(|\vec{k}_1-\vec{p}_1|)\right.\\
\left.+f_{NL}(p_2,|\vec{k}_1-\vec{p}_1+\vec{p}_2|,|\vec{k}_1-\vec{p}_1|)P_\zeta(p_2)\right]\\
+\zeta_l(\vec{k}_1-\vec{p}_1+\vec{k}_2-\vec{p}_2)\delta^{(3)}(\vec{p}_1+\vec{p}_2)P_\zeta(p_1)\\
\times\left[f_{NL}(|\vec{k}_1-\vec{p}_1|,|\vec{k}_1-\vec{p}_1+\vec{k}_2-\vec{p}_2|,|\vec{k}_2-\vec{p}_2|)P_\zeta(|\vec{k}_1-\vec{p}_1|)\right.\\
\left.+f_{NL}(|\vec{k}_2-\vec{p}_2|,|\vec{k}_1-\vec{p}_1+\vec{k}_2-\vec{p}_2|,|\vec{k}_1-\vec{p}_1|)P_\zeta(\vec{k}_2-\vec{p}_2)\right]\Big].
\end{aligned}
\tag{D.1}
$$

Proceeding as in the main text, we solve the $\vec{p}_2$ integral by making use of the Dirac deltas. It is then possible to perform the substitution $\vec{p}_1 \to \vec{k}_1 - \vec{p}_1$ in the last two contributions, in such a way

that we can express the previous result in the following way:

$$
\begin{aligned}
\langle \rho_{GW}(\tau,\vec{x})\rangle = \frac{M_P^2}{81\tau^2 a^2}\int\frac{d^3\vec{k}_1}{(2\pi)^3}\int\frac{d^3\vec{p}_1}{(2\pi)^3}\int\frac{d^3\vec{q}}{(2\pi)^3}e^{i\vec{q}\vec{x}}\frac{1}{k_1^2|\vec{q}-\vec{k}_1|^2}\\
\times\Bigg\{\langle\big[\mathcal{I}_s(p_1,|\vec{k}_1-\vec{p}_1|)\cos(k_1\tau)-\mathcal{I}_c(p_1,|\vec{k}_1-\vec{p}_1|)\sin(k_1\tau)\big]\\
\times\big[\mathcal{I}_s(|\vec{q}-\vec{p}_1|,|\vec{k}_1-\vec{p}_1|)\cos(|\vec{q}-\vec{k}_1|\tau)\\
-\mathcal{I}_c(|\vec{q}-\vec{p}_1|,|\vec{k}_1-\vec{p}_1|)\sin(|\vec{q}-\vec{k}_1|\tau)\big]\rangle_T\\
\times\sum_{\lambda,\lambda'}e_{ij}^{(\lambda)}(\hat{k}_1)e^{(\lambda')ij}(\widehat{\vec{q}-\vec{k}_1})e^{(\lambda)}(\hat{k}_1,\vec{p}_1)e^{(\lambda')}(\widehat{\vec{q}-\vec{k}_1},\vec{q}-\vec{p}_1)\\
+\langle\big[\mathcal{I}_s(p_1,|\vec{k}_1-\vec{p}_1|)\cos(k_1\tau)-\mathcal{I}_c(p_1,|\vec{k}_1-\vec{p}_1|)\sin(k_1\tau)\big]\\
\times\big[\mathcal{I}_s(|\vec{k}_1-\vec{p}_1|,|\vec{q}-\vec{p}_1|)\cos(|\vec{q}-\vec{k}_1|\tau)\\
-\mathcal{I}_c(|\vec{k}_1-\vec{p}_1|,|\vec{q}-\vec{p}_1|)\sin(|\vec{q}-\vec{k}_1|\tau)\big]\rangle_T\\
\times\sum_{\lambda,\lambda'}e_{ij}^{(\lambda)}(\hat{k}_1)e^{(\lambda')ij}(\widehat{\vec{q}-\vec{k}_1})e^{(\lambda)}(\hat{k}_1,\vec{p}_1)e^{(\lambda')}(\widehat{\vec{q}-\vec{k}_1},\vec{p}_1-\vec{k}_1)\\
+\langle\big[\mathcal{I}_s(|\vec{k}_1-\vec{p}_1|,p_1)\cos(k_1\tau)-\mathcal{I}_c(|\vec{k}_1-\vec{p}_1|,p_1)\sin(k_1\tau)\big]\\
\times\big[\mathcal{I}_s(|\vec{q}-\vec{p}_1|,|\vec{k}_1-\vec{p}_1|)\cos(|\vec{q}-\vec{k}_1|\tau)\\
-\mathcal{I}_c(|\vec{q}-\vec{p}_1|,|\vec{k}_1-\vec{p}_1|)\sin(|\vec{q}-\vec{k}_1|\tau)\big]\rangle_T\\
\times\sum_{\lambda,\lambda'}e_{ij}^{(\lambda)}(\hat{k}_1)e^{(\lambda')ij}(\widehat{\vec{q}-\vec{k}_1})e^{(\lambda)}(\hat{k}_1,\vec{k}_1-\vec{p}_1)e^{(\lambda')}(\widehat{\vec{q}-\vec{k}_1},\vec{q}-\vec{p}_1)\\
+\langle\big[\mathcal{I}_s(|\vec{k}_1-\vec{p}_1|,p_1)\cos(k_1\tau)-\mathcal{I}_c(|\vec{k}_1-\vec{p}_1|,p_1)\sin(k_1\tau)\big]\\
\times\big[\mathcal{I}_s(|\vec{k}_1-\vec{p}_1|,|\vec{q}-\vec{p}_1|)\cos(|\vec{q}-\vec{k}_1|\tau)\\
-\mathcal{I}_c(|\vec{k}_1-\vec{p}_1|,|\vec{q}-\vec{p}_1|)\sin(|\vec{q}-\vec{k}_1|\tau)\big]\rangle_T\\
\times\sum_{\lambda,\lambda'}e_{ij}^{(\lambda)}(\hat{k}_1)e^{(\lambda')ij}(\widehat{\vec{q}-\vec{k}_1})e^{(\lambda)}(\hat{k}_1,\vec{k}_1-\vec{p}_1)e^{(\lambda')}(\widehat{\vec{q}-\vec{k}_1},\vec{p}_1-\vec{k}_1)\Bigg\}\\
\times\frac{6}{5}\zeta_l(\vec{q})P_\zeta(|\vec{k}_1-\vec{p}_1|)\big[f_{NL}(p_1,q,|\vec{q}-\vec{p}_1|)P_\zeta(p_1)\\
+f_{NL}(|\vec{q}-\vec{p}_1|,q,p_1)P_\zeta(|\vec{q}-\vec{p}_1|)\big],
\end{aligned}
\tag{D.2}
$$

where we have also made the change of variable $\vec{q}=\vec{k}_1+\vec{k}_2$ and replaced the integration over $\vec{k}_2$ with the integration over $\vec{q}$. In this way we see that terms involving the primordial curvature power spectra and scale-dependent f_{NL} have all been grouped into the final two lines.

It is possible to realize that expression (D.2) would simplify a lot if we were able to neglect the $\vec{q}$-dependence inside all the terms in the curly brackets. If this was the case, all these 4 contributions would end up being identical to the one combination present in (6.23) for the Gaussian case.

We do not prove explicitly that this approximation is reasonable, but, since we are considering here an expansion up to first order in $\frac{q}{k_*}$, the outcome can be twofold: either the contributions we are neglecting are second order or higher, and then the result we will give at first order is the correct one, or these neglected terms actually give rise to additional first-order contributions and thus our result is incomplete. Either way, the computations we present here should come in handy when looking for the correct way to derive an expression linear in $\frac{q}{k_*}$. In the worst case scenario, our result has to be complemented with linear terms coming from the contributions we are neglecting here.

The fact that we are resorting to this further assumption should make clear why we have decided to not include this treatment in the main text, and we have instead settled to just keep the leading-order terms of the expansion.

Having clarified the strength and limits of our approximations, we are now left with the following expression:

$$\begin{aligned}\langle\rho_{GW}(\tau,\vec{x})\rangle = \frac{M_P^2}{81\tau^2a^2}\int\frac{d^3\vec{k}_1}{(2\pi)^3}\int\frac{d^3\vec{p}_1}{(2\pi)^3}\int\frac{d^3\vec{q}}{(2\pi)^3}e^{i\vec{q}\vec{x}}\frac{1}{k_1^2|\vec{q}-\vec{k}_1|^2}\\ \langle\big[\mathcal{I}_s(p_1,|\vec{k}_1-\vec{p}_1|)\cos(k_1\tau)-\mathcal{I}_c(p_1,|\vec{k}_1-\vec{p}_1|)\sin(k_1\tau)\big]^2\rangle_T\\ \times\sum_{\lambda,\lambda'}e_{ij}^{(\lambda)}(\hat{k}_1)e^{(\lambda')ij}(-\hat{k}_1)e^{(\lambda)}(\hat{k}_1,\vec{p}_1)e^{(\lambda')}(-\hat{k}_1,-\vec{p}_1)\\ \times\frac{24}{5}\zeta_l(\vec{q})P_\zeta(|\vec{k}_1-\vec{p}_1|)\big[f_{NL}(p_1,q,|\vec{q}-\vec{p}_1|)P_\zeta(p_1)\\ +f_{NL}(|\vec{q}-\vec{p}_1|,q,p_1)P_\zeta(|\vec{q}-\vec{p}_1|)\big],\end{aligned} \tag{D.3}$$

where the 4 previous contributions, linear in f_{NL}, contribute equally under our assumption. The in the last line can be made equal to the one in the line above by further making both the substitutions $\vec{q}-\vec{p}_1\to\vec{p}_1$ and $\vec{q}-\vec{k}_1\to\vec{k}_1$.
Following the treatment in the main text, we can now assume the coordinate system where the third axis is directed in the $\hat{k}_1$-direction. In such a system we express the wavevectors in the following way:

$$\begin{aligned}\vec{k}_1 &= k_1(0,0,1),\\ \vec{p}_1 &= p_1(\sin\theta_p,0,\cos\theta_p),\\ \vec{q} &= q(\sin\theta_q\cos\phi_q,\sin\theta_q\sin\phi_q,\cos\theta_q),\end{aligned} \tag{D.4}$$

where all the angles are taken with respect to $\hat{k}_1$. It is then possible to exploit these expressions in order to make explicit the rightmost dependence $|\vec{q}-\vec{p}_1|$ in f_{NL}:

$$|\vec{q}-\vec{p}_1| = q^2+p_1^2-2qp_1(\sin\theta_q\cos\phi_q\sin\theta_p+\cos\theta_q\cos\theta_p). \tag{D.5}$$

Remembering to account also for the Gaussian parts of the 4-point correlator (6.59), we can now perform the remaining integrations in the usual way and we obtain the following result, written in terms of the GW energy density per logarithmic interval:

$$\Omega_{GW}(\tau,\vec{x},k) = \bar{\Omega}_{GW}(\tau,k)\rangle\left[1+\frac{24}{5}\int\frac{d^3\vec{q}}{(2\pi)^3}e^{i\vec{q}\vec{x}}\zeta_l(\vec{q})f_{NL}(k_*,q,|\vec{q}-\vec{p}|)\right], \tag{D.6}$$

where expression (D.5) for the dependence of f_{NL} becomes:

$$\begin{aligned}|\vec{q}-\vec{p}| &= \left[q^2+k_*^2-2qk_*\left(\sin\theta_q\cos\phi_q\left(1-\frac{k^2}{4k_*^2}\right)^{\frac{1}{2}}+\cos\theta_q\frac{k}{2k_*}\right)\right]^{\frac{1}{2}}\\ &\simeq k_*\left[1-\frac{q}{k_*}\left(\sin\theta_q\cos\phi_q\left(1-\frac{k^2}{4k_*^2}\right)^{\frac{1}{2}}+\cos\theta_q\frac{k}{2k_*}\right)\right],\end{aligned} \tag{D.7}$$

which we have expanded up to first order in $\frac{q}{k_*}$ in the second line. Comparing result (D.6) with the (6.61) in the main text, we see that, as a consequence of keeping the linear terms in the expansion, the rightmost dependence in f_{NL} has changed from the simple wavenumber k_* and has acquired new contributions dependent on q and $\hat{q}$. Notice in particular that the third wavenumber on which f_{NL} depends is not equal to the first one anymore. This was in fact an approximated result which held only at the leading order in $\frac{q}{k_*}$. In this case, instead, the third wavenumber results indeed from a combination of the small and large scales wavevectors.

We want now to explicitly express the scale-dependent f_{NL} in (D.6) by means of the same two parametrizations considered in the main text. It is straightforward to realize that expression (3.53) for the running is not affected by the new contributions linear in $\frac{q}{k_*}$, since it depends on the first

two wavenumbers which are left unchanged from the leading-order treatment. Therefore, we conclude that, for such a parametrization of the running, our computations here would lead to the very same result (6.69) of the main text for the CGWB anisotropies angular power spectrum. Of course, it is still possible for eventual, additional contributions, linear in $\frac{q}{k_*}$, to arise from the terms we are neglecting, as already mentioned in the previous discussion.
We are then left to treat with just the simple power-law parametrization of the running (3.49), which in fact depends on the third wavenumber and it is thus affected by the new linear contributions in $\frac{q}{k_*}$. In this case we have explicitly:

$$f_{NL}(k_*,q,|\vec{q}-\vec{p}|)=\mathcal{A}|\vec{q}-\vec{p}|^{n_{f_{NL}}}\simeq k_*^{n_{f_{NL}}}\left[1-n_{f_{NL}}\frac{q}{k_*}\left(\sin\theta_q\cos\phi_q\left(1-\frac{k^2}{4k_*^2}\right)^{\frac{1}{2}}+\cos\theta_q\frac{k}{2k_*}\right)\right], \tag{D.8}$$

where in the second equality we have substituted (D.7) and kept only terms up to linear order in $\frac{q}{k_*}$. Repeating the procedure outlined in the main text to obtain (6.62), we now write the expansion coefficients over spherical harmonic of the CGWB initial condition anisotropy term:

$$\Gamma_{\ell m,I}(k)=4\pi(-i)^\ell\frac{3}{5}\int\frac{d^3\vec{q}}{(2\pi)^3}\zeta_l(\vec{q})Y^*_{\ell m}(\hat{q})j_\ell\big(q(\tau_0-\tau_{\rm in})\big)\tilde{f}_{NL}(k,k_*,\vec{q}), \tag{D.9}$$

where the rescaled non-linear parameter has the following expression:

$$\tilde{f}_{NL}(k,k_*,\vec{q})=8\mathcal{A}k_*^{n_{f_{NL}}}\left[1-n_{f_{NL}}\frac{q}{k_*}\left(\sin\theta_q\cos\phi_q\left(1-\frac{k^2}{4k_*^2}\right)^{\frac{1}{2}}+\cos\theta_q\frac{k}{2k_*}\right)\right]\left(4-\frac{\partial\ln\bar{\Omega}_{GW}}{\partial\ln k}\right)^{-1}. \tag{D.10}$$

Combining the previous result (D.9) with the scalar sourced anisotropy term (5.78), in the large-scale limit, we obtain the following 2-point correlation function:

$$\begin{aligned}\langle\Gamma_{\ell_1m_1,I+S}(k)\Gamma^*_{\ell_2m_2,I+S}(k)\rangle=4\pi\frac{9}{25}(i)^{\ell_1}(-i)^{\ell_2}\mathcal{P}_{\zeta_l}\int\frac{dq}{q}j_{\ell_1}\big(q(\tau_0-\tau_{\rm in})\big)j_{\ell_2}\big(q(\tau_0-\tau_{\rm in})\big)\\ \times\int d\Omega_qY_{\ell_2m_2}(\hat{q})Y^*_{\ell_1m_1}(\hat{q})\Bigg\{1+16\mathcal{A}\left(4-\frac{\partial\ln\bar{\Omega}_{GW}}{\partial\ln k}\right)^{-1}\\ \times k_*^{n_{f_{NL}}}\left[1-n_{f_{NL}}\frac{q}{k_*}\left(\sin\theta_q\cos\phi_q\left(1-\frac{k^2}{4k_*^2}\right)^{\frac{1}{2}}+\cos\theta_q\frac{k}{2k_*}\right)\right]\\ +64\mathcal{A}^2\left(4-\frac{\partial\ln\bar{\Omega}_{GW}}{\partial\ln k}\right)^{-2}\\ \times k_*^{2n_{f_{NL}}}\left[1-2n_{f_{NL}}\frac{q}{k_*}\left(\sin\theta_q\cos\phi_q\left(1-\frac{k^2}{4k_*^2}\right)^{\frac{1}{2}}+\cos\theta_q\frac{k}{2k_*}\right)\right]\Bigg\},\end{aligned} \tag{D.11}$$

where the Dirac delta arising from 2-point correlators of the long mode ζ_l has already been integrated. It is clear from this result that the new dependencies on the angular components of $\vec{q}$ have to be considered carefully when integrating the spherical harmonics, since the orthonormality condition (B.8) cannot be simply applied anymore. We need to perform, in particular, the following two non-trivial integrations:

$$\begin{aligned}&\int_0^{2\pi}\int_0^{\pi}d\phi_qd\theta_q\sin\theta_qY_{\ell_2m_2}(\hat{q})Y^*_{\ell_1m_1}(\hat{q})\sin\theta_q\cos\phi_q,\\ &\int_0^{2\pi}\int_0^{\pi}d\phi_qd\theta_q\sin\theta_qY_{\ell_2m_2}(\hat{q})Y^*_{\ell_1m_1}(\hat{q})\cos\theta_q.\end{aligned} \tag{D.12}$$

We show here explicitly the steps to solve the first one, with the treatment of the second being analogous. We start by expressing the spherical harmonics in terms of the associated Legendre polynomials via definition (B.7), in such a way that we can factorize the two integrals over θ_q and

ϕ_q. The latter can be solved straightforwardly:

$$\begin{aligned}\int_0^{2\pi} d\phi_q e^{im_2\phi_q} e^{-im_1\phi_q}\cos\phi_q &= \int_0^{2\pi} d\phi_q e^{im_2\phi_q} e^{-im_1\phi_q}\frac{e^{i\phi_q}+e^{-i\phi_q}}{2}\\ &= \frac{1}{2}\int_0^{2\pi} d\phi_q\big(e^{i(m_2-m_1+1)\phi_q}+e^{i(m_2-m_1-1)\phi_q}\big)\\ &= \pi\big(\delta_{m_1-1,m_2}+\delta_{m_1+1,m2}\big).\end{aligned} \tag{D.13}$$

In order to perform the integration over θ_q we now exploit the Legendre polynomials recursive relations (B.4) and (B.5), along with the normalization condition (B.3). We obtain the following result:

$$\int d\Omega_q Y_{\ell_2 m_2}(\hat{q}) Y^*_{\ell_1 m_1}(\hat{q})\sin\theta_q\cos\phi_q = \mathcal{C}_{\ell_1-1,m_1-1}+\mathcal{C}_{\ell_1+1,m_1-1}+\mathcal{C}_{\ell_1-1,m_1+1}+\mathcal{C}_{\ell_1+1,m_1+1}, \tag{D.14}$$

where the symbols after the equality are defined with the following notation:

$$\mathcal{C}_{\ell_1 m_1} \propto \delta_{\ell_1\ell_2}\delta_{m_1 m_2}. \tag{D.15}$$

Their exact expressions can be computed to be:

$$\begin{aligned}\mathcal{C}_{\ell_1-1,m_1-1} &= -\frac{1}{2}\delta_{\ell_1-1,\ell_2}\delta_{m_1-1,m_2}\sqrt{\frac{(\ell_1+m_1)(\ell_1+m_1-1)}{(2\ell_1+1)(2\ell_1-1)}},\\ \mathcal{C}_{\ell_1+1,m_1-1} &= \frac{1}{2}\delta_{\ell_1+1,\ell_2}\delta_{m_1-1,m_2}\sqrt{\frac{(\ell_1-m_1+2)(\ell_1-m_1+1)}{(2\ell_1+1)(2\ell_1+3)}},\\ \mathcal{C}_{\ell_1-1,m_1+1} &= \frac{1}{2}\delta_{\ell_1-1,\ell_2}\delta_{m_1+1,m_2}\sqrt{\frac{(\ell_1-m_1)(\ell_1-m_1-1)}{(2\ell_1+1)(2\ell_1-1)}},\\ \mathcal{C}_{\ell_1+1,m_1+1} &= -\frac{1}{2}\delta_{\ell_1+1,\ell_2}\delta_{m_1+1,m_2}\sqrt{\frac{(\ell_1+m_1+2)(\ell_1+m_1+1)}{(2\ell_1+1)(2\ell_1+3)}}.\end{aligned} \tag{D.16}$$

Similar arguments to the one just outlined allow to also recover the following expression for the second integral in (D.12):

$$\int d\Omega_q Y_{\ell_2 m_2}(\hat{q}) Y^*_{\ell_1 m_1}(\hat{q})\cos\theta_q = \mathcal{C}_{\ell_1-1,m_1}+\mathcal{C}_{\ell_1+1,m_1}, \tag{D.17}$$

where the recursive relation (B.6) has been used and the exact expressions for the symbols on the right side are:

$$\begin{aligned}\mathcal{C}_{\ell_1-1,m_1} &= \delta_{\ell_1-1,\ell_2}\delta_{m_1 m_2}\sqrt{\frac{(\ell_1-m_1)(\ell_1+m_1)}{(2\ell_1+1)(2\ell_1-1)}},\\ \mathcal{C}_{\ell_1+1,m_1} &= \delta_{\ell_1+1,\ell_2}\delta_{m_1 m_2}\sqrt{\frac{(\ell_1-m_1+1)(\ell_1+m_1+1)}{(2\ell_1+1)(2\ell_1+3)}}.\end{aligned} \tag{D.18}$$

Substituting results (D.14) and (D.17) back in (D.11), we are left to solve the integral containing the spherical Bessel functions. Exploiting relations (B.13) we get the following expression for the

2-point correlator (D.11):

$$\begin{aligned}\langle\Gamma_{\ell_1 m_1, I+S}(k)\Gamma^*_{\ell_2 m_2, I+S}(k)\rangle &= \left[1+\tilde{f}_{NL}(k,k_*)\right]^2 \frac{2\pi}{\ell(\ell+1)}\frac{9}{25}\mathcal{P}_{\zeta_I}\delta_{\ell_1\ell_2}\delta_{m_1 m_2} \\ &- i\frac{n_{f_{NL}}}{k_*(\tau_0-\tau_{\rm in})}\left[\tilde{f}_{NL}(k,k_*)+\left(\tilde{f}_{NL}(k,k_*)\right)^2\right] \\ &\times\left[\frac{1}{\ell_1}\left(\left(\mathcal{C}_{\ell_1-1,m_1-1}+\mathcal{C}_{\ell_1-1,m_1+1}\right)\left(1-\frac{k^2}{4k_*^2}\right)^{\frac{1}{2}}+\frac{k}{2k_*}\mathcal{C}_{\ell_1-1,m_1}\right)\right. \\ &\left.-\frac{1}{\ell_1+1}\left(\left(\mathcal{C}_{\ell_1+1,m_1-1}+\mathcal{C}_{\ell_1+1,m_1+1}\right)\left(1-\frac{k^2}{4k_*^2}\right)^{\frac{1}{2}}+\frac{k}{2k_*}\mathcal{C}_{\ell_1+1,m_1}\right)\right],\end{aligned} \tag{D.19}$$

where $\tilde{f}_{NL}(k,k_*)$ is defined as in equation (6.65). It has to be stressed that relations (B.13) have been applied here in an approximate form. Remember in fact that the q-integration is cut off at the largest wavenumber associated to a long mode of the split. As a consequence, in analogy to what we have already pointed out in the main text, we conclude that result (D.19) describes correctly only large-scales, i.e. low multipoles, anisotropies.

The inclusion of terms linear in $\frac{q}{k_*}$ in the treatment has brought up some interesting features which we now briefly discuss.

Notice first of all that the first line in result (D.19) corresponds to expression (6.66) for the angular power spectrum at leading order in $\frac{q}{k_*}$. The other contributions are what comes instead from linear terms in $\frac{q}{k_*}$. Remembering the notation convention for the symbols (D.16) and (D.18), it is clear that these are actually off-diagonal contributions to the angular power spectrum of the CGWB anisotropies. This is a unique feature which does not arise when sticking only to the leading order, as we have seen in the main text. Furthermore, this happens only with specific forms of the running, since we know for example that it is not the case for the other parametrization (3.49).

Another interesting fact about result (D.19) is that the suppressed expansion term $\frac{q}{k_*}$ is converted into $\frac{1}{k_*(\tau_0-\tau_{\rm in})}$ after the integration over q. This is analogous to what happens in result (6.69) in the main text, on which we have already commented. The corrective nature of the off-diagonal terms in (D.19) is evident from the fact that the combination $\tau_0-\tau_{\rm in}\simeq\tau_0$ approximately corresponds to the largest observable scale, in such a way that $\frac{1}{k_*(\tau_0-\tau_{\rm in})}\ll 1$ still holds.

Do keep in mind that all these conclusions may well change when correctly accounting for all the terms linear in $\frac{q}{k_*}$ that we are currently neglecting. Nevertheless, we have decided to give in this appendix the result of our calculations, even if incomplete, both because these ended up to be a major part of our work and also with the hope that our findings may prove to be somewhat useful for any future research on this same topic.

Bibliography

[1] P. Coles, F. Lucchin, *Cosmology: The Origin and Evolution of Cosmic Structure*, John Wiley & Sons, (2002).

[2] D. Baumann, *Cosmology Part III Mathematical tripos*.

[3] Planck Collaboration, *Planck 2018 results. VI. Cosmological parameters*, arXiv:1807.06209 [astro-ph.CO], (2018).

[4] A. H. Guth, *Inflationary universe: A possible solution to the horizon and flatness problems*, Phys. Rev. D 23, 347, (1981).

[5] A. Riotto, *Inflation and the Theory of Cosmological Perturbations*, arXiv:hep-ph/0210162, (2017).

[6] D. Baumann, *TASI Lectures on Inflation*, arXiv:0907.5424 [hep-th], (2012).

[7] E. W. Kolb, M. S. Turner, *The Early Universe*, Westview Press, (1990).

[8] N. Bartolo, E. Komatsu, S. Matarrese, A. Riotto, *Non-Gaussianity from Inflation: Theory and Observations*, Phys. Rept. 402 103-266, (2004).

[9] A. R. Liddle, D. H. Lyth, *Cosmological inflation and large-scale structure*, Cambridge University Press, (2000).

[10] Planck Collaboration, *Planck 2018 results. IX. Constraints on primordial non-Gaussianity*, arXiv:1905.05697 [astro-ph.CO], (2019).

[11] P. Daniel Meerburg, D. Green et al. *Primordial Non-Gaussianity*, arXiv:1903.04409 [astro-ph.CO], (2019).

[12] X. Chen, *Primordial Non-Gaussianities from Inflation Models*, Adv. Astron., 638979, (2010).

[13] J. Maldacena, *Non-Gaussian features of primordial fluctuations in single field inflationary models*, JHEP 0305 013, (2003).

[14] M. Celoria, S. Matarrese, *Primordial Non-Gaussianity*, arXiv:1812.08197 [astro-ph.CO], (2018).

[15] M. Liguori, A. Yadav, F. K. Hansen, E. Komatsu, S. Matarrese, B. Wandelt, *Temperature and Polarization CMB Maps from Primordial non-Gaussianities of the Local Type*, Phys. Rev. D 76, 105016, (2007).

[16] E. Komatsu, D. N. Spergel, *Acoustic Signatures in the Primary Microwave Background Bispectrum*, Phys. Rev. D 63, 063002, (2001).

[17] E. Komatsu, D. N. Spergel, B. D. Wandelt, *Measuring primordial non-Gaussianity in the cosmic microwave background*, Astrophys. J. 634 14-19, (2005).

[18] H. Kodama, M. Sasaki, *Cosmological perturbation Theory*, Progress of Theoretical Physics Supplement No. 78, (1984).

[19] K. A. Malik, D. Wands, *Cosmological perturbations*, Phys. Rept. 475 1-51, (2009).

[20] S. Matarrese, S. Mollerach, M. Bruni, *Relativistic second-order perturbations of the Einstein-de Sitter Universe*, Phys. Rev. D 58, 043504, (1998).

[21] J. M. Bardeen, *Gauge-invariant cosmological perturbations*, Phys. Rev. D 22, 1882, (1980).

[22] E. Komatsu, N. Afshordi, N. Bartolo, D. Baumann et al. *Non-Gaussianity as a Probe of the Physics of the Primordial Universe and the Astrophysics of the Low Redshift Universe*, arXiv:0902.4759 [astro-ph.CO], (2009).

[23] H. M. Hodges, G. R. Blumenthal, L. A. Kofman, J. R. Primack, *Nonstandard primordial fluctuations from a polynomial inflation potential*, Nucl. Phys. B, 335, 197, (1990).

[24] D. S. Salopek, J. R. Bond, *Nonlinear evolution of long-wavelength metric fluctuations in inflationary models*, Phys. Rev. D 42, 3936, (1990).

[25] L. Kofman, G. R. Blumenthal, H. Hodges, J. R. Primack, *Generation of Non-Flat and Non-Gaussian Perturbations from Inflation*, Large-Scale Structures and Peculiar Motions in the Universe, ASP Conference Series, Vol. 15, D.W. Latham and L.N. daCosta, Eds., p. 339, (1991).

[26] A. Gangui, F. Lucchin, S. Matarrese, S. Mollerach, *The Three–Point Correlation Function of the Cosmic Microwave Background in Inflationary Models*, Astrophys. J. 430 447-457, (1994).

[27] V. Acquaviva, N. Bartolo, S. Matarrese, A. Riotto, *Second-Order Cosmological Perturbations from Inflation*, Nucl. Phys. B, 667, 119-148, (2003).

[28] L. Senatore, K. M. Smith, M. Zaldarriaga, *Non-Gaussianities in Single Field Inflation and their Optimal Limits from the WMAP 5-year Data*, JCAP 1001:028, (2010).

[29] C. T. Byrnes, M. Gerstenlauer, S. Nurmi, G. Tasinato, D. Wands, *Scale-dependent non-Gaussianity probes inflationary physics*, JCAP 10 004, (2010).

[30] F. Oppizzi, M. Liguori, A. Renzi, F. Arroja, N. Bartolo, *CMB constraints on running non-Gaussianity*, arXiv:1711.08286 [astro-ph.CO], (2017).

[31] R. Emami, E. Dimastrogiovanni, J. Chluba, M. Kamionkowski *Probing the scale dependence of non-Gaussianity with spectral distortions of the cosmic microwave background*, Phys. Rev. D 91, 123531, (2015).

[32] N. Bartolo, S. Matarrese, A. Riotto, *Non-Gaussianity of Large-Scale Cosmic Microwave Background Anisotropies beyond Perturbation Theory*, JCAP 0508:010, (2005).

[33] A. Becker, D. Huterer, K. Kadota *Scale-Dependent Non-Gaussianity as a Generalization of the Local Model*, JCAP 01 006, (2011).

[34] A. Becker, D. Huterer, *First constraints on the running of non-Gaussianity*, Physical Review Letters, vol. 109, Issue 12, id. 121302, (2012).

[35] M. Liguori, S. Matarrese, L. Moscardini, *High-Resolution Simulations of Cosmic Microwave Background non-Gaussian Maps in Spherical Coordinates*, Astrophys. J., 597, 57-65, (2003).

[36] R. Scoccimarro, L. Hui, M. Manera, K. C. Chan, *Large-scale Bias and Efficient Generation of Initial Conditions for Non-Local Primordial Non-Gaussianity*, Phys. Rev. D 85, 083002, (2012).

[37] F. Schmidt, M. Kamionkowski, *Halo Clustering with Non-Local Non-Gaussianity*, Phys. Rev. D 82, 103002, (2010).

[38] W. Hu, S. Dodelson, *Cosmic Microwave Background Anisotropies*, Ann. Rev. Astron. Astrophys., 40, 171-216, (2002).

[39] A. Jones, A. Lasenby, *The Cosmic Microwave Background*, Living Reviews in Relativity 1, 11, (1998).

[40] A.A. Penzias, R.W. Wilson, *A Measurement of Excess Antenna Temperature at 4080 m/s*, Astrophys. J., 142, 419-421, (1965).

[41] S. Dodelson, F. Schmidt, *Modern Cosmology*, Academic Press, (2020).

[42] D. J. Fixsen, E. S. Cheng, J. M. Gales et al. *The Cosmic Microwave Background Spectrum from the Full COBE FIRAS Data Set*, Astrophys. J., 473, 576, (1996).

[43] D. J. Fixsen, *The temperature of the cosmic microwave background*, Astrophys. J., 707 (2), 916–920, (2009).

[44] G. F. Smoot, M. V. Gorenstein, R. A. Muller, *Detection of anisotropy in the cosmic blackbody radiation*, Phys. Rev. Lett., 898-901, (1977).

[45] G. F. Smoot et al. *Structure in the COBE Differential Microwave Radiometer First-Year Maps*, Astrophys. J Lett., 396 L1, (1992).

[46] Planck Collaboration, *Planck 2018 results. I. Overview and the cosmological legacy of Planck*, arXiv:1807.06205 [astro-ph.CO], (2018).

[47] https://www.cosmos.esa.int/web/planck

[48] R. K. Sachs, A. M. Wolfe, *Perturbations of a Cosmological Model and Angular Variations of the Microwave Background*, Astrophys. J., 147, 73, (1967).

[49] N. Bartolo, D. Bertacca, S. Matarrese et al. *Characterizing the Cosmological Gravitational Wave Background: Anisotropies and non-Gaussianity*, Phys. Rev. D 102, 023527, (2020).

[50] U. Seljak, M. Zaldarriaga, *A Line-of-Sight Integration Approach to Cosmic Microwave Background Anisotropies*, Astrophys. J., 469, 437, (1996).

[51] *https://camb.info/*

[52] C. Caprini, D. G. Figueroa, *Cosmological Backgrounds of Gravitational Waves*, arXiv:1801.04268 [astro-ph.CO], (2018).

[53] M. C. Guzzetti, N. Bartolo, M. Liguori, S. Matarrese, *Gravitational waves from inflation*, Rivista del Nuovo Cimento, Vol. 39, Issue 9, 399-495, (2016).

[54] M. Maggiore, *Gravitational Waves. Vol. 1: Theory and Experiments*, Oxford University Press, (2007).

[55] G. M. Harry and the LIGO Scientific Collaboration, *Advanced LIGO: the next generation of gravitational wave detectors*, Classical and Quantum Gravity 27, 084006, (2010).

[56] B. P. Abbott et al. (LIGO Scientific Collaboration and Virgo Collaboration), *Observation of Gravitational Waves from a Binary Black Hole Merge*, Phys. Rev. Lett. 116, 131102, (2016).

[57] N. Christensen, *Stochastic Gravitational Wave Backgrounds*, Reports on Progress in Physics, Vol. 82, 016903, (2019).

[58] N. Christensen, *Measuring the stochastic gravitational-radiation background with laser-interferometric antennas*, Phys. Rev. D 46, 5250, (1992).

[59] T. Regimbau, *The astrophysical gravitational wave stochastic background*, arXiv:1101.2762 [astro-ph.CO], (2011).

[60] B. Allen, J. D. Romano, *Detecting a stochastic background of gravitational radiation: Signal processing strategies and sensitivities*, Phys. Rev. D 59, 102001, (1999).

[61] P. D. Lasky et al. *Gravitational-Wave Cosmology across 29 Decades in Frequency*, Phys. Rev. X 6, 011035, (2016).

[62] S. Vitale *Space-borne gravitational wave observatories*, Gen Relativ Gravit 46:1730, (2014).

[63] P. Cabella, M. Kamionkowski, *Theory of cosmic microwave background polarization*, arXiv:astro-ph/0403392, (2005).

[64] W. Hu, M. White, *CMB anisotropies: Total angular momentum method*, Phys. Rev. D 56, 596-615, (1997).

[65] Planck Collaboration, *Planck 2018 results. X. Constraints on inflation*, arXiv:1807.06211 [astro-ph.CO], (2018).

[66] Keck Array, BICEP2 Collaborations, *BICEP2 / Keck Array x: Constraints on Primordial Gravitational Waves using Planck, WMAP, and New BICEP2/Keck Observations through the 2015 Season*, Phys. Rev. Lett. 121, 221301, (2018).

[67] C. R. Contaldi, *Anisotropies of Gravitational Wave Backgrounds: A Line Of Sight Approach*, arXiv:1609.08168 [astro-ph.CO], (2016).

[68] C. W. Misner, K. S. Thorne, J. A. Wheeler, *Gravitation*, W. H. Freeman, (1973).

[69] K. Tomita, *Non-Linear Theory of Gravitational Instability in the Expanding Universe*, Progress of Theoretical Physics 37 831, (1967).

[70] S. Matarrese, O. Pantano, D. Saez, *General-relativistic approach to the nonlinear evolution of collisionless matter*, Phys. Rev. D 47, 1311, (1993).

[71] S. Matarrese, O. Pantano, D. Saez, *General relativistic dynamics of irrotational dust: Cosmological implications*, Phys. Rev. Lett. 72, 320, (1994).

[72] C. Carbone, S. Matarrese, *Unified treatment of cosmological perturbations from superhorizon to small scales*, Phys. Rev. D 71, 043508, (2005).

[73] K. N. Ananda, C. Clarkson, D. Wands, *The cosmological gravitational wave background from primordial density perturbations*, Phys. Rev. D 75, 123518, (2007).

[74] D. Baumann, K. Ichiki, P. J. Steinhardt, K. Takahashi, *Gravitational Wave Spectrum Induced by Primordial Scalar Perturbations*, Phys. Rev. D 76, 084019, (2007).

[75] R. Saito, J. Yokoyama, *Gravitational-Wave Background as a Probe of the Primordial Black-Hole Abundance*, Phys. Rev. Lett. 102, 161101, (2009).

[76] S. Mollerach, D. Harari, S. Matarrese, *CMB polarization from secondary vector and tensor modes*, Phys. Rev. D 69, 063002, (2004).

[77] N. Bartolo, S. Matarrese, A. Riotto, *CMB Anisotropies at Second-Order II: Analytical Approach*, JCAP 0701:019, (2007).

[78] J. R. Espinosa, D. Racco, A. Riotto, *A Cosmological Signature of the SM Higgs Instability: Gravitational Waves*, arXiv:1804.07732 [hep-ph], (2018).

[79] M. Maggiore, *Gravitational Wave Experiments and Early Universe Cosmology*, Phys. Rept. 331 283-367, (2000).

[80] N. Bartolo, S. Matarrese, A. Riotto, A. Vaihkonen, *The Maximal Amount of Gravitational Waves in the Curvaton Scenario*, Phys. Rev. D 76, 061302, (2007).

[81] M. Sasaki, T. Suyama, T. Tanaka, S. Yokoyama, *Primordial Black Holes - Perspectives in Gravitational Wave Astronomy* -, Class. Quantum Grav. 35, 063001, (2018).

[82] R. Saito, J. Yokoyama, *Gravitational-Wave Constraints on the Abundance of Primordial Black Holes*, Prog. Theor. Phys. 123, 867-886, (2010).

[83] N. Bartolo, V. De Luca, G. Franciolini, M. Peloso, D. Racco, A. Riotto, *Testing Primordial Black Holes as Dark Matter through LISA*, Phys. Rev. D 99, 103521, (2019).

[84] N. Bartolo, V. De Luca, G. Franciolini, A. Lewis, M. Peloso, A. Riotto, *The Primordial Black Hole Dark Matter - LISA Serendipity*, Phys. Rev. Lett. 122, 211301, (2019).

[85] S. Young, C. T. Byrnes, *Signatures of non-gaussianity in the isocurvature modes of primordial black hole dark matter*, JCAP 1504 04, 034, (2015).

[86] G. Franciolini, A. Kehagias, S. Matarrese, A. Riotto, *Primordial Black Holes from Inflation and non-Gaussianity*, JCAP03 016, (2018).

[87] N. Bartolo, D. Bertacca, V. De Luca, G. Franciolini, S. Matarrese, M. Peloso, A. Ricciardone, A. Riotto, G. Tasinato, *Gravitational Wave Anisotropies from Primordial Black Holes*, arXiv:1909.12619 [astro-ph.CO], (2019).

[88] C. Gordon, D. Wands, B. A. Bassett, R. Maartens, *Adiabatic and entropy perturbations from inflation*, Phys. Rev. D 63, 023506 (2001).

[89] A. L. Erickcek, M. Kamionkowski, S. M. Carroll, *A Hemispherical Power Asymmetry from Inflation*, Phys. Rev. D 78, 123520, (2008).

[90] Y. Tada, S. Yokoyama, *Primordial black holes as biased tracers*, Phys. Rev. D 91, 123534, (2015).

[91] J. Baker, T. Baker, C. Carbone et al. *High angular resolution gravitational wave astronomy*, arXiv:1908.11410 [astro-ph.HE], (2019).

[92] A. Kalaja, N. Bellomo, N. Bartolo et al. *From Primordial Black Holes Abundance to Primordial Curvature Power Spectrum (and back)*, JCAP10 031, (2019).